TRACKING AND DATA RELAY SATELLITE SYSTEM CONFIGURATION AND TRADEOFF STUDY–PART II FINAL REPORT

Volume III
Atlas Centaur Launched TDRSS

HUGHES AIRCRAFT COMPANY
Space and Communications Group
El Segundo, California 90009

1 April 1973
Part II Final Report

Prepared For
GODDARD SPACE FLIGHT CENTER
Greenbelt, Maryland 20771

TECHNICAL REPORT STANDARD TITLE PAGE

1. Report No.	2. Government Accession No.	3. Recipient's Catalog No.
4. Title and Subtitle Tracking and Data Relay Satellite System Configuration and Tradeoff Study - Atlas Centaur Launched TDRSS		5. Report Date 1 April 1973 6. Performing Organization Code
7 Author(s)		8. Performing Organization Report No.
9. Performing Organization Name and Address Hughes Aircraft Company, Space and Communications Group, NASA Systems Division 1950 E. Imperial Highway El Segundo, California 90009		10. Work Unit No. 11. Contract or Grant No. NAS 5-21704
12. Sponsoring Agency Name and Address National Aeronautics and Space Administration - Goddard Space Flight Center Greenbelt, Maryland 20771 G. Clark		13. Type of Report and Period Covered Final Report, Part II 22 August 1972 to 1 April 1973 14. Sponsoring Agency Code

15. Supplementary Notes

16. Abstract

Configuration data and design information for the Atlas Centaur launched configuration are contained herein. Overall system definition, operations and control, and telecommunication service system, including link budgets, are discussed in Sections 1, 2, and 3, respectively. A brief description of the user telecommunications equipment and ground station is presented. Section 4 includes a summary description of the TDR spacecraft and all the subsystems. The data presented are largely in tabular form for easy reference.

Section 5 contains a brief treatment of an optional configuration with enhanced telecommunications service.

17. Key Words (Selected by Author(s))	18. Distribution Statement
Atlas Centaur Launched TDRSS	

19. Security Classif. (of this report)	20. Security Classif. (of this page)	21. No. of Pages	22. Price*
Unclassified	Unclassified	246	$14.50

*For sale by the Clearinghouse for Federal Scientific and Technical Information, Springfield, Virginia 22151.

CONTENTS

ILLUSTRATIONS

TABLES

1. SYSTEM DEFINITION

1.1 INTRODUCTION

An Atlas Centaur launched TDRSS concept is described in this volume.

- Section 1, System Definition, identifies the system concept, the spacecraft configuration, and the telecommunications service.

- Section 2, Operations and Control, contains an orbit insertion profile, a brief description of the spacecraft on-orbit control, including a listing of auxiliary propulsion, and a description of the telecommunications service operation.

- Section 3, Telecommunications Service System, contains a summary of the telecommunications services and link budgets as well as general TDRS repeater characteristics. It also contains a brief description of the user transceiver and ground station design.

- Section 4, TDR Spacecraft Design, is comprised of three subsections:

  4.1 Design Concept discusses the spacecraft design objectives and the requirements and the implementation of the telecommunications service system.

  4.2 Configuration Summary contains a discussion of the TDR spacecraft design characteristics including an artist's concept of the spacecraft configuration drawing. This section also contains a compilation of the spacecraft parameters, electrical power budgets, mass summaries and a listing of the subsystem components.

  4.3 Subsystem Description contains descriptive material of the subsystem design and a summary of pertinent data, namely, subsystem block diagrams, requirement tables and mass summaries.

- Section 5, Atlas Centaur launched Option 1 discusses briefly a configuration option with enhanced telecommunications service, namely, the addition of more HDR channels, with the related changes in repeater, antennas, and electric power.

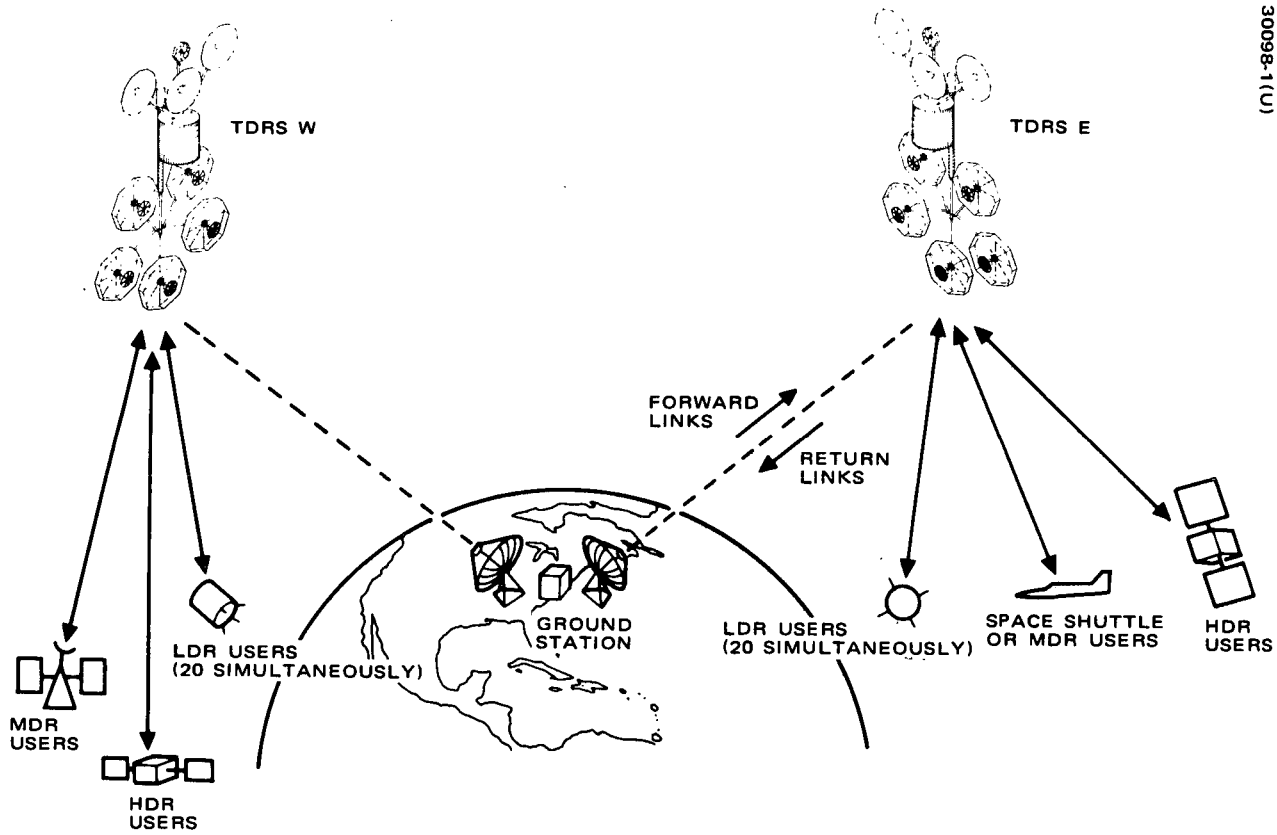

Figure 1. TDRS System Concept

1.2 SYSTEM CONCEPT

The TDRSS concept employs two geostationary satellites to provide relay links for telemetry, tracking, and command (TT&C) between multiple low earth-orbiting user satellites and a centrally located ground station, as shown in Figure 1, making possible nearly continuous reception of data in real time.

The TDRSS comprises the following major elements:

- GSFC network scheduling and data processing facilities
- TDRS ground station
- TDRS control center
- Two operational TDR satellites, one in orbit spare

The communication links from the ground station to the TDRS to the user are defined as forward links, and the links from the user spacecraft to the TDRS to the ground station are defined as return links. The forward links contain user command, tracking signals, and voice transmissions, whereas the return links contain the user telemetry, return tracking signals, and voice. The users are categorized as low data rate (LDR), medium data rate (MDR), and high data rate (HDR) according to their telemetry rates.

1.3 TDRS CONFIGURATION

The baseline configuration for the Atlas Centaur launched TDRS was derived from the successful Intelsat IV spacecraft design. These spacecraft are gyrostats which provide a fully stabilized platform for the communication payload while exploiting the simplicity and long life advantages associated with spinning satellites. The principal elements of the spacecraft are the spinning rotor, comprising 60 percent of the on station vehicle mass, and the despun earth oriented platform containing the communication repeater and its antennas. A rotating interface sustains the relative motion between the two bodies, permits signal transfers to take place, and affords an electrical path over which power from the solar panels and batteries can flow to the repeater payload. The spinning rotor provides a basic gyroscope stability to the spacecraft.

The use of the improved Atlas Centaur launch vehicle was postulated for the study. It is capable of placing 1780 kg spacecraft (including adapters) into transfer orbit for final spacecraft operation at synchronous altitude.

The Atlas Centaur configuration of the deployed TDR spacecraft shows the arrangement of antennas about the spacecraft spinning body. This arrangement of antennas was selected to provide control of solar torque and minimize propellant and number of attitude correction maneuvers. An artists concept of the configuration is shown in Figure 2.

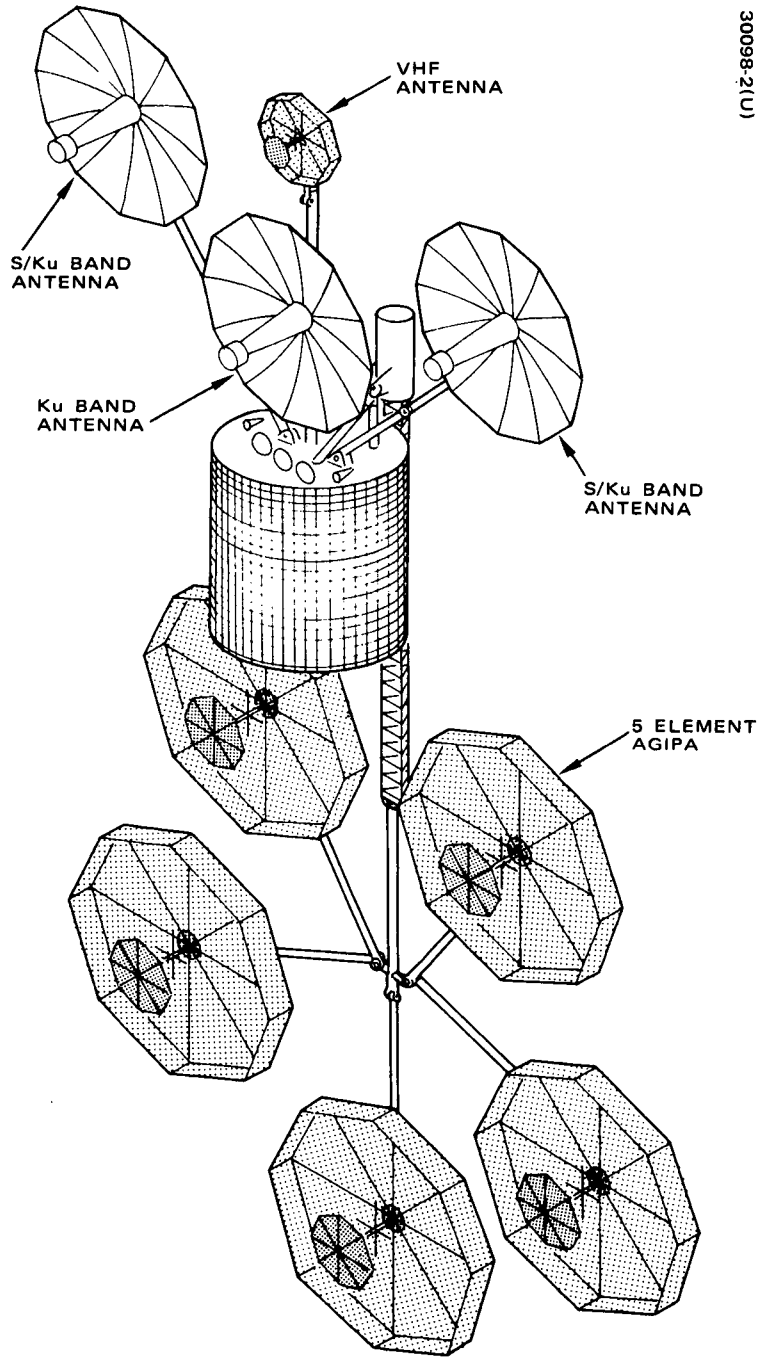

Figure 2. Atlas Centaur Launched TDR Satellite

The high gain MDR, HDR, and return link antennas are mounted forward. This position minimizes cable and waveguide runs to electronic equipment mounted in the spacecraft, and also provides for a more rigid and thermally stable mount for these narrowbeam antennas. A forward location of the UHF broadbeam antenna is also selected to minimize power loss in the transmission lines running from the transmitter to the antenna.

The LDR return link is implemented with a five element AGIPA configuration which is deployed aft. The antenna is deployed by a system combination of an Astromast and pivoted linkages. The Astromast is a low mass deployable truss structure which can achieve the long deployment required with a high stiffness and highly compact stowage.

A despun section houses the communication equipment and some of the tracking, telemetry, and command equipment. Electronic equipment are mounted on a thermally controlled platform. Antennas are mounted off the platform on a mast type support structure.

The spinning section supports and houses the propulsion, electrical power, attitude control, and some of the tracking, telemetry, and command equipment. The apogee motor is installed in the central thrust tube.

1.4 TELECOMMUNICATIONS SERVICE

The user service provided is summarized in Table 1.

TABLE 1. TDRSS USER SERVICE

LDR Service	Forward, UHF	Sequential to one user at a time.
	Return, VHF	Simultaneous from all users, AGIPA for added RFI Suppression.
MDR(1) Service Stand	Forward	Two Links(2): One link at an EIRP of 47 dBW 50 percent of the time One link at an EIRP of 41 dBW continuous
	Return	Two links, 1 Mbps maximum each
HDR(1) Service Ku Band	Forward	One link at an EIRP of 59 or 51 dBW continuous.
	Return	One link 100 Mbps maximum

(1) Separate transmitters and receivers are provided for MDR and HDR service, however, only two antennas (with dual feeds) are used for both types of services.

(2) Two continuous links at an EIRP of 41 dBW are also feasible.

2. OPERATIONS AND CONTROL

The TDRS operations and control involve three major functions:

1) TDRS launch and orbital deployment

2) TDRS on-orbit control

3) TDRSS telecommunication service operations.

Each of these topics will be discussed briefly in the following sections.

2.1 TDRS ORBIT INSERTION PROFILE

The improved Atlas Centaur launch vehicle is utilized for this study. The spacecraft design requirements are summarized in Table 2. The payload of 1780 kg includes spacecraft and adapters. Orbital operations require flexibility in assignment of spacecraft and a reasonable allowance is provided for station change maneuvers. The lifetime of 5 years is the minimum required orbital lifetime. In order to provide a more cost effective design, solar cell arrays and propellant budgets are sized for 7 years. If operations are benign, this spacecraft lifetime could easily extend to 10 years or more.

TABLE 2. SPACECRAFT DESIGN REQUIREMENTS ATLAS CENTAUR CONFIGURATIONS

Launch vehicle	Improved Atlas Centaur
Payload to transfer orbit	1780 kg maximum
Operational orbit	Synchronous
Initial inclination	3 degrees
Deployment	±65 degrees from ground station
Station change	2 to 4.3 degrees/day maneuvers
Stationkeeping	East-west only
Lifetime	5 years minimum

The Atlas Centaur launched TDRS mission profile consists of the following phases:

1) Atlas Centaur launch of the TDRS due east into a low altitude circular parking orbit.

2) Injection into a synchronous transfer orbit at the first node, the spacecraft is separated and spun up.

3) The transfer orbit phase for the spacecraft will be similar to typical synchronous communication satellite missions, e.g., Intelsat IV, and will not be discussed in this report.

4) The apogee injection is scheduled to minimize the time required to drift to station. The nominal plan is as follows:

   - Fire apogee motor of TDRS E at second apogee and drift 5 degrees (from 50° W to 105° W) to station in 2 ±1 days.

   - Fire apogee motor of TDRS spare at second apogee and drift 55 degrees (from 50° W to 105° W) to station in 50 ±20 days.

   - Fire apogee motor of TDRS W at third apogee and drift 42 degrees (from 210° W to 168° W) to station in 16 ±6 days.

4) Drift to station and station acquisition will be similar to Intelsat IV.

6) Antenna deployment is discussed in Section 4.3.3.

7) On-orbit operations are discussed in Sections 2.2 and 2.3.

A typical mission profile is shown in Figure 3.

2.2 TDRS ON-ORBIT CONTROL

There are two systems for TDRS telemetry and command: Ku band and S band. The Ku band system is prime with the S band system, which employs an omni antenna on the TDRS for backup.

TDRS tracking can be accomplished by using either the LDR forward link or the S band transponder. Using the former, a signal is continuously sent to each TDRS via the Ku band system. Each TDRS repeats the signal at UHF via the broad coverage antenna. A relatively low gain UHF antenna can be used to receive these signals at the ground station, where they are processed to provide range and range rate measurements for the TDRS.

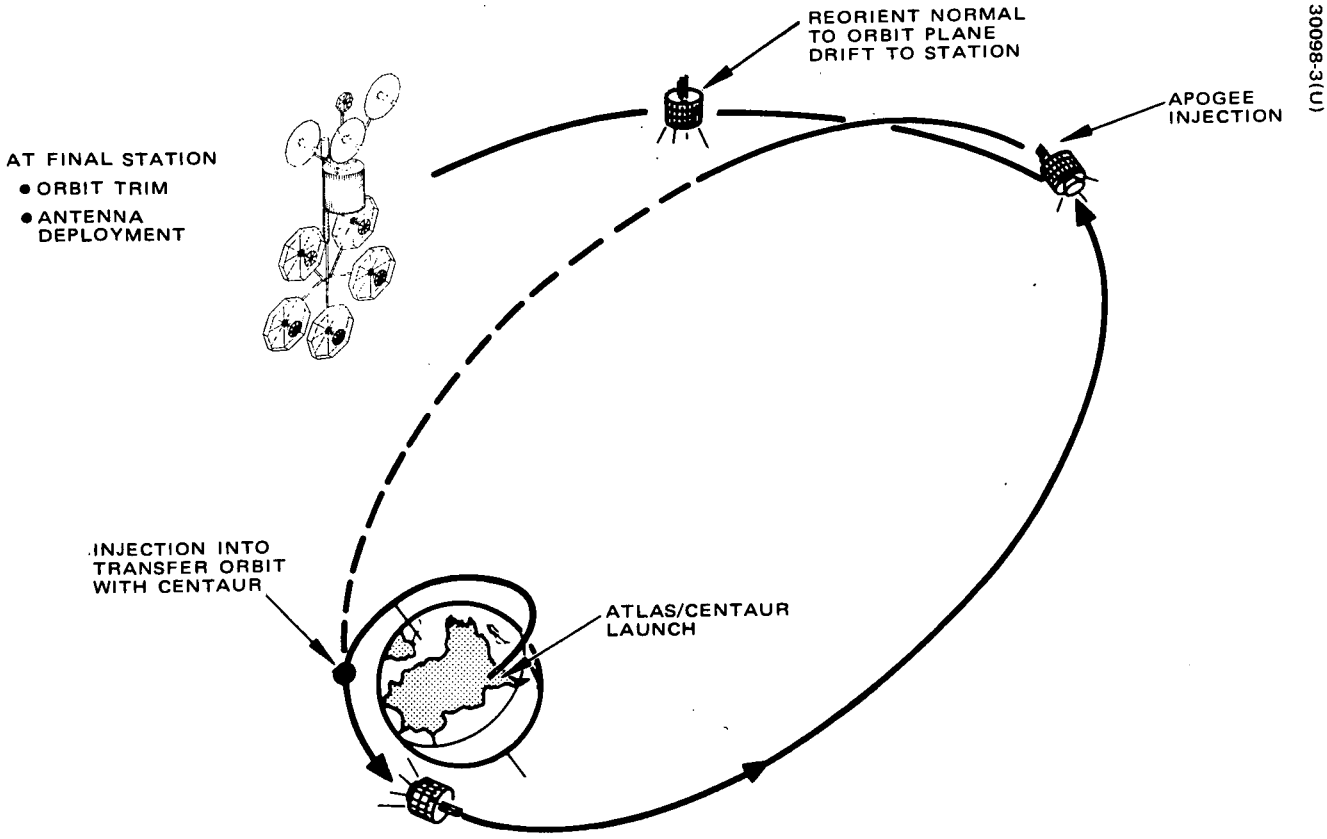

Figure 3. Orbit Insertion Profile

The S band transponder has an earth coverage antenna and is well suited to trilateration ranging using the Goddard Range and Range Rate System.

The on-orbit control operations for the TDRS are:

- East-west stationkeeping
- Attitude maneuvers
- S band and Ku band antenna pointing
- TDRS repeater channel settings for MDR users.

The frequency of east-west stationkeeping maneuvers is approximately one maneuver every 100 days and the frequency of the attitude maneuvers is one maneuver every 2 days. The satellite has sufficient angular momentum so that antenna pointing will not require any attitude correction maneuvers. The stationkeeping and attitude correction maneuvers do not require an interruption of the telecommunication service to the users. A summary of the requirements imposed on the auxiliary propulsion is shown in Table 3.

TABLE 3. AUXILIARY PROPULSION REQUIREMENTS

ΔV			146.6 m/sec
Cumulative impulse predictability for		< 10 pulses	20 percent
		> 10 pulses	10 percent
Burn time:	Steady state		None
	Pulse	Axial	70,000
		Radial	30,000
Cold starts:		Axial	1250
		Radial	30

The ground link antenna has autotrack capability and under normal conditions will require no ground control. The two dual feed antennas have tracking Ku band feeds but must be slewed to their acquisition position for each HDR user pass. The scan motion for link acquisition will be generated in the TDRS and will only need an activation command from the Control Center. When used for MDR service at S band, the dual feed antennas are pointed open-loop by commands from the TDRS Control Center. The 2.5 degrees beamwidth will require a pointing command to be sent no more often than once every 20 seconds. All antenna pointing, slewing, and acquisition commands will be based on spacecraft ephemerides and a master schedule for TDRSS services.

2.3 TDRS TELECOMMUNICATIONS SERVICE OPERATIONS

The TDRS system consists of five major elements: 1) GSFC communications control and processing facility, referred to as GSFC; 2) satellite control centers for users and TDR spacecraft; 3) ground station; 4) tracking and data relay satellites; and 5) user spacecraft. The overall functional relationship among these elements is shown in Figure 4. Note that GSFC has the responsibility for scheduling the TDRSS communications services and providing most data processing. The TDRSS link availability will be defined by Network Scheduling and Control similar to the present NASA ground station scheduling and will be forwarded to the users on a regular schedule. During the scheduled times, the user spacecraft command data are compiled at the GSFC Control Center into a forward link data stream which is sent to the TDRSS ground station for transmission to the user spacecraft.

The TDRS control center computes commands for the TDR satellites and forwards commands to the ground station for transmission to the satellites. These commands configure the repeater and point the steerable antennas, as well as produce housekeeping and subsystem control functions. Each user control center will issue commands to assigned spacecraft, limited only by the predetermined schedule.

The ground station is the interface between the TDRSS control center, GSFC, and the TDR satellites. All modulation/demodulation, multiplexing/demultiplexing, and RF transmitting/receiving is performed at this facility.

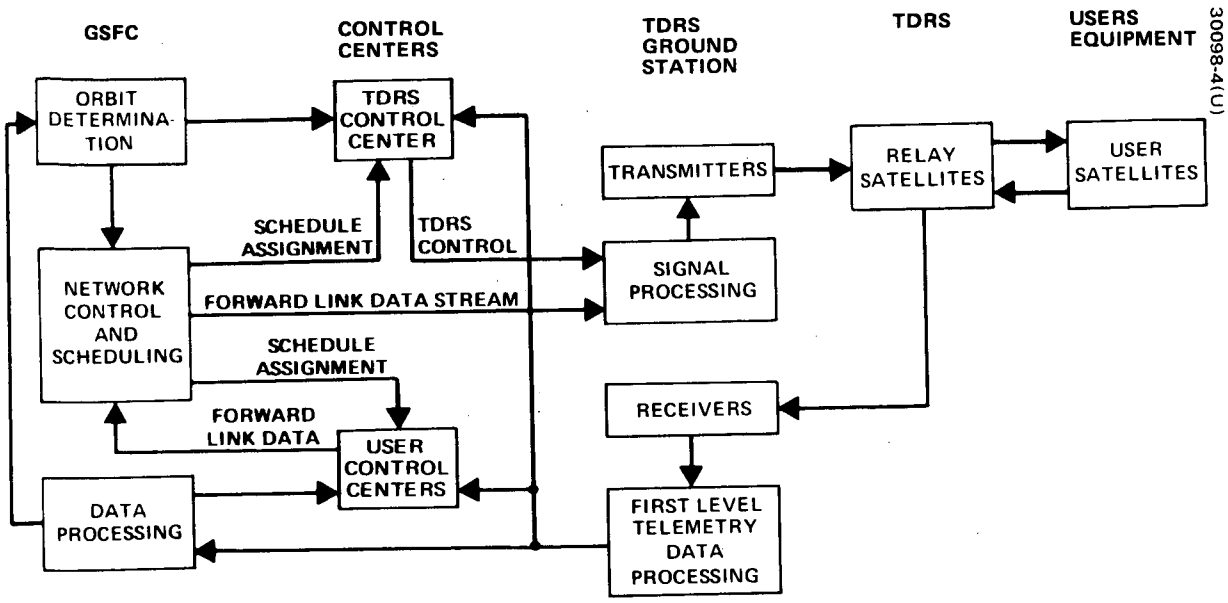

Figure 4. TDRSS Functional Operations

The return link data can be sent directly to the user program offices and/or to GSFC for further data processing. Orbit determination for both the TDRS and user satellites is performed at GSFC and made available to the user program offices and to the TDRSS control center which is responsible for TDRS control.

Figure 5 illustrates how the TDRSS augments the current ground network and employs much of the existing scheduling, switching, and data processing capability of GSFC. The control center operations have been briefly mentioned on the previous page. The major ground station functions include:

- Ground station antenna pointing
- Transmitting to and receiving from TDRSs
- Demultiplexing signals from GSFC into forward link channels plus additional status, scheduling, and control signals
- Spreading spectra of forward link signals as required
- Carrier modulation

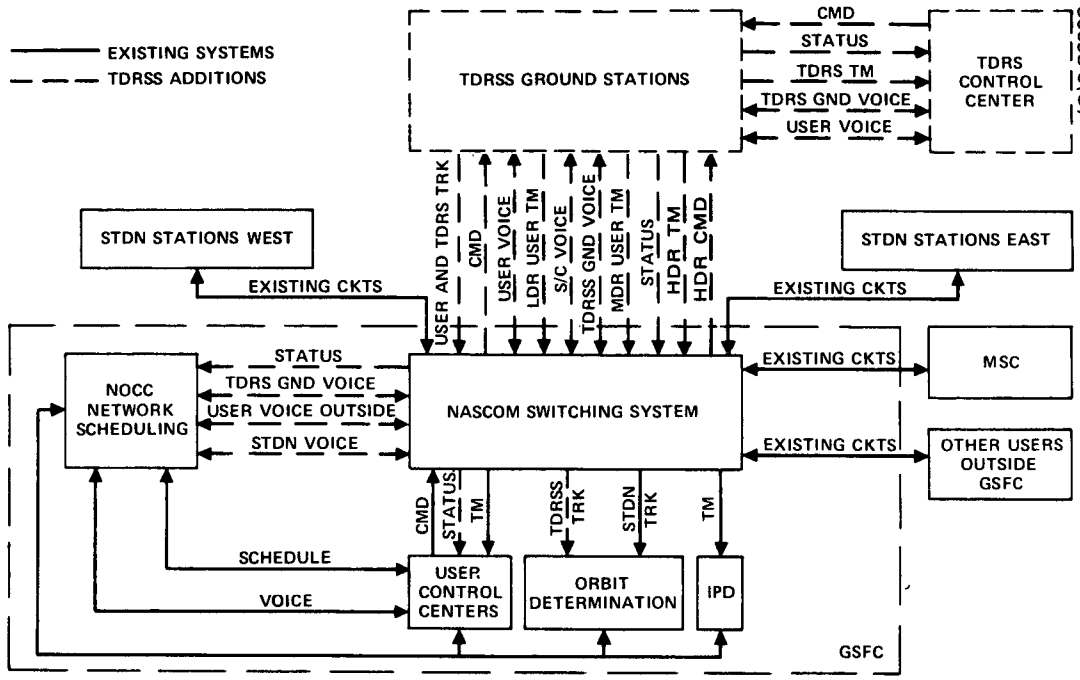

Figure 5. TDRS Ground Network

- Filtering and processing as required to separate received signals and to reduce RFI in LDR return channels
- Configuration of demodulation equipment according to schedule for all services
- Multiplexing of all return link signals, range, and range rate measurements, and status data for transmission to GSFC
- Internal forward links verification, comparing what was transmitted to the TDR satellites in each link to outputs of forward link demultiplexer

The LDR return link service is operationally the most difficult because there will be many telemetry signals simultaneously present in the ten channels from each TDRS. The choice of which TDRSs channels to connect a particular user's processing and demodulation equipment is made initially at GSFC and may be automated based on the GSFC handover schedule. MDR and HDR functions are conceptually the same as for the LDR, but only one signal per TDRS at any time will be received per channel, and acquisition and demodulation will be simpler.

3. TELECOMMUNICATIONS SERVICE SYSTEM

The telecommunication service system consists of the communication equipment in the TDRS, user spacecraft, and ground station. The services and their operational aspects have been briefly discussed above and are depicted in Figure 6. The frequency plan is shown in Figure 7. The telecommunication services provided via each TDRS are summarized below.

3.1 SERVICES AND LINK PARAMETERS

This section consists of two major subsections. Subsection 3.1.1 presents a very brief summary of the services provided by the TDRSS. Subsection 3.1.2 contains the major assumptions, characteristics, parameters and parametric relationships associated with each of the services. The order of presentation is LDR, MDR, HDR, Order Wire, and S band Transponder. Following these, the parameters of the TDRS/Ground Station link are listed. The link power budgets which are the basis for all link analysis and service capability are presented in Tables 4 and 5.

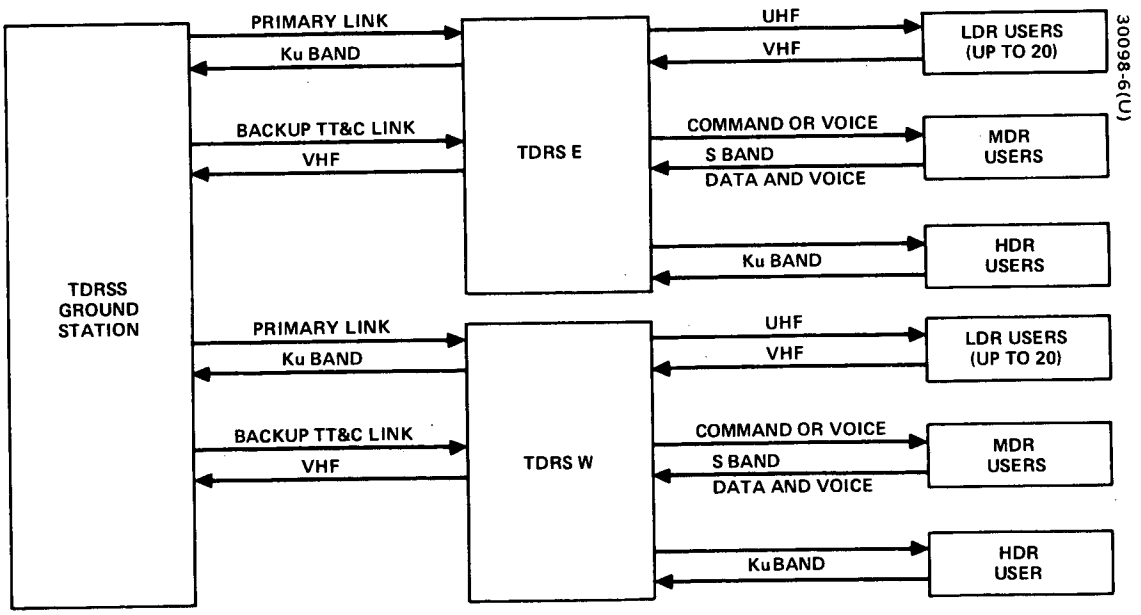

Figure 6. Telecommunications Service System

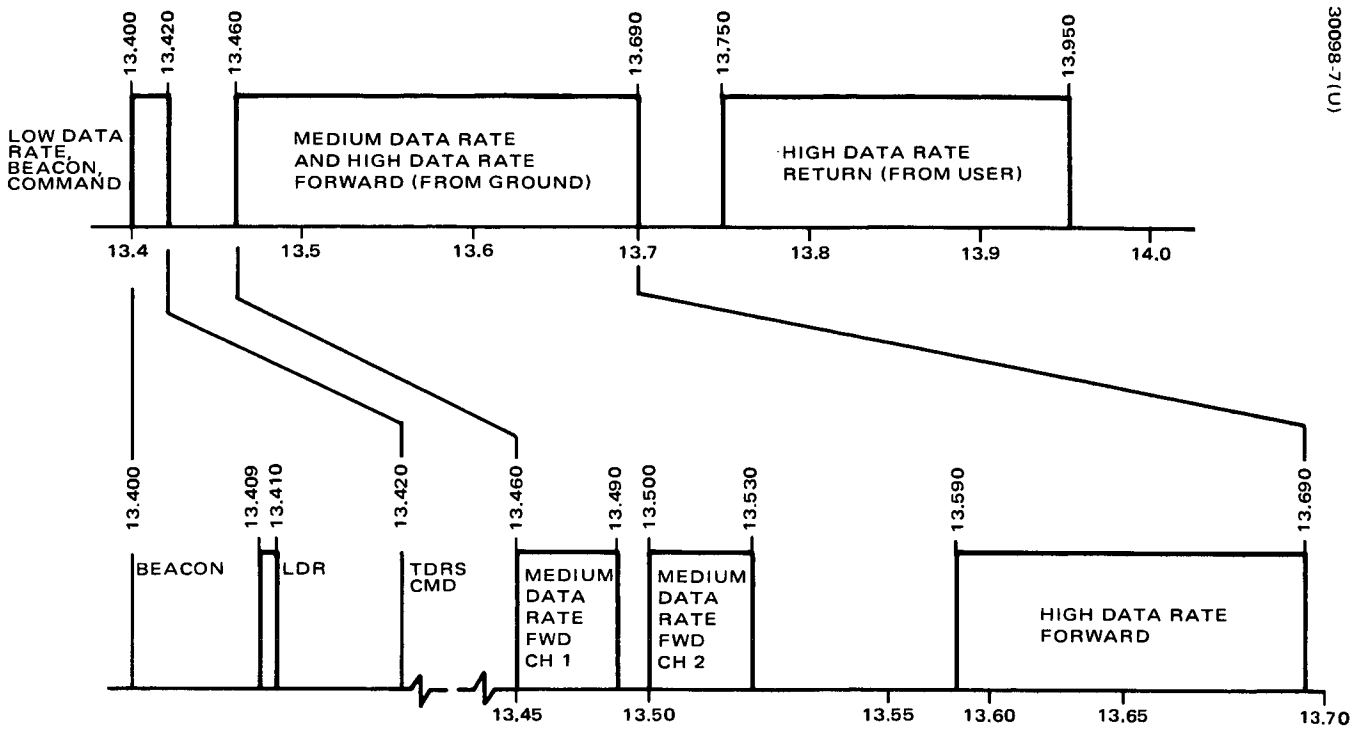

a) Ku BAND RECEIVE

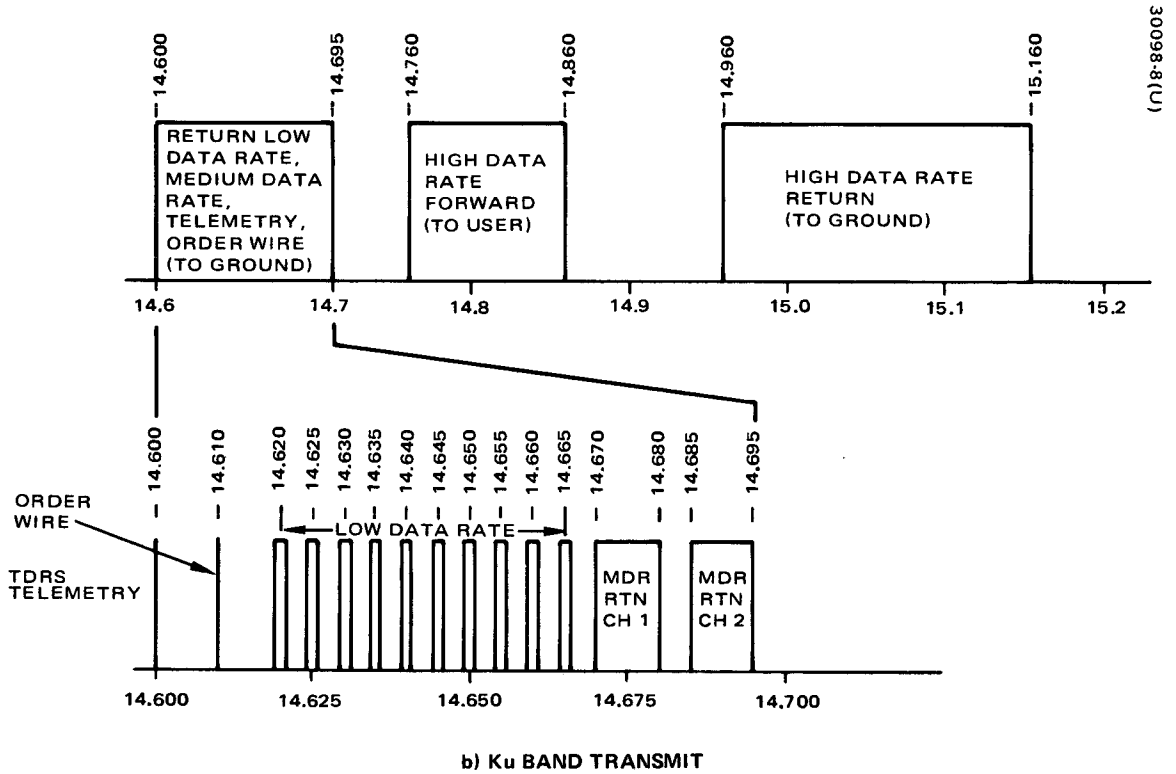

b) Ku BAND TRANSMIT

Figure 7. TDRS Frequency Plan

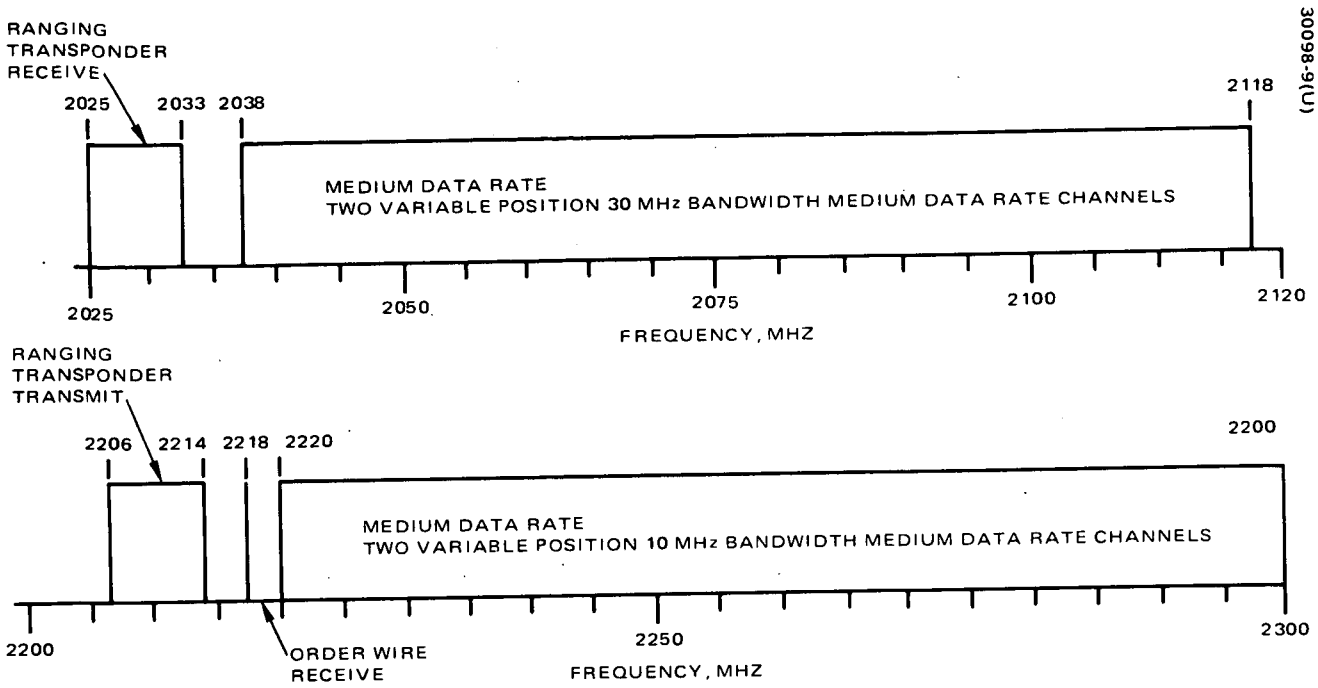

c) S BAND TRANSMIT AND RECEIVE

Figure 7 (Continued). TDRS Frequency Plan

TABLE 4. TDRS TRANSMIT LINK BUDGETS

Parameter	LDR Command UHF	MDR Forward S Band		Ground Ku Band	HDR Forward Ku Band
		High Power	Low Power		
TDRS EIRP	30.0*	47.0	41.0	EIRP	59
TDRS pointing loss	–	-0.5	-0.5	-0.5	-0.5
Space loss	-177.5	-192.0	-192.0	-208.4	-208.9
Receive antenna gain	-3.0	G_u	G_u	63.0	G_u
Receive pointing loss	–	-0.5	-0.5	-0.5	-0.5
Receive line loss (L)	-0.5	-2.0	-2.0	-0.3	-2.0
Receive ellipticity loss	-3.0	-1.0	-1.0	-0.2	-0.2
Receive power, P_r	-154.0	G_u-149	G_u-155	EIRP-146.9	G_u-153.1
Receive noise figure, dB*	3.75	5.1		3.8	7.0
Receiver noise temperature, K	300.0	650.0		400.0	1160.0
Background noise temperature, K**	50.0	50.0		5.0	5.0
(1-L(290K – Line loss noise temperature	31.0	100.0		20.0	100.0
Total system noise temperature at receiver input, K	481.0	800.0		420.0	1280.0
Noise density, η_T dBW/Hz	-201.8	-199.6		-202.3	-197.5
Pr/η_T dB-Hz	47.8	G_u +50.6	G_u +44.6	EIRP +55.4	G_u +44.4

*For 26-degree conical coverage, 29.3 dBW for 30 degree coverage.

**Adjusted for line loss.

TABLE 5. TDRS RECEIVE LINK BUDGETS

Parameter	Return LDR VHF (Minimum)	Return MDR S Band	Order Wire S Band	Forward LDR From Ground Ku Band	Forward HDR, MDR From Ground Ku Band	Return HDR Ku Band
Transmit power	7.0		20.0	P	P	
Transmit antenna gain	-3.0	EIRP	0	62.0	62.0	EIRP
Transmit line loss	–		–	-2.5	-2.5	
Transmit pointing loss	–		–	-0.5	-0.5	-0.5
Space loss	-167.5	-192.7	-192.7	-207.5	-207.5	-208.3
TDRS antenna gain	18.8*	36.2	13.2	18.5	51.5	51.9
TDRS pointing loss	–	-0.5	–	-2.0	-0.5	-0.5
TDRS line loss, L	-1.0	-0.8	-1.0	-1.0	-2.0	-2.0
TDRS ellipticity loss	-0.5	-0.2	-0.2	0	-0.2	-0.2
Receiver power, P_r	-146.2	EIRP-157.5	-160.7	P-133	P-99.7	EIRP-159.8
Noise figure, dB	3.9	1.3	3.9	9.0	10.0	4.0
Receiver noise temperature, K	940.0***	100.0	420.0	1170.0	2600.0	440.0
Earth noise temperature, K**	150.0	240.0	240.0	240.0	195.0	195.0
(1-L) 290K – Line loss noise temperature, K	60.0	58.0	60.0	60.0	105.0	105.0
Total system noise temperature, K	1250.0	398.0	720.0	1470.0	2900.0	740.0
Noise density, η_T, dBW/Hz	-197.6	-202.6	-200.0	-196.9	-194.0	-199.9
P_r/η_T dB-Hz	51.4	EIRP+44.6	39.3	P+63.9	P+94.3	EIRP+40.1

* For 30 degree conical coverage.
** Adjusted for line loss.
*** Rms sum of five receivers.

3.1.1 Services

3.1.1.1 Low Data Rate at UHF/VHF

Command of, tracking of, and telemetry from up to 20 users; command is sequential, tracking and telemetry are simultaneous for all users.

3.1.1.2 Medium Data Rate at S Band

Two simultaneous two-way links, each with the following capability:

Forward links: Two 24 kbps delta modulated voice signals plus 2 kbps to the Space Shuttle (this service is restricted to 50 percent usage and corresponds to a high power transmitter mode) or up to 2 kbps data continuously to a user spacecraft with a 0 dB gain antenna.

Return links: Up to 1 Mbps data from a user spacecraft.

3.1.1.3 High Data Rate at Ku Band

One two-way link.

Forward Link: Up to 50 Mbps

Return Link: Up to 100 Mbps

3.1.1.4 Order Wire at S Band

An S band antenna has been provided for an order wire service. This is a broad coverage antenna; thus a request can be made by a manned spacecraft with an omni antenna for MDR service, even if the TDRS narrowbeam S band antenna is not pointed at this user. The order wire service channel bandwidth is 1 MHz.

3.1.1.5 S Band Transponder

A turnaround S band transponder has been provided to allow accurate TDRS range measurements. The bandwidth is 8 MHz centered at 2029 for receive and 2210 for transmit. The transmitted EIRP is 20 dBW. This transponder will allow the use of trilateration techniques and is compatible with the Goddard Range and Range Rate System. This transponder is also used for backup TT&C when used in conjunction with an omnidirectional antenna.

3.1.2 Link Parameters

The features, characteristics, and parameters associated with each link of each service are presented below.

3.1.2.1 Low Data Rate Service

Forward Link

The forward link, user command channel will be time shared; that is, only one user can be commanded at a time. However, commands may be sent to many users within a period of 1 minute. All users will receive the TDRS transmitter RF signal, thus each command will have a prefix that will activate the command decoder of the intended user.

Other operational features include:

- Automatic user acquisition — User available for command shortly after becoming visible.
- Time shared link — Requires synchronized sequencing of user commands.
- Fixed timing — User receivers can be standardized.

- Variable format — Number of bits and their significance in a user command can be different for every user if desired, i.e., command format flexibility.
- Baseline bit rate — 300 bps
- Probability of bit error — $P_e \leq 10^{-5}$
- PN code length — 2048
- One code per bit
- Chip rate — 614.4 kilochips per second
- Carrier frequency — 401.0 MHz
- Biphase PSK IF carrier modulation
- EIRP — See Table 6

Analysis of the low data rate links and a study of ground emitters have revealed that RFI is most likely the limiting factor in these links. Figure 8 shows how the bit rate is limited by RFI. The parameter chosen to quantify RFI is the average spectral density of the RFI power at the receiver input.

TABLE 6. LDR FORWARD LINK EIRP

	26 Degree Field of View	30 Degree Field of View
Antenna gain, dB	12.5	11.8
Radiated Power, dBW	17.5	17.5
EIRP, dBW	30.0	29.3

Return Link

Up to 20 users may simultaneously return telemetry. Code Division Multiplexing (CDM) will be used to allow simultaneous telemetry return. The PN codes for CDM will be different for each user spacecraft's telemetry.

Convolutional encoding will be employed on user telemetry for bit error correction; link quality is improved significantly with this technique.

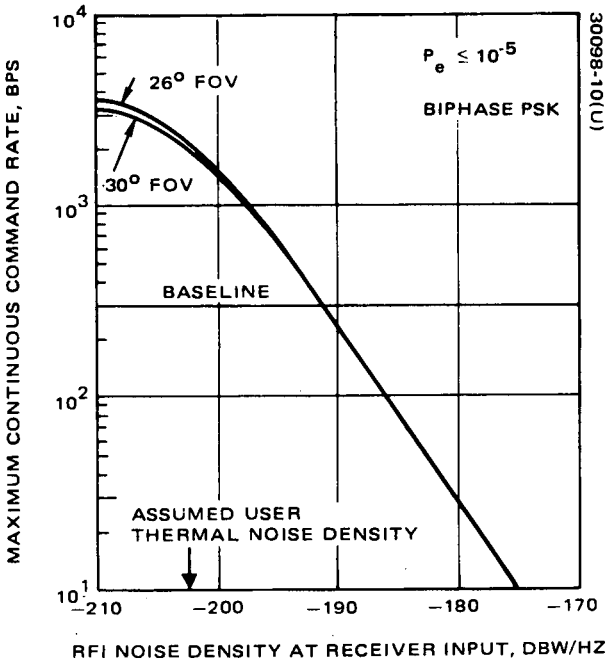

Figure 8. Low Data Rate Forward Link

The baseline approach assumes that the return bit is standardized for all users but this is not a system requirement. With this standardization, the baseline parameters and techniques are as follows:

- Bit rate: 1200 bps
- Probability of error $P_e \leq 10^{-5}$
- Adaptive processing of the ten array antenna signals
- Rate one-half convolutional encoding
- One gold code per convolutional code symbol
- Gold code length: 512
- Chip rate: 1.2288 megachips/sec
- Carrier frequency: 136.5 MHz
- Biphase PSK carrier modulation

- Estimated degradation due to ground link and processing (same as for the Part I TDRS) — 3.0 dB
- Required $E_b/$ at decoder for $P_e = 10^{-5}$ — 4.1 dB-Hz
- User EIRP — 4 dBW
- TDRS G/T per element (considering receiver generated noise only) is shown in Table 7 below

The LDR return link bit rate per user is shown in Figure 9 as a function of the RFI power density at the TDRS receiver inputs. A performance range exists because the signal-to-interference ratio depends on the location of the user spacecraft with respect to the RFI pattern as seen by a TDRS. If the figure is correct, the baseline bit rate of 1200 bps from 20 users simultaneously is possible with an RFI noise density up to 180 dBW/Hz.

Figure 9 was the result of AGIPA analysis using a digital computer to simulate the RFI distribution and compute the signal-to-noise ratio after ground processing as a function of total RFI level and user position. The analysis is discussed in Volume 2 of this report.

TABLE 7. LDR RETURN LINK G/T

	26 Degree Field of View	30 Degree Field of View
VHF antenna element gain, dB	12.7	12.0
Receiver noise figure, dB	3.9	3.9
Receiver noise temperature, K	420.0	420.0
Equipment G/T (at receiver), dB/K	-13.5	-14.2

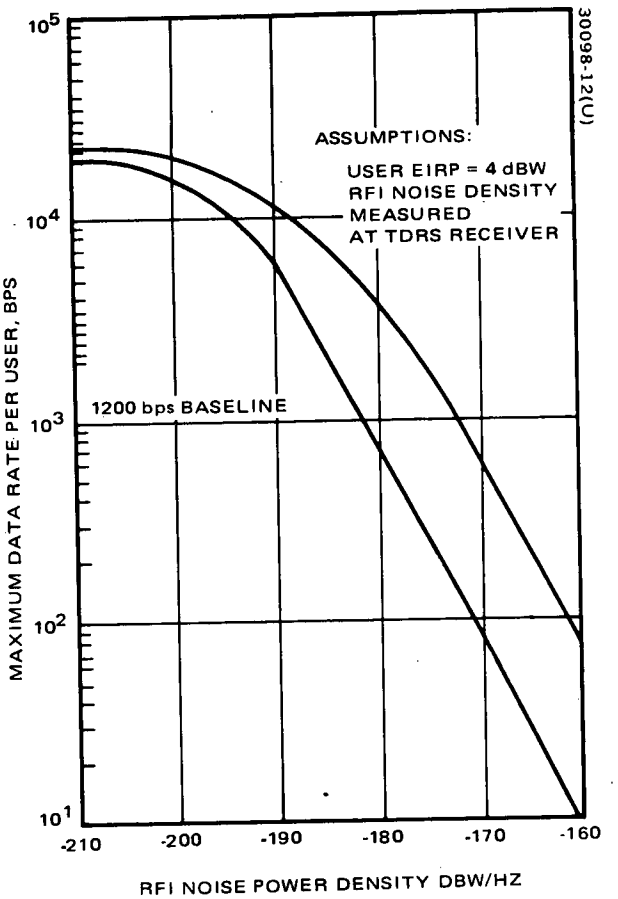

Figure 9. LDR Return Link Capability

Tracking

Due to the PN code signaling, user spacecraft receivers automatically acquire and synchronize to the signal transmitted from a TDRS. After the brief acquisition period, range and range rate measurements can be made. However, the user's transmitter must be turned on, and the return signal acquired at the ground station. A particular operational advantage of the signaling concepts used here is that both range and range measurements can be made simultaneous with telemetry reception and no forward link commands are required.

Range measurement uncertainty is affected by system noise, of which RFI appears to be the most severe. Figure 10 shows the RMS uncertainty as a function of RFI noise density for both forward and return levels. The total RMS uncertainty is the sum of the two link contributions.

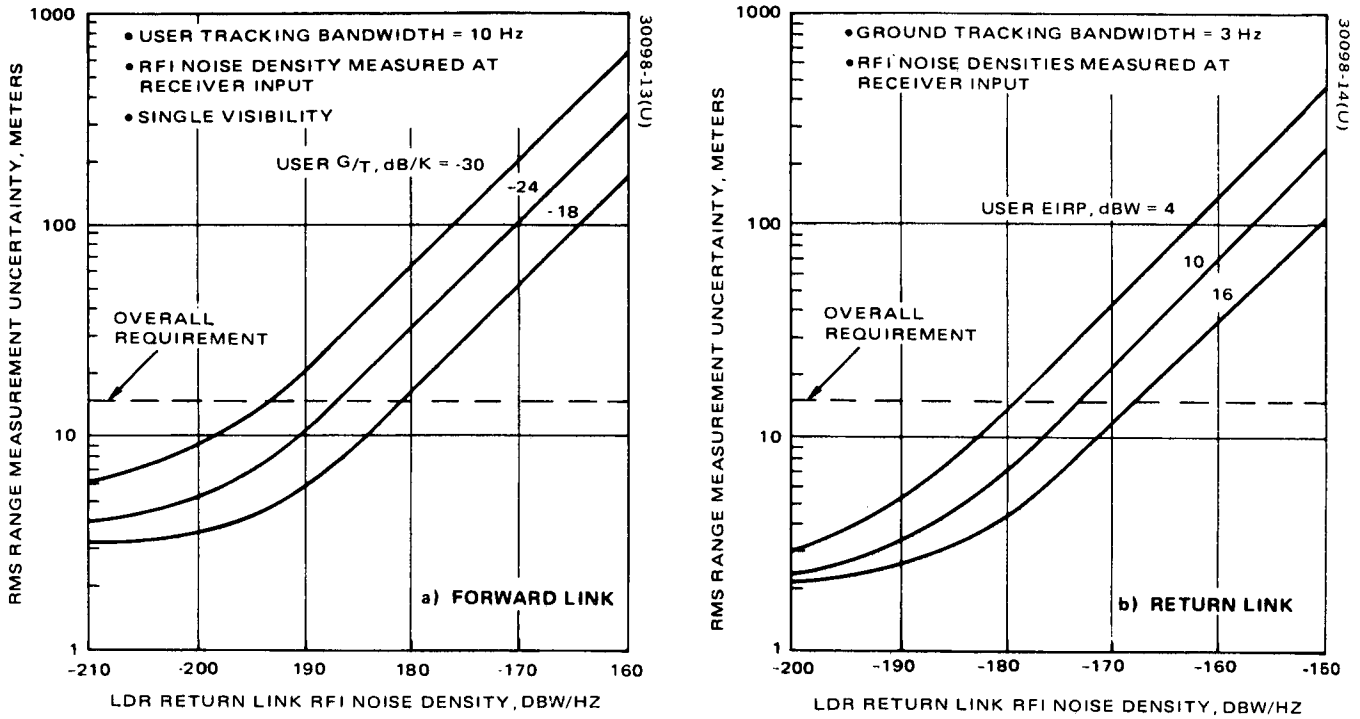

Figure 10. RMS Range Measurement Uncertainty

3.1.2.2 Medium Data Rate Service

Two independent two way channels are provided via the two dual feed antennas. The power subsystem and ground link transmitter have been designed to support these two links simultaneously with the required margin. Each two way link has the following characteristics:

Forward Links

- Channel bandwidth — 30 MHz
- Channel center frequency placeable by ground command anywhere from 2038 to 2118 MHz with 1 MHz discrete steps.
- High power mode

Antenna gain	36 dB
Radiated power	11 dBW
EIRP	47 dBW

- Low power mode

Antenna gain	36 dB
Radiated power	5 dBW
EIRP	41 dBW

Figure 11 shows the maximum possible data rate which may be sent to an unmanned user assuming no error correction encoding, a receiver system noise temperature of 800 K, and 3 dB receive losses.

The link capacity for transmitting to the Space Shuttle is shown in Figure 12. The major assumptions of the link analysis accompany the figure. Note that the requirement for 54 Kbps which includes two digital voice signals plus 2 Kbps data can be accommodated with the high power mode.

Return Links

- Channel bandwidth 10 MHz
- Channel center placeable by ground command anywhere from 2220 to 2300 MHz with 1 MHz discrete steps.
- G/T = 10.2 dB/K at receiver input considering all noise sources.

The bandwidth of the return channels is smaller than that of the forward channels because the energy is radiated away from the earth most of the time. Consequently, the spectrum spreading required to reduce the earth-incident flux density to acceptable levels is less.

Figure 13 shows the relationship between the return data rate, radiated power, and antenna gain for an unmanned user. No link margin and no error correcting encoding has been assumed. Figure 14 shows the relationship between data rate, transmitter power and antenna for the Space Shuttle. A number of assumptions have been made for this link as listed with the figure. The use of coding and the 10^{-4} bit error rate (BER) allow a bit energy to noise density of 5.2 dB, whereas 10 dB was used in Figure 13. The assumed line loss plus margin tends to cancel the increase in link capacity due to coding relative to Figure 13. However, note that the requirement of 192 Kbps can be achieved with a 40 watt transmitter and 3 dB gain antenna on the Shuttle.

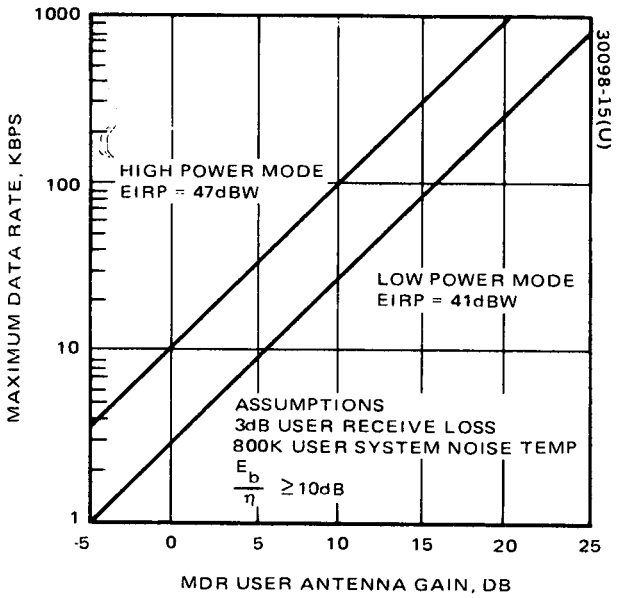

Figure 11. MDR Forward Link Capability for Unmanned User

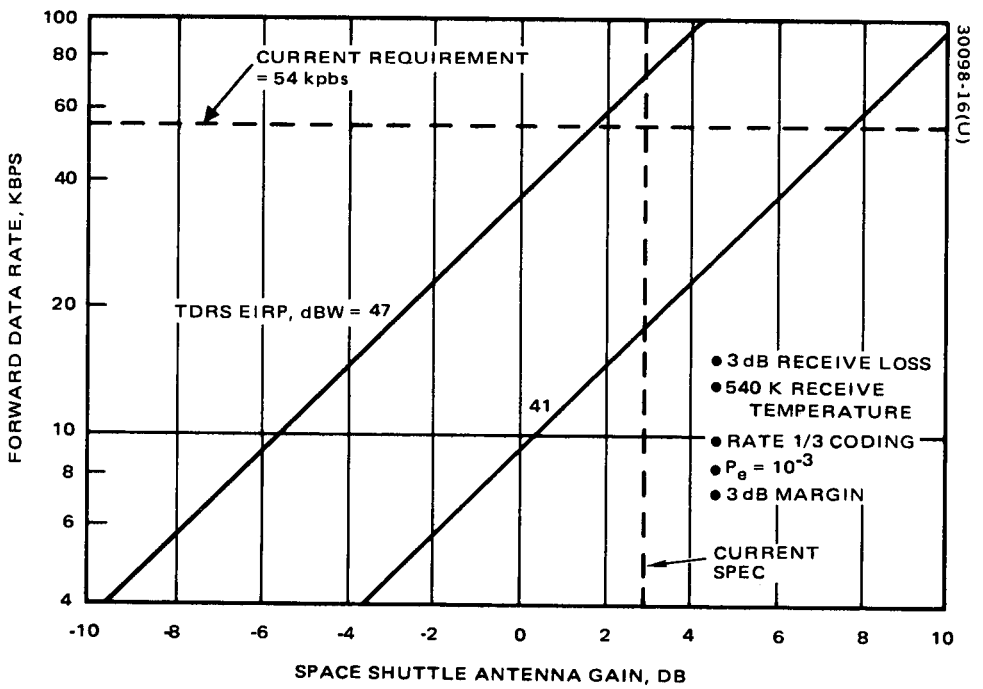

Figure 12. Space Shuttle Service Via TDRS Forward Command Plus Voice

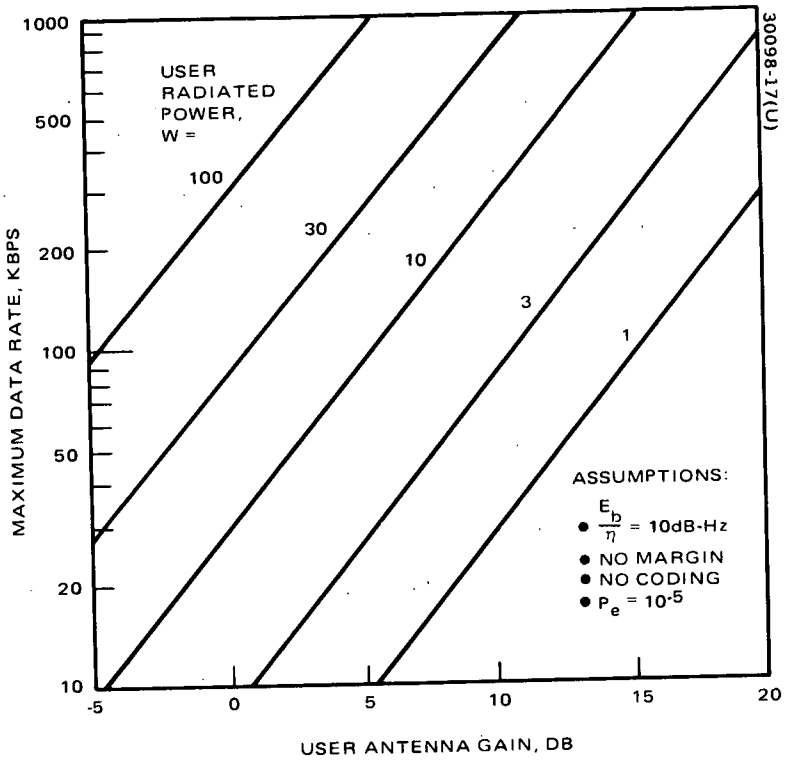

Figure 13. MDR Return Link Capability for Unmanned User

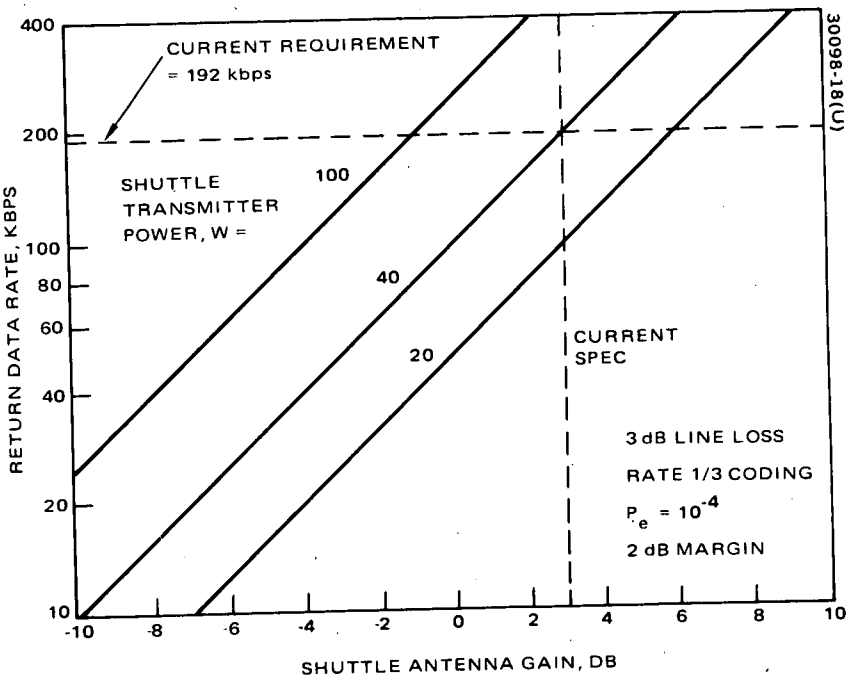

Figure 14. Space Shuttle Service Via TDRS, Return Telemetry Plus Voice

3.1.2.3 High Data Rate Service

Either of the two dual feed antennas may be used for this service, but must also be shared with the MDR service. The TDRS/user link employs Ku band frequencies. If a user spacecraft has the capability, the dual feed and independence of the MDR and HDR repeater channels will allow a two way link simultaneously at both S band and Ku band.

Forward Link

- TDRS to user frequency band — 14.760 to 14.860 GHz (100 MHz)
- EIRP is given in Table 8.

TABLE 8. HDR FORWARD LINK EIRP

	High Power Mode	Low Power Mode
Antenna gain, dB	52.8	52.8
Radiated power, dBW	6.2	-1.8
EIRP, dBW	59.0	51.0

Figure 15 shows the required user antenna diameter as a function of bit rate for the two power modes assuming a tunnel diode user receiver (7 dB noise figure).

Return Link

Variable bandwidth	200, 100, 50, 10 MHz
Center frequency of the TDRS/user link	13.850
G/T	23.2 dB/K
G	51.9
T	740 K including all noise sources

Figure 16 shows the relationship between the required user antenna size, radiated power and return data rate. Figure 17 shows the relationship between the required user antenna diamter and radiated power for a data rate of 100 Mbps with and without the use of error correcting encoding.

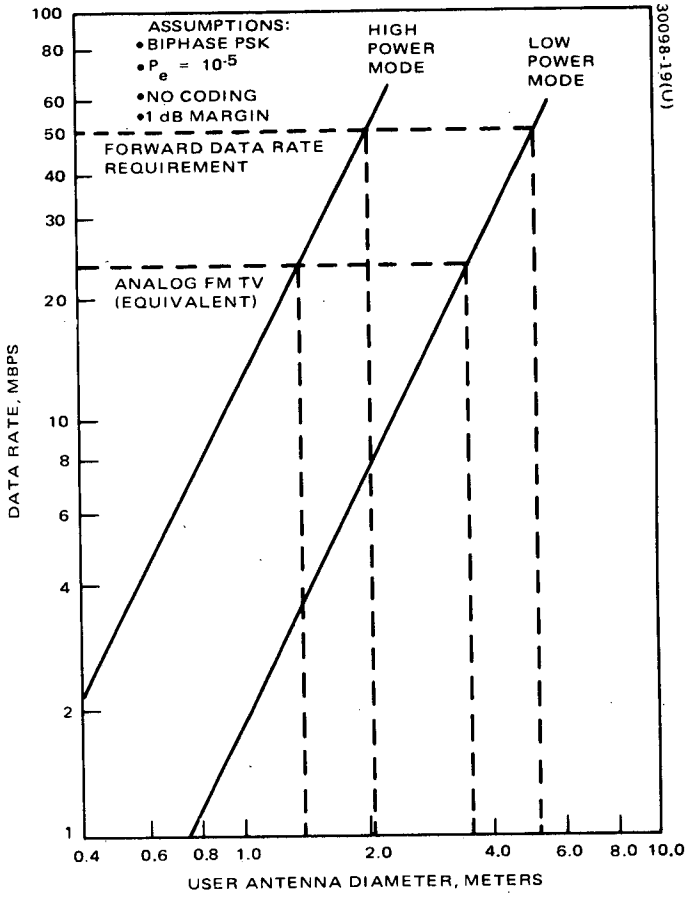

Figure 15. TDRS to HDR User (Forward Link)

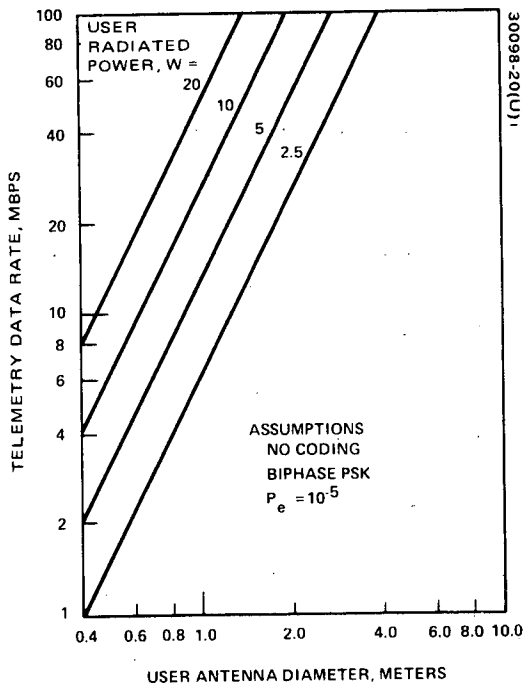

Figure 16. HDR Return Link

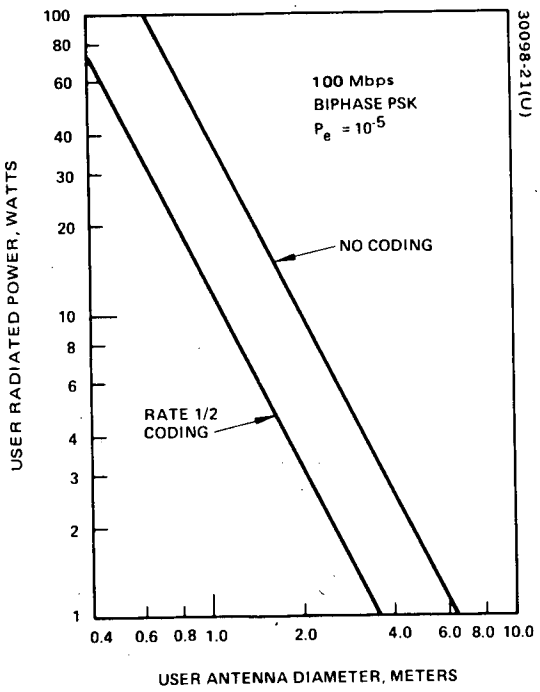

Figure 17. HDR User Requirements for 100 Mbps Telemetry

3.1.2.4 Order Wire Service

Center frequency	2218 MHz
Bandwidth	1 MHz
G/T	-15.2 dB/K at receiver over 19.5 degree earth centered cone considering all noise sources.

3.1.2.5 S Band Transponder

Frequency band	
Receive	2025 to 2033 MHz
Transmit	2206 to 2214 MHz
EIRP	
Antenna gain	13.5 dB
Radiated power	6.5 dBW
EIRP	20.0 dBW

3.1.2.6 Ground Links

A weather margin of 17.5 dB has been provided for all channels in both the forward and return links between the TDRS and Ground Station.

Forward Link

A northern hemisphere coverage horn is used to receive the LDR, beacon, and TDRS command channels from the Ground Station. A 3.82 meter reflector antenna is used to receive the two MDR and the HDR channels.

High gain antenna (HGA) G/T	17.3 dB/K
G	51.9 dB
T	2900 K including all noise sources
Low gain antenna (LGA) G/T	-13.2 dB/K
G	18.5 dB
T	1470 K including all noise sources
The minimum carrier to noise power at the TDRS receiver in each channel	15 dB

Frequency bands: 13.400 to 13.420 GHz for LGA receiver

13.460 to 13.700 GHz for HGA receiver.

Return Link

There are two power amplifiers, the outputs of which are multiplexed and transmitted to the Ground Station via the 3.82 meter Ku band antenna. One of the power amplifiers contains the HDR signal and operates in a saturated mode. The other power amplifier provides linear amplification required by the multiple signals and by the LDR adaptive processing. Bit energy-to-noise density for each signal is given in Table 9.

TABLE 9. HDR RETURN LINK BIT ENERGY-TO-NOISE DENSITY

Return Service	Minimum Ground Link E_b/η, dB	Maximum Data Rate Per User, Kbps	Minimum Weather Margin, dB
Low rate telemetry	14	1.2	17.5
LDR voice	14	20.0	17.5
Medium rate data	20	1,000.0	17.5
High data rate	15	100,000.0	17.5
TDRS telemetry	15	1.0	20.0
Order wire	15	1.0	20.0

3.2 HDR ANALYSIS

Analysis of the major aspects of the LDR and MDR services is presented in Volume 4 of the Part 1 Final Report of the TDRSS Configuration and Tradeoff Study. This subsection treats, in order, three aspects of the HDR System: 1) TDRS/user frequency selection, 2) Link analysis and TDRS EIRP selection, and 3) Link acquisition.

3.2.1 Space Link (TDRS/User) Frequency Selection

The first choice to be made in the HDR system design was the frequency band for the TDRS/user link. A 600 MHz transmit band (14.6 to 15.2 GHz) and a 600 MHz receive band (13.4 to 14.0 GHz) have been allocated for TDRS use at Ku band. These bands must be used for the TDRS/ground station link as well as any TDRS/user links. At X band, two 200 MHz bands have been allocated for transmitting to and receiving from users; 8.3 to 8.5 GHz and 7.7 to 7.9 GHz, respectively. In preliminary design, approximately 300 MHz of the TDRS receive band was required for the forward ground link including LDR, MDR, and HDR (with 50 Mbps capability), leaving 300 MHz for the HDR return user-to-TDRS link. The effects of these bandwidth limitations on link capacity are shown in Table 10.

TABLE 10. HDR FREQUENCY SELECTION

Frequency Band	PSK Modulation	Error Correcting Coding*	Return Data Rate						
			50	75	100	150	200	250	300
Ku	Biphase	Coding	X	X					
		No coding	X	X	X	X			
	Quadphase	Coding	X	X	X	X			
		No coding	X	X	X	X	X	X	X
X	Biphase	Coding	X						
		No coding	X	X	X				
	Quadphase	Coding	X	X	X				
		No coding	X	X	X	X	X		

*Rate 1/2 convolutional encoding.

Biphase and quadriphase PSK modulation and the effect of rate one-half convolutional encoding for bit error correction were considered. Quadriphase PSK will allow the same bit rate in one-half the bandwidth of biphase PSK. The use of rate one-half encoding doubles the rate in the transmission channel. Thus, biphase phase-shift-keying without coding and quadriphase phase-shift-keying with rate one-half coding requires the same bandwidth. Note that in Table 10 for the baseline data rate of 100 Mbps, the allocated bands at both frequencies allow the same signaling combinations. That is, 200 MHz is all the bandwidth required for data rates up to 100 Mbps. However, note that the greater bandwidth of the Ku band allocation offers more options at 150 Mbps and is necessary if rates above 200 Mbps are required.

The user requirements for HDR communications provide a more compelling reason for choosing Ku band in preference to X band. Figure 18 shows the combination of user radiated power and parabolic reflector antenna diameter required to return 100 Mbps via the TDRS which has a 3.82 meter antenna and a parametric amplifier receiver. The radiated power is the power amplifier output reduced by line losses. The Ku band link should have an advantage proportional to the square of the ratio of the Ku band and X band frequencies, that is, $(13.8/7.8)^2 = 3.13$ (5.0 dB). However, the poorer expected performance of receivers at Ku band reduces this advantage by about 0.5 dB. Thus, Ku band offers an advantage factor of 2.8 (4.5 dB) over X band for user power or antenna aperture area, i.e., a factor of approximately 1.67 in antenna diameter. Thus, for instance, if the user has a 15 watt power amplifier and 2 dB of line loss, the radiated power will be approximately 9.3 watts and referring to the figure, a 2.2 meter (7.2 feet) antenna will be required at Ku band, while a 3.6 meter (12 feet) antenna will be required at X band.

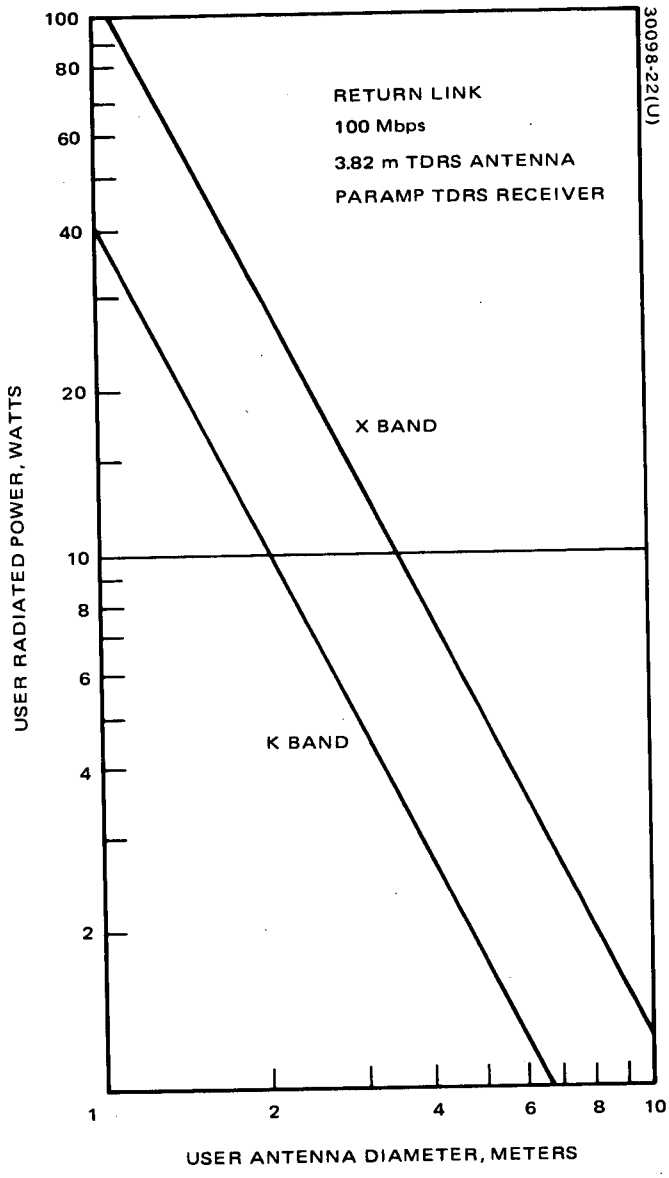

Figure 18. HDR User Impact

A more accurate comparison of user requirements must consider transmitter efficiency, receiver, power supply requirements, heat exchanger, antenna, and positioner. This comparison was made using a computer program which uses state-of-the-art technology data to determine the major variable parameters of the above listed subsystems such that the total mass is minimized. The results of such computations are shown in Figure 19, indicating a significant difference between both the mass and power for the two frequencies. At data rates above 80 Mbps, the estimated difference in mass between X and Ku band user terminals is approximately 9 kg (20 pounds).

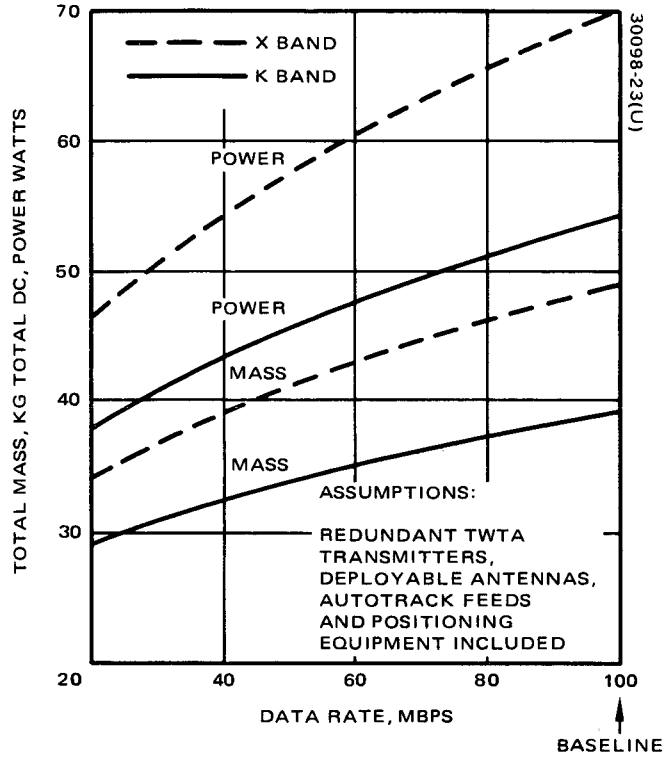

Figure 19. User Terminal Characteristics

For the baseline data rate of 100 Mbps, Table 11 shows the parameters selected by the optimization program. If user constraints require a different combination of user power and antenna gain, the total mass is expected to be somewhat greater.

The trade study described above assumed technology expected in the near term at both frequencies. Hardware at X band is currently available because of the many military communications satellites that have operated in that band. In the late 1970's, Ku band technology is also expected to be readily available because of the new civilian and military satellite systems.

In conclusion, it is the smaller user impact that makes Ku band preferable to X band.

3.2.2 HDR Link Analysis and EIRP Selection

Having chosen Ku band for the HDR TDRS/user communications link, the next objective was to select the TDRS EIRP for both the forward link to the user spacecraft and the return link to the Ground Station. The link requirements are:

TABLE 11. MASS OPTIMUM HDR USER COMMUNICATIONS TERMINAL (100 MBPS DATA)

	X Band	Ku Band
Communications characteristics		
Transmitter power, dBw	12.1 (16.3W)	8.2 (6.6W)
Output losses, dB	-2.0	-2.0
Antenna gain, dB	45.4 (3.52M)	49.8 (3.09M)
EIRP, dBw	55.5	56.0
Mass Summary (kg)		
Antenna and feeds	12.0	8.9
ACQ and track equipment	5.0	5.0
Transmitters (2)	6.2	5.5
Prime power supply	22.8	17.8
Heat exchanger	3.2	2.2
Total mass	49.2	39.4
Power summary, watts		
Transmitter input	48.5	32.6
ACQ and track	22.0	22.0
Total dc power	70.5	54.6

1) 100 Mbps data at a bit error rate of 10^{-5} in the return link

2) 50 Mbps data at a bit error rate of 10^{-5} in the forward link

Two other design objectives included:

1) Keep earth incident flux density less than -152 dBW/m^2 in any 4 kHz band.

2) Minimize user impact.

These two objectives are in direct conflict in the HDR forward link. There were three design constraints as follows:

1) Diameter of ground station antenna = 12.8 meters

2) Weather margin for ground link must be at least 17.5 dB

3) Diameter of a TDRS Ku band reflector antenna = 3.82 meters

The third constraint is imposed because the HDR space link antenna is also used for the MDR space link which requires this size. The TDRS ground link antenna was arbitrarily chosen to have the same size reflector in order to minimize cost.

The analysis led to a choice of identical EIRP values for both the forward TDRS to user link and return TDRS to ground link. This choice allows the same transmitter design to be used for both links. Two EIRP levels, 59 dBW and 51 dBW, were selected for these links. The higher level provides the required margin for the ground link and allows a user antenna diameter less than 3 meters for 50 Mbps on the forward link. The lower level satisfies the CCIR flux density requirements for both links.

The HDR system design assumed the use of biphase PSK without coding, but is compatible with quadriphase and rate one-half convolutional coding. A user employing the latter would require less EIRP. The TDRS design employs a 3.82 meter unfurlable antenna and a low noise parametric amplifier receiver. In meeting the 17.5 dB downlink margin requirement, it was found that the CCIR requirements on incident flux density were exceeded. The low power mode was chosen so that the limit need not be exceeded in clear weather.

3.2.2.1 Link Analysis

The design of the high data rate (HDR) return link followed the procedure illustrated in Figure 20. This procedure permits the designer to

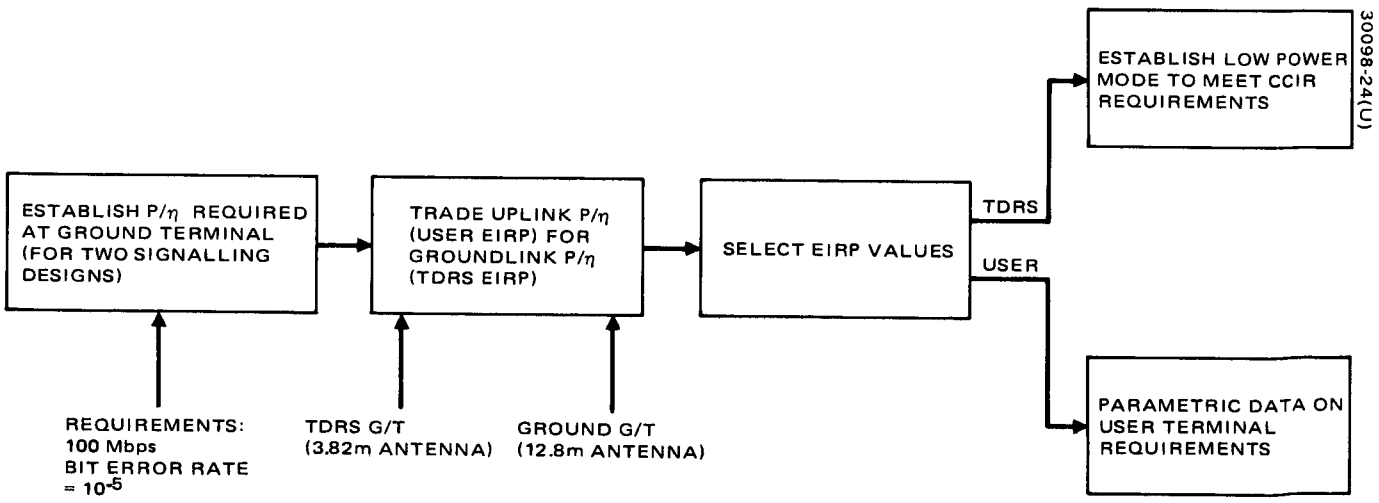

P/η = CARRIER POWER-TO-NOISE DENSITY RATIO

Figure 20. HDR Return Link Design Procedure

vary the relative burden placed on the TDRS and the user in terms of link signal-to-noise ratio. The design of the HDR forward link essentially involves only the TDRS-to-user portion since the ground-to-TDRS link has a very high signal-to-noise ratio.

Requirement on P/η

The first step in the design of both the forward and return links is to establish the final required signal power-to-noise spectral density ratio. Table 12 summarizes this calculation for a 100 Mbps return link capacity for two signaling schemes and for the forward link for both 50 Mbps data and television.

Table 12 is best explained by moving from the bottom to the top in the first column for biphase PSK without error control coding. In a linear, non-bandlimited communications channel with additive white Gaussian noise, biphase PSK requires an energy per bit-to-noise spectral density ratio of 9.6 dB for a bit error rate of 10^{-5}. At a data rate of 100 Mbps, the theoretically required P/η is given by

$$\frac{P}{\eta} = \frac{E_B}{\eta} R_B$$

$$= 9.6 + 80.0 \text{ dB} \cdot \text{Hz}$$

$$= 89.6 \text{ dB} \cdot \text{Hz}$$

A departure from theoretical of 1.5 dB has been allocated for bandlimiting effects including inter-symbol interference and for imperfect performance of the carrier recovery and bit synchronization loops. This value is quite optimistic but not unrealistic. Figure 21 shows that bandlimiting effects at the design time-bandwidth product of two will be about 0.9 dB. With the addition of a 3 tap transversal equalizer at the ground terminal, the inter-symbol interference would be reduced such that the degradation due to bandlimiting would be only 0.5 dB. Carrier and bit sync recovery loops have been built for high rate systems with quite satisfactory performance. The limiting factor in maintaining a coherent reference will probably prove to be the phase jitter of the modulator's reference.

The first column of Table 12 also includes an entry for degradation due to the limiter/TWTA combination used in the TDRS repeater. A limiter is employed as a power control device since the input power from the HDR user is expected to vary by 3 or 4 dB. The limiter prevents overdriving the output amplifier with the accompanying power reduction. Based on previous

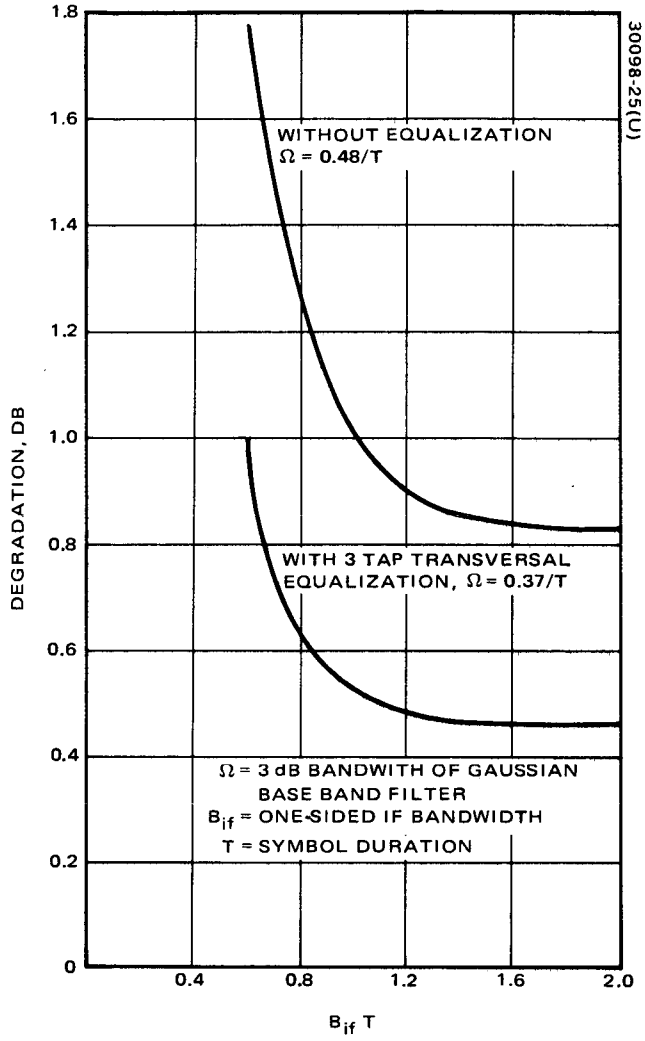

Figure 21. Degradation in E/N_o as Function of IF Bandwidth for Biphase Modulation and Gaussian Filter Detection

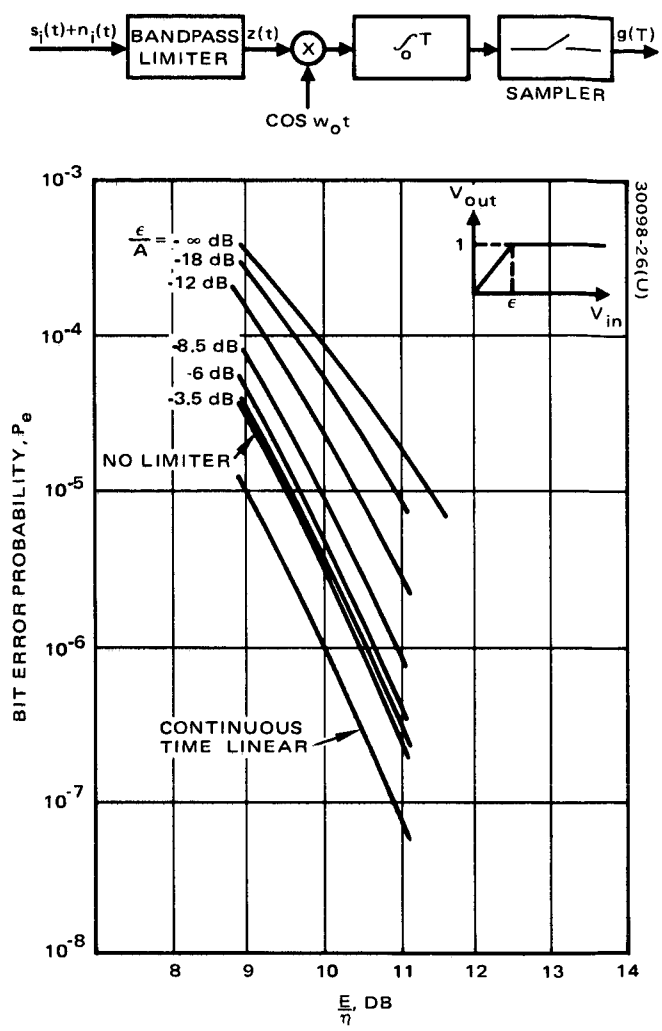

Figure 22. PSK Degradation Due to Bandpass Limiter

work at Hughes, an allocation of 1 dB is adequate to account for the signal distortion caused by this limiter.* From Figure 22, taken from *, the estimated degradation for a given error probability is the difference between the continuous time linear case and the case of interest. The limiter/TWTA combination is a soft limiter; the degradation should be much less than that corresponding to the curve labelled $\epsilon/A = \infty$ in Figure 22.

Based on these considerations, the required P/η at the ground terminal for 100 Mbps return link was set at 92.1 dB-Hz for biphase PSK. With quadriphase, the P/η should theoretically be the same, but an additional 0.5 dB has been allocated for phase imbalance between the two orthogonal carriers. With the use of rate one half convolutional coding, the E_b/η requirement will be reduced from 9.6 to between 5 and 6 dB. Figure 23 gives recent results for the performance of rate one half codes with sequential decoding.** For 100 Mbps, two or more coder/decoder pairs in parallel may be required. With two of the currently available Linkabit decoders in parallel, a 100 Mbps data stream would have an error rate of 10^{-5} at $E_b/\eta = 5.6$ dB.

The last column of Table 12 also shows the minimum P/η required for an analog television system meeting CCIR performance standards. This design assumes a baseband bandwidth of 4.55 MHz (including aural subcarrier) and a signal-to-noise ratio of 40 dB. An SNR of 39.8 dB rms signal to rms noise ratio is equivalent to the CCIR recommended 56 dB peak-to-peak signal to weighted rms noise (10.2 dB noise weighting plus 6 dB form factor). Figure 24 shows the power/bandwidth tradeoff possible in FM and the fact that a 90 MHz bandwidth provides a minimum P/η for an output SNR of 40 dB. The results in the figure assumes a threshold of 6 dB which is currently available with threshold extension demodulators.

Return Spacelink P/η Versus Ground Link P/η

For a linear repeater, the overall return link P/η value can be attained with P/η values in the user-to-TDRS link (space link) and the TDRS-to-ground links (ground link) according to the expression:

$$\left(\frac{P}{\eta}\right)_{U/T/G} = \frac{\left(\frac{P}{\eta}\right)_{T/G} \frac{P}{\eta B}_{U/T}}{\left(\frac{P}{\eta B}\right)_{T/G} + \left(\frac{P\eta}{\eta B}\right)_{U/T} + 1}$$

*L. D. Davisson and L. B. Milstein, "On the Performance of Digital Communication Systems with Bandpass Limiters," IEEE Trans., Vol. COM-20, No. 5, October 1972, pp. 972-75.

**K. S. Gilhousen and D. R. Lumb, "A Very High Speed Hard Decision Sequential Decoder," Proceedings of the International Telemetering Conference, Los Angeles, 1972.

TABLE 12. HDR LINKS DESIGN PARAMETERS

Parameter	Return Link(1)		Forward Link(2)	
	2Ø PSK/No Coding	4Ø PSK/Coding	Data	TV
$\left(\frac{P}{\eta}\right)_{U/T}$	95.2	91.2		
$\left(\frac{P}{\eta \bar{B}}\right)_{U/T}$	12.2	8.4		
$\left(\frac{P}{\eta}\right)_{T/G}$	95.2	91.2	89.1	
$\left(\frac{P}{\eta \bar{B}}\right)_{T/G}$	12.2	8.4	9.2	
$\left(\frac{P}{\eta}\right)_{U/T/G}$ (*see equation below)	92.1	88.1	89.1	85.8
Degradation in Limiter/TWTA	1.0	1.0	1.0	
Bandlimiting Effects, Etc.	1.5	2.0	1.5	
Bit Rate	80.0	80.0	77.0	
Theoretical $E_{b/\eta}$ Required	9.6	5.1	9.6	
	92.1	88.1	89.1	

*For a linear Repeater:

$$\frac{P}{\eta}_{U/T/G} = \frac{\left(\frac{P}{\eta}\right)_{T/B}\left(\frac{P}{\eta \bar{B}}\right)_{U/T}}{\left(\frac{P}{\eta \bar{B}}\right)_{T/G} + \left(\frac{P}{\eta \bar{B}}\right)_{U/T} + 1}$$

(1) SNRs equal in each link

(2) Ground link SNR ≥ 20 dB

Note: U denotes user
T denotes TDRS
G denotes ground station

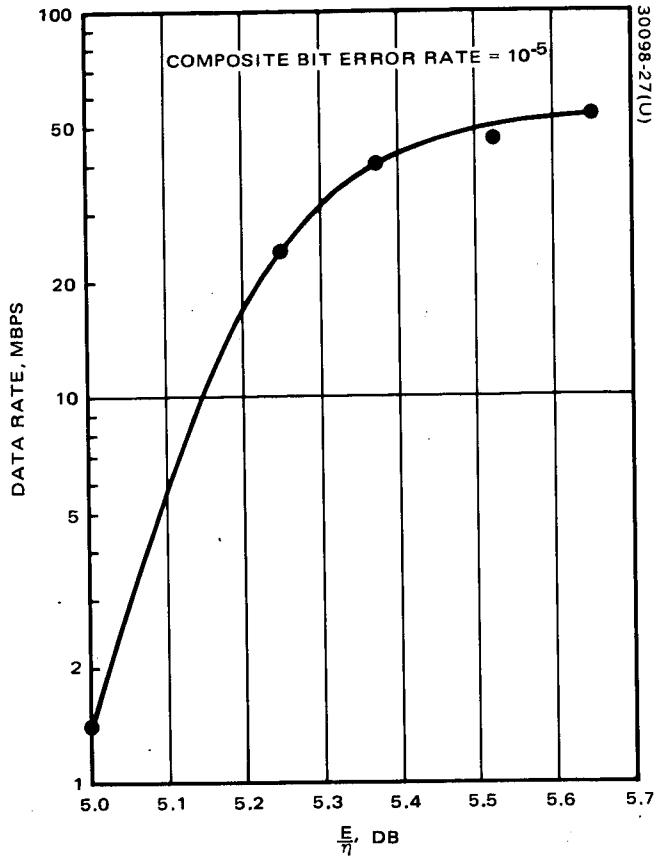

Figure 23. "Linkabit" Very High Speed Sequential Decoder Performance

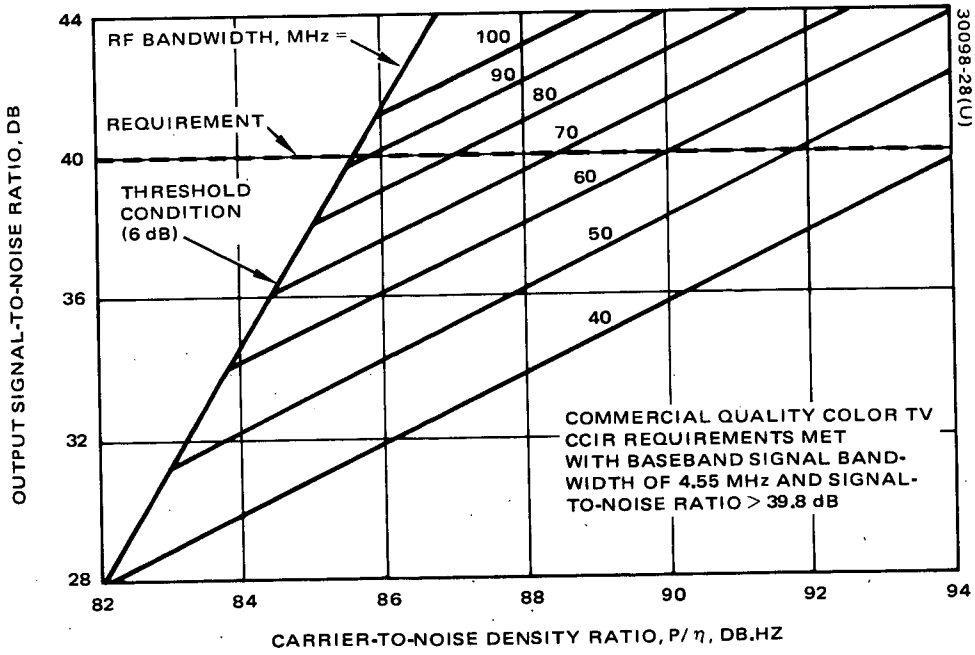

Figure 24. Power/Bandwidth Tradeoff in FM Design

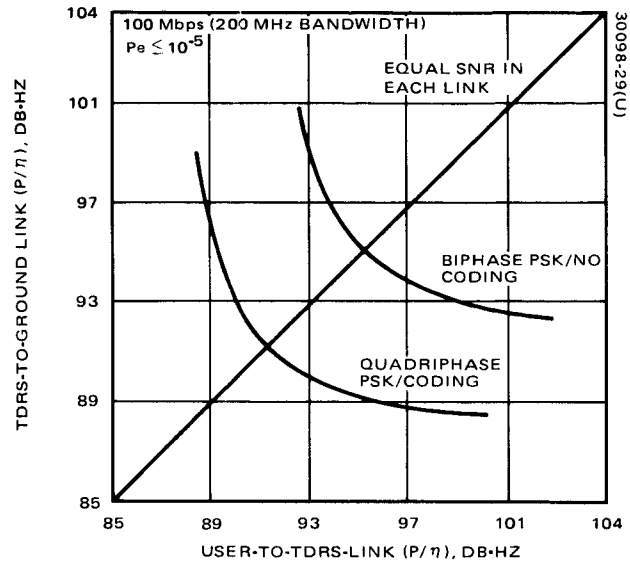

Figure 25. $(P/\eta)_{U/T}$ Versus $(P/\eta)_{T/G}$

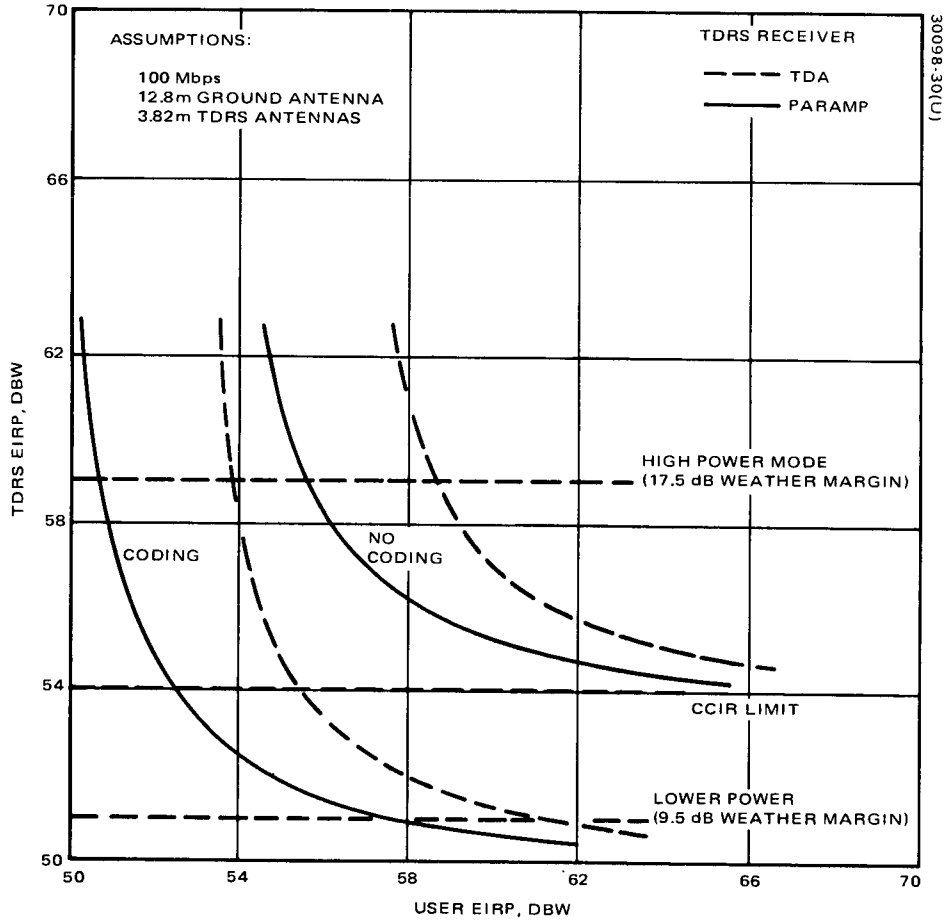

Figure 26. Ku Band HDR Return Link Design

where B is the noise bandwidth of the repeater. Although the repeater design includes a limiter for power control, this equation is still useful for preliminary design. System performance with the limiter is only 1 dB less than the linear case. Figure 25 shows the trade of spacelink versus groundlink P/η which results from use of the above equation. Note that when one P/η value is increased by 10 dB, that the other is within 0.4 dB of the minimum.

3.2.2.2 Link Budgets and EIRP Selection

Tables 4 and 5 contain the TDRS transmit and receive link budgets, respectively. The final entries allow the P/η values arrived at previously to be expressed in terms of system parameters such as EIRP, gain, or transmit power. In these budgets, several important parameters have been fixed; the TDRS antenna diameter (3.82 meters), the ground terminal antenna diameter (12.8 meters), and ground receive system temperature (420 K).

Referring to the ground link column of Table 4 and the return HDR link column of Table 5, the antenna gains used assume 48 percent efficient parabolic reflectors. This value is rather low because large unfurlable antennas are used with relatively poor surface tolerance. Pointing losses are assumed to be 0.5 dB with the autotrack system. The space loss for the user/TDRS link is the maximum geometrically possible for a 550 km user. Line loss values are based on preliminary design estimates and should be achievable. Polarization mismatch of the various antennas should be such that a 0.2 dB ellipticity loss is reasonable. The noise figure estimates are based on Hughes experience with parametric amplifiers. The background sky temperature is higher for the spacelink than for the groundlink, because the TDRS receives noise radiated from the earth. Note that the receive system noise temperatures have been referred to the receiver input.

These power budgets and the P/η requirements of Table 12 result in the curves of Figures 25 and 26. Although a paramp has been selected for the TDRS receiver, if this unit fails, the noise figure will be essentially that of the TDA second stage. Curves for both paramp operation and backup TDA operation are shown in Figure 26. The two upper right hand curves assume biphase PSK and no coding; the bottom curves assume quadriphase PSK and rate one-half coding.

The selection of the 59 dBW for the TDRS ground link EIRP was made by letting the required EIRP for the TDRS and user be the same under the conditions of TDA backup operation and no coding. This corresponds to the upper right hand dashed curve of Figure 26 which passes through the point corresponding to 59 dBW for both spacecraft. Thus, with the paramp, the user EIRP requirement for 100 Mbps is reduced by a factor of 2 (3 dB) to 56 dBW. If, in addition, convolutional encoding is used, the users EIRP may be as low as 51 dBW. Figure 26 also shows the EIRP to which the HDR ground link must be limited in order to satisfy the CCIR regulations on earth-incident power flux density. But, as can be seen from the figure, to use this

value would severely burden the user if coding is not employed and if the return link weather margin of 17.5 dB is required. To partially resolve this problem, a lower power mode was selected which will not violate CCIR regulations but which will also not provide the required margin. However, studies have shown that the 9.5 dB margin provided in the low power mode is adequate more than 99 percent of the time. The low power EIRP was selected to be the same as that required for the forward link (discussed shortly) so that the transmitter design could be identical.

From Figure 26, with the paramp receiver operating properly, the required user EIRP for 100 Mbps return data is 56 dBW, if coding is not used and 51 dBW, if it is. Figure 27 shows the relationship between the user antenna diameter (assuming 48 percent efficiency) and radiated power for these two values. Radiated power is that which emerges from the antenna feed; the transmitter final power amplifier output stage must provide additional power as required to compensate for line losses. The use of coding requires additional processing equipment at the ground station but offers significant reduction in user requirements. For instance, referring to Figure 27, 100 Mbps can be returned with a combination of 12.5 radiated watts and a 1 meter (3.3 feet) diameter antenna if coding is employed. However, without coding the same transmitter power, a 1.8 meter (5.9 feet) antenna is required.

The required user EIRP is very nearly proportional to the return data rate. This is illustrated in Figure 16 where the data rate is related to user antenna diameter and radiated power.

The high power mode for the forward link TDRS to user transmitter was arbitrarily chosen to be the same as that of the return ground link transmitter. Since this level violated the CCIR flux density regulations, a higher level did not appear justified and the use of two identical transmitters will reduce costs. Attention was turned to a lower EIRP level which would not violate the CCIR regulations. A brief analysis of the flux density problem leads to the following equation for the incident flux density (IFD) in 4 kHz.

$$IFD = -126 + EIRP - R_b \ \text{dBW/m}^2/4\ \text{kHz}$$

where EIRP and bit rate, R_b, are expressed in decibel units for 50 Mbps or an equivalent spectrum spreading rate.

$$IFD = -126 + EIRP - 77 \leq -152$$

Thus, the EIRP must be less than or equal to 51 dBW, and it is this value that was chosen for the low power mode. Again, it was arbitrarily decided to provide this power mode for both Ku band transmitters to reduce cost. The effect on the return link is to lower the weather margin by about 8 dB as mentioned previously.

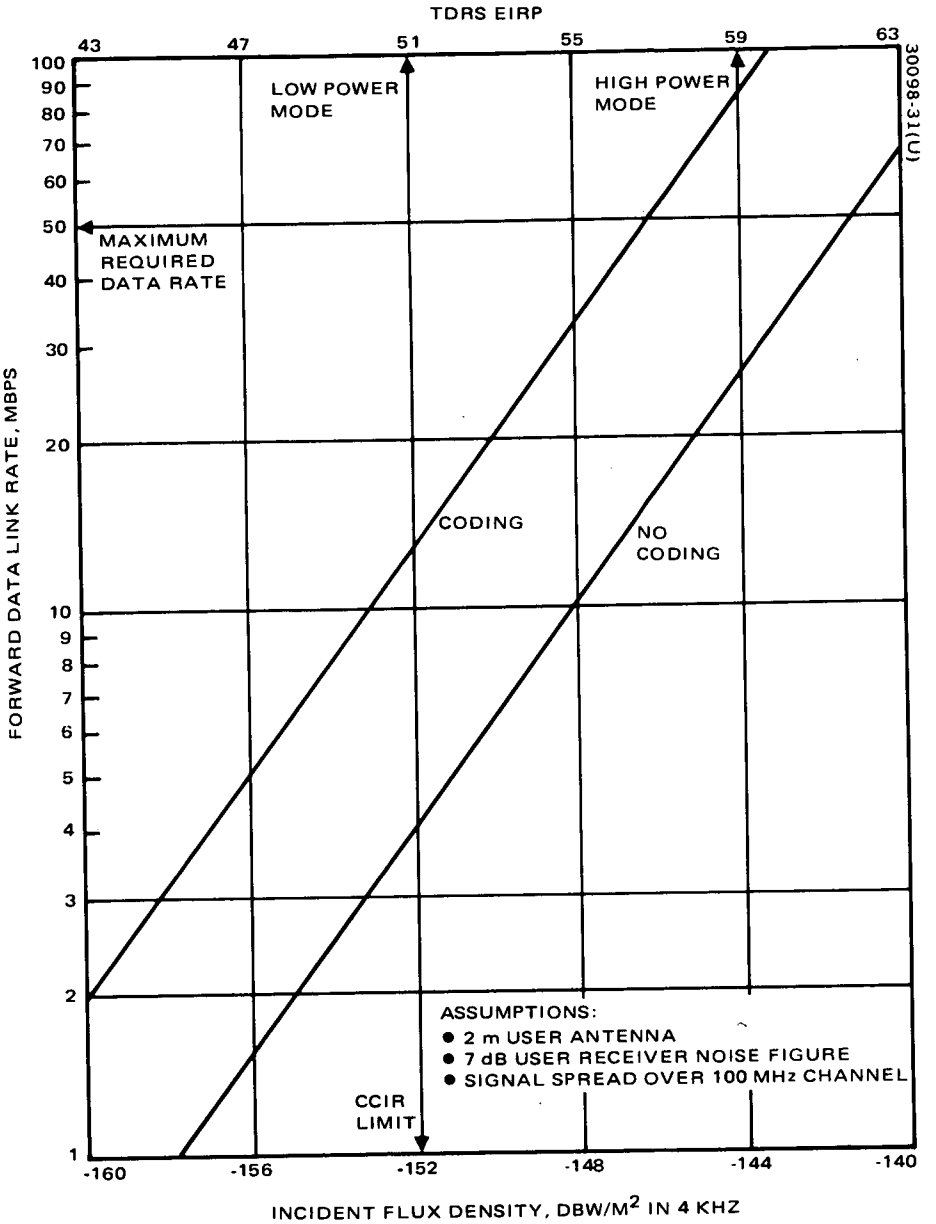

Figure 27. Forward Data Rate Versus Flux Density

For the two power modes, the HDR forward power budget of Table 4 was used to derive Figure 15. Note that use of the low power mode severely penalizes the user by requiring a much larger antenna for any desired bit rate.

The relationship between forward link data rate and incident flux density is shown in Figure 27 for a user spacecraft with a two meter (6.5 feet) diameter antenna and a receiver with a 7 dB noise figure. The advantage of using error correction encoding is shown, but the processing burden is borne by the user spacecraft and may be excessive for unmanned users. Thus, without the use of coding and employing the low power mode to meet CCIR regulations, the data rate is limited to 4 Mbps.

3.2.3 Link Acquisition

There are two major aspects of link acquisition which were addressed in this study: (1) procedure and (2) performance analysis. The first is qualitative in nature and requires the establishment of the sequence of procedural steps required to achieve link acquisition. The second aspect naturally follows the first and requires analysis of the relationships between the many parameters to establish those parameters which are variable and to determine the major performance characteristics. Both of these aspects are discussed in this subsection.

3.2.3.1 Acquisition Sequence

Both the TDRS and user will have mechanically steerable antennas with relatively narrow beamwidths. The TDRS half-power beamwidth is approximately 0.4 degree. From Figure 16, it can be seen that in order to utilize the capability of the HDR service, the user will require an antenna with a diameter of 1 to 2 meters; this corresponds to a half-power beamwidth in the range of 1.5 to 0.8 degree. Radiation beamwidths this small require a sequence which will result in each spacecraft lying and remaining the beamwidth of the other. Correct continuous pointing is maintained by autotrack subsystems employing feedback.

To achieve acquisition, either the TDRS or the user spacecraft must transmit a Ku band signal to the other. This signal is then detected and detection followed by autotracking antennas. Communication can then begin.

A prime objective in choosing the sequence is to allow the user to be initially passive. That is, with the user's transmitter off, and the user's antenna in an arbitrary orientation, the acquisition sequence must be started by ground control via the TDRS. Thus, the first commands to initiate action by the user must be transmitted via the TDRS by pointing its antenna such that the user lies within the beam. This may be possible with the narrow beam at Ku band, but from the pointing error budget of Table 13, the estimated 3σ uncertainty is 0.7 degree before calibration, which is approximately twice the half-power beamwidths. Thus, a wider beam must be used to be certain that the user lies within it. A logical choice was to use the dual frequency capability of the HDR/MDR antennas and begin acquisition by transmitting commands to the user at S band. The beamwidth at this frequency is approximately 2.7 degrees which is significantly greater than the estimated 3σ error. The use of S band to initiate the acquisition requires the user to have a receiver and broad coverage antenna at this frequency. However, this may be required anyway in order to provide backup direct-to-ground compatibility.

The user is commanded via his S band receiver to point a Ku band antenna at the TDRS with crude accuracy. The beamwidth of this antenna should be in the range of 3 to 5 degrees corresponding to a reflector diameter in the range of 0.3 to 0.45 meter (1.0 to 1.5 feet). The commanded pointing accuracy must then be in this range; from Table 13, this should present no difficulty. The user is then commanded to transmit via this

TABLE 13. POINTING ERROR BUDGETS

	3σ Angular Error, degrees (±)	
	TDRS	User
Spacecraft attitude stabilization	0.2	0.4
Alignment of antenna support*	0.1	0.1
Deployment mechanisms*	0.05	0.1
Thermal deflection of antenna support**	0.2	0.1
Antenna positioner	0.05	0.05
Antenna boresight alignment*	0.1	0.1
Boresight deflection due to thermal distortion**	0.1	0.1
Orthogonality of gimbal axis*	0.02	0.02
Accuracy of ephemerides	0.02	0.02
Operational time delays	0.2	0.5
Rss error	0.345	0.680
Maximum sum error	1.04	1.49

*These errors can be reduced by calibration.

**These time varying errors can be reduced after data analysis.

broadbeam antenna an unmodulated carrier which serves as a beacon for the TDRS. The TDRS is then commanded to perform a scanning search with its antenna over the angular region of user position uncertainty. With a high probability (discussed later), this search will result in a detection of the user signal which will cause the TDRS to automatically stop the search and begin autotracking. An unmodulated Ku band carrier is then transmitted via the TDRS antenna which is the beacon for the user. The user is then commanded, still via S band, to perform a similar scan search which will result in a detection of the TDRS beacon signal followed by an automatic switch to autotrack and a switching of the Ku band transmitter to the higher gain communication antenna. At this point, Ku band communication antennas on each spacecraft are automatically tracking signals transmitted by the other. One more command via S band may be used to transfer command reception to the user's Ku band receiver if desired, but for command reliability, it may be preferable to maintain the command link at S band.

In the above sequence, two Ku band user antennas have been mentioned; one with low gain (30 to 33 dB) for transmitting the beacon, and the high gain communication antenna for receiving the beacon signal from the

TDRS and transmitting the return data via the TDRS. Thus, the low gain antenna is used only for transmission while the high gain antenna is used for both transmission and reception and must provide the RF signals for auto-tracking. These user requirements are summarized in Table 14. It is expected that these two antennas will be rigidly attached to each other with their boresights aligned. A popular mechanical configuration uses a high gain cassegrain antenna with the low gain direct feed reflector mounted on the subreflector of the high gain antenna.

The alternate to scanning for signal detection is the general technique called beam broadening. With this method, the beam of the receiving antenna is made larger at the beginning of the acquisition sequence to insure that the transmitting spacecraft lies within the beam. The transmitting antenna beam may also need to be broadened to ensure that the receiving spacecraft is illuminated.

Several methods are available for achieving varying beam sizes. These include: 1) using separate antennas, 2) using a section of the main antenna, if an array antenna is used, or 3) changing the feed position such that the antenna beam is defocused. When antennas have a beam size which is a fraction of a degree, it is often advantageous to achieve beam broadening by using a second antenna with an area in the order of 1/100 of the main antenna. This second antenna may then cover the necessary angular sector to sense the transmitted signal. Once the signal has been sensed, the auto-track processing electronics directs the antenna positioner to align the beam of the smaller antenna toward the target. That is, the smaller antenna is boresighted on the target. Since the larger and smaller antennas have their electrical axes aligned, pointing the smaller antenna directly at the target also aligns the large antenna. The acquisition procedure then switches antennas, and the larger antenna develops error signals that cause it to be accurately boresighted on the target.

TABLE 14. USER REQUIREMENTS FOR HDR LINK ACQUISITION

- S Band system with omni antenna for command
- Dual-gain Ku band antenna (probably different antennas and feeds)
  - Low gain: 30 dB, transmit only
  - High gain: 47 dB, tracking feed, transmit and receive

The major disadvantage of beam broadening is the additional RF and mechanical complexity because the RF error signals for autotracking must be generated for both beamwidths. Scanning requires no additional RF or mechanical complexity, but will cause additional gimbal wear. However, it is felt that this additional wear can be more easily accommodated by gimbal design than beam broadening. However, in the above discussed acquisition sequence, the use of two antennas on the user, one with a broader beam for a beacon is a form of beam broadening. Since this broader beam is used only for transmission, most of the additional RF complexity is eliminated. The acquisition sequence is summarized in Table 15.

3.2.3.2 Scan Analysis

Typical patterns for scanning the search area are shown in Figure 28. The bar scan approach has the advantage of relatively simple pointing commands. Its disadvantage is that, for complete coverage of the search area, turnaround occurs outside the search area, thereby increasing scan time. A bar scan is also less efficient because it begins scanning over an area that has low probability of containing the signals, whereas, a spiral scan starts at the point of highest probability of finding the target. A spiral scan is most efficient in terms of early acquisition of the target, and the beam is always in the search area. The disadvantage of a spiral scan is that the positioner drive signal generation is more complex. But, since the

TABLE 15. HDR LINK ACQUISITION SEQUENCE

- TDRS points dual feed antenna at User ±1.0 degree accuracy
- User commanded via S band omni to
  - point dual gain Ku band antenna at TDRS ±3 degrees
  - Switch to low gain antenna mode
  - Transmit unmodulated Ku band carrier
- TDRS acquires user by antenna scan search and transmits Ku band beacon signal
- User is commanded via S band to perform scan acquisition with high gain antenna followed by autotracking
- User automatically switches transmitter to the high gain antenna

same scan pattern will be used each time, the advantages of spiral scan in minimizing acquisition time outweigh the disadvantages of on-board signal generator complexity.

A scan pattern of interest is shown in Figure 29. The pattern consists of a set of semicircles with centers alternating between points A and B and diameters increasing in increments as shown. If the center of the antenna beam is to travel the pattern at a constant rate during each semicircle, the motion in the plane of Figure 29 is expressed by

$$\left.\begin{aligned} x_n &= nd(a - \cos \omega_n t) \\ y_n &= nd(-1)^{n-1} \sin \omega_n t \end{aligned}\right\} \quad 0 \le t < \frac{\pi}{\omega_n} \qquad (1)$$

where

$$a = \begin{cases} 0 \text{ if } n \text{ is even} \\ 1 \text{ if } n \text{ is odd} \end{cases}$$

Two independent motors with orthogonal drive axes are used to position the antenna and hence their motion corresponds to the x and y coordinates of the figures. These positioners and the control electronics will have an angular rate limit, R, which will be assumed here to be the same for each motor drive. Thus,

$$\left|\dot{x}_n\right|_{max} = n\omega_n d = R = \left|\dot{y}_n\right|_{max}$$

If a maximum speed scan is to be achieved, then for the h^{th} semicircle

$$\omega_n = \frac{R}{nd} \qquad (2)$$

The motor drive signals will be the functions of Equation (1). The time, t_n, to trace the n^{th} semicircle is given by

$$t_n = \frac{nd\pi}{R}$$

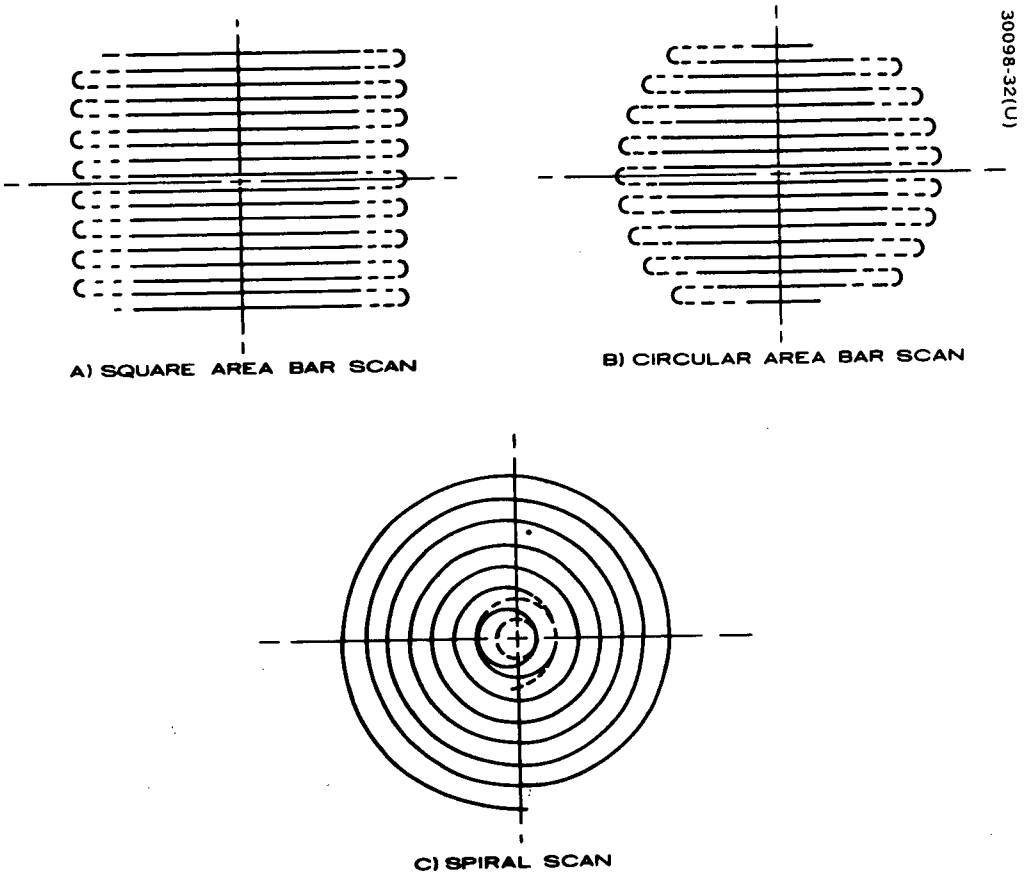

Figure 28. Scan Patterns

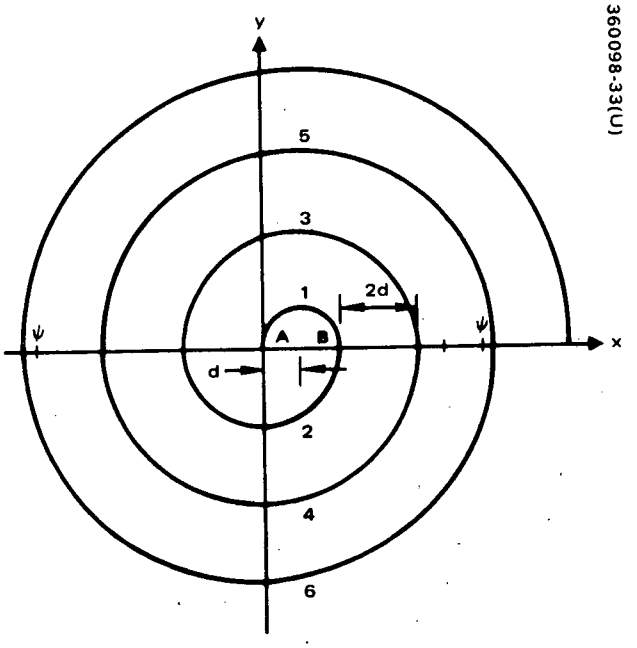

Figure 29. Spiral Pattern Consisting of Joined Semicircles

And the total scan time T_s is given time

$$T_s = \sum_{n=1}^{k} t_n = \frac{k(k+1)\,d\pi}{2R} \tag{3}$$

where K is the number of required semicircle segments of the scan pattern.

Denoted by ψ, the half angle of the cone to be covered by the scanning antenna beam, to ensure complete coverage by this area the number of required semicircles, k, is given by

$$k = 1 + \text{the next integer larger than } \frac{\psi}{d} \tag{4}$$

For reliable acquisition there should be overlap of the antenna beam 3 dB illumination area between adjacent semicircles. A conservative approach would be to make the angular distance d equal to one-fourth the 3 dB beamwidth, θ, i.e.,

$$4d = \theta \tag{5}$$

If this is done, the relationship between the scan area radius ψ, beamwidth, θ, maximum positioner rate, R, and total search time, T_s, can be approximated by letting $k = 1 + 4\,\psi/\theta_o$. The result is

$$T_s R = \frac{\pi\theta}{4}\left(\frac{8\psi^2}{\theta^2} + \frac{6\psi}{\theta} + 1\right) \tag{6}$$

This relationship is shown in Figure 30 for typical parameter values.

The maximum positioner rate for the TDRS is approximately 1 degree/second. If the same rate is assumed for the user, then for TDRS and user antenna beamwidths of 0.4 and 0.8 degree, respectively, Figure 30 indicates the required search times corresponding to the estimated 3σ errors of Table 13 are approximately 6 and 8 seconds, respectively. Operational delays during the sequence are expected to be longer. If the scan radii, ψ, are increased to 1 and 2 degrees, respectively for the TDRS and user for greater certainty of acquisition, the search times are 20 and 40 seconds, respectively.

The functional elements of the signal detector are shown in Figure 31. The envelope detector assumed in the analysis below is the square law device. Both linear and square law devices have been analyzed and shown to have nearly identical detection characteristics. The envelope detector is preceded by a bandpass filter and followed by a sampler. The sampler is, in turn, followed by an adder which sums the last m outputs from the sampler. A threshold switch is used to indicate a signal detection when the added output voltage exceeds a bias level, b.

Available statistical analysis is valid only if the samples of the detector output are independent. They may be considered to be independent if the sampling interval, t_s, is greater than the reciprocal of the input IF filter bandwidth, B, i.e.,

$$t_s \geq 1/B \tag{7}$$

In order to assure that the signal will remain within a beamwidth during a full cycle of the sample and add process, this cycle time, t_c, must be less than one-half the minimum time that a transmitter may lie in the antenna beam during the scan. Analysis of the scan motion of Figure 29 where Equation (5) is valid shows that the minimum time, t_{min}, for a transmitter to lie in the 3 dB beamwidth is given by

$$t_{min} \geq \frac{4d}{R} \tag{8}$$

and if Equations (5) and (8) are combined,

$$t_{min} \geq \frac{\theta}{R} \tag{9}$$

Thus, a sample and add cycle period, t_c, must satisfy

$$t_c = mt_s \leq \frac{2d}{R} = \frac{\theta}{2R} \tag{10}$$

3.2.3.3 Detection Analysis

When no signal is present, the noise alone may cause the adder output to exceed the threshold level. The probability of error during a

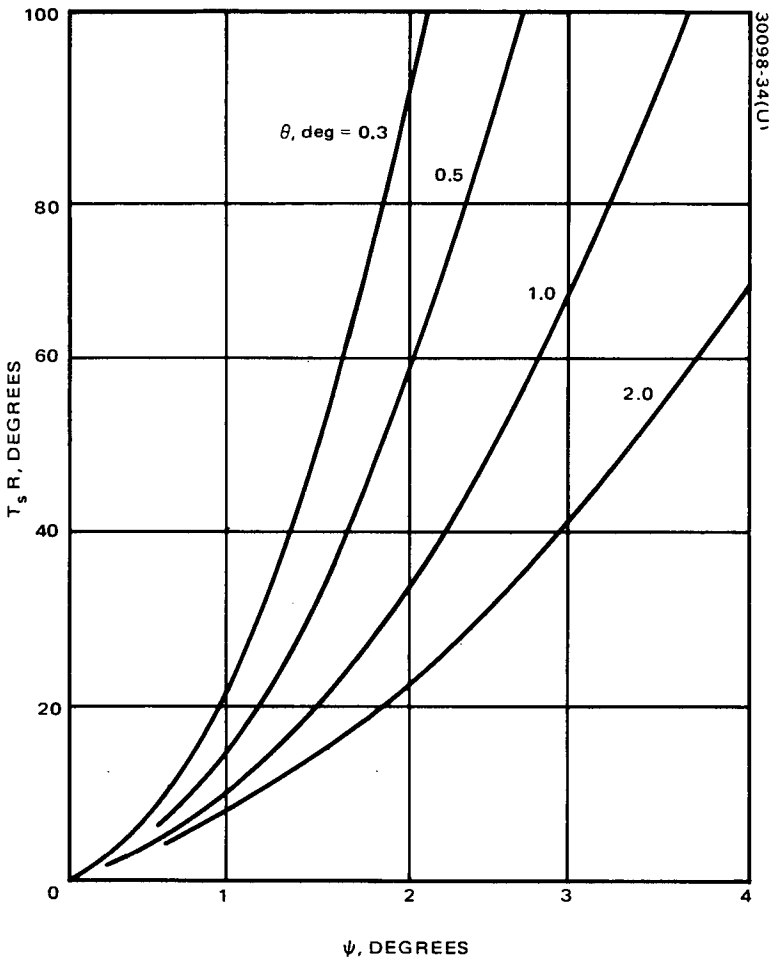

Figure 30. Search Time Parametric Curves

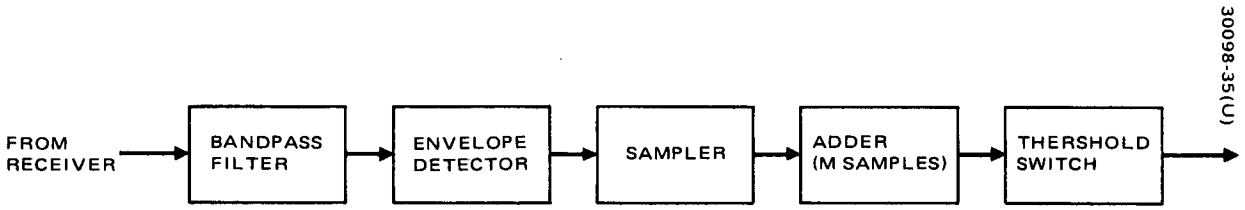

Figure 31. Signal Detector

sample and add cycle, P_e, is the probability that this will occur and is given by

$$P_e = \int_b^\infty P_m(y)\, dy$$

where b is the normalized threshold level and $P_m(y)$ is the density function for the normalized adder output voltage and is given by

$$P_m(y) = \begin{cases} \dfrac{y^{m-1} e^{-y}}{(m-1)!} & y \geq 0 \\ 0 & y < 0 \end{cases}$$

In Reference 1, b is computed as a function of P_e and m.

A false alarm occurs during the search when the detector registers a signal detection and there is no signal present at the time. This happens if the output of the adder exceeds the threshold bias level due to noise alone. The probability of false alarm during one complete search is given by

$$P_{fa} = 1 - (1 - P_e)^r \tag{11}$$

where

$$r = \text{next integer greater than } \frac{T_s}{t_c} \tag{12}$$

From Equation (11) above it follows that:

$$\left.\begin{array}{ll} P_e = P_{fa} & r = 1 \\ P_e = \dfrac{P_{fa}}{r} & r \geq 2,\ P_e r << 1 \end{array}\right\} \tag{13}$$

It may be noted from Equation (11) that $P_e \leq P_{fa}$. Thus, if $rP_{fa} << 1$ then $rP_e << .$

When the signal is present, the probability of detection during a sample and add cycle, P_{dc}, is given by

$$P_{dc} = \int_b^\infty q_m(v)\, dv$$

where $q_m(v)$ is the probability density function of the adder output when both signal and noise are at the input. It is shown in Reference 2 that this integral may be expressed as

$$P_{dc} = 1 - T\sqrt{b}\left(2m - 1,\ m - 1,\ \sqrt{mQ}\right)$$

where T represents the incomplete Toronto function (see Reference 2) and Q is the signal-to-noise ratio at the envelope detector input.

The probability of acquisition, P_{acq}, satisfies the inequality

$$P_{acq} \geq P_A(1 - P_{fa}) \sum_{i=1}^{q} P_{dc}\,(1 - P_{dc})^{i-1} \qquad (14)$$

The expression on the right is the product of the probabilities that the transmitter is in the angular search area (P_A), that no false alarm will occur during a search, and that a detection will be made when the transmitter is in the 3 dB antenna beam. The parameter q is the total number of sample and add cycles that occur while the transmitter lies in the beam.

The probability of acquisition is greater than or equal to the right-hand expression because a detection will probably occur before the scan process is completed, and P_{fa} is the probability of a false alarm occurring anytime during the complete scan if no transmitter were in the search area. Substituting Equation (11) in Equation (14) and performing the summation

$$P_{acq} \geq P_A(1 - P_e)^r \left[1 - (1 - P_{dc})^q\right] \qquad (15)$$

Equations (9) and (10) provide a lower bound on q, i.e.,

$$q_{min} = \frac{t_{min}}{t_c} \geq \frac{\theta}{mRt_s} \geq 2 \tag{16}$$

In almost all cases $P_{fa} \leq 10^{-5}$ by design, and from Equations (11) and (13), $P_{fa} \approx rP_e$ and so

$$(1 - P_e)^4 \approx 1 - rP_e \tag{17}$$

A conservative design to satisfy Equation (7) is to let

$$t_s = \frac{2}{B} \tag{18}$$

Substituting this in Equation (16)

$$q_{min} = \frac{t_{min}}{t_c} \geq \frac{\theta B}{2mR} \tag{19}$$

The inequality is thus strengthened by the use of q_{min}, i.e.,

$$P_{acq} \geq P_A(1 - P_e)^r \left[1 - (1 - P_{dc})^{q_{min}}\right] \tag{20}$$

Figure 32 shows the relationship between $q_{min} = t_{min}/t_c$ and the right-hand factor of Equation (20).

As an illustrative sample design, let

$$m = 100$$

$$P_A = 1.0$$

$$P_{fa} = 10^{-6}$$

$$P_{acq} = 0.9999$$

Letting $P_A = 1.0$ implies that the search area has been chosen large enough to ensure that the transmitting spacecraft lies within it. With $P_{fa} = 10^{-6}$ and $P_A = 1.0$

$$P_{acq} \geq 1 - (1 - P_{dc})^{(t_{min}/t_c)} \tag{21}$$

From the previous scan analysis it appears that the required search time, T_s, will be less than 100 seconds. It can be shown that the doppler shift at 14 GHz can be as large as ±400 kHz. Then allowing for oscillator instabilities, if a frequency search in addition to the scanning spatial search is to be avoided, $B \approx 10^6$ Hz.

If the sampling interval is chosen according to Equation (18), then from Equation (10)

$$t_c = mt_s = \frac{2m}{B} = 2 \times 10^{-4} \text{ second}$$

From Equation (12) and the estimate $T_s \leq 100$ seconds

$$r = \frac{T_s}{t_c} \leq 50 \times 10^4$$

From Equation (13), the required P_e is given by

$$P_e \approx \frac{P_{fa}}{r} \geq \frac{10^{-6}}{50 \times 10^4} = 2 \times 10^{-11} \tag{22}$$

As a conservative approach, let $P_e = 10^{-12}$. From Reference 1 the required threshold value, b, is 186.7.

The TDRS 3 dB beamwidth is approximately 0.4 degree and R is 1 degree per second. Thus, $\theta/R = 0.4$ and this ratio is expected to be larger than 0.1 for the user spacecraft. Using the latter value in Equation (19) along with other numerical values mentioned above,

$$\frac{t_{min}}{t_c} \geq \frac{\theta B}{2mR} \geq 500$$

And from Equation (21) and Figure 32 the maximum required value of P_{dc} is 0.015.

Figure 33 shows a plot of P_{dc} versus bias level for various values of signal-to-noise power ratio, Q. As mentioned above for $P_e = 10^{-12}$, $b \approx 187$, and thus for $P_{dc} \geq 0.015$, $Q \geq 0.4$ (-4 dB).

For the TDRS, the transmitter power was chosen to be 100 mW for reliable acquisition. From the link budget of Table 4, the signal-to-noise ratio in a 10^6 Hz bandwidth is approximately 8 dB for a 1 meter user antenna diameter. Since the user is expected to have an antenna at least this large, the probability of signal detection when the TDRS is in the user's beam during the user's search is greater than 0.9999. The same is true for the search by the TDRS if the user's EIRP is greater than 20 dB. The user's steerable beacon antenna will have a gain greater than 30 dB and his transmitter power will be larger than 1 watt as can be seen from Figure 16.

3.2.3.4 Conclusion

The conclusion of the above analysis is that:

1) The probability of acquisition success on each trial is extremely high, greater than 0.9999.

2) The maximum acquisition search time will be less than 1 minute. The average acquisition time will be less.

It should be noted that antenna slewing prior to the scanning search and other operational procedures may require several minutes, but these can be reduced by automating some functions and by prepositioning the user's antenna prior to stopping communication.

3.2.3.5 References

1) J. Pachares, "A Table of Bias Levels Useful in Radar Detection Problems," IRE Trans. on Information Theory, IT-4, No. 1 (1958), pp. 38-45.

2) J. I. Marcum, "A Statistical Theory of Target Detection by Pulsed Radar," with mathematical index, RAND Research Memo RM-754, 1 December 1947.

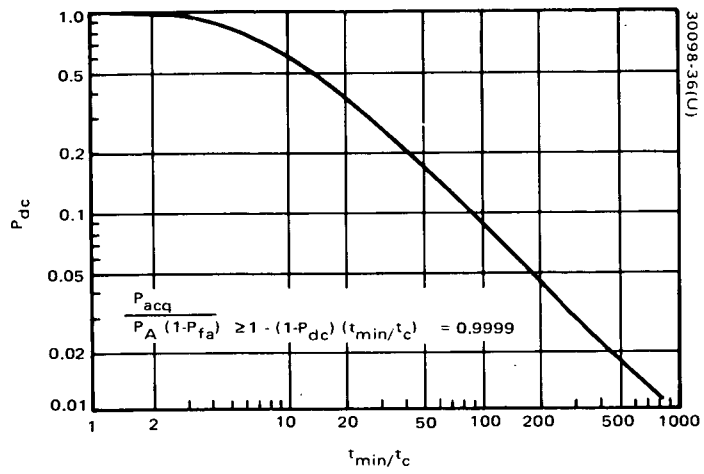

Figure 32. Detection Probability Versus t_{min}/t_c

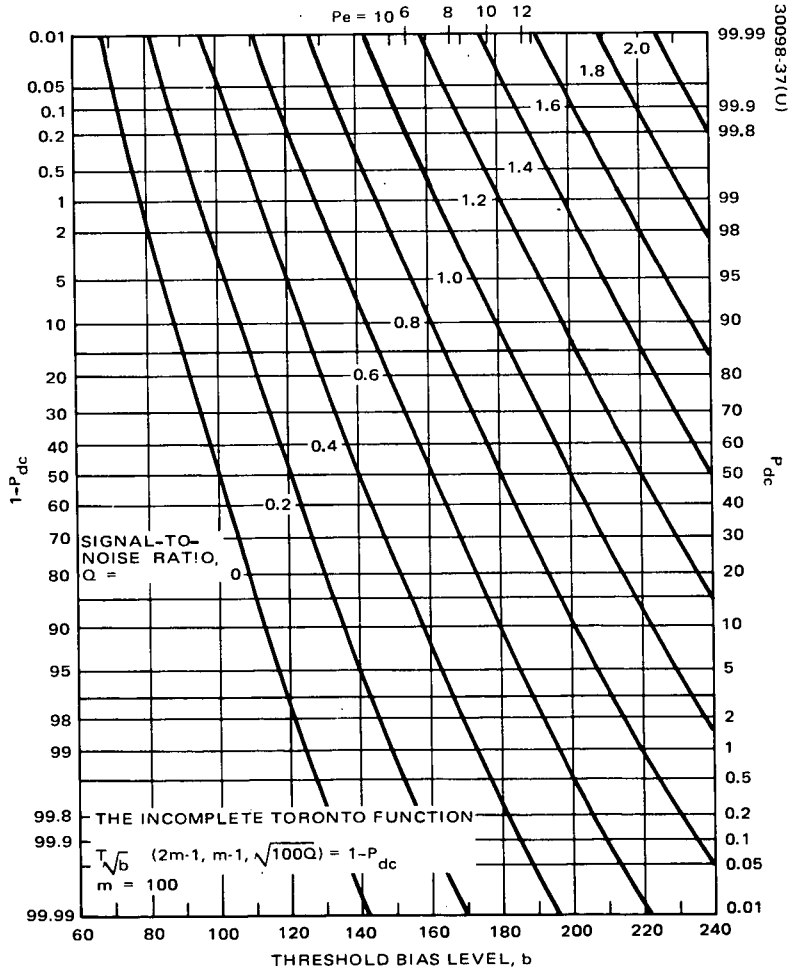

Figure 33. P_{dc} Versus Bias Level for Various Values of Signal-to-Noise Power Ratio

3.3 TDRS REPEATER

A simplified functional diagram of the repeater is shown in Figure 34. The antennas on the left are for communication with the Ground Station and the antennas on the right are for communication with user spacecraft. The forward LDR channel, TDRS commands, and frequency reference beacon are received from the Ground Station via a northern hemisphere coverage Ku band horn as shown in the lower left of the figure. The LDR signal is up-converted and transmitted to users via the broad coverage UHF antenna. The command signal is sent to the TDRS decoder and the reference beacon to the frequency synthesizer to provide system coherency for all frequency conversions.

The HDR and two MDR forward channels are received from the Ground Station via the 3.82 meter reflector antenna with the Ku band feed. The MDR channels are appropriately downconverted to S band and amplified for transmission. The HDR channel is upconverted from the receive Ku band frequency to the transmit Ku band frequency as shown in the frequency plan of Figure 7b.

The two return MDR channels, the 10 return signals from the LDR VHF array antenna, the order wire channel and the TDRS telemetry are added together in frequency multiplex, up converted to Ku band, and linearly amplified for transmission. Linear amplification is required to reduce intermodulation between channels and to allow adaptive processing at the Ground Station for up to 20 LDR users simultaneously. The return HDR channel is upconverted from Ku band receive frequency to Ku band transmit frequency and amplified in a saturated, i.e., limiting, amplifier for power efficiency. The outputs of the two power amplifiers are multiplexed and the resultant diplexed with the incoming combined forward MDR and HDR band for transmission to the Ground Station via the 3.82 meter Ku band dish.

The switches associated with the ground link signals and the HDR signal provide subsystem redundancy which will allow only slightly reduced service if one of the large reflector antenna subsystems should fail including positioner, feed, and tracking electronics. The 3.82 meter antenna at the left of Figure 34 has only a Ku band feed and is the initial and primary ground link antenna. If it should fail, however, either dual feed antenna may be used for the ground link. If, for instance, antenna 2 were used, then antenna 1 would be used for the HDR channel and would be time shared with MDR service. Lost would be the capability to provide the second two way MDR link simultaneous with the other link either MDR or HDR. The ability to provide two backup antenna subsystems for the ground link greatly enhances the system reliability and long life service potential.

If the primary ground link antenna operates as designed, then the switches allow the HDR channel to be provided by either of the dual feed antennas. The major antenna parameters are summarized in Table 16. More detailed discussion of the repeater is presented in Subsections 4.3.1 and 4.3.2.

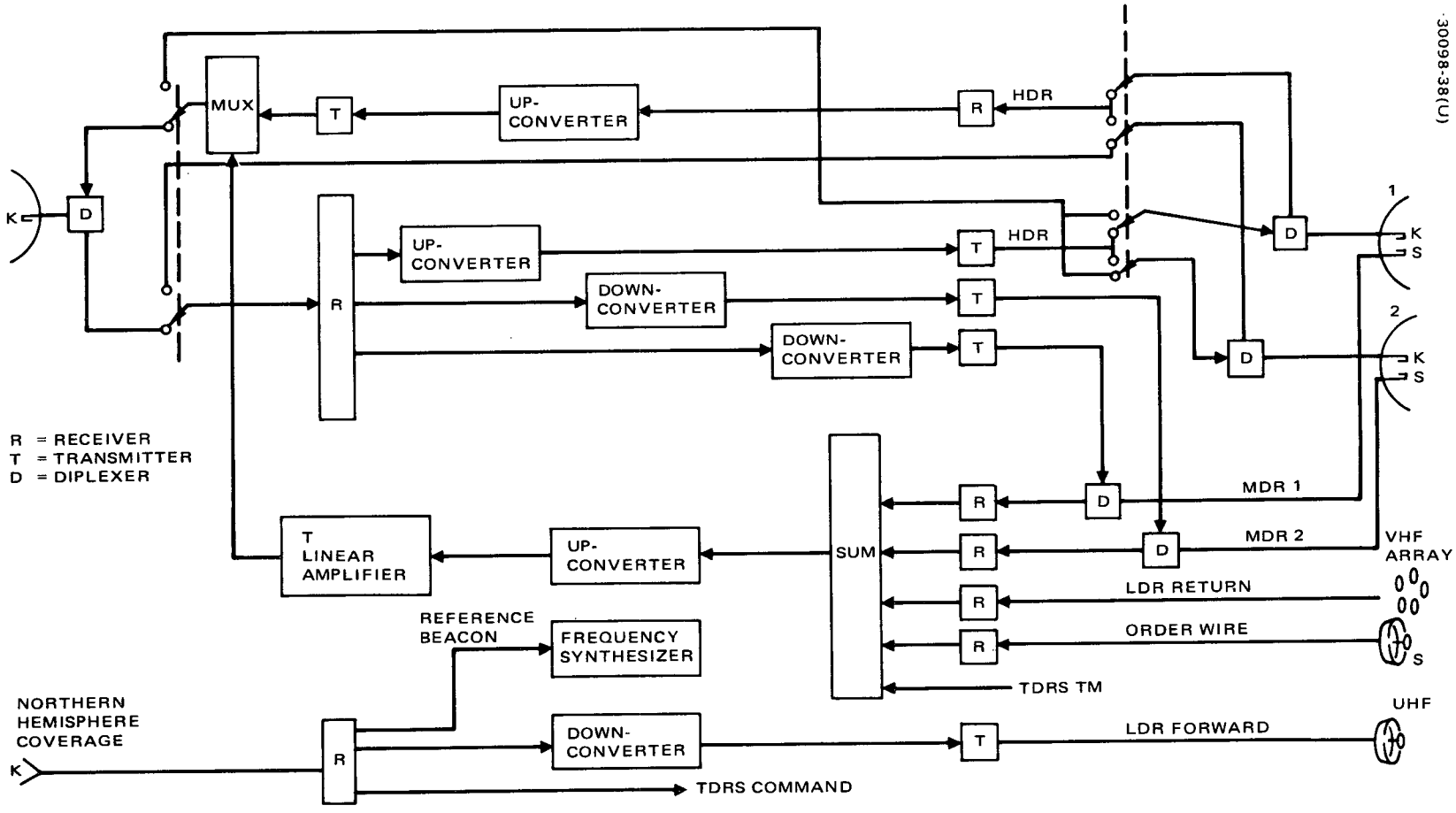

Figure 34. TDRS Repeater

TABLE 16. TDRS ANTENNA PARAMETERS

Link	Antenna Frequency, MHz	Antenna Diameter, meters	Minimum Antenna Gain over FOV, dB
Low data rate forward	UHF	1.43	12.5
Low data rate return	VHF	3.82	18.5
Medium data rate forward	S band	3.82	35.5
Medium data rate return	S band		36.2
High data rate forward	Ku band	3.82	52.8
High data rate return	Ku band		51.9
Order wire	S band	0.267	13.1
TDRS/ground	Ku band	3.82	52.8
Ground/TDRS	Ku band	Horns	18.5

3.4 USER EQUIPMENT

3.4.1 LDR and MDR Users

Both low data rate and medium data rate users will require spread spectrum transceivers. The carrier signals are modulated by binary PN sequences (codes), which in turn have been modulated by data. The use of PN coding for spectrum spreading accomplishes four objectives: 1) it allows code division multiplexing, 2) it reduces multipath interference, 3) it reduces the earth incident flux density (to meet CCIR requirements), and 4) it improves range measurement accuracy. All four of these reasons are important in the LDR system, and all but the first are important in the medium data rate system. The low data rate PN symbol (chip) rate is 614,000 chip/sec in the allocated 1 MHz (400.5 to 401.5 MHz) band. The forward link bandwidth of the medium data rate service is 30 MHz, and the signal must be spread over most or all of this band to minimize the flux density. Thus, the MDR signaling rate may be more than 30 times greater than that of the LDR system. However, the transceiver (receiving/transmitting equipment) consists of the following major components, interrelated as shown in Figure 35: receiver, command data correlator, telemetry modulator, transmitter, interface buffers, and a signal acquisition, matched filter correlator.

The acquisition correlator permits rapid forward link signal acquisition and provides PN code timing to the command correlator, which maintains pattern and frequency lock after initial acquisition. The telemetry transmitter frequency may be phase locked to the received frequency for ranging, but may also be allowed to run free during telemetry data transmission enabling handover between TDRSs without interrupting data flow.

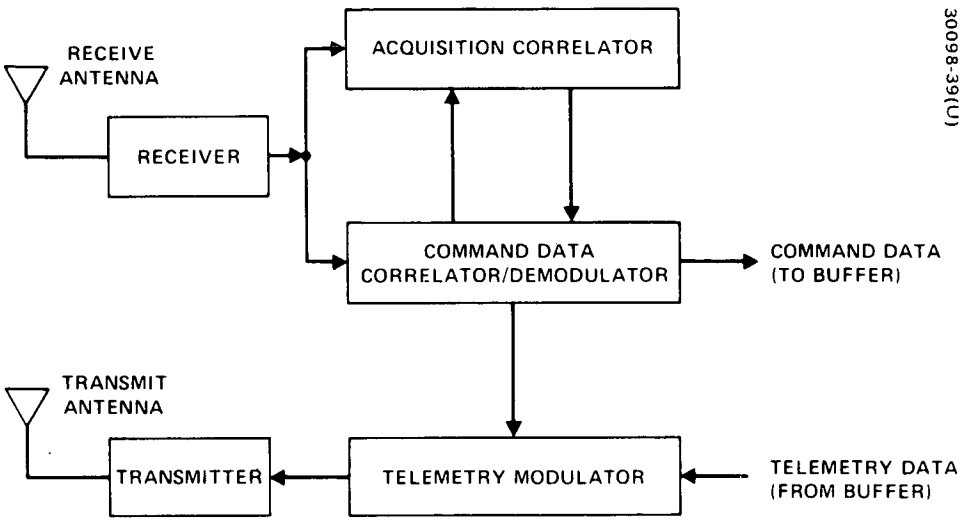

Figure 35. User Transceiver

To operate with the TDRS system, a user spacecraft does not need to replace or modify its NASA ground station compatible equipment, but must supplement it with the TDRS compatible transceiver and antennas. Two types of standard transceivers are envisioned, one for LDR users and one for MDR users. These transceivers can be connected with a switch to the regular command decoder and telemetry encoder. The choice between the ground station or TDRSS operation could be made any time during the user's mission by a simple command of the switch setting. If the data and command rates for both modes of operation are different, an interface buffer unit will also be required as part of the transceiver package. In addition to the standard transceiver, the LDR users will probably require a UHF antenna. The VHF link to a TDRS is compatible in frequency with the user to ground station link.

Figure 36 presents a more detailed transceiver description with numerical values corresponding to the baseline parameters of LDR forward command and return telemetry links. For this implementation, the acquisition correlator gives the following performance when the bit energy-to-noise density, E_b/η at the receiver is 0 dB, which is 10 dB below the link design value.

Mean time to threshold (synchronous signal output)	0.1 second
Probability of correct acquisition	0.99
Probability of a false synchronization output	0.01

In order for MDR users to realize the 1 Mbps capacity of the return link, a directive antenna will be required for expected transmitter power levels less than 30 watts. The relationship between user antenna gain and return data rate is shown in Figure 7c. In order to allow communication during a major portion of the user's orbit, or whenever the user is visible to a TDRS, the directive antenna radiation must be steered. The most straightforward approach is to provide the capability to mechanically orient a single antenna structure, but whatever technique is employed, a steerable directive radiation pattern will be necessary for data rates near 1 Mbps.

3.4.2 HDR Users

Whereas the principal problem with the LDR and MDR links is code acquisition, i.e., signal synchronization, the principal problem of the HDR link is antenna beam acquisition and steering. The antenna half-power beamwidth will be less than 1 degree for most HDR users, necessitating special equipment for rapidly establishing the HDR user/TDRS link.

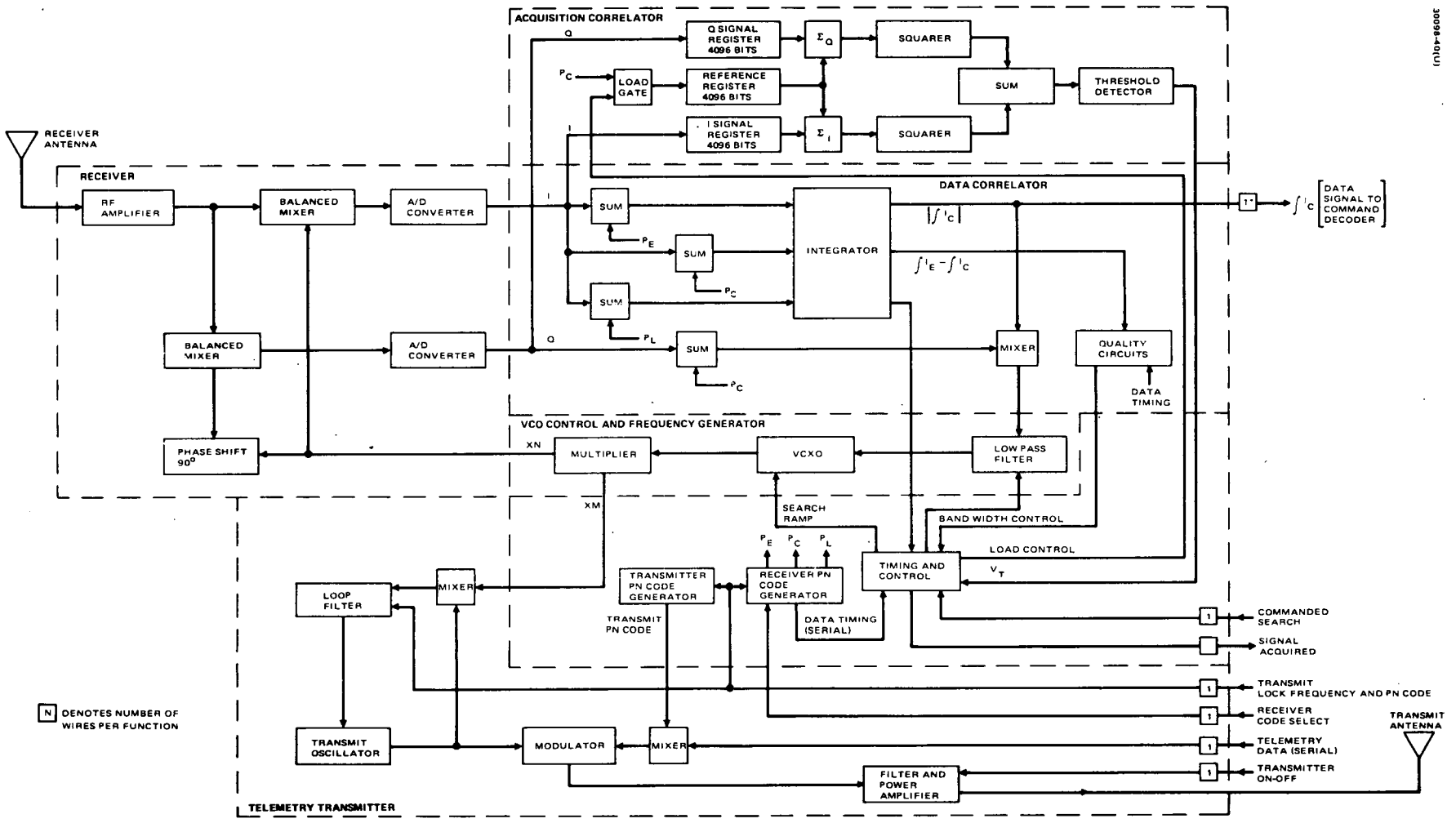

Figure 36. User Transceiver Detailed Diagram

A possible communication subsystem implementation is shown in Figure 21. The basic equipment required is as follows:

1) S band receiver with an omnidirectional antenna for command

2) Steerable, dual gain antenna

   Low gain - transmit only

   High gain - tracking feed, transmit and receive

The dual gain antenna shown in Figure 37 consists of two separate antennas and feeds rigidly connected to each other with parallel boresights. Only the high gain antenna has a tracking feed. With this equipment the acquisition sequence is as follows:

1) The TDRS is commanded to point a dual feed antenna at the user with ±1.0 degree accuracy and an unmodulated carrier is transmitted at Ku band.

2) The TDRS transmits the following commands at S band which are received, verified, and executed via the user's S band omnidirectional antenna:

   Point antenna at TDRS with ±3 degree accuracy

   Switch power amplifier output to low gain antenna

   Turn off carrier modulator

   Turn on transmitter

3) The TDRS performs a spatial scan acquisition of the user carrier.

4) The user is commanded via S band to perform a scan acquisition of the TDRS signal (see Step 1).

5) Following acquisition, the autotrack system is automatically activated, the user switches its transmitter to the high gain antenna and data transmission begins.

In Figure 37 an output of the S band receiver provides a reference for the user's frequency synthesizer. This is not required, but if a frequency reference properly adjusted on the ground based on ephemerides is sent to the user, the effect of doppler shift can be compensated and the acquisition time greatly reduced.

The maximum time required to perform steps 3 through 5 above is estimated to be 45 seconds. The antenna slewing of steps 1 and 2 will probably require more time. For instance, with the TDRS antenna slew rate of approximately 1 degree per second, slewing across the earth disc will require approximately 20 seconds. The user may be required to slew 180 degrees which would take 120 to 240 seconds depending on its positioner capability. However, this delay could be eliminated by prepositioning the antenna for the next communication period at the end of the current period.

3.4.3 User Equipment Implementation

User transponder equipment may be constructed using design approaches described for the TDRS repeaters. The principal difference in the detailed design is that the user equipment must operate in the complimentary transmit and receive bands. Minimum mass designs are required to minimize the impact on user satellites. The power consumption of power amplifiers and transceiver equipment must also be minimized by using high efficiency components in their design and construction. Complete redundancy in all electronic equipment is included. Equipment mass and power parameters are summarized in Table 17.

Low data rate transceiver equipment is implemented with microwave integrated circuit construction. The receivers utilize a transistor preamplifier to achieve a moderate noise figure as RFI will generally limit the command link performance. Transmitters feature high efficiency transistor power amplifiers developing 5 watts of output power. Overall efficiency of the transmitter is estimated to be 50 percent. An omnidirectional whip array antenna may be used on satellites using the Low Data Rate Service. Pseudo noise correlators are constructed with integrated circuits to minimize equipment mass and production cost. A crystal oscillator is provided for equipment operation prior to acquisition of the TDRS carrier which then provides the frequency reference for the transponder.

Medium data rate transceiver equipment at S band is also implemented with microwave integrated circuit construction. Command receivers for unmanned users utilize a transistor preamplifier to achieve a moderate noise figure. Higher data rates required for manned users are achieved by using a low noise parametric preamplifier and by operating the TDRS in the high power mode. A 5 watt transmitter is provided for unmanned user satellites. The required link performance of 1 Mbps may be achieved with a 5 watt transmitter and directional antenna with approximately 20 dB gain. The directional antenna is controlled by commands received through an omnidirectional antenna. A mechanical positioner with stepper motor drive is used to position the antenna. Applications requiring lower data rates may be implemented with an array of antennas which are switched to achieve beam steering. Beams are broad and can be controlled by computer generated ground commands. The MDR transceiver is also compatible with ground based satellite control and data acquisition facilities. Pseudo noise equipment is provided. It is implemented with integrated circuit construction.

The high data rate user equipment consists of a Ku band transmitter, a Ku band tracking receiver, a Ku band directional antenna and Ku band transceiver equipment for initial acquisition and contact with ground stations directly. The Ku band transmitter utilizes a TWT amplifier and a receiver implemented with waveguide circuitry. For a data link operating at 100 Mbps, an eight watt transmitter operating into a 2 meter antenna is required. As the beam width is less than one degree, autotracking is employed after acquisition of the link is achieved. The antenna is positioned with a mechanical motor employing a stepper motor driver.

3.5 GROUND STATION DESIGN

The Ground Station is the interface element between the TDRS and the two control centers – GSFC and the TDRS control center. The general relationship of the Ground Station to the other elements is shown in Figure 38. Also shown in the figure are three major portions of the basic Ground Station: 1) a terminal for maintaining RF communication with TDRS east, 2) a terminal for maintaining RF communication with TDRS west, and 3) a common area containing demodulation and processing equipment, which will be applied to signals from both terminals.

The RF terminals are of conventional design, but the signal demodulation and processing equipment, although not new in concept, has not been previously applied in the complexity required for simultaneous multiple user communication via the TDRSS. It should be mentioned that a third terminal may be required for communication with the in-orbit spare TDRS and for redundancy. This will require only a slight increase in the processing equipment and its configuration controls.

The terminals consist of five major portions: 1) the antenna structure, 2) the antenna tracking subsystem, 3) the Ku band RF/IF subsystem, 4) the VHF backup system, and 5) the UHF antenna for TDRS tracking. The signal processing can be functionally separated into ten portions:

1) LDR user telemetry demodulation
2) MDR channel 1 telemetry demodulation
3) MDR channel 2 telemetry demodulation
4) HDR telemetry demodulation
5) LDR forward link modulation
6) MDR channel 1 forward link modulation
7) MDR channel 2 forward link modulation

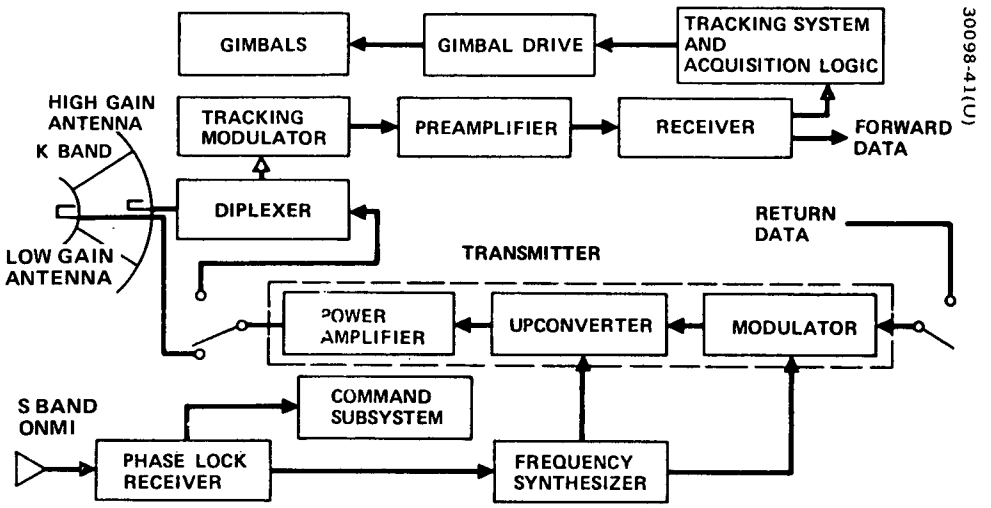

Figure 37. HDR User Communication Subsystem for TDRSS Operation

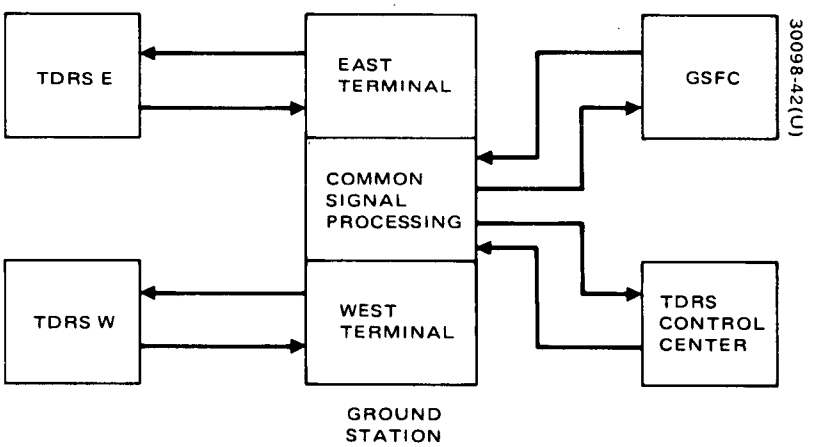

Figure 38. Overall Ground Station Concept and External Interfaces

TABLE 17. USER TELECOMMUNICATIONS EQUIPMENT

Item	Number	Mass, kilograms	Power, watts
LDR User VHF/UHF		5.8	15.0
Receiver	2	1.0	1.0
Telemetry transmitter*	2	2.0	10.0
VCO control and frequency generator	2	0.3	1.0
Acquisition and data correlator	2	1.0	3.0
Antennas	1 Set	1.5	–
MDR User (1 Mbps) S Band		14.9	32.0
Command receiver	2	0.8	1.0
Telemetry transmitter*	2	2.7	20.0
Frequency synthesizer	2	0.3	1.0
Signal processor	2	1.0	3.0
Diplexer	1	1.7	–
Antenna, omnidirectional	1	1.0	–
Antenna, directional	1	1.4	–
Gimbal	1	4.2	–
Gimbal driver	2	1.8	6.0
HDR User (100 Mbps) Ku Band		27.2	62.3
Command receiver, S Band	2	0.8	1.0
Telemetry transmitter, S Band	2	2.7	(20.0)
Tracking receiver, Ku Band	2	5.1	5.8
Telemetry transmitter,** Ku Band	2	5.2	45.5
Frequency synthesizer	2	0.5	1.0
Signal processor	2	1.0	3.0
Diplexer, S Band	1	1.7	–
Diplexer, Ku Band	1	0.2	–
Antennas, S Band	1	1.0	–
Antennas, Ku Band	1	3.0	–
Gimbal	1	4.2	–
Gimbal driver	2	1.8	6.0

*5 watts RF power.
**12 watts RF power.

8) HDR forward link modulation

9) TDRS telemetry, tracking, and command

10) User range and range rate measurements

3.5.1 Ground Terminal Design

The equipment and associated parameters for a terminal are listed below:

3.5.1.1 Antennas

Ku band/VHF antenna

1) Reflector diameter, 12.8 meter (42 feet)

2) Ku band cassegrain feed

3) S band near focus feed

4) Polarization

   a) Ku band, circular, C/CC

   b) S band, circular, C/CC

5) Gain

   a) 13.5 GHz, 62 dB

   b) 15.0 GHz, 63 dB

   c) 2040 MHz, 46 dB

   d) 2220 MHz, 47 dB

6) Pedestal type: AZ/EL

7) Autotrack system, single RF channel amplitude comparison, monopulse type

UHF antenna for TDRS tracking

1) Frequency, 400.5 to 401.5 MHz

2) Gain, 5 dB

3.5.1.2 Receivers

Ku band receiver

1) Location, rear of reflector

2) Noise figure, 3.9 dB

S band receiver

1) Location, within terminal structure

2) Noise figure, less than 4 dB

UHF receiver

1) Location, within terminal structure

2) Noise figure, less than 4 dB

3.5.1.3 Power Amplifiers

Two 2 kW klystrons operational and two in standby.

The two HDR signals and three MDR signals are amplified in one power amplifier; the LDR, TDRS command, and beacon are amplified in the other.

Power output allocations at the Ku band antenna feed:

LDR: 1 kW

MDR: 70 watts per channel

HDR: 200 watts

Beacon: 20 watts

TDRS command: 20 watts

Figure 39 shows the forward link RF/IF equipment and power amplifier arrangement.

3.5.2 Signal Processing

The ground station return signal processing equipment must separate the individual channels in the two signals from each terminal, demodulate the data signals, and then multiplex all data for transmission to the GSFC telecommunications control center. These functions are illustrated in Figure 40, where for simplicity, range and range rate measurements have

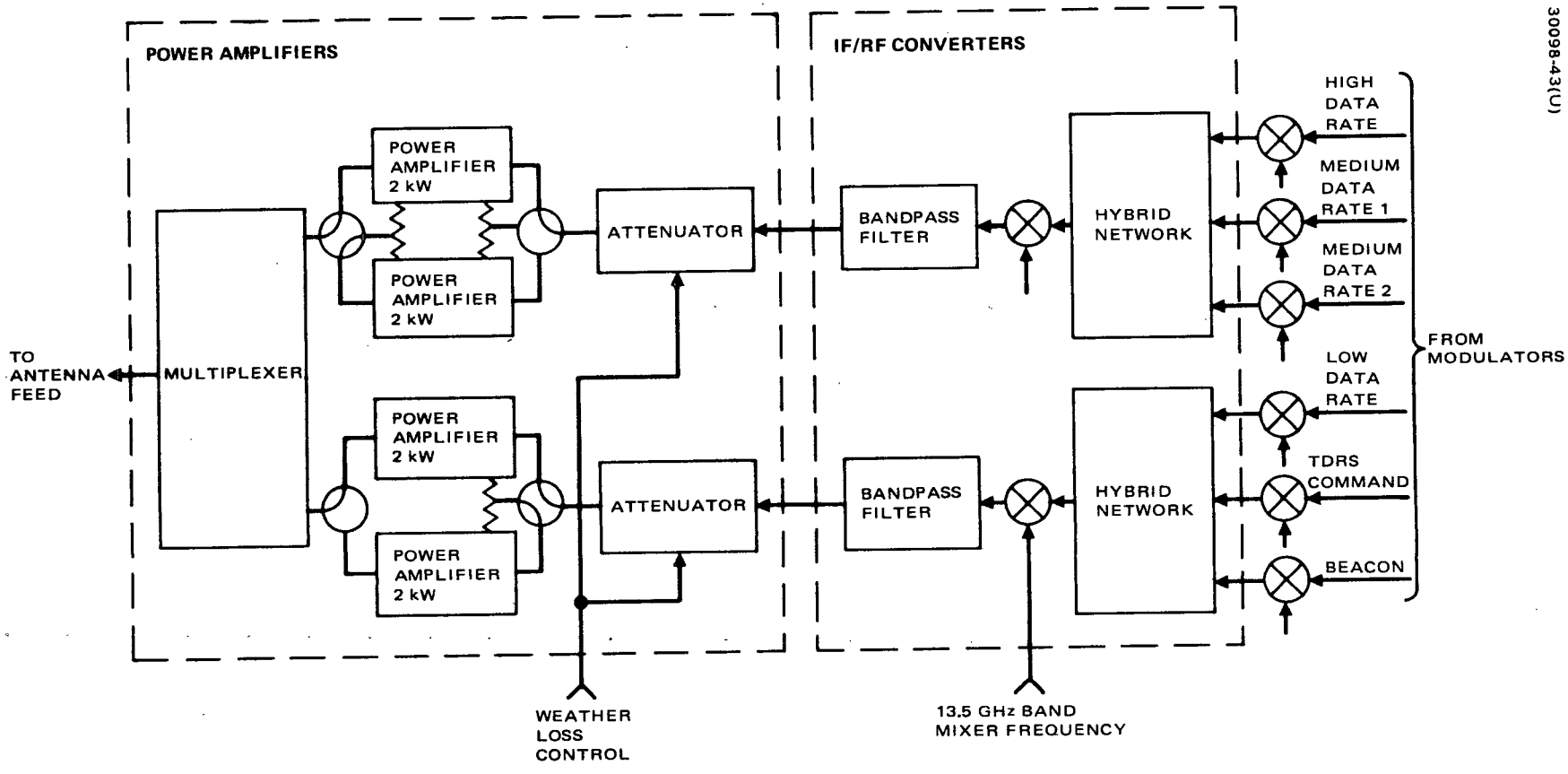

Figure 39. Power Amplifier and RF/IF Configuration

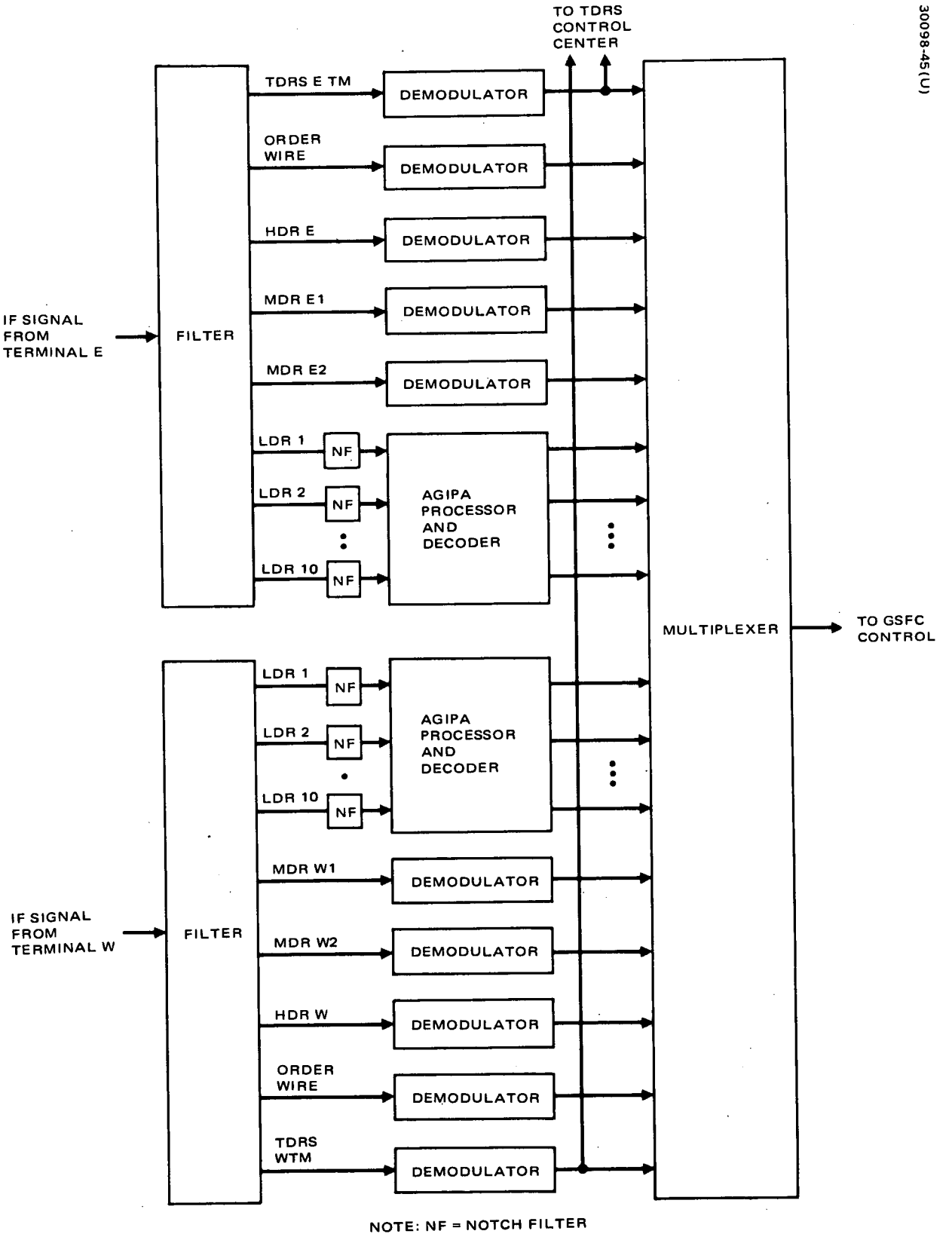

Figure 40. Ground Station Return Signal Processing

been made part of the general demodulation process. The forward signal processing as shown in Figure 41 includes demultiplexing the signals from GSFC, modulating the LDR and MDR with PN codes, IF carrier modulation of all signals, and transmission to the two terminals. The voice must be switched to the correct LDR or MDR channel as directed from GSFC.

The major task required for the signal processing equipment is one of integration, control, checkout, maintenance, and replacement provision. All equipment, except the LDR return channel demlutiplexing and demodulation equipment, is conceptually conventional. The equipment and major parameters follows:

3.5.2.1 Forward Links

LDR telemetry PN/PSK modulator

1) Quantity, 2

2) Rate, 614.4 Kchips/sec

MDR PN/PSK modulator

1) Quantity, 4

2) Rate, 10 Mchips/sec

HDR PSK modulator

1) Quantity, 2

2) Rate, 50 Mbps

TDRS telemetry

1) Quantity, 2

2) Type, three tone GSFC AM-FSK

3) Bit rate 128 bps

3.5.2.2 Return Links

LDR telemetry – Notch filters will be used at IF in each LDR component signal as necessary to reduce high power, narrowband interference (see Figure 40). For each user the following equipment is required:

One AGIPA processor

One convolutional decoder

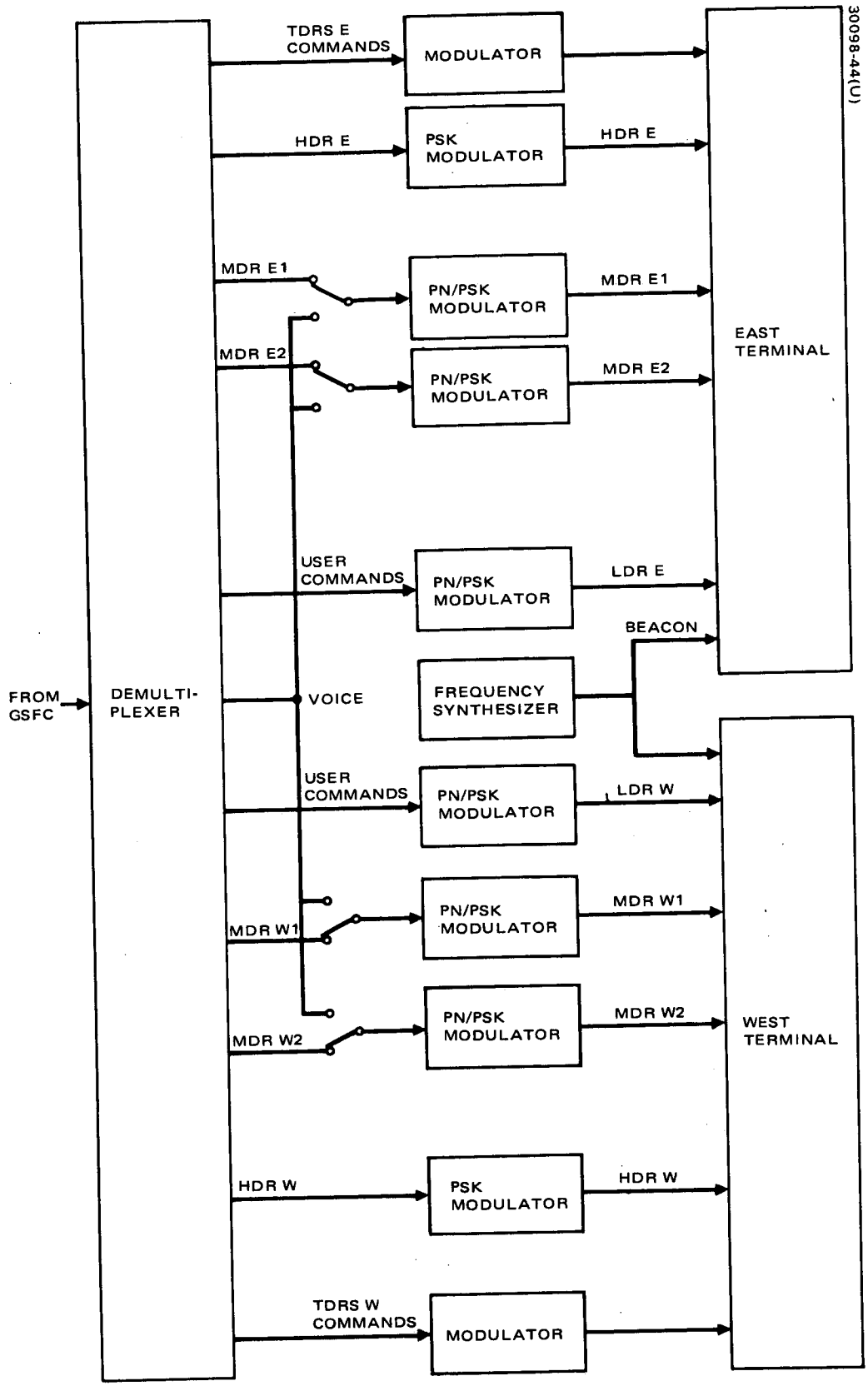

Figure 41. Ground Station Forward Signal Processing

One range measurement unit

One range rate measurement unit

The AGIPA processor includes the PN correlation process. A functional arrangement of the above equipment is illustrated in Figure 42.

MDR - Biphase PSK correlation receivers must be used to demodulate the return signals and procure output bit streams corresponding to the current user spacecraft telemetry rates; a standardized but variable bit rate device is envisioned.

HDR - A biphase PSK demodulator is required; the bit rate will depend on user requirements but rates up to 100 Mbps are possible.

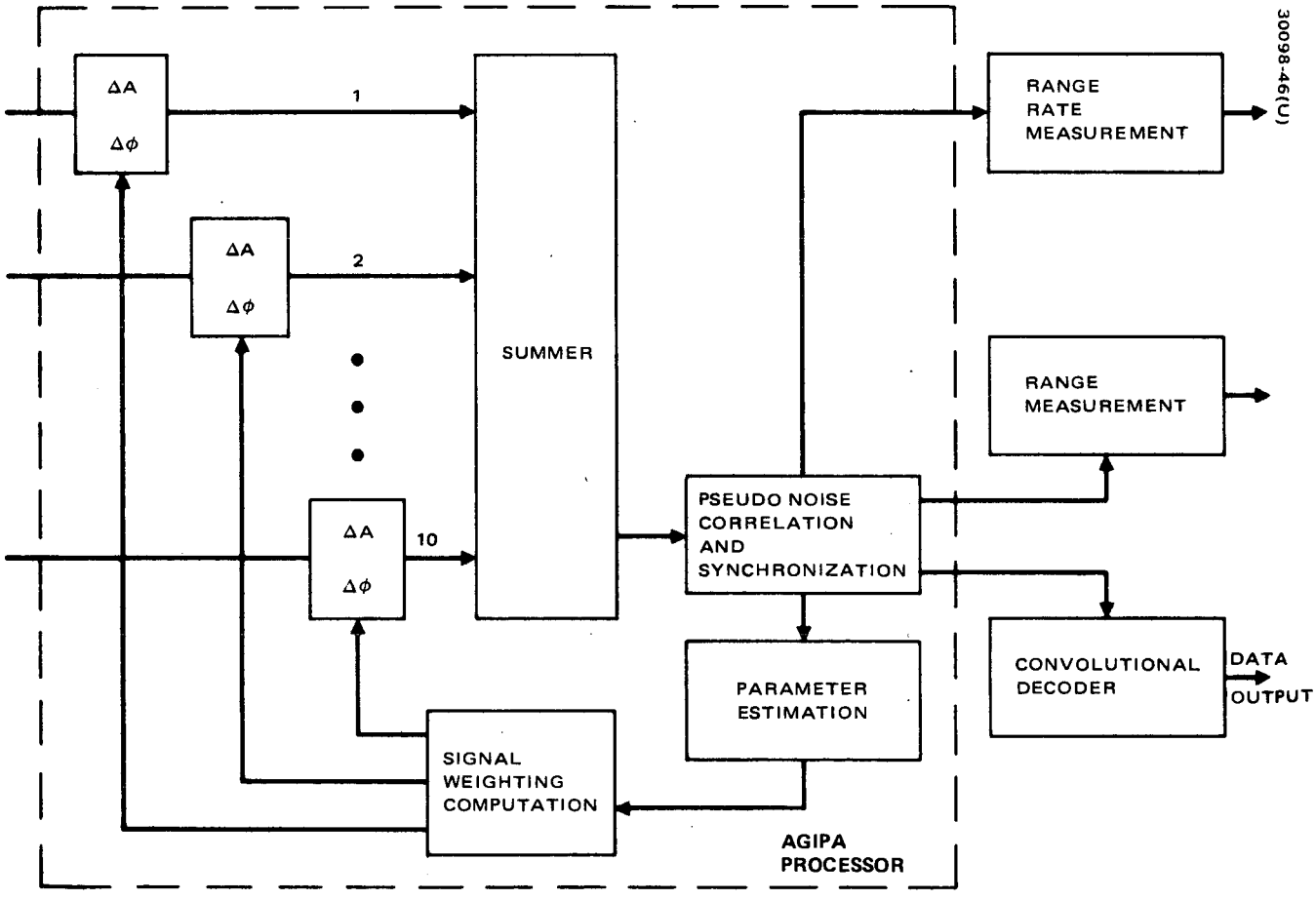

Figure 42. LDR Signal Processing

4. TDR SPACECRAFT DESIGN

4.1 DESIGN CONCEPT

The TDR spacecraft is designed to provide command and data relay capability for low, medium, and high data rate unmanned user spacecraft and voice, command, and data relay capabilities for manned user spacecraft. All transmissions from the TDRS ground station are at Ku band. In the spacecraft repeater, a frequency translation is performed prior to transmission to the various users. Low data rate (LDR) user commands are frequency translated to UHF for transmission to the user satellites. The UHF forward link channels utilize broad beam antennas oriented toward earth center. An independent voice channel is also provided in this frequency band. Medium data rate (MDR) user commands are frequency translated to S band for transmission and high data rate (HDR) user commands and data are frequency translated to the Ku band frequencies.

For the MDR and HDR service, two dual S/Ku band feed 3.82 meter (12.5 foot) diameter paraboloid reflector antennas are provided. These antennas are time shared between the MDR and HDR service. Switching circuitry is provided so that each antenna may be used for either service. However, two separate S band channels and two separate Ku band channels are implemented in the TDRS repeater so that each antenna may be used in the MDR and HDR modes simultaneously.

The LDR and MDR data and voice return links are provided at VHF and S bands respectively. A broad beam return link is also provided at S band to provide an emergency "order wire" service for manned users. The VHF, LDR return is designed with a five element AGIPA. Both horizontal and vertical polarization of the return signal from each antenna element is transmitted to the ground in an independent channel, where it is processed to maximize the signal/interference ratio of the return beam.

The HDR return links are implemented at Ku band. The links from the TDRS to the ground station are also at Ku band and are implemented with a narrow beam antenna. A VHF backup service for TDRS telemetry, tracking, and command and an S band transponder for TDRS tracking are also provided.

The TT&C subsystem uses the Ku band links for primary operations. A VHF transponder provides a backup capability in the event that contact cannot be made with the TDRS with the Ku band links. The primary command subsystem uses the 128 bps PCM-FSK/AM format to send the commands. A real time execute capability is desirable to simplify equipment. This requirement is met by providing an execute tone at a different frequency than the 0 and 1 tones employed in the command signals.

Pointing of the high gain S band antennas is easily accomplished by ground command. In the case of the S band antenna with a beamwidth of approximately 2.5 degrees, open loop pointing with an accuracy of the order of 0.5 degree is feasible. The Ku band antennas with a beamwidth of approximately 0.35 degrees require an autotrack capability. Acquisition is accomplished for those antennas equipped with dual S/Ku band feeds by initially making contact with a user at S band and then going through a search at the user satellite for a broadened Ku band beacon signal transmitted by the TDRS. After the user has acquired the TDRS, the TDRS then searches and locks into the Ku band transmission from the user.

Attitude control requirements are to provide a stable platform for antenna pointing. It is not essential to control the despun platform orientation to less than 0.5 degree but it is necessary to measure the orientation of the spin vector and the despun platform azimuth to an accuracy of the order of 0.1 degree. Thus short term dynamic variations in pointing should be restricted by the design to be less than that amount. This requirement leads to a specification for nutation stability and also to a requirement to balance the spinning section. The despin control must be stable and any limit cycle shall not exceed 0.005 degree.

Propellant for 7 years of spacecraft operations has been included. In the event that the solar cell array has not degraded to the point conservatively predicted and the spacecraft has not failed, the TDRS will continue to function and provide relay service as specified. This will provide a longer time to write off development and deployment costs of the system, and the expected cost effectiveness of the system will be enhanced.

Considerable attention has been devoted during the study to cost effectiveness. The general approach has been to utilize well proven technology for the satellite subsystems and, if compatible with launch vehicle performance limitations, to utilize hardware designed for earlier satellite programs.

4.2 CONFIGURATION SUMMARY

The improved Atlas Centaur launch vehicle was utilized for this study. The spacecraft design requirements are summarized in Table 18. The payload of 1780 kg includes spacecraft and adapters. Orbital operations require flexibility in assignment of spacecraft and a reasonable allowance is provided for station change maneuvers. The lifetime of 5 years is the minimum required orbital lifetime. In order to provide a more cost effective

TABLE 18. SPACECRAFT DESIGN REQUIREMENTS FOR ATLAS CENTAUR CONFIGURATIONS

Launch vehicle	Improved Atlas Centaur
Payload to transfer orbit	1780 kg maximum
Operational orbit	Synchronous
Initial inclination	3 degrees
Deployment	±65 degrees from ground station
Station change	2 to 4.3 degrees/day maneuvers
Stationkeeping	East - west only
Lifetime	5 years maximum

design, solar cell arrays and propellant budgets are sized for 7 years. If operations are benigh, this spacecraft lifetime could easily extend to 10 years or more.

The Atlas Centaur configuration of the deployed TDR spacecraft shows the arrangement of antennas about the spacecraft spinning body. This arrangement of antennas was selected to provide control of solar torque and minimize propellant and number of attitude correction maneuvers. An artist's concept of the configuration is shown in Figure 43 and Figure 44 shows the spacecraft layout in the orbital configuration.

The high gain MDR, HDR, and return link antennas are mounted forward. This position minimizes cable and waveguide runs to electronic equipment mounted in the spacecraft, and also provides for a more rigid and thermally stable mount for these narrowbeam antennas. A forward location of the UHF broadbeam antenna is also selected to minimize power loss in the transmission lines running from the transmitter to the antenna.

The LDR return link is implemented with a five element AGIPA configuration which is deployed aft. The VHF elements are less sensitive to alignment errors and cable runs over the required distance do not result in excessive losses. The antenna is deployed by a system combination of an Astromast and pivoted linkages. The Astromast is a light weight deployable truss structure which can achieve the long deployment required with a high stiffness and highly compact stowage. The lattice type structure also minimizes shadowing of the solar cell arrays arising from the aft deployment of the LDR return antenna.

The Intelsat IV spacecraft has been adapted for the bus. This design utilizes Gyrostat stabilization. The principal elements of the spacecraft are the spinning rotor, comprising 60 percent of the on station vehicle mass, and the despun earth oriented platform containing the communication repeater and its antennas. A rotating interface (consisting of conventional ball bearings, a rotary transformer, and slip rings) sustains the relative motion between the two bodies, permits signal transfers to take place, and affords an electrical path over which power from the solar panels and batteries can flow to

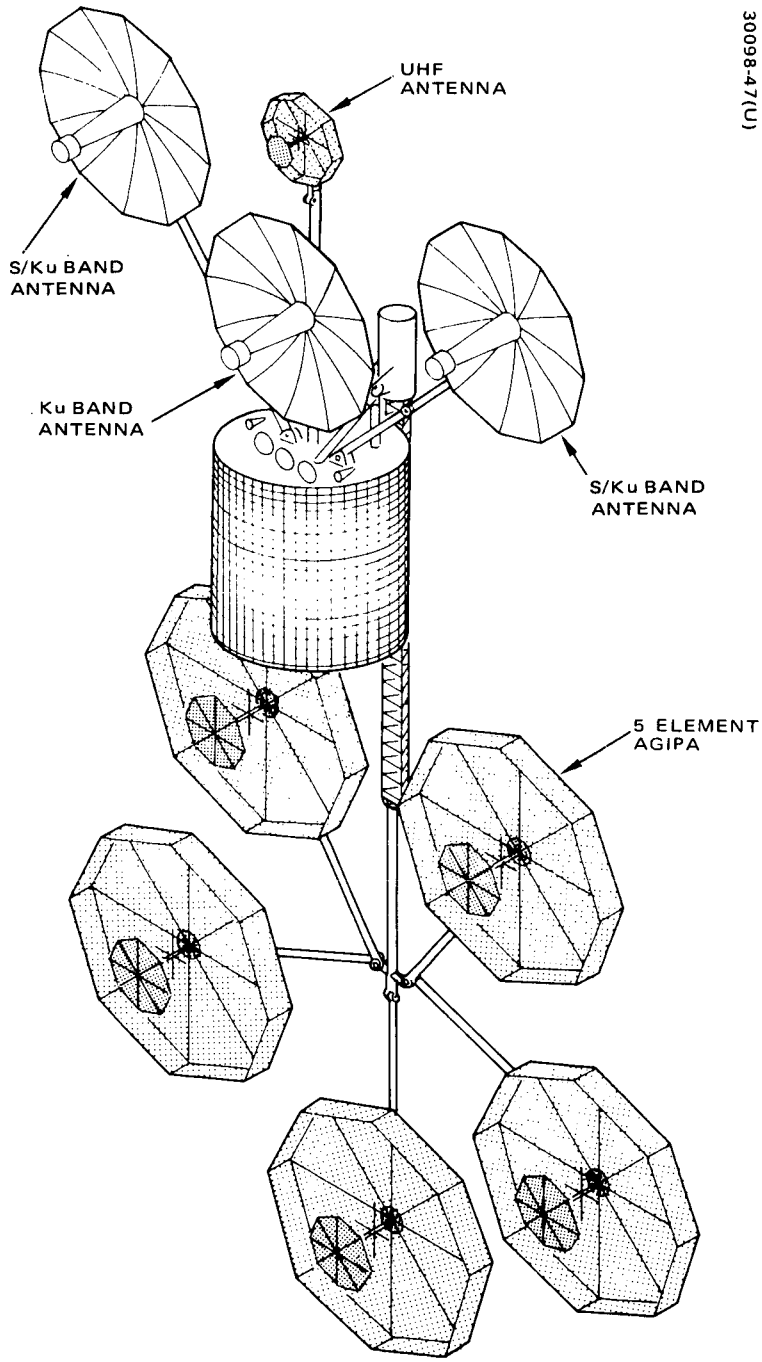

Figure 43. Atlas-Centaur Launched TDR Spacecraft

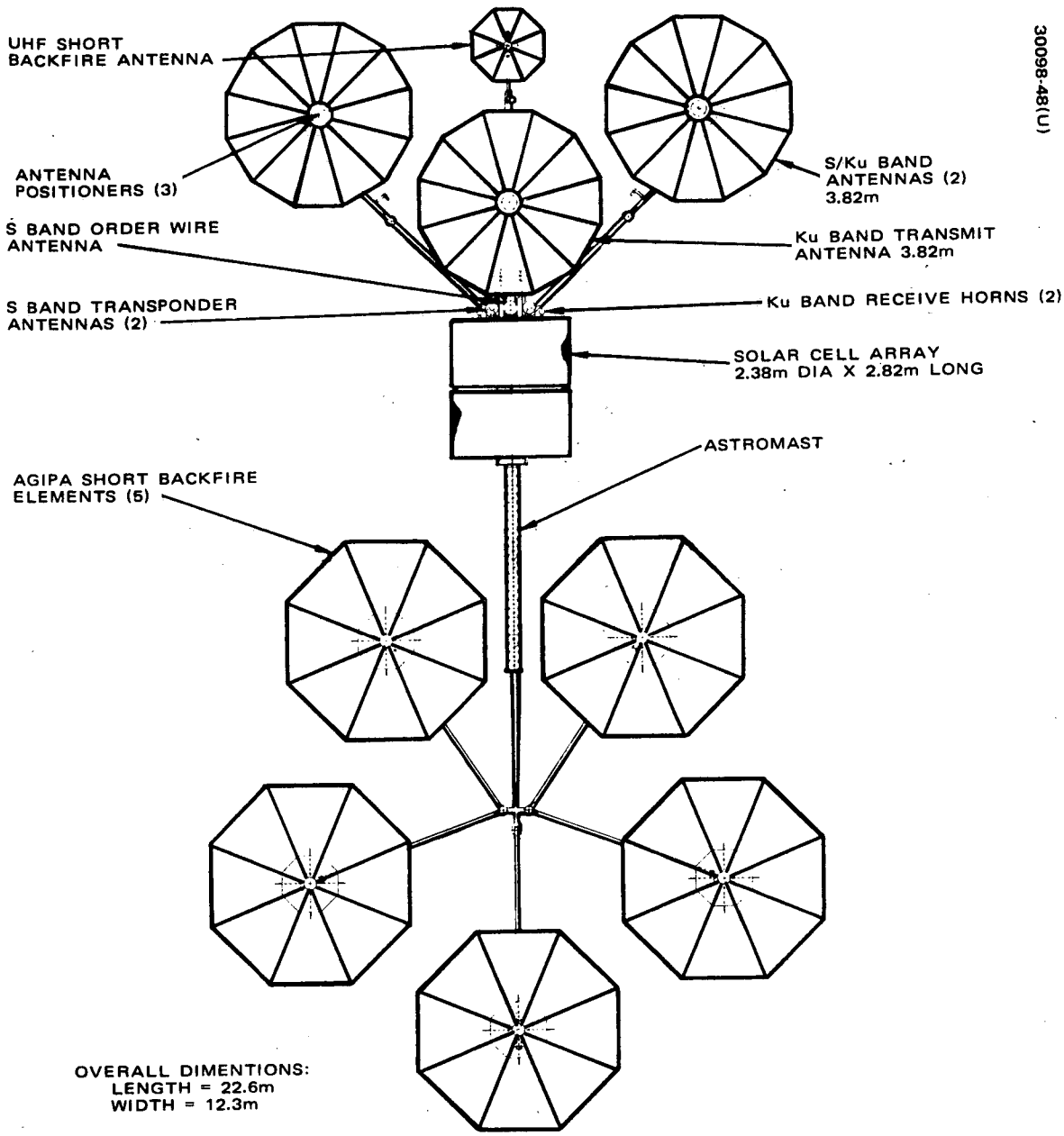

Figure 44. Atlas-Centaur Launched TDRS Orbital Configuration

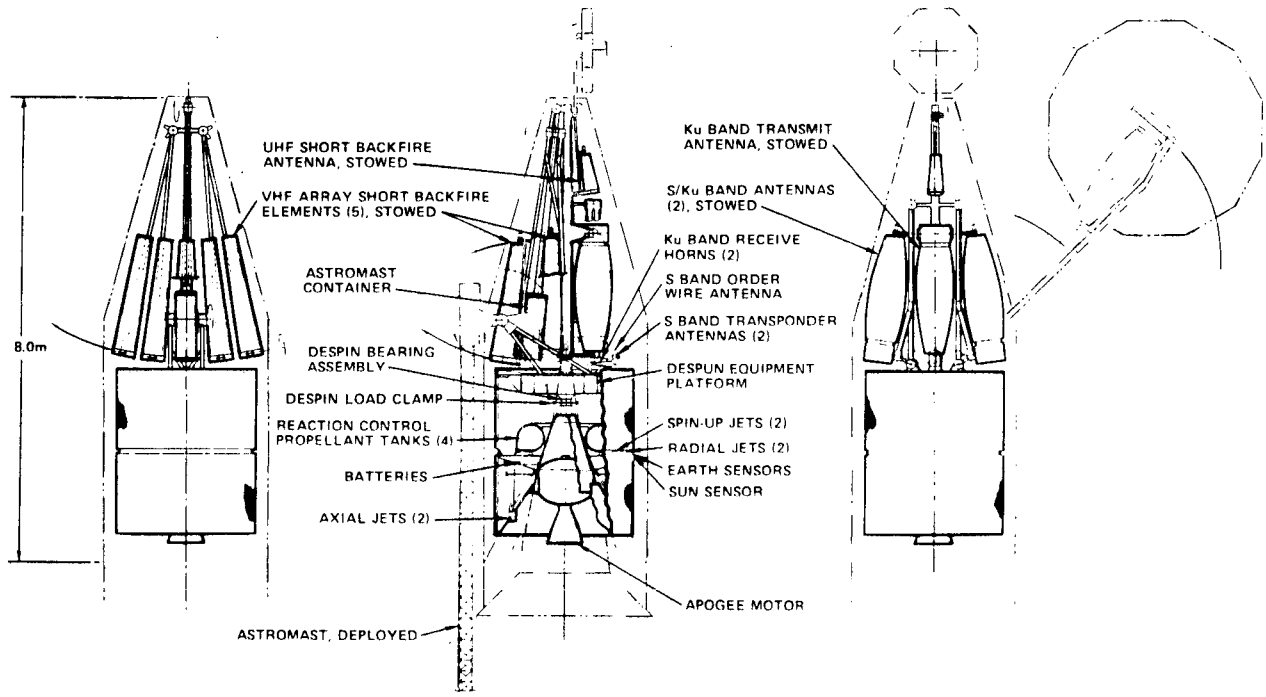

Figure 45. Atlas-Centaur Launched TDRS Stowed Configuration

the repeater payload. The spinning rotor provides a basic gyroscope stability to the spacecraft.

The TDR spacecraft equipment is located in the body of the vehicle on either spinning or despun equipment platforms as appropriate. Modification of Intelsat IV hardware is required for the TT&C, attitude control, and structure subsystems to meet TDRS specifications or mission performance requirements. Intelsat IV propulsion and thermal control subsystems are not affected by the TDRS payload requirements. TT&C modifications are required to meet system interface and capacity requirements. The despin subsystem will require redesign of the Intelsat IV control electronics unit because of the large change in payload configuration and to mass properties. Structural changes are required because of the change in spacecraft loading during launch. The principal item affected is the despun launch load clamp.

Stowage of the TDR antenna complement in the Intelsat IV payload fairing requires an extensive amount of folding of these structures in Figure 45. A 4λ AGIPA size was selected to avoid a more complex deployment or the necessity of extending the length of the payload fairing. The antenna elements are folded using the umbrella principle developed by Radiation, Inc. for the high gain S and Ku band antennas.

A despun section houses the communication equipment and some of the telemetry, tracking, and command equipment. Electronic equipment are mounted on a thermally controlled platform. Antennas are mounted off the platform on a mast type support structure.

The spinning section supports and houses the propulsion, electrical power, attitude control, and some of the telemetry, tracking, and command equipment. The apogee motor is installed in the central thrust tube. Hydrazine tanks, batteries, battery controllers, despin control electronics, and tracking, telemetry, and command equipment are mounted on the ribs and small equipment platforms spanning the ribs. Attitude control sensors, radial control jets, and umbilical connectors are installed in an annular section between parts of the solar cell array. The axial jets are mounted on truss supports and protrude through the aft thermal barrier.

An estimate of the mass of the spacecraft and subsystem is presented in Table 19. The propulsion selected for this design is the Intelsat IV apogee motor with a preburn of 77 kg of hydrazine to maximize the injected mass using the SVM-4A apogee motor. A contingency mass of 100.5 kg is available which is adequate in view of the extensive use of Intelsat IV equipment.

Component masses are based on the use of developed hardware or extrapolated from recent program developments. See Table 20 for a summary of the mass properties of subsystems and components. Repeater equipment estimates are based on TACSAT UHF equipment and more recent laboratory developments. Microwave equipment masses are extrapolated from developments at X and Ku band. TT&C component frames are based on the use of modified Intelsat IV equipment and a transponder being developed for SMS by Philco-Ford.

TABLE 19. SPACECRAFT MASS SUMMARY

Subsystem	Mass, kg
Repeaters	73.0
Telemetry, tracking and command	19.5
Antennas	96.5
Attitude control	32.8
Reaction control, dry	18.0
Electrical power	93.9
Wire harness	30.0
Apogee motor burned out	57.0
Structure	236.3
Thermal control	30.0
Contingency	134.3
Spacecraft, final orbit	821.3
Hydrazine synchronous orbit	58.8
Spacecraft, initial orbit	880.1
Apogee motor expendables	652.7
Hydrazine, orbit injection	77.4
Spacecraft, transfer orbit	1610.2
Hydrazine, transfer orbit	4.8
Spacecraft, separation	1615.0
Spacecraft adapter	61.0
Payload at launch	1676.0

Antenna masses are based on prototype development by Radiation, Inc. and on antenna developments for ATS, TACSAT, and Intelsat IV. Attitude control and reaction control equipment are derived from Intelsat IV. The BAPTA mass is quoted for the bearing assembly and power and signal transfer assemblies. The despin load clamp mass has been itemized under the structure subsystem.

Electrical power equipment is derived from Intelsat IV. More efficient solar cells have been selected and the solar cell array mass adjusted for this change. Larger battery cells have also been selected to match the increased output of the solar cell array.

The apogee motor for this configuration is the SVM-4A which is used in the Intelsat IV spacecraft. Propellant and expended inerts are tabulated in the summary mass statement.

TABLE 20. SUBSYSTEM AND COMPONENT MASS PROPERTIES

Subsystem/Item	Quantity		Mass, kg
	Available	Required	
Repeater subsystem			73.0
Transmitter; LDR/MDR/HDR Return	2	1	11.4
Transmitter; HDR Forward	2	1	6.2
Receiver; CMD/LDR Forward	2	1	3.4
Receiver; HDR Return	2	1	6.9
Receiver; MDR/HDR Forward	2	1	5.1
Transmitter; MDR Forward	4	2	11.6
Receiver; MDR Return	4	2	3.0
Receiver; order wire	2	1	1.9
Transponder; S band	2	1	4.0
Transmitter; LDR Forward	2	1	4.6
Receiver; LDR Return	16	8	6.4
Frequency synthesizer	2	1	8.5
Telemetry and command subsystem			19.5
Despun decoder	2	1	2.7
Despun encoder and multiplexer	2	1	4.2
Spun decoder	2	1	2.7
Spun encoder and multiplexer	2	1	5.0
Despun squib driver	1	1	3.5
Spun squib and solenoid driver	1	1	1.4
Antenna subsystem			96.5
Paraboloid reflector, Ku band	1	1	7.9
Horns, Ku band	2	2	0.5
Paraboloid reflector, S and Ku band	2	2	17.8
Backfire, S band	2	2	1.0
Backfire, UHF	1	1	2.5
Backfire, VHF	5	5	30.0
Bicone, S band	1	1	1.0
Antenna positioner	3	3	12.6
Position controller	3	3	2.7
Coax waveguide			20.0
Attitude control subsystem			32.8
BAPTA	1	1	13.7
Earth sensors	3	2	2.8
Sun sensors	1	1	0.1
Despun control electronics	2	1	4.4
Active nutation control	2	1	1.8
Nutation damper	2	1	10.0

Table 20 (continued)

Subsystem/Item	Quantity		Mass, kg
	Available	Required	
Electrical power subsystem			93.9
Solar cell arrays	2	2	39.8
Batteries	2	2	47.2
Battery controller	2	2	2.6
Heater controllers	1	1	1.1
Miscellaneous hardware	1	1	0.5
Voltage limiter	6	4	2.7
Reaction control subsystem			18.0
Tanks	4	4	9.5
Thrusters	6	3	3.0
Filters	4	4	0.6
Valves fill vent	1	1	0.3
Valves latching	5	5	0.5
Pressure transducer	2	2	0.5
Plenum chambers	2	2	0.2
Manifold fittings		2	2.3
P- Pressurant			1.1
Apogee motor burned out	1		57.0
Structure			236.3
Solar array substrate	2	2	34.3
Spin structure	1	1	50.0
Despun equipment platform	1	1	60.0
Equipment support	1	1	20.0
Antenna support			60.0
Despun clamp	1	1	7.0
Balance mass			5.0
Thermal control			30.0
Spin thermal equipment	1	1	25.0
Despun thermal equipment	1	1	5.0
Wire harness			30.0

Structure and thermal control masses estimates are based on adaptation of Intelsat IV design practice to this TDR spacecraft design. The principal change derives from the large mass of antennas which are carried forward of the spacecraft despun platform during launch. The resulting launch loads will require local strengthening of the Intelsat IV structure. The tabulated values are a preliminary estimate of the required structure mass. Similarly, thermal control is tailored to meet the specific TDRS design requirements. Addition of insulation is required for antenna support structure and the estimated mass has been adjusted from the Intelsat IV thermal control mass accordingly.

The primary TT&C requirements are to provide telemetry data and command control of the spacecraft using the GSFC standard TT&C formats. These requirements are satisfied via either the primary telecommunication service system at the Ku band frequency, Figure 46, or the backup telemetry transmitter and command receiver at S band. The S band transponder system is to be compatible with the GRARR operational requirements to provide data for orbit determination during this phase. Once the spacecraft is on station, the S band transponder system will be used as a backup to the Ku band system in providing TDRS TT&C links to the ground station. The telemetry system provides data for the determination of the TDRS performance, status, operational mode, attitude, and antenna pointing. The command system provides control of the spacecraft for selection of redundant units, operational mode changes, stationkeeping, and orientation of the spacecraft and the antenna.

The electrical power subsystem provides power continuously for a minimum of 7 years. The power requirement for the different operating modes for both the sunlit and eclipse portion of the orbit are listed in Table 21. The payload includes a continuously operating command and data relay for both LDR and MDR users. In addition, a voice relay will be provided to orbiting manned spacecraft. With the user spacecraft in an approximately 100 minute orbit, an S band forward voice link can be operational up to a maximum of 50 percent of the time. No UHF voice link is provided. Voice operation on the return links is unrestricted except for time sharing the S band channels with various users. These power requirements include a 7 to 10 percent contingency reserved for future growth.

The power levels required for the TDRS mission can be achieved using an Intelsat IV size solar cell array with currently available higher efficiency solar cells. This minimum change is planned for all programs which will use the Intelsat IV spacecraft in the future.

The reliability prediction was obtained by developing a model for each of the subsystems based on the subsystem configuration. Failure rates were derived for each functional element in the model. The failure rates were obtained by the parts count method with the Hughes E factor applied, or from estimates of similar units. Subsystem and system reliability was calculated by using the failure rates in the subsystem mathematical model.

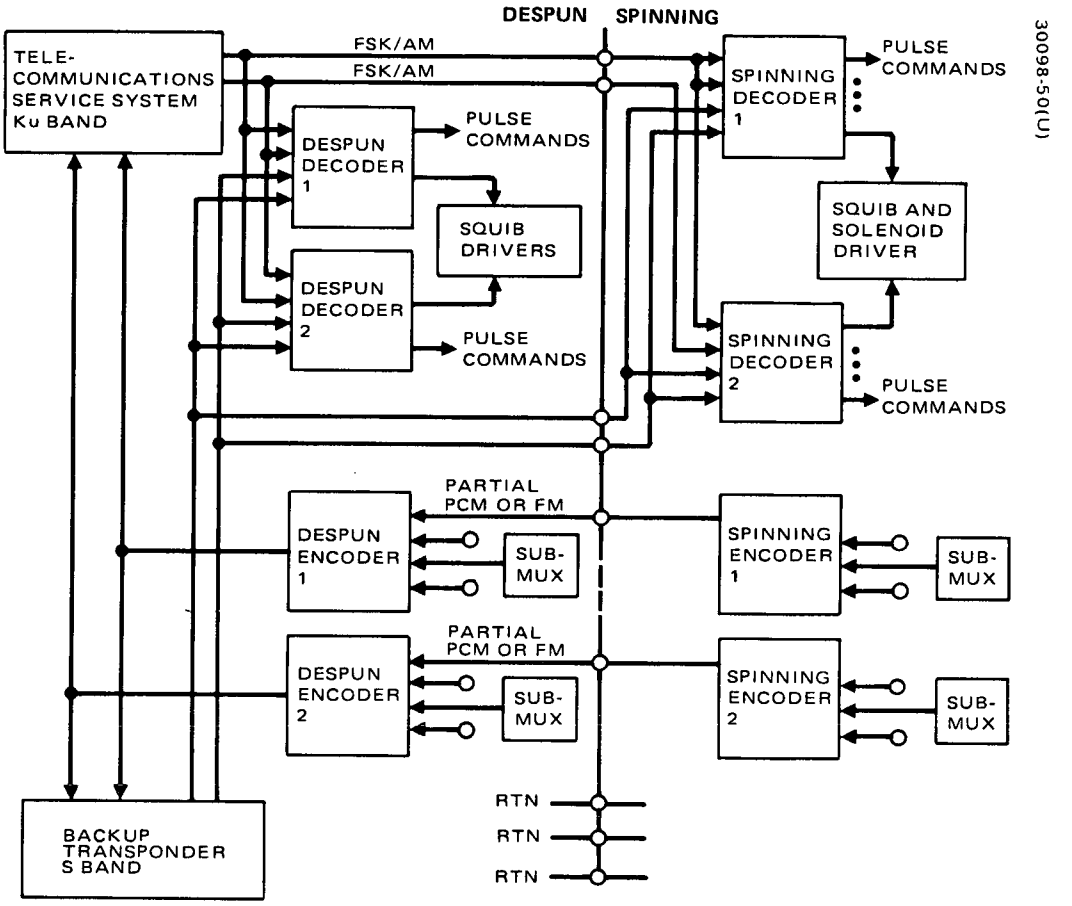

Figure 46. Tracking, Telemetry, and Command Subsystem

TABLE 21. ELECTRICAL POWER REQUIREMENTS

Equipment	Watts at 24.5 Volts			
	Eclipse Season		Solstice Season	
	Command Mode	Intermittent S Band Voice	Command Mode	Intermittent S Band Voice
HDR return TX (Ku)	30	30	30	30
LDR/MDR return TX (Ku)	9	9	9	9
HDR forward TX (Ku)	27	27	27	27
MDR Forward TX No. 1 (S) Command Voice and data	25	25	25	25
MDR forward TX No. 2 (S) Command	25	–	25	–
Voice and data	–	100	–	100
LDR forward TX (UHF) Command and data	146	146	146	146
S Band transponder	24/2	24/2	24/2	24/2
Receivers, processors, etc.	48	48	48	48
Telemetry, tracking and command	16	16	16	16
Antenna position control	12	12	12	12
Despin control	20	20	20	20
Thermal control	6	6	6	6
Power electronics	1	1	1	1
Battery charging	109	36	36	36
Distribution losses	14	14	14	14
Power required	512/490	514/492	439/417	514/492
Contingency	60/82	58/80	101/123	26/48
Solar power available	572	572	540	540

The results of these calculations are listed in Tables 22 and 23 for the launch and deployment and operational spacecraft, respectively. The communication and antenna positioning subsystem reliability is lower than the other subsystems in spite of the incorporation of practical redundancy due to the complexity of this subsystem.

4.3 SUBSYSTEM DESCRIPTION

The Atlas Centaur launched TDRS is comprised of nine major subsystems whose functional and performance characteristics are described in the following sections.

C-2

TABLE 22. LAUNCH AND DEPLOYMENT

Subsystem	Reliability Estimate	Estimate Basis
Apogee kick stage	0.9924	Intelsat IV program estimates Estimates (flights: 4 for 4 successful)
TT&C	0.9999	Subsystem analysis
Separation and deployment	0.995	Subsystem analysis
ACS and RCS	0.9999	Subsystem analysis
Launch booster	0.85	Launch experience
Total	0.839	

TABLE 23. OPERATIONAL SPACECRAFT

Subsystem	5 Year Reliability Estimate
Communication and antenna positioning	0.826
Telemetry and command	0.926
Attitude control	0.956
Electric power	0.984
Harness	0.984
Reaction control	0.972
Total	0.688

4.3.1 Telecommunications Service System

The TDRS telecommunications service system is designed to provide low data rate (LDR), medium data rate (MDR), and high data rate (HDR) services. The low data rate return link includes a VHF AGIPA concept for RFI rejection and includes voice data transmissions for manned spacecraft users. The MDR service is provided at S band with a 2 Kbps command data rate capability plus voice data to manned users. Two simultaneous channels are provided with a return link data rate capability of 1 Mbps. Other S band services include an order wire receiver and an S band transponder. The transponder provides the capability of direct ranging by trilateration from ground stations other than the TDRSS ground terminal. Initial acquisition and backup TT&C are also provided by the S band transponder using an omnidirectional antenna. One HDR channel is provided at Ku band frequencies where adequate bandwidths are available for the necessary 50 Mbps forward and 100 Mbps return link data rates. Available technology allows the performance requirements to be met with state of the art hardware devices.

The space-to-space MDR and HDR links use three interchangeable dual feed S/Ku band antennas. The TDRS Telecommunications Service Subsystem requirements are summarized in Table 24.

The simplified block diagram of Figure 47 illustrates the TDRS repeater subsystem design configuration providing the required telecommunications service. The repeater is a frequency translation type providing coherent frequency translations at all bands. Every active element in the repeater subsystem is redundant.

A multichannel Ku band receiver receives ground transmitted command, voice, and beacon signals through an earth coverage horn antenna. TDRS commands are sent to the TT&C subsystem, the beacon signal is processed and phase locked to a frequency synthesizer reference source to provide coherency, and the LDR command and voice data are distributed via a power divider to the UHF transmitter for frequency upconversion and radiation to user spacecraft. A multichannel Ku band receiver and high gain antenna is used for the two MDR channels and the HDR channel. The MDR signals may be transmitted to the user spacecraft over three S band links. Upon return, the S band MDR data from user spacecraft is double conversion frequency translated to a Ku band link for transmission to the ground. A linear Ku band transmitter is used for MDR, LDR, and telemetry information. The HDR channel is transmitted to the users at Ku band and received at Ku band.

The VHF antenna is a five element array utilizing the AGIPA concept. Therefore the LDR return link contains 10 separate signal channels to be processed on the ground in an attempt to overcome RFI degradations. The HDR and MDR user links utilize dual feed parabolic reflectors, one for each MDR channel, and an RF switch to select the antenna to be used for the HDR channel.

The communications repeater receiver characteristics listed in Table 25 are those of typical current state of the art hardware. The Ku band receivers having noise temperatures of 440, 1170, and 2600 K are achieved using parametric amplifiers, tunnel diode amplifiers, and low noise mixers in various combinations. Transistor low noise preamplifiers are used at VHF frequencies to achieve a 420 K noise temperature, and parametric amplifiers are employed for the S band MDR return link receivers to achieve a noise temperature of 100K.

The transmitter characteristics are listed in Table 26. The required EIRP for each transmitter is shown and the major gain and loss contributors leading to the required DC power are listed also to illustrate the derivation of the total power required of each transmitter.

The repeater has several bands of operating frequencies and requires a variety of transmitters. The transmitters are the repeaters' largest power consumer, therefore, design emphasis is placed upon transmitter efficiency. All but the Ku band TWTs are solid state devices. The TWTs have a dual

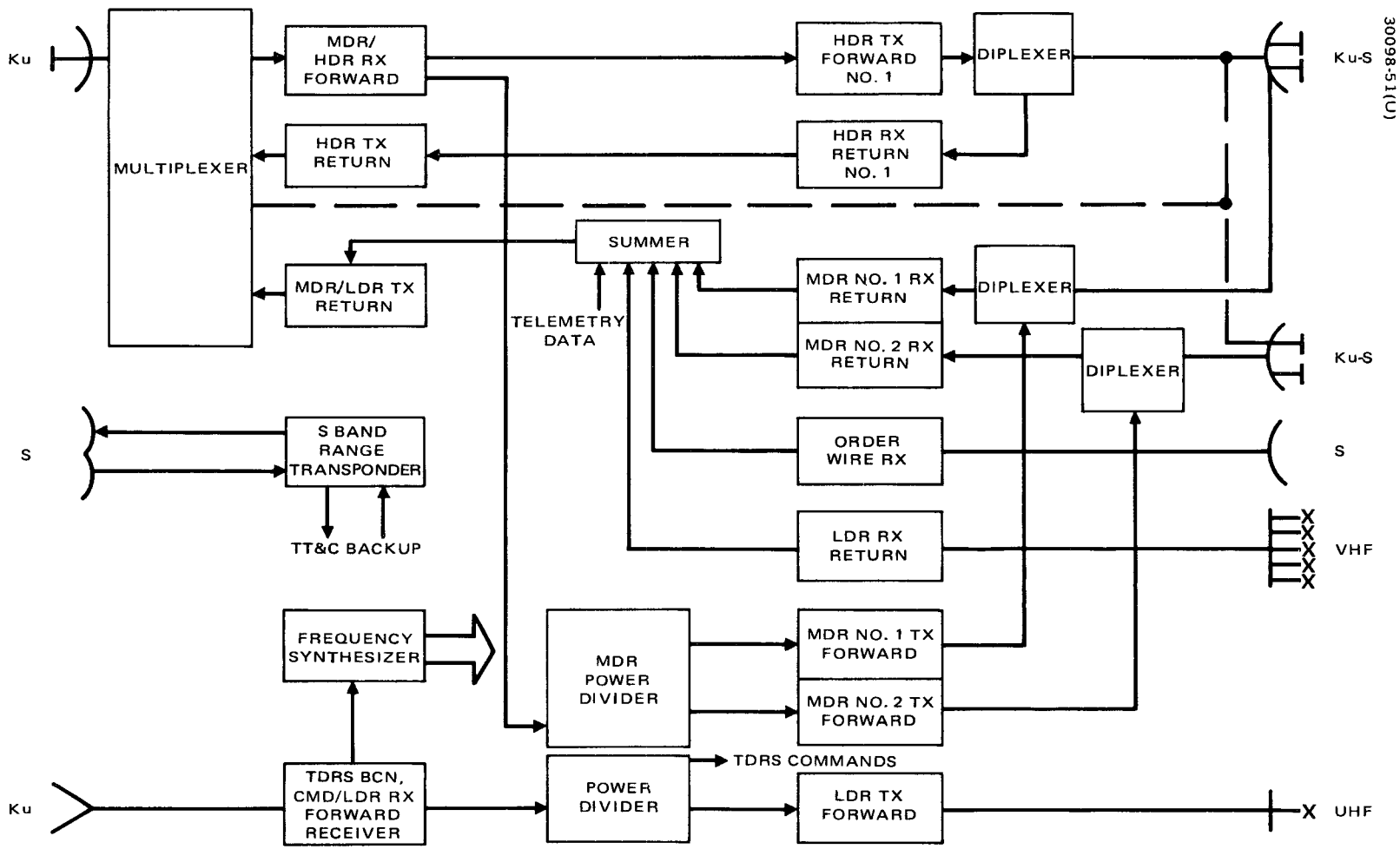

Figure 47. TDRS Repeater

TABLE 24. TDRS TELECOMMUNICATIONS SERVICE SUBSYSTEM REQUIREMENTS

LDR Forward Link (to user)	
Forward link EIRP	30 dBW/channel
Number of channels	1
Frequency	400.5 to 401.5 MHz
Field of view	30 degrees
Coding	PN
Antenna	Backfire, single UHF
Data rate	300 bps command
RF bandwidth	1 MHz
LDR Return Link (from user)	
Return link G/T	-10.2 dB/Kelvin
Number of channels	20
Frequency	136 to 138 MHz
Voice modulation	Delta modulation
Telemetry coding	Code division multiplexing Convolution encoding
Antenna	Five element AGIPA
Data rate	19.2 kbps voice, 1.2 kbps telemetry
RF bandwidth	2 MHz
MDR Forward Link (to user)	
Forward link EIRP	47 dBW 41 dBW
Number of channels	2
Frequency	2038 to 2118 MHz
Field of view	2.8 degrees
Antenna	Dual feed paraboloid
Data rate	1-2 kbps command channel 2-24 kbps voice channels
RF bandwidth	30 MHz/channel
MDR Return Link (from user)	
Return link G/T	10.2 dB/Kelvin
Number of channels	2
Frequency	2220 to 2300 MHz
Antenna	Dual feed paraboloid
Data rate	1 Mbps telemetry (maximum)
Order wire G/T	-15.2 dB/Kelvin
RF bandwidth	10 MHz
HDR Forward Link (to user)	
Forward link EIRP	59 dBW 51 dBW
Number of channels	1
Frequency	14.76 to 14.86 GHz
Antenna	Dual feed paraboloid
Data rate	50 Mbps
RF bandwidth	100 MHz

Table 24 (continued)

HDR Return Link (from users)	
Return link G/T	23.2 dB/K
Number of channels	1
Center frequency	13.850 GHz
RF bandwidth	200/100/50/10 MHz
Antenna	Dual feed paraboloid
Data rate	100 Mbps
MDR/LDR Return Link (to ground)	
Return link EIRP	53.1 dBW
Number of channels	2 MDR (10 MHz each) 10 LDR (2 MHz each) 1 TDRS TLM 1 order wire
Frequency	14.60 to 14.695 GHz
Antenna	Paraboloid
Data rate	1 Mbps maximum
RF bandwidth	95 MHz
HDR Return (to ground)	
Return link EIRP	59 dBW 51 dBW
Number of channels	1
Frequency	14.96 to 15.16 GHz
Antenna	Paraboloid
Data rate	100 Mbps
RF bandwidth	200 MHz
MDR/HDR Forward Link (from ground)	
Forward link G/T	17.3 dB/Kelvin
Number of channels	1 HDR (100 MHz) 2 MDR (30 MHz)
Frequency	13.460 to 13.690 GHz
Antenna	Paraboloid - HDR MDR
Data rate	HDR 50 Mbps MDR 1 Mbps maximum
RF bandwidth	230 MHz
S Band Ranging Transponder	
Transmit EIRP	20 dBW
Number of channels	1
Frequency	
Transmit	2210 MHz
Receive	2029 MHz
Antennas transmit and receive	Short backfire type
RF bandwidth	8 MHz

Table 24 (continued)

TDRS CMD, Beacon, and LDR Forward Link (from ground)	
Forward link G/T	-13.2 dB/Kelvin
Number of channels	1 LDR 1 beacon 1 command
Frequency	13.4 to 13.42 GHz
Antenna	Horn
RF bandwidth	20 MHz

TABLE 25. TDRS REPEATER RECEIVER CHARACTERISTICS

Receiver	Frequency Band	Bandwidth, MHz	Noise Temperature, K	Preamplifier Type
MDR/HDR forward	Ku	230	2600	None
HDR return	Ku	200/100/50/10	440	Paramplifier/ TDA
TDRS BCN, CMD, LDR forward	Ku	20	1170	TDA
MDR return	S	10	100	Paramp
Order wire	S	1	420	Transistor
LDR return	VHF	2	420	Transistor
S band transponder	S	8	420	None

TABLE 26. TDRS TRANSMITTER CHARACTERISTICS

Transmitter	HDR Return	LDR/MDR Return	HDR Forward	LDR Forward	MDR Forward	S Band Transponder
Frequency band	Ku	Ku	Ku	UHF	S	S
EIRP, dBW, Hi/Lo	59/51	53.1	59/51	30	47/41	20
Antenna Gain, dB	52.8	52.8	52.8	12.5	35.5	13.5
RF Loss, dB	2.7	2.7	2.2	1.0	2.8/3.0	1.5
PA Output, watts, Hi/Lo	7.8/1.2	2.0	6.9/1.1	71	27/6.3	6.3
Effeciency Amplifier, percent, Hi/Lo	33/20	30	33/20	51	28/30	30
PA dc Power, watts, Hi/Lo	23.6/6.0	6.7	20.9/5.5	140	96/21	22
Total dc Power,* watts, Hi/Lo	30/10	9	27/9	146	100/25	24/2

*Including power conversion losses.

mode power capability that is accomplished by command control of the tube anode and helix voltages. The transistor power amplifiers used in the S band and UHF transmitters are operated at maximum efficiency and are paralleled to satisfy the total power output requirement. The TWT amplifiers are redundant and the transistor amplifiers are selectable as 3 of 4 or 4 of 6 to provide excellent reliability.

The repeater subsystem component mass summary is shown in Table 27. Available quantities represent the redundancy and spare components. The required quantity represents the portions used or turned on to provide the telecommunications service.

4. 3. 2 Telecommunications Repeater Design Description

The TDRS communications repeater subsystem is designed to provide LDR, MDR, and HDR links between the user spacecraft and a central ground station. The LDR link is accomplished at VHF frequencies using the senior AGIPA antenna system for RFI rejection. Two independent MDR links are provided at S band. Each link will allow two voice signals plus 2 kbps data to be transmitted to a user spacecraft and up to 1 Mbps telemetry data to be returned.

Other S band services include an orderwire receiver and an S band ranging transponder. The transponder is compatible with present GRARR ground terminals and will provide direct ranging measurements for trilateration with three ground stations. HDR services are provided at Ku band with a 50 Mbps capability forward (to the user) and a 100 Mbps capability on the return link (from the user).

Repeater features include:

- Coherent frequency translation type
- All active elements are redundant
- Dual mode TWT power amplifiers at Ku band
- Selectable Ku band transmitter/receiver and antenna combinations
- Solid state S band and VHF power amplifiers
- Design includes IC and MIC components
- VHF senior AGIPA antenna concept in the LDR return link
- Ku band tracking antennas
- Low noise receivers with minimum complexity
- High efficiency transmitters

TABLE 27. MASS AND POWER REQUIREMENTS FOR THE REPEATER COMPONENTS

	Spacecraft Quantity	Mass, kg	DC Power at 24 Volts
Transmitter; HDR/MDR/LDR RTN		11.4	39.6
Antenna switches	2	0.4	–
Multiplexer (two transmit and one receive)	1	0.4	–
TWT and EPC	4	8.2	38.0
Driver upconverter	4	2.2	1.6
Summer	1	0.2	–
Transmitter; HDR Forward		6.2	27.0
Antenna switches	4	0.8	–
Diplexer (transmit/receive)	1	0.2	–
TWT and EPC	2	4.1	26.2
Driver upconverter	2	1.1	0.8
Receiver; CMD/LDR FWD		3.4	2.1
TDA and BPF	2	0.7	0.4
Mixer/amplifier and phase lock loop	2	2.5	1.7
Hybrid and divider	1	0.1	–
EPC	1	0.1	–
Receiver; HDR RTN		6.9	10.0
Tracking modulator	2	2.2	1.7
Preamplifier	2	2.5	5.4
Mixer/amplifier/filter	2	1.2	0.6
Tracking demodulator	2	0.9	1.8
EPC	1	0.1	0.5
Receiver; MDR/HDR FWD		5.1	5.8
Tracking modulator	1	1.1	1.7
BPF	1	0.1	–
Mixer/amplifier/filters	2	2.9	2.0
Tracking demodulator	1	0.9	1.8
EPC	1	0.1	0.3
Transmitter; MDR FWD		11.6	100/25
Driver	4	5.4	4.0
Power amplifier (4 of 6)	2	2.6	96/21
Diplexer and cable	2	3.4	–
EPC	2	0.2	–
Receiver; MDR Return		3.0	11.1
Preamplifier	4	1.6	10.0
Mixer/filter/amplifier/attenuator	4	1.2	1.0
EPC	2	0.2	0.1

Table 27 (continued)

	Spacecraft Quantity	Mass, kg	DC Power at 24 Volts
Receiver; Order Wire		1.9	1.7
BPF	1	1.1	–
Preamplifier	2	0.2	0.5
Mixer/filter amplifier/Mixer amplifier	2	0.5	1.0
EPC	1	0.1	0.2
Transponder, S Band		4.0	24.0/2.0
Receiver	2	0.6	1.0
Transmitters	2	0.9	22.0
Frequency reference	2	0.3	1.0
Filter	1	2.2	–
Transmitter; LDR FWD		4.6	146.0
Driver	2	0.6	6.0
Power amplifier (4 of 6)	6	1.5	140.0
Summer and switch	1	0.5	–
LPF	1	1.0	–
Cable	1	0.9	–
EPC	1	0.1	–
Receiver; LDR RTN		6.4	9.6
Preamplifier/BPF/amplifier	20	1.7	1.0
LO frequency source and selector	2	0.2	0.3
Preamplifier/mixer/amplifier (8 channels)	20	1.1	7.0
BPF/limiter/summer	1	0.7	–
Mixer/amplifier/filter	2	0.1	0.8
EPC	1	0.1	0.5
Cable and integrated package		2.5	–
Frequency synthesizer		8.5	7.8
Master oscillators and multiplier	2	8.4	7.3
EPC	1	0.1	0.5

The repeater design description which follows is divided into groups of units according to their operating frequency. The repeater frequency plan in Figure 48 summarizes the operational bands.

4. 3. 2. 1 Ku Band Repeater Units

The TDRS repeater subsystem units operating at Ku band consists of three transmitters and three receivers. Each of the receivers are designed to provide antenna tracking error signals derived from the antenna tracking modulators. The Ku band antennas used for the TDRS user link are dual feed S/Ku band parabolic reflectors interchangeable between Ku band transmitters and receivers.

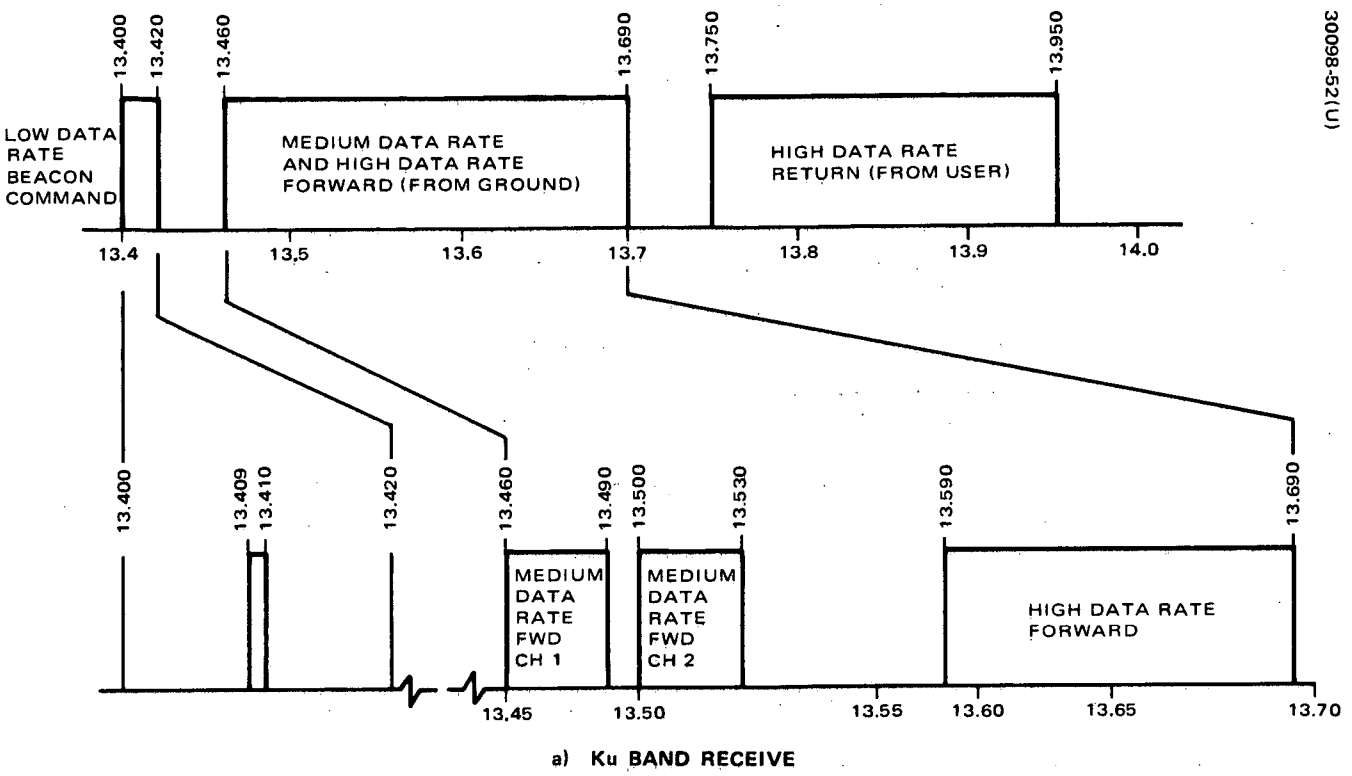

a) Ku BAND RECEIVE

Figure 48. TDRS Frequency Plan

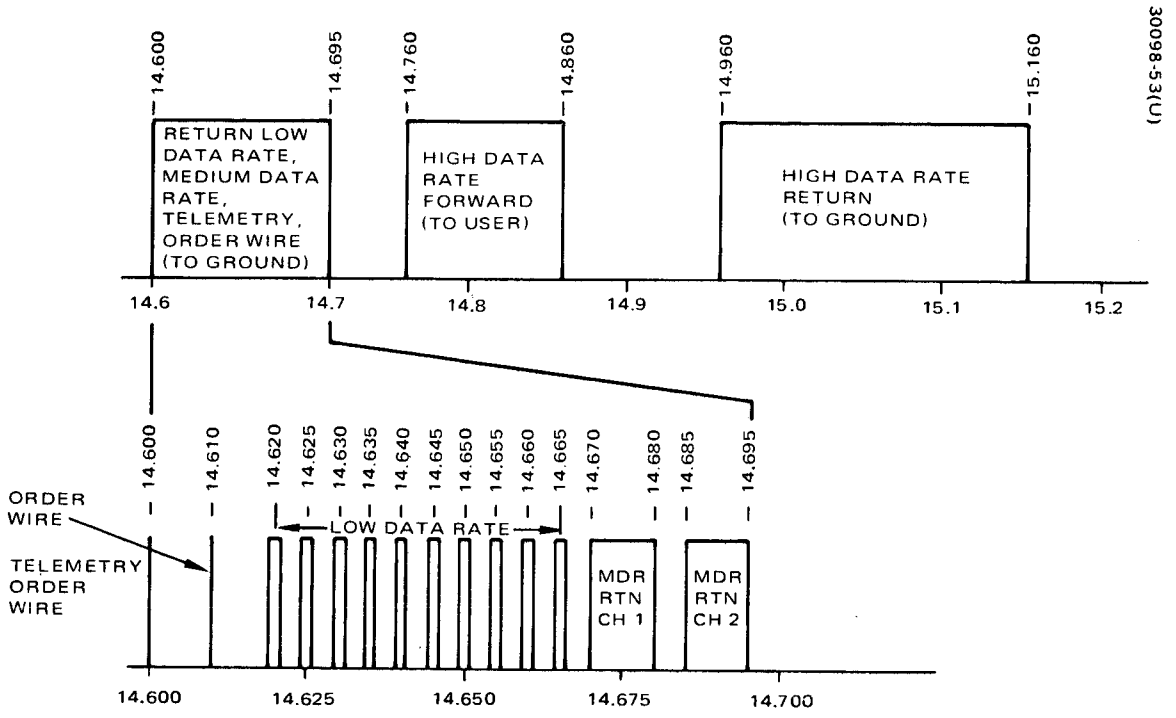

b) Ku BAND TRANSMIT

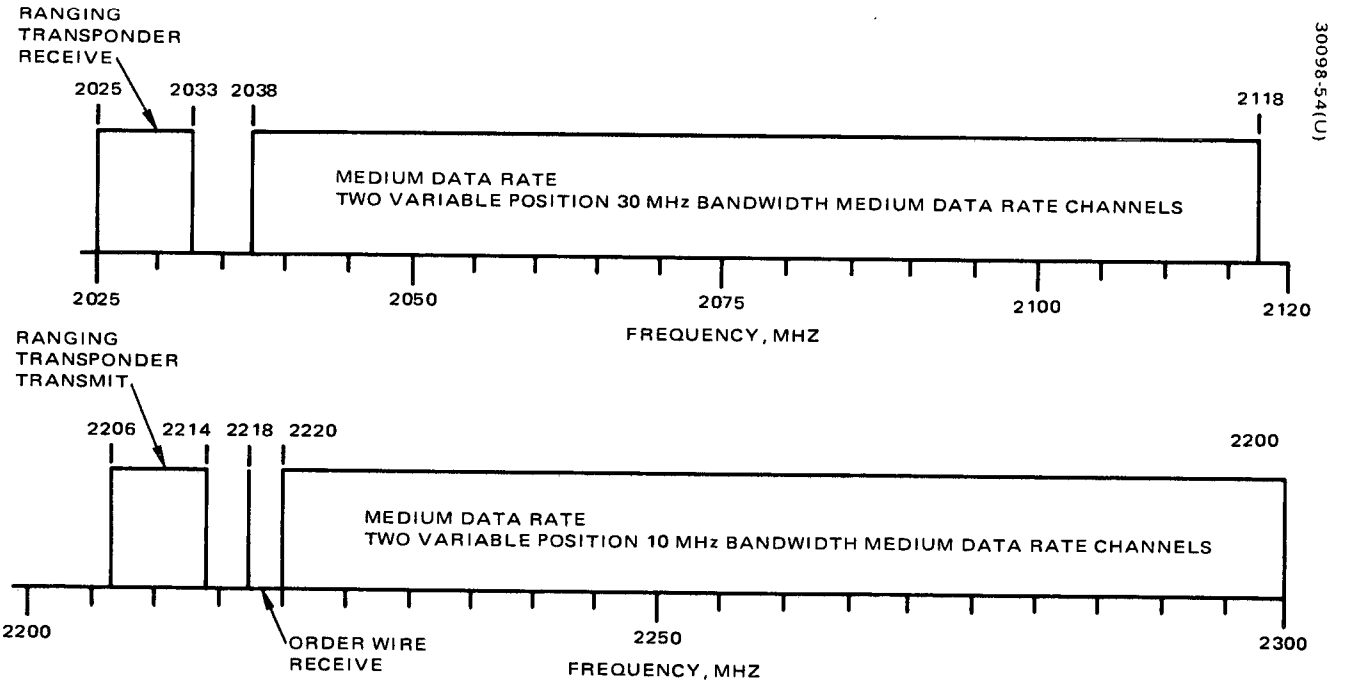

c) S BAND TRANSMIT AND RECEIVE

Figure 48 (continued). TDRS Frequency Plan

The Ku band antenna tracking modulator is shown in Figure 49. The narrowbeam Ku band antennas require precision tracking to maintain the HDR link performance requirements. This is provided by a ferrite switch modulator in the monopulse difference channel outputs from the antenna. The sum channel is diplexed with the transmitter and receiver and the receiver input is therefore a composite signal containing data and tracking modulation. The tracking error signals are processed by a tracking demodulator in each Ku band receiver and applied to the antenna tracking control circuits. Dual switch drivers provide redundancy for the only active circuits in the modulator/diplexer.

The antenna switching network is shown in Figure 50. The Ku band antennas may be used interchangeably with the Ku band transmitter and receiver. Two antennas have dual feeds for the two S band transmitters and receivers. A Ku band forward link and return link may be completed using any one of the two Ku band antennas. The switches are of the ferrite latching switch type and this configuration or matrix represents the maximum switching capability within reasonable RF loss considerations. The switches will provide added assurance of a completed HDR link in the event of antenna deployment failure. Antennas A, B, or C may be connected to the ground link transmitter and receiver, and antennas B or C to the HDR TDRS/user transmitter and receiver. The S band MDR transmitters and receivers are assigned specific antennas, B and C.

The HDR forward link transmitter provides a 100 kHz channel to the user spacecraft. The upconverter and traveling wave tube power amplifier are shown in the block diagram of Figure 51. The HDR channel signals leave the TDRS on a 14.775 or 14.875 GHz carrier. A 50 dB gain TWT operated near saturation provides the required 8.8 dBW output power. A low power 0.8 dBW mode is possible by command control of the TWT anode and helix voltages. The TWT amplifier selected is a version of space TWT designs under present development. The key performance parameter is efficiency which is about 33 percent in the high power mode and 20 percent in the low power mode. This efficiency is achieved by operating the TWT at a voltage 8 percent over that corresponding to maximum gain. A cathode wearout life of 10 years is well within the state of the art.

The HDR return link receiver provides the 100 Mbps service from user spacecraft. The input signal level of -104 dBW is received on a 13.850 GHz carrier. A block diagram of a return link HDR receiver is shown in Figure 52. The HDR return link receiver requires a 440 K noise temperature preamplifier. To meet this requirement, a two stage preamplifier will be employed consisting of a parametric amplifier first stage followed by a tunnel diode amplifier providing an overall gain of 24 dB. Pump power for the parametric amplifier will be provided by a Gunn diode oscillator and, with the thermal stabilization, reliable stable gain operation of the preamplifier can be assured. A receiver bandwidth of 200, 100, 50, or 10 MHz may be selected by ground command, thus enabling optimization of the link for any user bandwidth requirements.

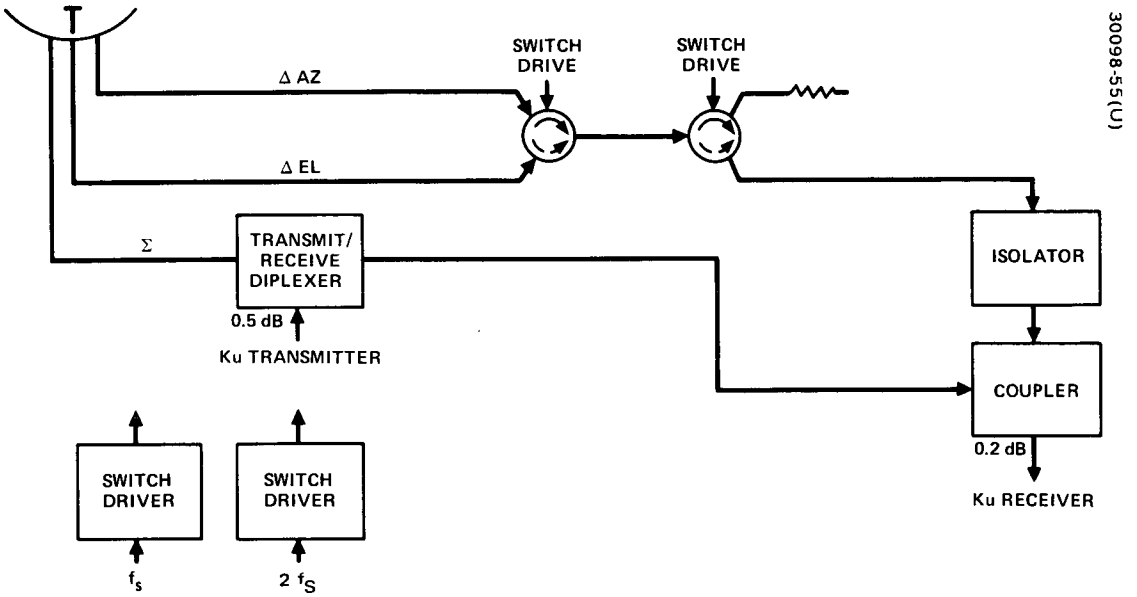

Figure 49. Ku Band Antenna Tracking Modulator/Diplexer

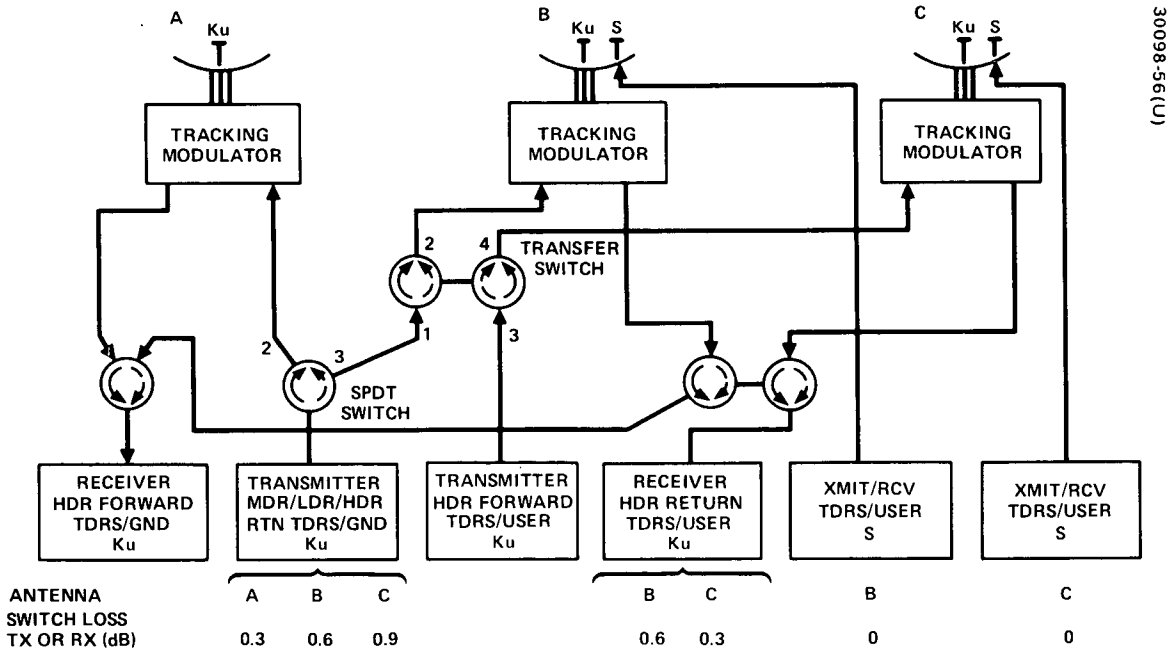

Figure 50. Antenna Switching Network

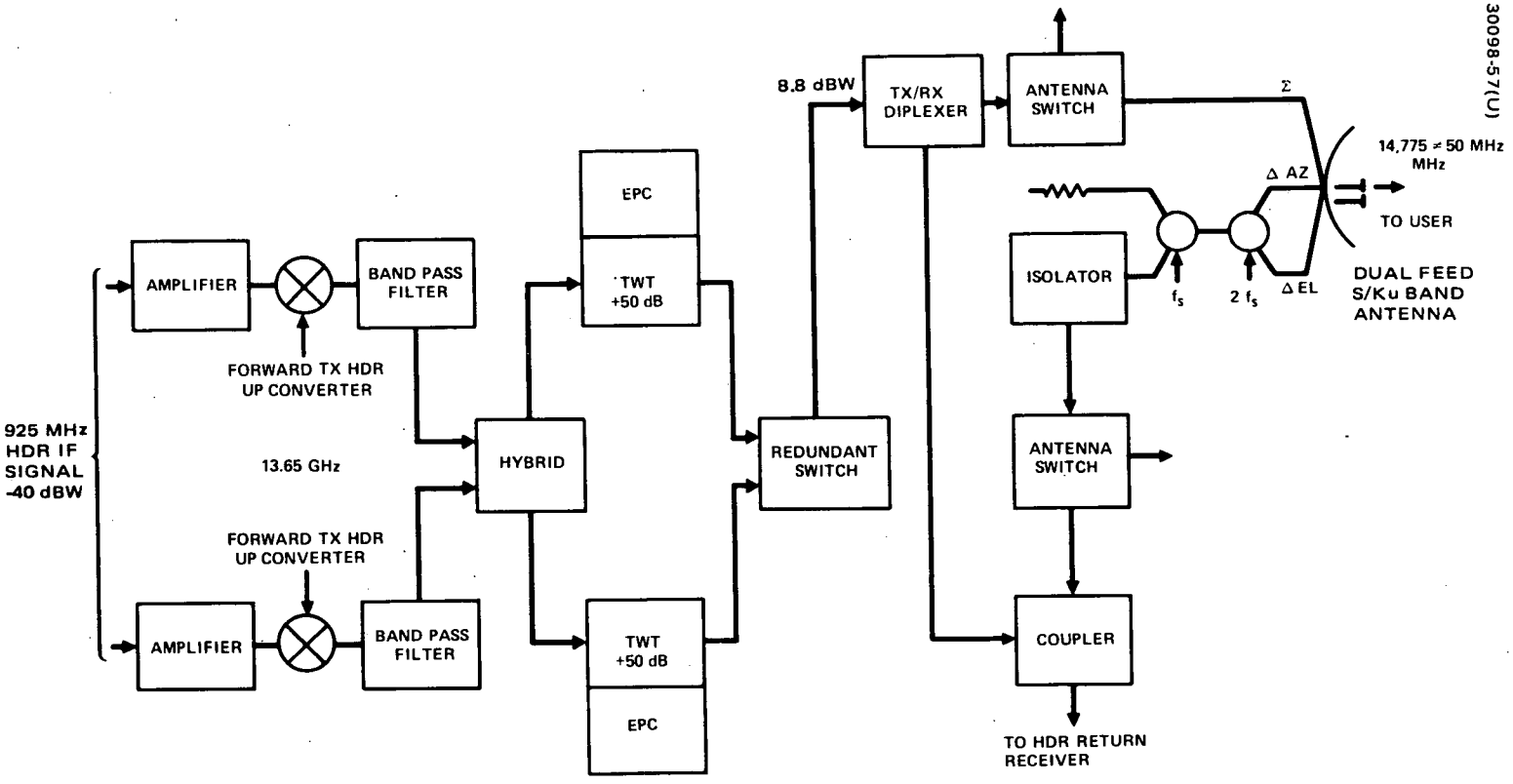

Figure 51. HDR Forward Link Transmitter and Upconverter

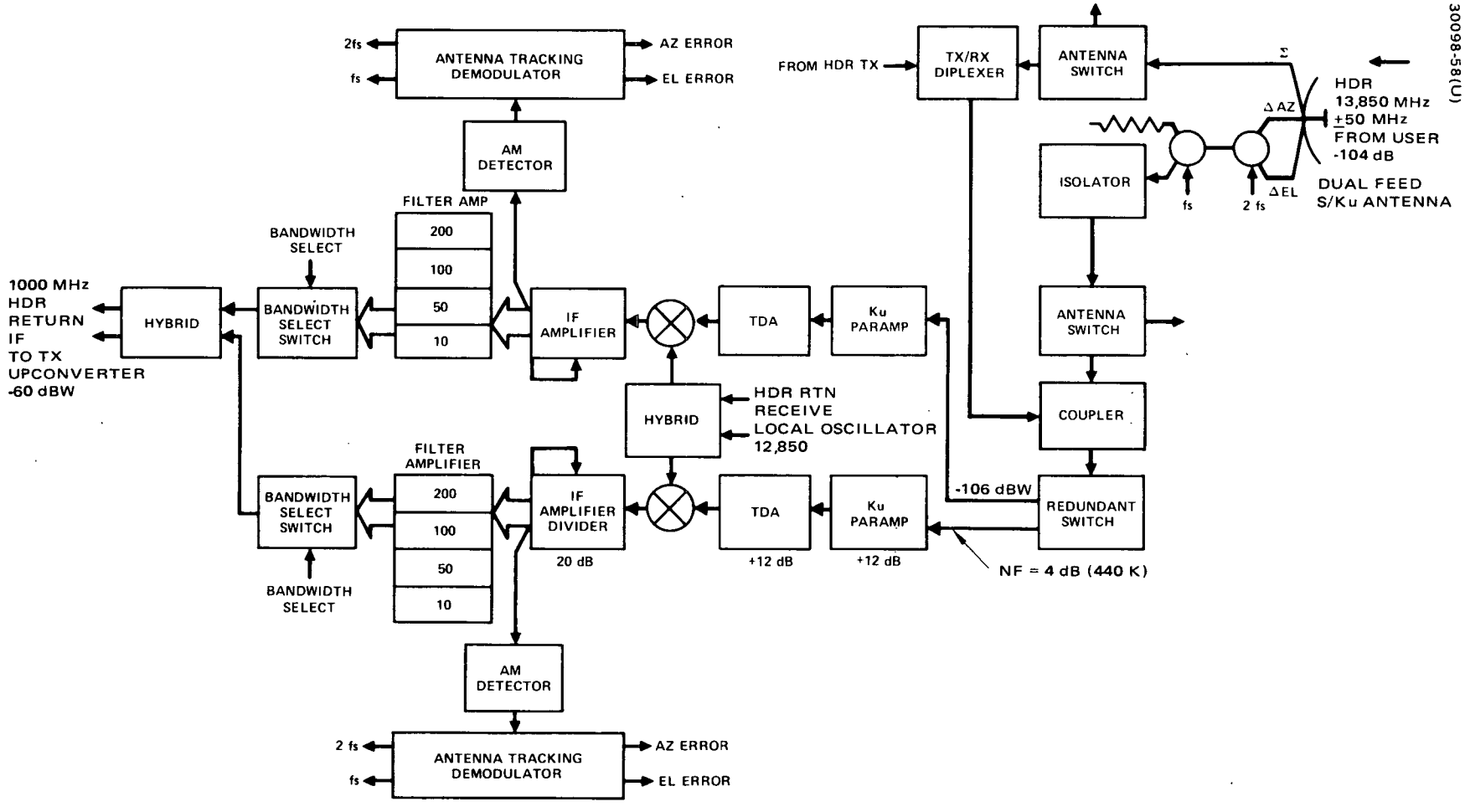

Figure 52. HDR Return Link Receiver

The data transmitted to the TDR spacecraft from the ground is received by two Ku band receivers. One receiver handles the HDR and MDR information channels and the other handles the LDR channel, as well as TDRS telemetry command signals and the reference frequency beacon signal.

The uplink MDR and HDR signals are received by a narrowbeam Ku band parabolic antenna. Difference channel outputs are combined with the sum channel output after switching and phase shifting accomplished in the tracking modulator. The input to the receiver contains the 13.46 to 13.69 GHz carrier with uplink data modulation and the pseudo monopulse amplitude modulation tracking error signals. A block diagram of the MDR/HDR forward receiver is shown in Figure 53.

The receiver processes the composite data and tracking signals through redundant mixer and amplifier filter circuits. The tracking modulation is processed in the antenna tracking demodulator to provide quadrature coordinate error signals. The demodulator is also the source of the two modulator switch driver signals. The receiver has no preamplifier and the noise temperature at the input bandpass filter is 2600 K. The moderate IF allows the use of transistor amplifiers for processing the tracking signal and increasing the drive level to the upconverter. The MDR and HDR signals are frequency multiplexed and there are separate receiver outputs for each service. The MDR IF signals are distributed to the MDR forward S band transmitters and the HDR IF signal is connected to the HDR forward Ku band transmitter.

The uplink TDRS commands, LDR, and beacon signals are received on a low gain earth coverage horn antenna having 1.85 dB gain. The carriers are within the 13.400 to 13.420 GHz band and arrive with a signal level of approximately -115 dBW. A diagram of the receiver is shown in Figure 54.

A tunnel diode preamplifier is used to establish a low noise temperature at the receiver input of 1170 K. After a first conversion to IF, the signals are separated and converted to a second IF. The beacon signal is used to phase lock a VCXO to the uplink carrier and establish a stable coherent reference signal as a source for all TDRS local oscillator and upconverter signals. The CMD/LDR forward link receiver is redundant and uses dual series dissipative regulators. Hybrid circuit designs are used to minimize mass. The receiver data outputs (MDR, LDR, and TDRS commands) are distributed to their respective transmitters or processors via a six way power divider.

The Ku band downlink MDR, LDR, and telemetry signals are transmitted on 14.6 to 14.695 GHz carriers and the HDR channels use the 14.96 to 15.160 GHz band. A block of the downlink transmitters is shown in Figure 55.

The HDR return link transmitter is similar to the HDR forward link transmitter. The HDR transmitter is combined with the MDR/LDR transmitter via a transmit diplexer to radiate from a common Ku band antenna. The MDR/LDR transmitter is operated in a linear region, at 5 dB backoff, since there are several data channels simultaneously processed. The TWT saturated output power is 3.6 dBW for the MDR/LDR transmitter. The TWT output for the HDR transmitter is 9.4 dBW for the high power mode and 1.3 dBW for the lower power mode.

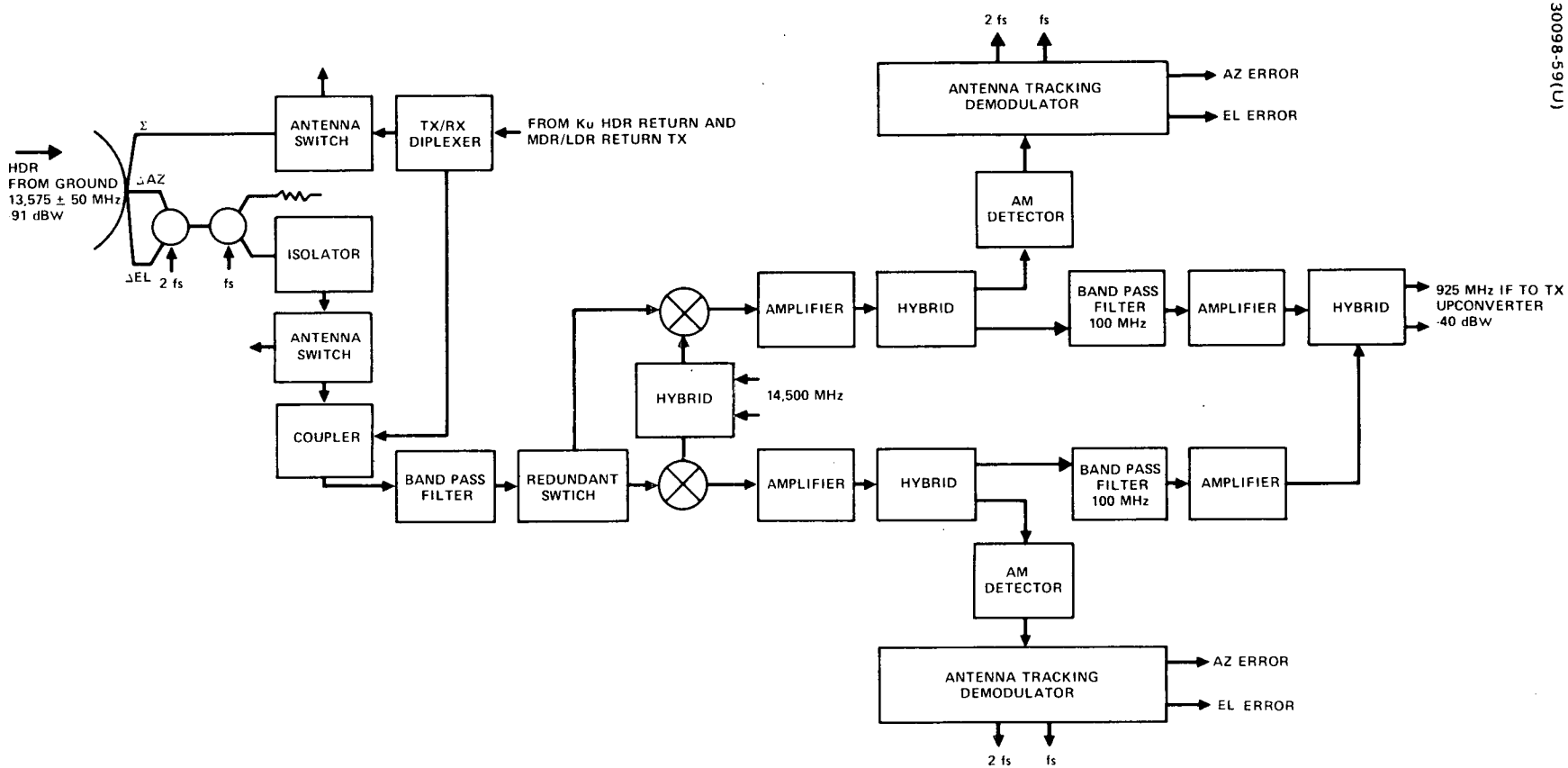

Figure 53. HDR Forward Link Receiver

30098-59(U)

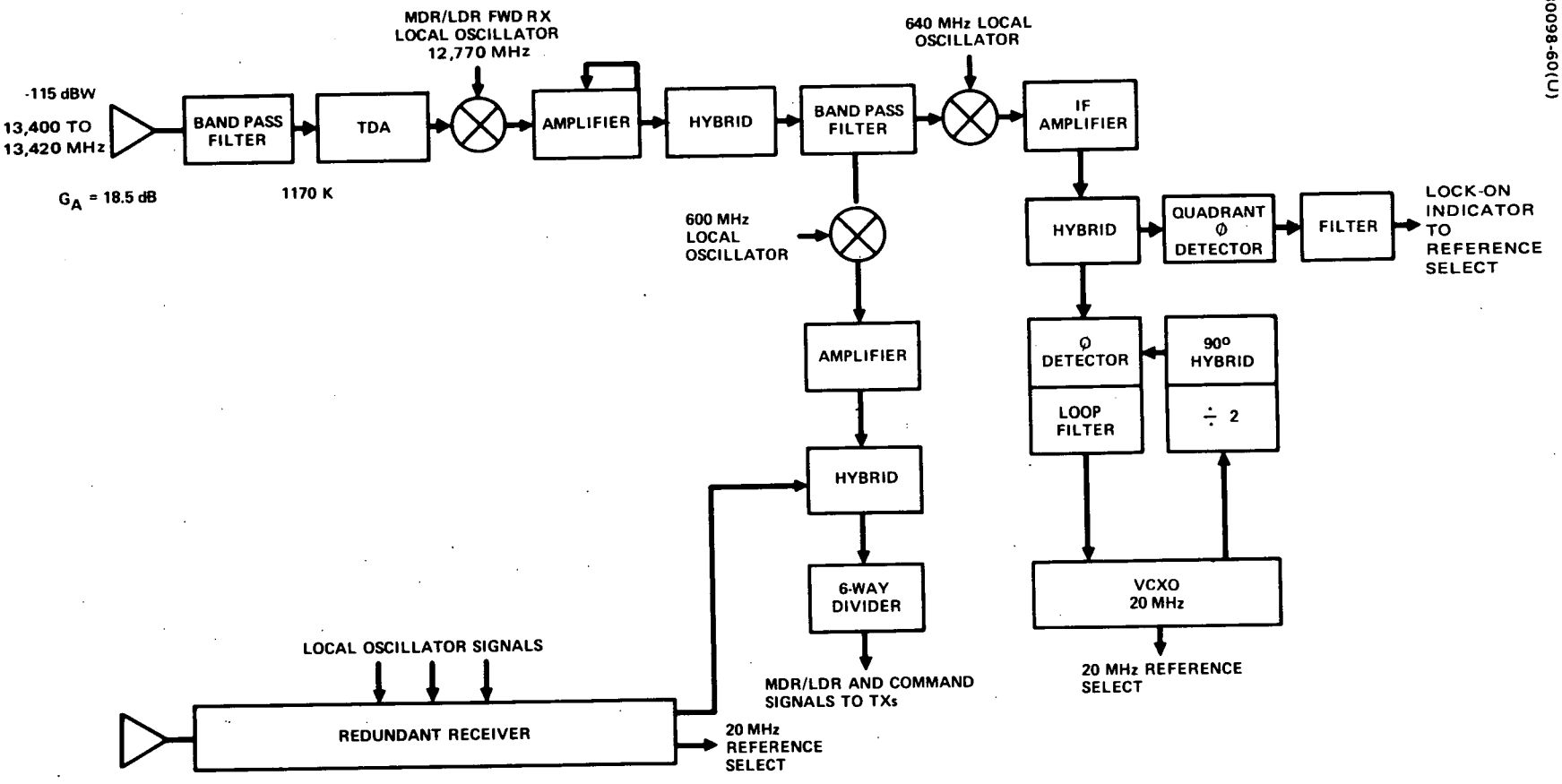

Figure 54. TDRS Command, LDR, and Beacon Receiver

30098-60(U)

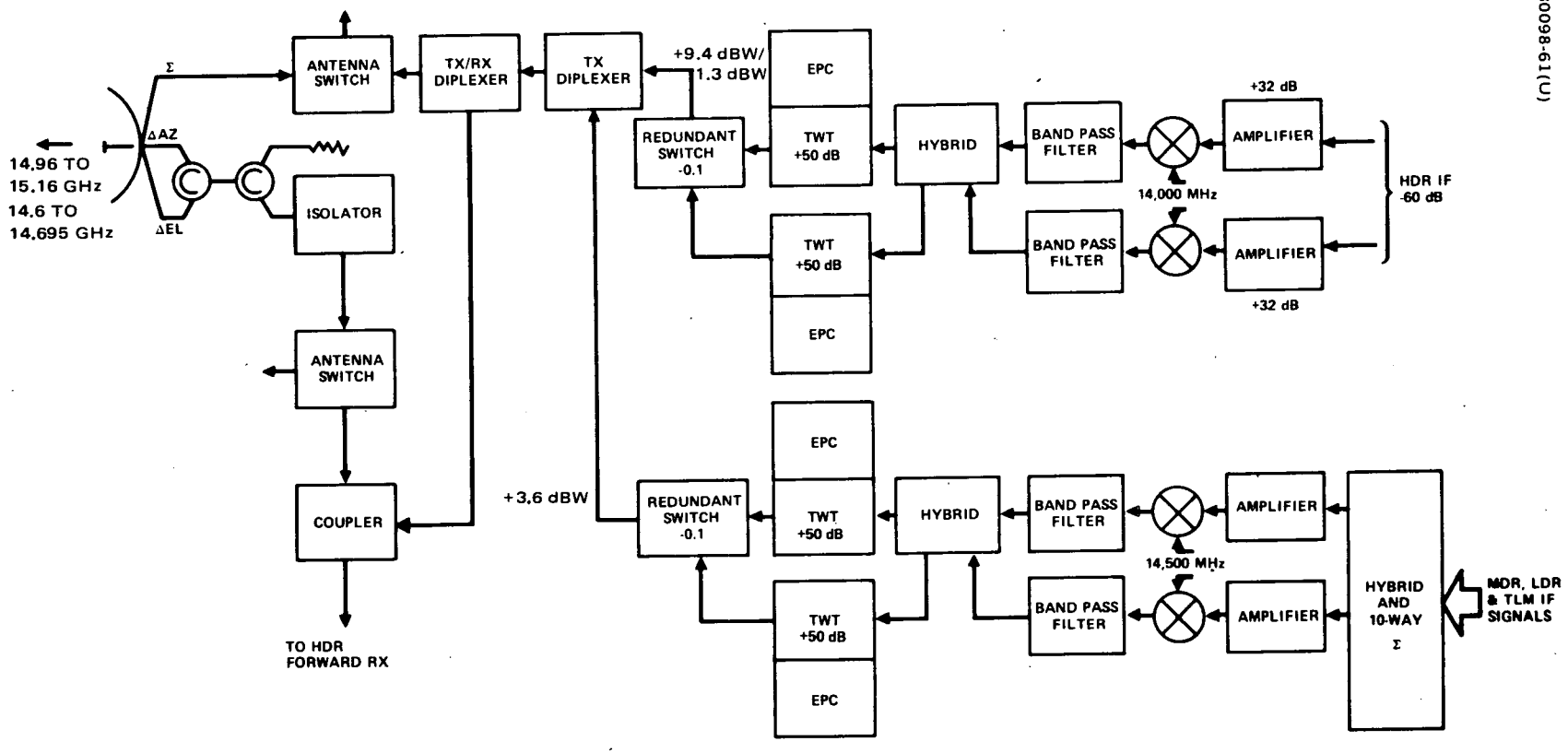

Figure 55. HDR and MDR/LDR Return Link Transmitters and Upconverters

4.3.2.2 S Band Repeater Units

The telecommunications repeater S band subsystem units provide the required MDR transmit and receive, order wire receive, and trilateral ranging functions. There are two MDR transmitters and receivers required to provide service to two separate user spacecraft. A single transmitter/receiver design is illustrated by the block diagram of Figure 56.

The MDR IF signal is frequency translated to S band antennas for solid state amplification to one of the three dual feed S/Ku band antennas for transmission to a user spacecraft. The transmit frequency is selectable in the 2025 to 2120 MHz band by a commandable upconversion local oscillator frequency 1968 to 2096 MHz. The driver output is switched directly to the antenna in the case of low power mode operation or is switched to pass through a bank of transistor amplifiers which are summed to provide a high power output. The receiver employs a parametric amplifier for the first stage, providing a noise temperature at the receiver input of 100 K. The receiver is also frequency selectable by command within the 2200 to 2300 MHz band. A step attenuator at the IF output controls the MDR return signal level driving the MDR return transmitter.

The order wire function is provided by receiving order wire signals at 2218 MHz and combining the data with the MDR and LDR IF signals for transmission on the Ku band downlink. A block diagram of the order wire receiver is shown in Figure 57. The order wire receiver is similar to the MDR receiver, however, it has a fixed frequency and narrow bandwidth. The double conversion utilizes mixing frequencies available from the frequency synthesizer to provide the proper IF. The receiver design includes redundancy and applies microstrip transmission techniques in the RF circuits to minimize mass.

TDRS ranging by trilateration is accomplished with an S band solid state transponder as shown in the block diagram of Figure 58. The S band ranging transponder is compatible with GRARR frequencies and is designed to transpond ranging data for trilateral ranging with three ground stations. The frequencies selected for TDRS ranging are near the edge of the band to minimize interference and RF filtering problems. It is a crystal transponder, having a self-contained conversion frequency source. The transmitter is completely solid state and the range code received is phase modulated on the carrier by a 222 MHz phase modulator in the transmit multiplier chain. S band microstrip techniques are used throughout to minimize the mass.

4.3.2.3 VHF and UHF Repeater Units

The TDRS LDR service provides command transmission to at least 20 user spacecraft and telemetry data from 20 users simultaneously. The transmitter power amplifier must provide a 71 watt output. The LDR forward link transmitter block diagram is shown in Figure 59. The LDR forward link transmitter features solid state driver with redundancy and

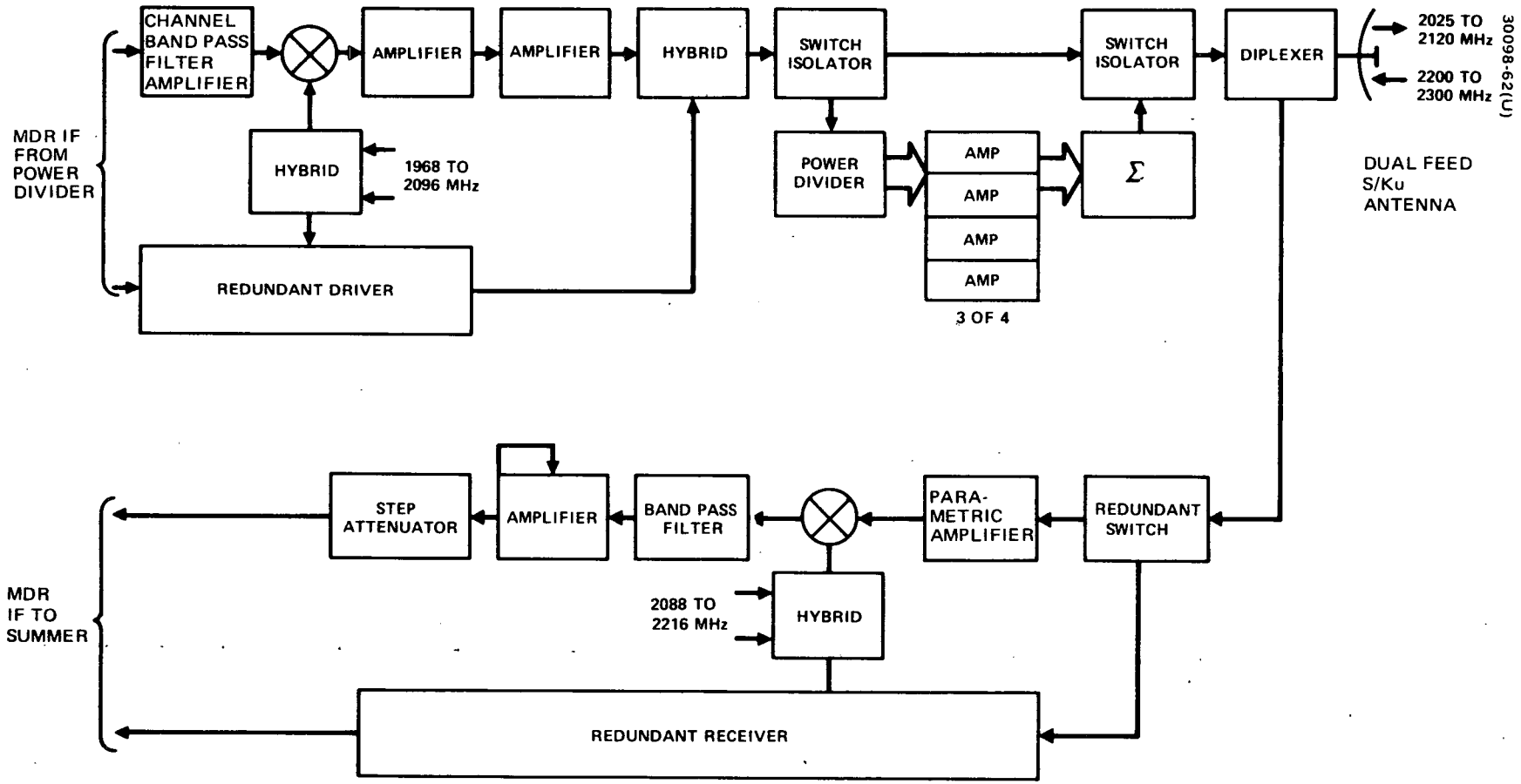

Figure 56. MDR Forward Link Transmitter and MDR Return Link Receiver

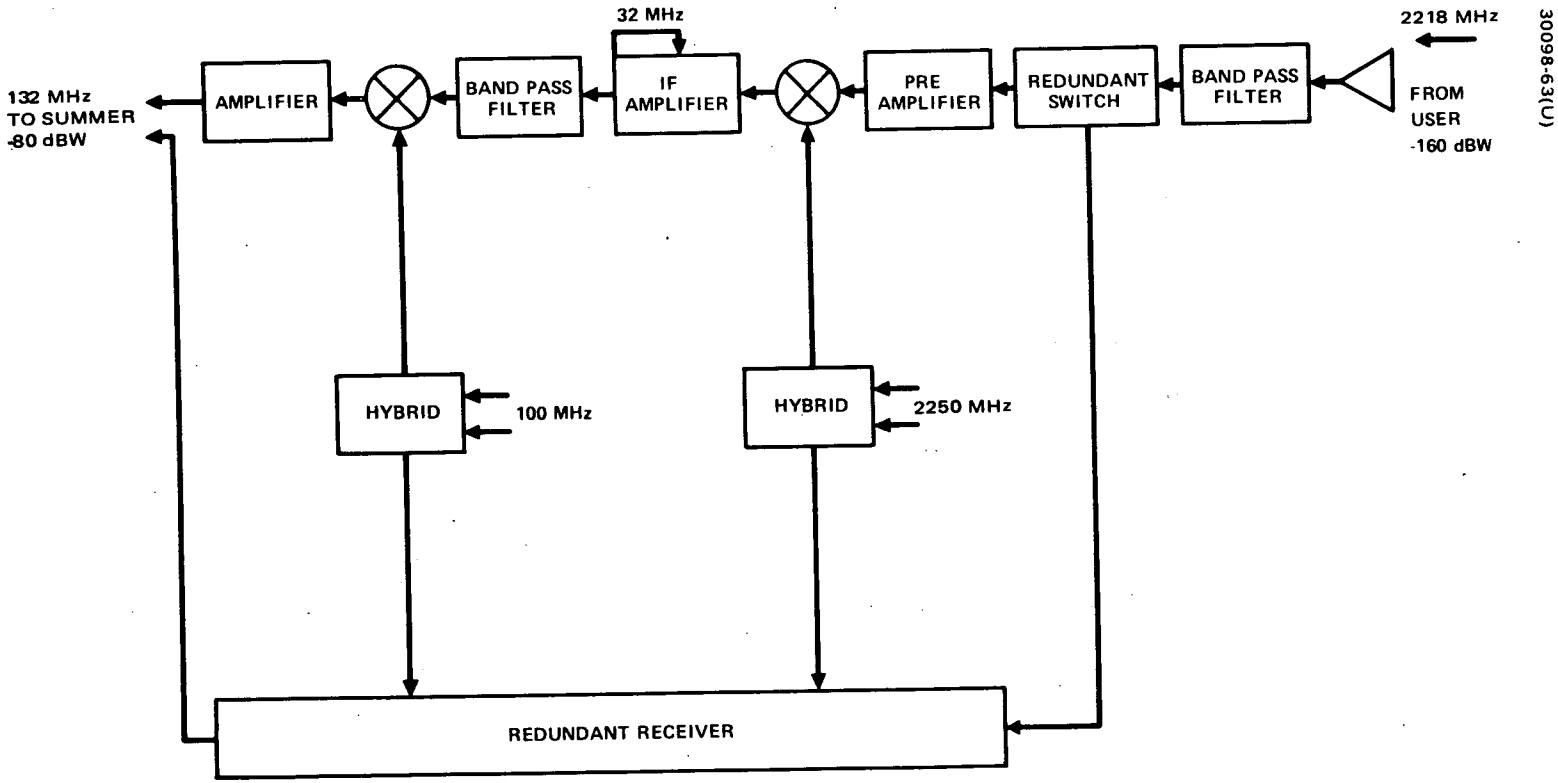

Figure 57. Order Wire Receiver

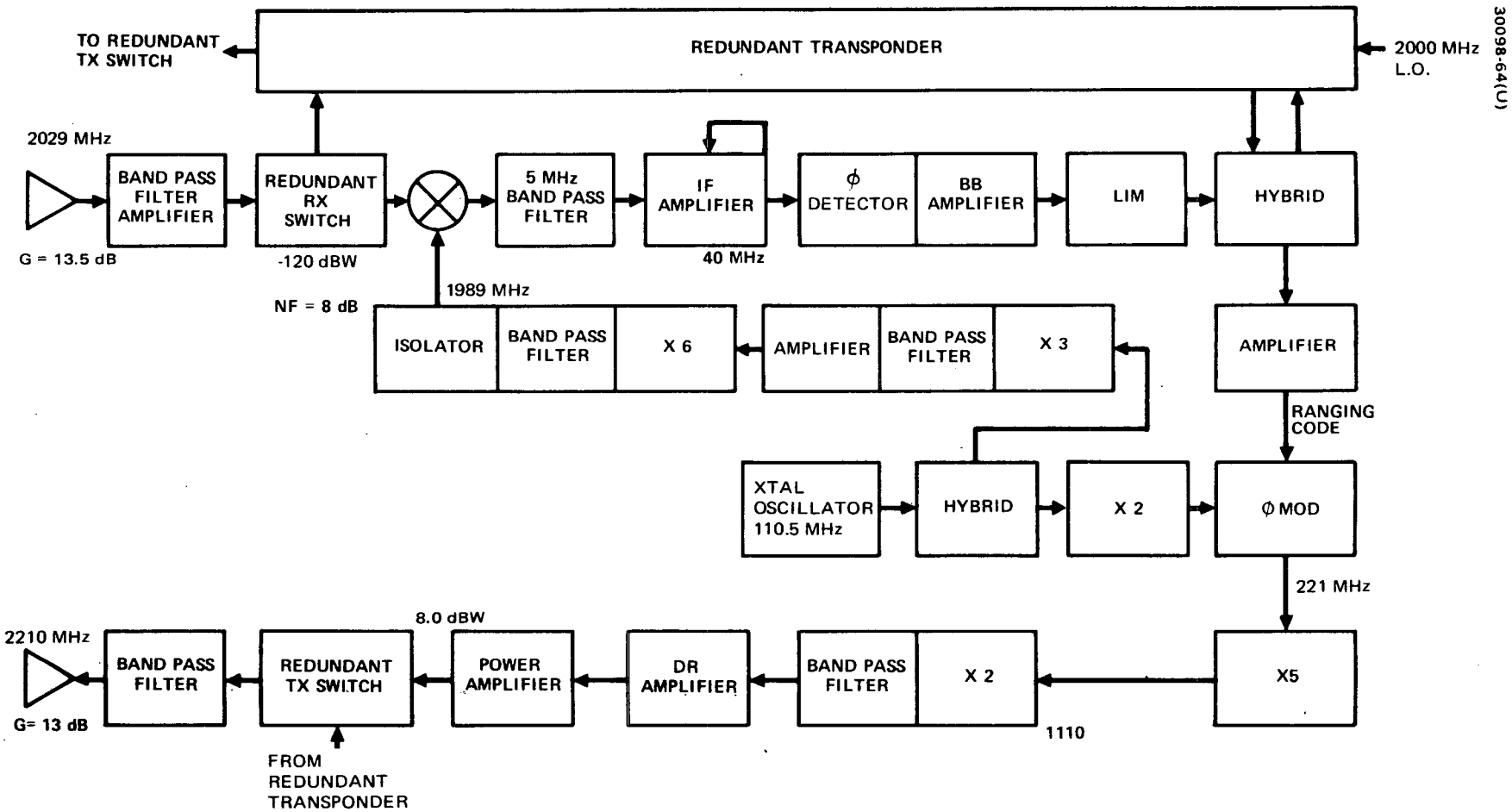

Figure 58. S Band Ranging Transponder

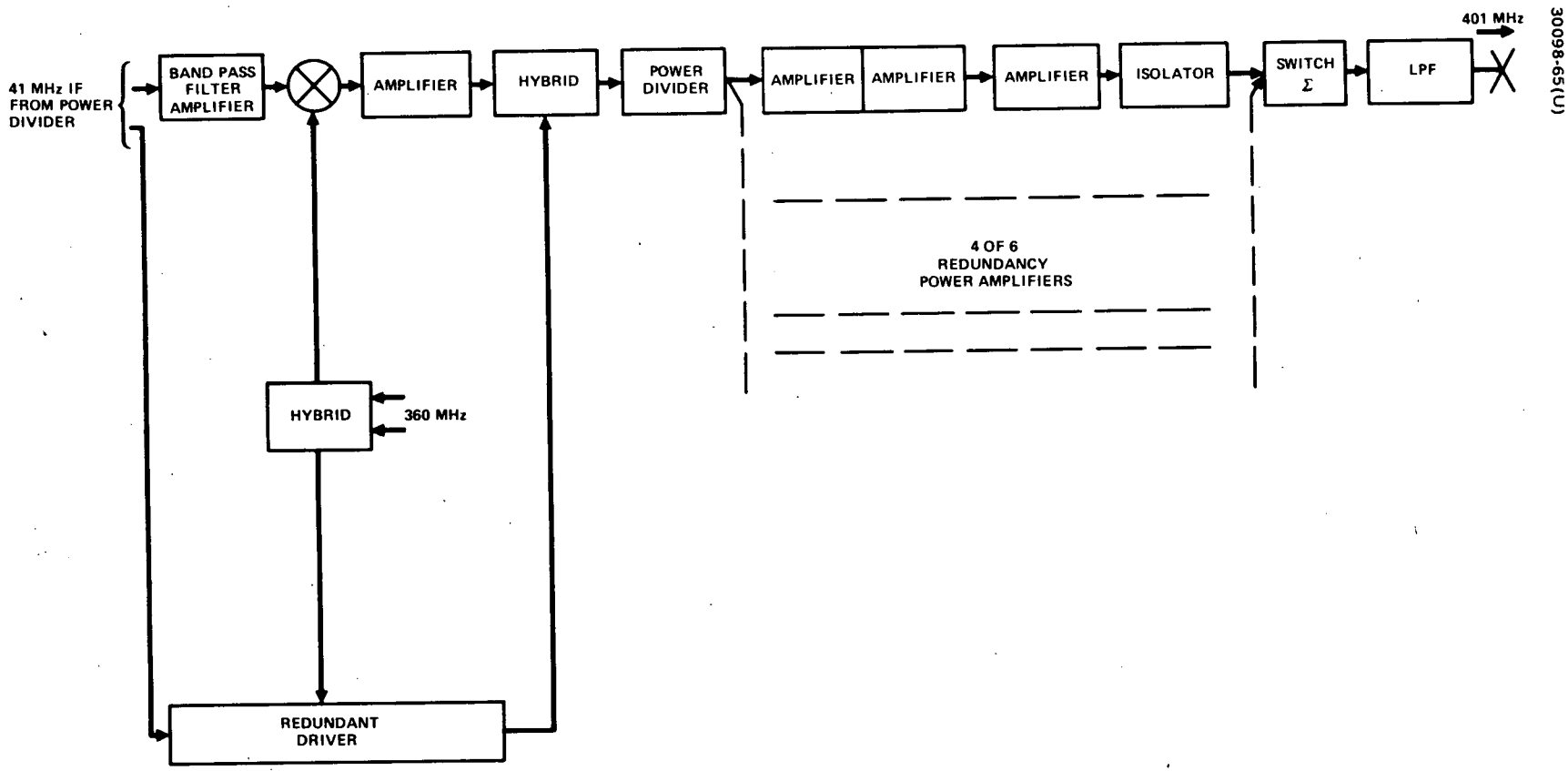

Figure 59. LDR Forward Link Transmitter

a final power amplifier using hybrid coupled transistor amplifiers. A selectable, by command, group of four power amplifier outputs are summed by a switched Wilkinson summer to provide the required 71 watt power control at 401 MHz; 142 watts are provided by eight parallel power amplifiers. The low pass filter at the output attenuates the harmonic and spurious signal outputs from the transmitter. The overall amplifier efficiency is 51 percent and includes regulator losses and 3 percent allowance for space environment and life degradation.

The LDR return link uses a five element AGIPA antenna to provide RFI rejection. The LDR receiver is designed to process the two outputs from each of the five AGIPA antenna elements independently through 10 channels. The channels are frequency translated to 10 Ku band frequencies for transmission to the ground station in the MDR/LDR return link transmitter. High reliability is achieved by complete redundancy of all channels. This is illustrated in Figure 60, which also shows the transistor preamplifier and the acoustic surface wave RF bandpass filter (BPF). The IF channel filter bank is made up of monolithic crystal filters. The outputs are summed and upconverted to frequencies between 120 and 155 MHz. The 10 channels are evenly spaced over this band with 5 MHz between center frequencies. Specific unequal frequency spacing may become necessary during detailed design to minimize intermodulation products. The LDR receiver contains an internal LO frequency source to simplify the distribution of the many LO signals required for the 10 channel receiver. A 5 MHz harmonic generator, frequency multipliers, and amplifiers are combined to provide the 10 local oscillator inputs between 85 and 120 MHz.

4.3.2.4 Frequency Synthesizers

The frequency synthesizer provides the necessary conversion frequencies for each of the receivers and transmitters in the TDRS communication subsystem. This requires a total of 14 frequencies to be derived from a stable crystal oscillator reference source. The primary reference source is a 20 MHz voltage controlled oscillator that is phase locked to an incoming pilot tone through the Ku band CMD/LDR receiver. When phase locked to the pilot tone, the reference oscillator becomes a coherent frequency reference source. A secondary or standby reference source is also provided for use when the primary reference source is not phase locked to the incoming pilot tone. The secondary reference source is a quartz crystal master oscillator, temperature controlled to maintain the required stability. The 14 output frequencies are generated by several solid state multiplier chains. Two pairs of S band outputs are programable in 1 MHz steps to provide repeater flexibility of user spacecraft interface frequencies.

4.3.3 Telemetry and Command

The major tasks of the telemetry, tracking, and command subsystem are to 1) monitor the relay to a ground control station all

spacecraft analog and status data required for mission management and control, power management, repeater gain adjustments, etc.; and 2) provide satellite range information at any phase of its mission.

The primary telemetry and command requirements are to provide telemetry data and command control of the spacecraft using the GSFC standard telemetry and command formats. These requirements must be satisfied via either the primary telecommunication service system at the Ku band frequency or the backup telemetry transmitter and command receiver at S band. The S band transponder system will be compatible with the GRARR operational requirements to provide data for orbit determination during launch and injection phase. Once the spacecraft is on station, the S band transponder system will be used as a backup to the Ku band system in providing TDRS telemetry and command links to the ground station. The telemetry subsystem must provide data for the determination of performance, status, operational mode, attitude, and antenna pointing of the TDRS. The command subsystem must provide control of the spacecraft for selection of redundant units, operational mode changes, stationkeeping, and orientation of the spacecraft and the antenna. Figure 61 is a schematic diagram of the telemetry and command subsystem (same as Figure 46; repeated for convenience only).

The units of the command subsystem, as shown in Figure 61, are fully redundant and cross-strapped so that either unit of every pair could fail completely without impairing the satellite's ability to receive and execute all commands. A command transmission consists of a microwave carrier modulated by a sequence of tones at three discrete frequencies, designated 1, 0, and execute. The tones are amplitude modulated at 128 Hz. The demodulated output of the Ku band receiver and the S band command receiver drive both the despun and spinning decoders. The despun decoders are designed for 155 commands and the spun decoders provide 127 commands. The selection of the executing decoder is by unique decoder address. Command verification is provided by telemetry readout of the command register before sending the execution tone.

The command subsystem is capable of executing jet firing commands in phase with the spin of the satellite. This is performed at the ground station by synchronizing the execute tones with sun or earth pulses, received via real time telemetry. The repetitive command mode is used for antenna pointing and jet firings. Slewing is accomplished at a rate of 24 steps per second. Tracking commands are transmitted as required to maintain the antenna beam on the user satellite.

Signal and word format of the demodulated command from a receiver output consists of a sequence of 1, 0, and execute tone pulses; these are arranged as shown in Figure 62. For convenience, the 1 and 0 pulses will referred to as bits, as they do, in fact, convey binary information to the decoder logic circuitry.

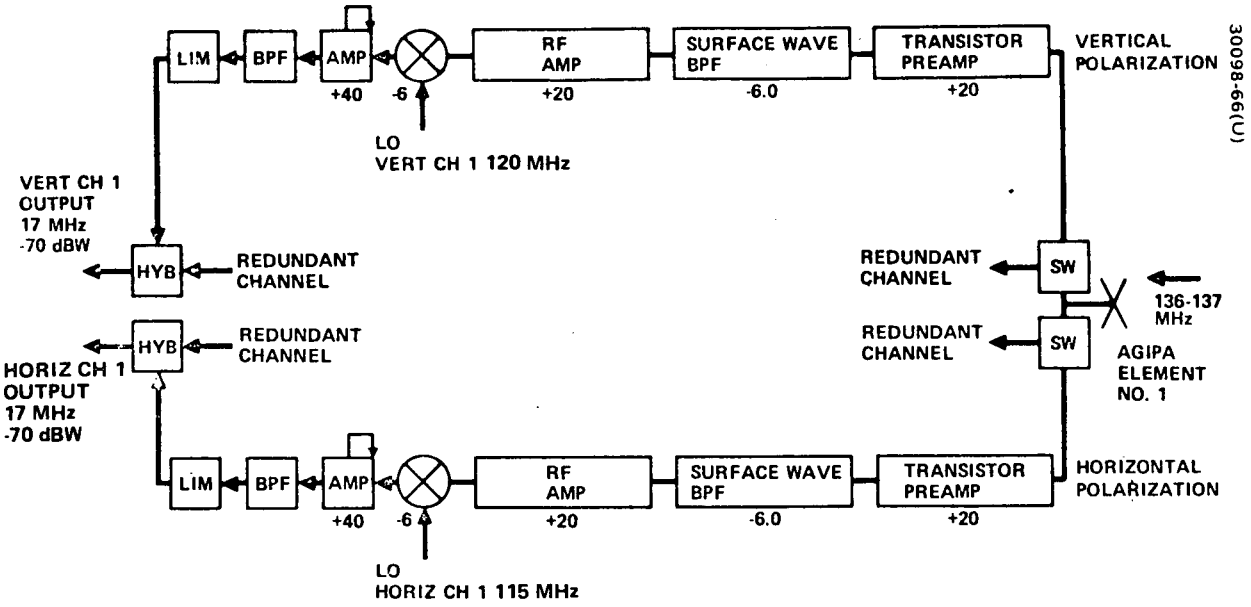

Figure 60. Redundant VHF Receiver

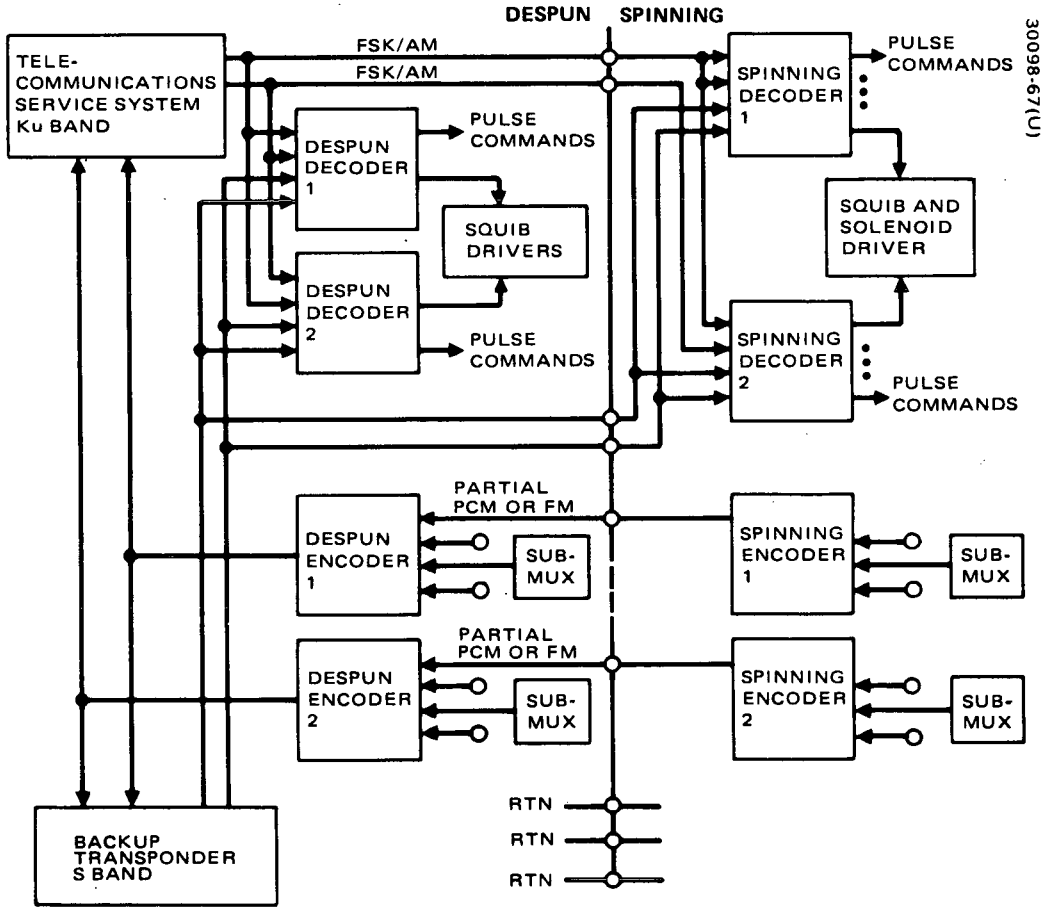

Figure 61. Tracking, Telemetry, and Command Subsystem

COMMAND GENERATOR CONTROL	FUNCTION PERFORMED	TONE	CODE	DURATION
ACTUATE XMIT				
	INTRODUCTION (CLEAR)	0	16 BITS	258 ms
		1	1 BIT	
	DECODER ADDRESS	0 AND 1	6 BITS	
		1	2 BITS	
	COMMAND	0 AND 1	8 BITS	
READ DECODER REGISTERS	COMMAND VERIFICATION VIA TELEMETRY			
ACTUATE EXECUTE				
	COMMAND EXECUTE	EXECUTE TONE	AS REQUIRED	VARIABLE TIME (40 ms FOR STANDARD SINGLE COMMAND)
ACTUATE CLEAR				
	CLEAR THE DECODER REGISTERS	0	16 BITS	133 ms
		1	1 BIT	

30098-68(U)

Figure 62. Command Format

The introduction portion of the command word consists of at least sixteen 0 bits followed by one 1 bit. During this time a receiver is selected and the decoder registers and logic are reset. The decoder is then able to process the remainder of the command word. The next eight bits comprise the address portion of the command word. The first six provide the coding for digital addresses. The address words are separated by a minimum Hamming distance of two, so that a single error in the transmission or reception of a decoder address will not result in the successful addressing of a wrong decoder. The last two bits are both ones, which ensures that the introduction sequence will never be repeated within the command word.

The command itself consists of eight bits. The eight command bits are entered into a storage register for verification via telemetry. Once a command word is entered into storage, further processing of data bits is inhibited and an introduction format must be sent to clear the register. Upon receipt of the execute tone, a coincident pulse will occur on the decoder output line corresponding to the stored command. Execute tone pulses can be sent for as long or as frequently as required. After the command has been executed (or if necessary at any time during the commanding sequence), the commanding ground station resets and clears the decoder by repeating the introduction. As shown in Figure 62, the time necessary for introduction, addressing, and entering a command into the register is 258 ms. This means that the minimum time required before executing a command is 258 ms (even when bypassing the telemetry verification step).

The despun and spinning command decoders differ from each other in only the following particulars:

1) Despun decoders are implemented with more command outputs from the output matrix than from the spinning output matrix.

2) Despun decoders each contain a TWT sequencer.

3) Spinning decoders each contain a spinup sequencer.

In all other aspects, including method of operation, the despun and spinning decoders are identical. Both types, therefore, will be described with reference to the block diagram of Figure 63.

There are two receiver sequencers. Each feeds a set of 1, 0, and execute tone filters (six different frequencies). This arrangement provides positive identification of the command link (S or Ku band) being used for a given command, as each sequencer drives only one set. Cross-strapping is achieved by connecting the two corresponding tone filter outputs together at the input to their respective detector circuits.

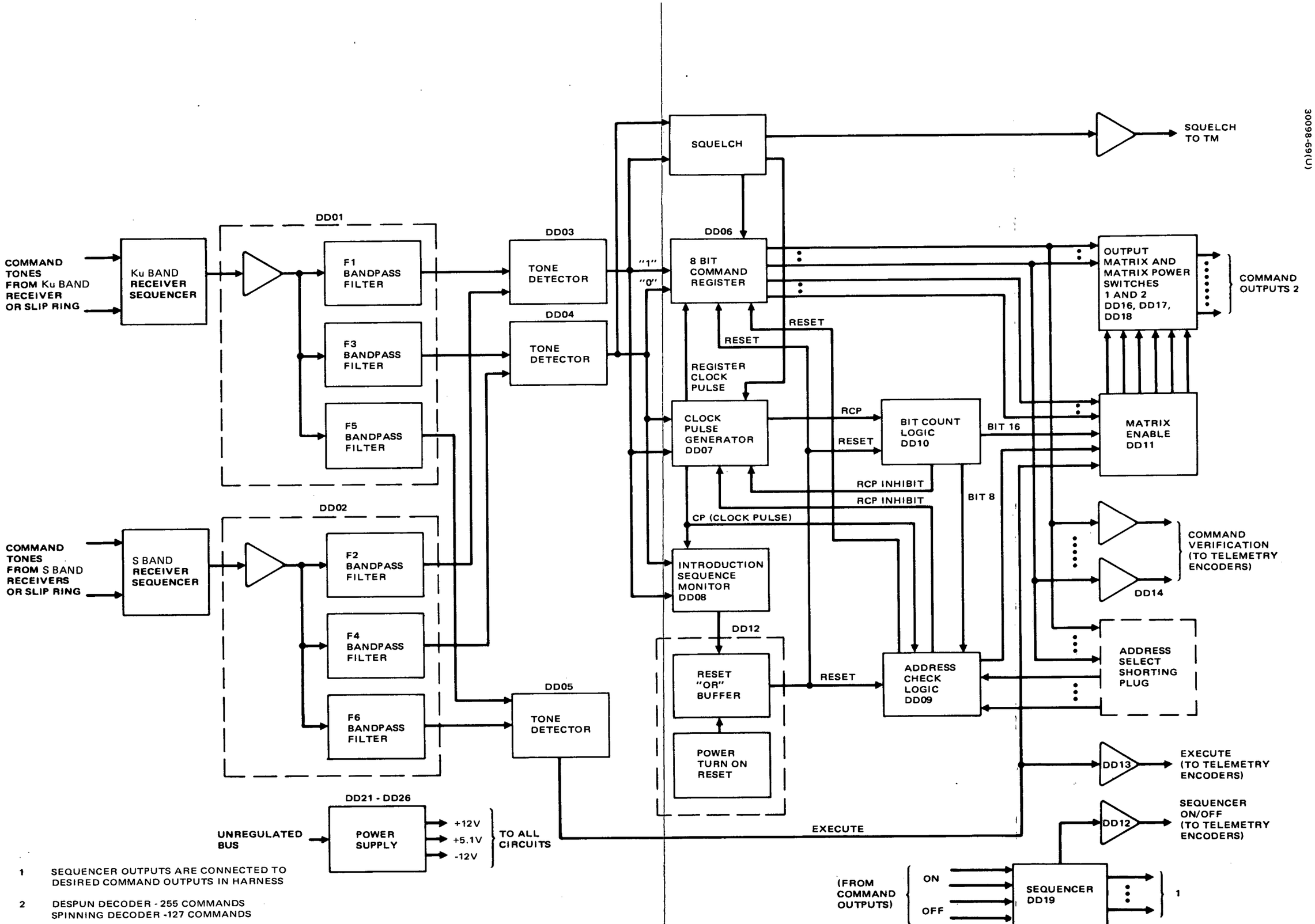

Figure 63. Despun or Spinning Decoder Block Diagram

FOLDOUT FRAME 1

FOLDOUT FRAME 2

The receiver sequencers sample the two S band and the two Ku band receiver outputs to select one which has a suitable output signal. The signal at the receiver output is shown in Figure 64. Tone filters are two-stage, stagger tuned, passive, bandpass filters with -3 dB bandwidths of approximately 1200 Hz. The output of the first stage of each filter goes to the AM detector where the two signals are summed and the composite signal is fullwave rectified and fed to a clock pulse generator which contains a narrow bandpass filter tuned to the 128 Hz bit rate. The output of the 128 Hz bandpass filter is the demodulated AM, a 128 Hz sine wave with an amplitude proportional to the signal strength of the received AM-FSK signal. The squelch circuit puts out a signal to enable the decoder processing when the input signal exceeds a preset threshold level. The 128 Hz sine wave is also fed to the clock pulse generator which generates the clock signals which drive the remainder of the demodulator.

When power is turned on, the decoder is initizlized by the power turnon reset circuit as follows: 1) the command register is cleared to all zeros (an illegal command), 2) the count register's count is set to zero, 3) the address check logic is reset, and 4) the full count logic is set to zero. Whenever an 0 or 1 pulse is detected, the clock pulse generator will provide a clock pulse (CP) to the introduction sequence monitor which checks the pattern of the incoming data. Upon receipt of eight or more 0s followed by a 1, it initializes the decoder in the same manner as the power turnon reset.

The command register is an 8 bit register. It receives 1s and 0s from the demodulator and RCPs (register clock pulses) from the clock pulse generator. Its output goes to the address check logic, output matrix, and to the telemetry buffers for parallel entry of its contents into redundant telemetry encoders.

The bit count logic provides a pulse to the address check logic when it has counted eight RCPs and a pulse to the full count logic when it has counted 16 RCPs. When the address check logic receives its pulse from the bit count logic, it checks the output of the command register (which now contains the address) and 1) if the address checks correctly, an enable signal is sent to the matrix enable or 2) if the address does not check, it inhibits further RCPs and clears the command register. Each decoder has an address plug which permits changing its address any time prior to launch. When the bit count logic has counted 16 RCPs, it inhibits further RCPs to prevent false clocking of the command register and also sends an enable signal to the matrix enable.

Use of two series matrix power switches prevents a single component failure in the matrix power switching circuitry from generating a false command. When both matrix power switches are enabled, an execute signal from the execute tone detector closes both power switches, cuasing a command pulse to occur on the output selected by the command portion of the command word. The command pulse is coincident with and lasts as long as the execute tone pulse.

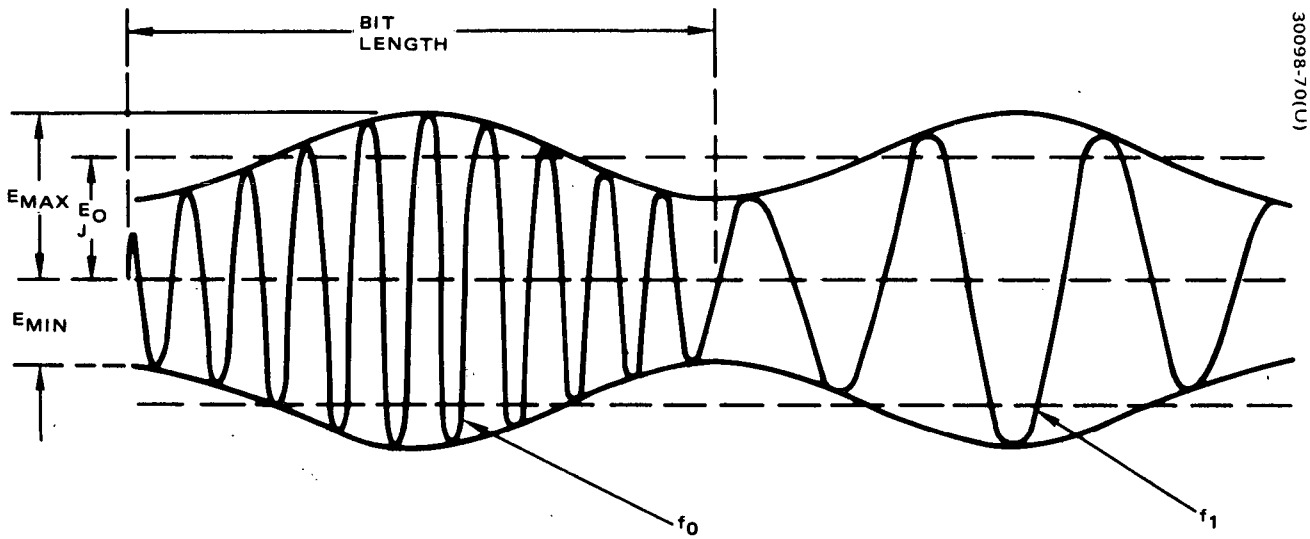

$$\text{MODULATION INDEX, } m = \frac{E_{MAX}-E_{MIN}}{2E_0} = 0.50 \pm 0.05$$

Figure 64. FSK/AM Signal Design

Each despun decoder contains a TWT sequencer which, when turned on by command, times for a specified period, then generates a sequence of eight command type output pulses spaced at 105 seconds, generates a second sequence of six pulses, and finally shuts itself off (it may also be commanded off, and thereby reset, at anytime during its cycle). The command type outputs that each TWT sequencer generates appear on a separate lines. Each line, in turn, is wired directly to selected command matrix output lines to execute those selected.

The squib and solenoid drivers actuate pyrotechnic and jet firing functions in the satellite. The squib drivers fire the apogee motor and bearing and power transfer assembly (BAPTA) release squibs, and the solenoid drivers actuate the axial, radial, and spinup jet valves and the latching valve in the spinup jet line. There are four squib driver and 10 solenoid drivers which are capable of firing three squibs and driving eight pairs of solenoids. All of the squib drivers apply power to their respective squibs after specified delay times. The BAPTA clamp release squib drivers are commanded by redundant separation switches. The apogee motor squib drivers are each commanded redundantly by the spinning decoders. After mating of the spacecraft to the adapter, until actuation of the separation switches, all squib driver power inputs are directly connected to ground.

The encoder units of the telemetry subsystem, as shown in Figure 61, are fully redundant and cross-strapped so that either unit or every pair could fail completely without impairing the satellite's ability to transmit all telemetry data. Normally one encoder unit or the despun pair operates with one unit of the spinning pair. Two modes of data processing are used: PCM and FM real time.

The PCM mode is used for all attitude, thermal, power, and status information, including command verification. In the PCM mode, the spinning encoder receives, processes, and formats data originating on the spinning portion of the satellite. The output, which is connected across the spinning/despun via slip rings, is an 8 kHz biphase waveform from which a despun encoder recovers the nonreturn to zero (NRZ-L) bit stream and derives a coherent clock. The despun encoder gathers and processes data originating in the despun compartment. It alternates its bit stream word-by-word with the spinning encoder bit stream, then converts the composite NRZ-L bit stream to a Manchester code format. The converted stream is used for phase modulating a Ku band carrier within the telecommunications repeater on the despun side and modulates the backup VHF transmitter on the spinning side.

The FM real time mode is used for real time attitude pulses (sun sensor pulses, earth sensors pulses, platform index pulses, and command execute pulses). The occurrence of a pulse coherently switches the frequency of an IRIG channel 13 subcarrier oscillator from its pilot tone to a different frequency, depending on the kind of pulse present. The output is connected via a slip ring to the despun encoder, the output of which phase modulates the Ku and S band telemetry transmitters.

In the PCM mode a spinning encoder conditions, multiplexes, and encodes the telemetry data originating on the spinning section of the satellite into a PCM bit stream. In the FM real time mode, the composite of real time pulses coherency switches the frequency of the SCO. All sequenced operations within the spinning encoder, including multiplexing, analog-to-digital conversion, attitude sensor pulse interval digitizing, and digital formatting, are timed by a 1.024 MHz crystal oscillator and count-down chain. The operation of the spinning encoder is described below with reference to the block diagram shown in Figure 65.

Multiplexers provide analog and digital gating circuits to time multiplex the telemetry inputs. The telemetry inputs consist of bilevel and analog data with a normalized range of 0.00 to 5.12 volts. Both analog and digital signals are multiplexed with the same type of circuitry, the digital signals being treated as analog signals up to the output stage of the digital multiplexer, which converts them to standard logic levels. The analog multiplexer output is fed to a successive approximation type analog-to-digital converter which encodes each analog input into a serial 8 bit NRZ-L word, providing resolution of better than 0.5 percent of full scale. The outputs of the analog-to-digital converter and digital multiplexer are combined at a data node to form the partial PCM bit stream.

The attitude data processor performs a sequence of ten time interval measurements (Figure 66), to facilitate the accurate and rapid determination of satellite attitude. Each measurement equals the number of cycles of a 32 kHz reference frequency, derived from the 1.024 MHz crystal oscillator, counted during the time of the interval being measured. The count is telemetered along with a 4 bit code identifying which measurement it represents. The inherent measurement resolution is ± 1/2 period of the 32 kHz reference, or approximately 16 microseconds. Measurement T2, from the occurrence of a sun or earth pulse to the start of the next telemetry frame, is of particular significance. It allows a suitably equipped ground station to synthesize a pulse train at the spin rate and at a known phase with respect to the generation of pulses on board the satellite. Such a pulse train (which can also be derived from the FM mode telemetry) is required for synchronous pulsing of the spacecraft jets.

The biphase modulator converts the NRZ bit stream to a coherent biphase format, in effect adding an easily recoverable clock for use by the despun decoder. It also adds a double maplitude pulse once each frame to which the despun decoder synchronizes its frame timing.

When the encoder is in the FM real time mode, it accepts and processes various real time pulses and transmits their occurrences as discrete changes in SCO frequency. The frequency transmitted and the duration of transmission correspond to the particular group that includes the occurring pulse (Table 28). All of the tone frequencies are within the IRIG channel 13 band. If two pulses in different groups should occur simultaneously, priority gating of the pulses permits the occurrence of only one pulse to be transmitted. The highest frequency group takes

FOLDOUT FRAME 1

FOLDOUT FRAME 2

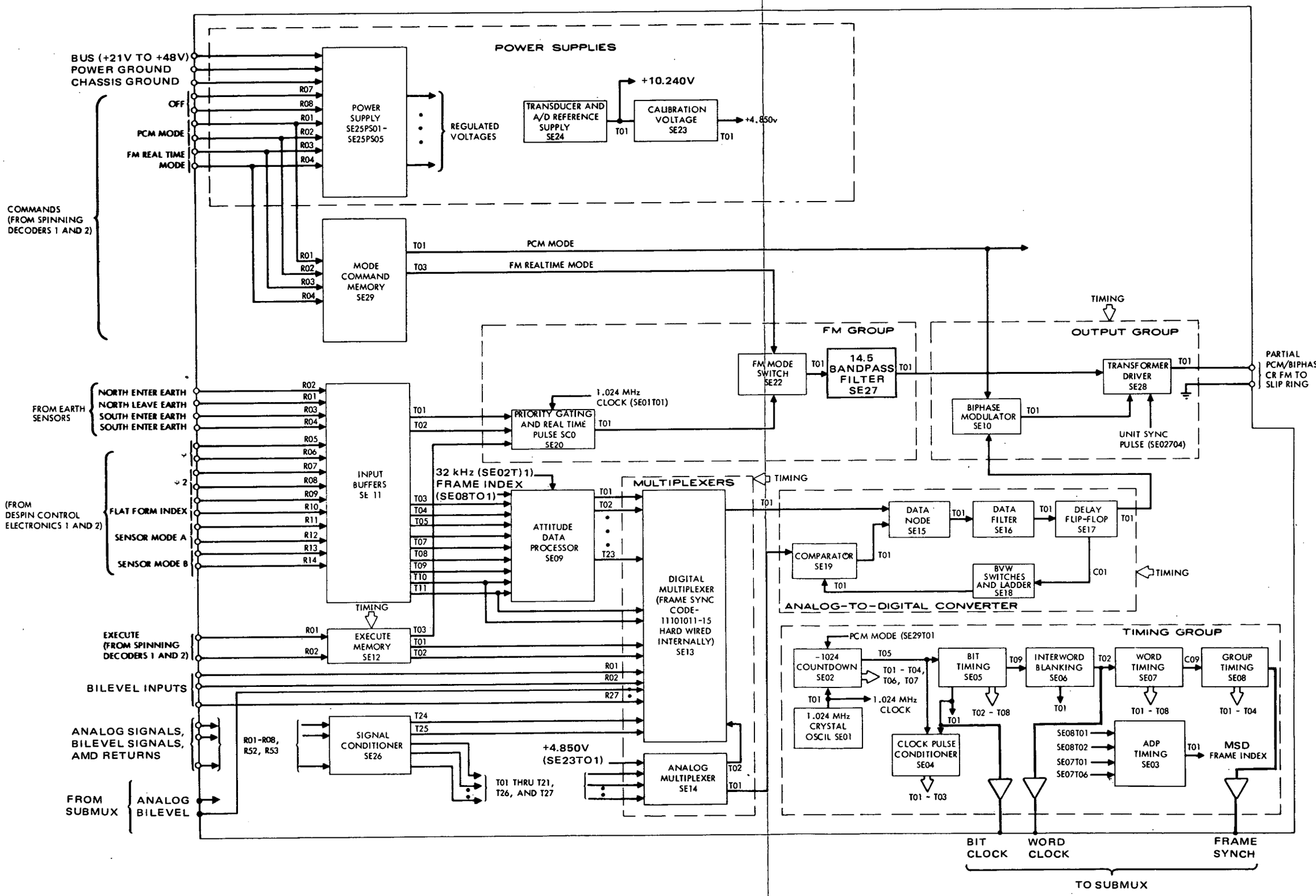

Figure 65. Spinning Encoder Block Diagram

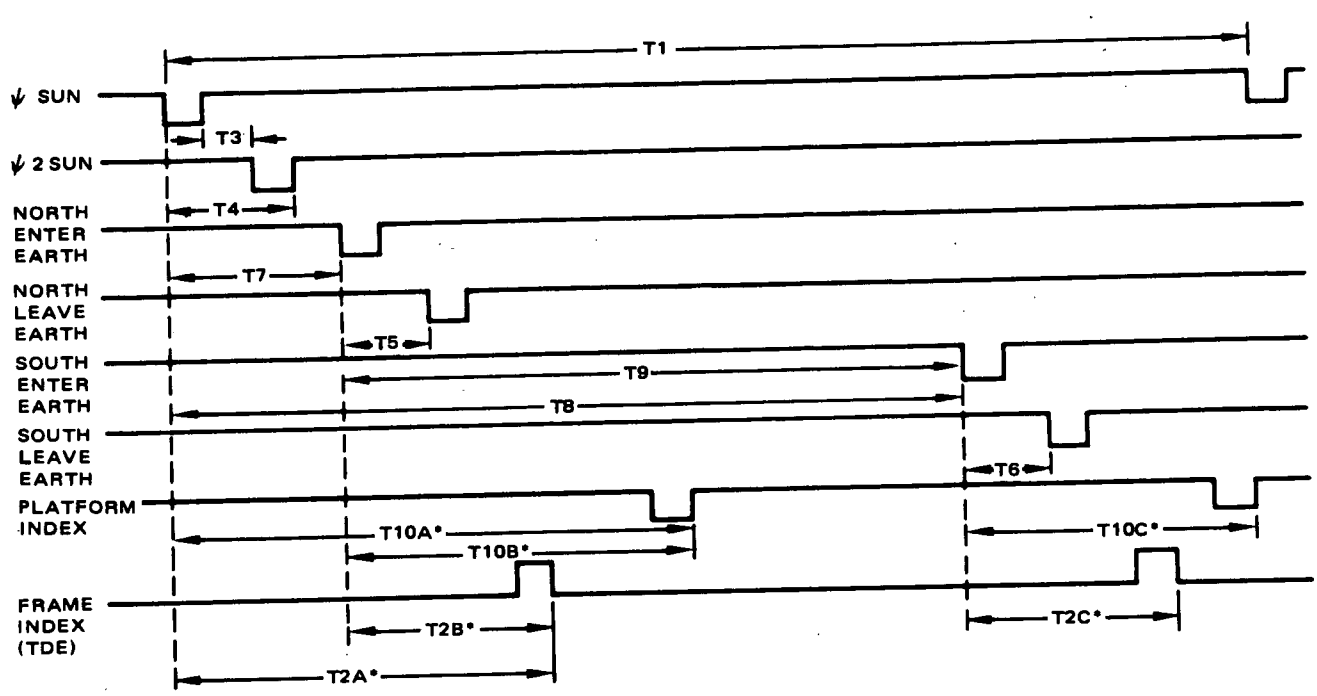

*THESE MEASUREMENTS ARE TAKEN RELATIVE TO THE SPECIFIC SENSOR IN USE AT THE TIME; THUS, A DENOTES THE MEASUREMENT TAKEN WHEN IN SUN MODE, B WHEN IN NORTH EARTH MODE, C WHEN IN SOUTH EARTH MODE.

Figure 66. Attitude Data Processor Time Interval Measurement

precedence. The most critical telemetry data are the attitude determination and execute pulses needed for spacecraft control. Except for a shared power supply and rotary transformer driver, the circuitry in the PCM path is entirely separate from that in the FM path to provide significant extra redundancy for these data.

In the PCM mode, a despun encoder condtions, multiplexes, and encodes the telemetry data originating in the despun compartment into a PCM bit stream, which it synchronizes and merges with the partial PCM from its associated spinning encoder. In the FM mode, a despun encoder switches the spinning encoder FM output to the telemetry transmitter. A comparison of block diagrams shows that the despun encoder (Figure 67) is identical in most respects to the PCM portion of the spinning encoder. In order to merge its PCM words with those of the spinning encoder, the despun encoder must derive its bit clock from the spinning encoder bit stream and synchronize the start of its telemetry frame with the spinning encoder double amplitude frame sync pulse. These tasks are performed, respectively, by the clock and data detector circuit and the sync detector circuit. It the clock detector is unable to derive a bit clock, either because the spinning encoder has failed or has been commanded off, the clock selector will switch the despun encoder to its internal 1.024 MHz crystal oscillator so that despun telemetry may continue to be transmitted. The

TABLE 28. FM MODE TRANSMISSION

Pulse	Frequency, kHz	Duration, ms	Remarks
Group 1			
Psi (ψ)	15.059	5	
Psi (ψ_2)	15.059	5	
Group 2			
North enter earth	14.222	10	
North leave earth	14.222	20 (exception)	For identification on ground
South enter earth	14.222	10	
South leave earth	14.222	10	
Platform index	14.222	10 to 120	Variable with spin speed
Group 3			
Command execute	13.838	Variable time	= execute duration (40 ms for standard single pulse)
Pilot Tone	13.474		Transmitted when no pulse is present

FOLDOUT FRAME 1

FOLDOUT FRAME 2

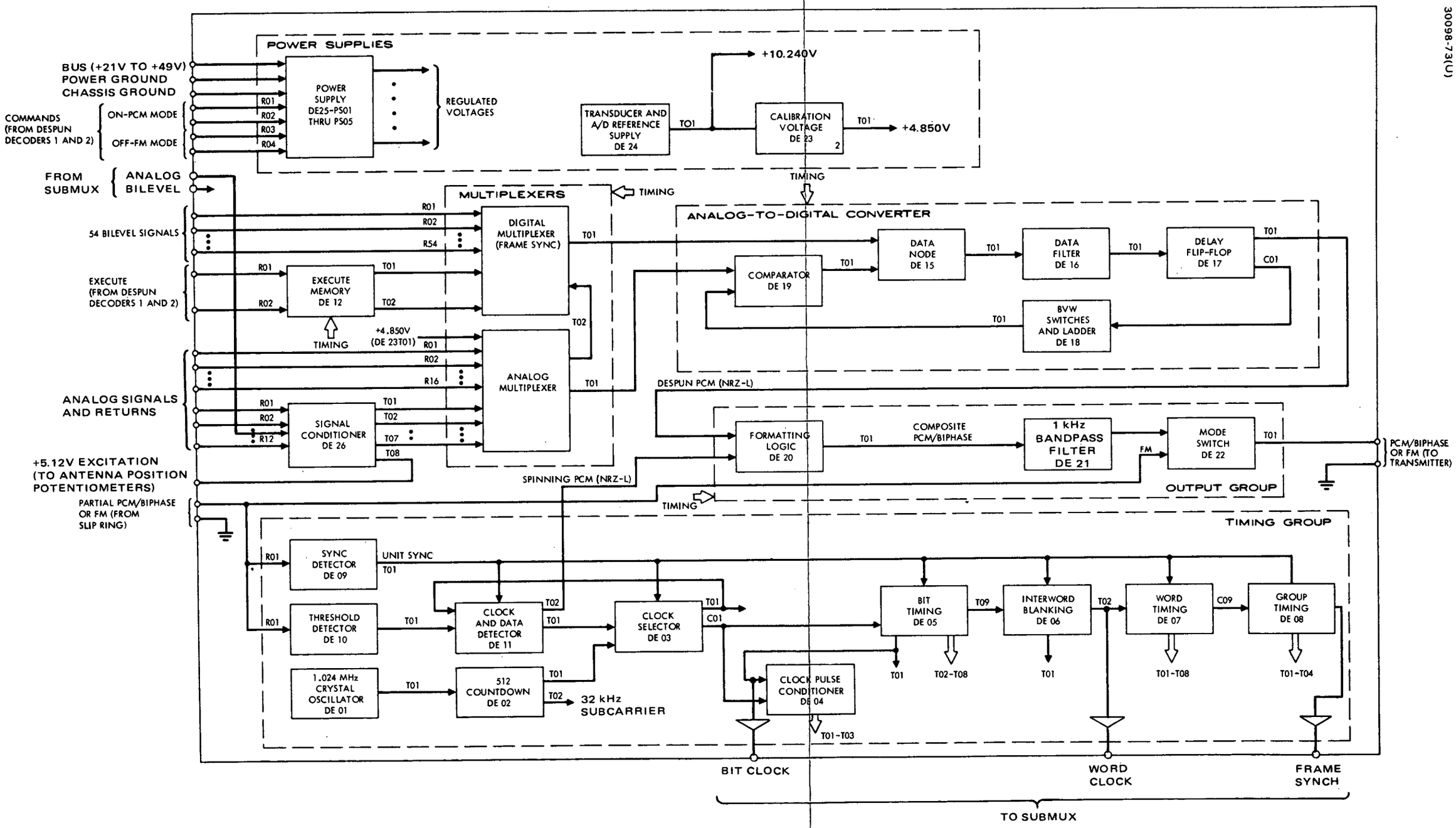

Figure 67. Despun Encoder Block Diagram

formatting logic performs the required merging of the partial PCM from the spinning encoder with despun encoder PCM. The combined NRZ-L bit stream is then coded into an NRZ-M waveform which biphase modulates the 32 kHz subcarrier output. Mass, power, and size data for selected components for the telemetry subsystem are listed in Table 29.

Telemetry and command performance characteristics are listed in Table 30. The command capacity may be divided as required between the spinning and despun sections of the spacecraft. Lists of telemetry requirements are provided in Tables 31 through 35. Table 36 lists the command requirements.

TABLE 29. TELEMETRY AND COMMAND COMPONENT PHYSICAL CHARACTERISTICS

Unit	Number per Spacecraft	Mass per Spacecraft, kg	28 Volt Bus		Size, cm			Program Identification
			Power Per Unit, watts	Spacecraft Standby Power, watts	Width	Length	Height	
Despun								
Decoder	2	2.7	0.9/1.8[2]	1.8	14.7	22.6[1]	6.9	HS 312
Encoder	2	4.2	4.0		14.7	22.6[1]	6.9	HS 312
Squib driver	1	2.5	–	–	14.7	15.2	3.6	MC
Spun								
Decoder	2	2.7	0.9/1.8[2]	1.8	14.7	31.0[1]	6.9	HS 312
Encoder	2	5.0	5.0	5.0	14.7	31.0[1]	6.9	HS 312 Mod
Solenoid and squib driver	1	0.9	–	–	14.7	34.3	3.6	HS 320
Latching valve – heater driver	1	0.5	–	–	6.6	8.9	7.4	–

NOTES: (1) Stackable units.

(2) Standby/execute.

TABLE 30. TELEMETRY AND COMMAND PERFORMANCE CHARACTERISTICS

Parameter	Characteristics
TELEMETRY – INTELSAT IV TYPE	
PCM Mode	
Word length	8 bits (11 words subcommutated)
Frame length	64 words (11 words subcommutated)
Analog words	110 words (8 subcommutations)
Digital words	31 total (8 subcommutations)
Bit rate	1000 bits/sec
Code type output	Manchester
FM Mode (attitude data)	
Subcarrier frequency	14.5 kHz
Data type	Real time pulses
Modulation	FM
Data transmitted	1) Sun pulses 2) North earth pulses 3) South earth pulses 4) Execute receipt
COMMAND – INTELSAT IV TYPE, MODIFIED	
Tones	1, 0, and execute
Input signal	FSK/AM
Bit rate	128 bits/sec
Command capacity, maximum	255 despun, 127 spinning
Command verification via	Telemetry
Command execution	Real time
Execution synchronization	Sun or earth pulses
Maximum command rate	Approximately 4 per second

TABLE 31. TELEMETRY CHANNEL ASSIGNMENTS

Main Frame Word	Spinning	Despun
0	Frame sync	
1		Frame sync
2	Decoder 1 command verify	
3		Decoder 1 command verify
4	Decoder 2 command verify	
5		Decoder 2 command verify
6	Status word 6	
7		Status word 7
8	Subcomm (Digital)	
9		Status word 9
10	Attitude determination	
11		Subcomm (Digital)
12	Attitude determination	
13		Subcomm (Digital)
14	Attitude determination	
15		Status word 15
16	Subcomm	
17		Subcomm
18	Subcomm	
19		Subcomm
20	Subcomm	
21		Subcomm
22	Subcomm	
23		Subcomm
24	Telemetry calibration	
25		Bus voltage
26	Bus current	
27		Antenna A azimuth*
28	Bus voltage	
29		Antenna A elevation*
30	Despin position torque command**	
31		Antenna B azimuth*
32	Motor torque command**	

*Digital output increases when antenna steers toward north or west.

**Both torque command signals are connected to each encoder via OR circuits, since only one despin control electronics unit is on at a time.

Table 31 (continued)

Main Frame Word	Spinning	Despun
33		Antenna B elevation*
34	Motor 1 current	
35		Antenna C azimuth*
36	Motor 2 current	
37		Antenna C elevation*
38	Spare	
39		Spare
40	Spare	
41		Spare
42	Spare	
43		Telemetry calibration
44	Spare	
45		Spare
46	Spare	
47		Spare
48	Spare	
49		Spare
50	Spare	
51		Spare
52	Spare	
53		Spare
54	Spare	
55		Spare
56	Spare	
57		Spare
58	Spare	
59		Spare
60	Spare	
61		Spare
62	Spare	
63		Spare

TABLE 32. TELEMETRY STATUS DIGITAL BIT ASSIGNMENTS – SPINNING

Main Frame Word	Subcomm Channel	Bit Assignments
6	–	Status Word 6 (8 bits) Spinning Encoder Bit 1 Spinning decoder 1 execute 2 Spinning decoder 2 execute 3 Spacecraft separation 4 Spinup sequencer 1/2 OFF 5 Subframe count 6 Subframe count 7 Subframe count 8 Spare
8	0	Reaction Control Status Bit 1 Latching valve 1 OPEN/CLOSE 2 Latching valve 2 OPEN/CLOSE 3 Latching valve 3 OPEN/CLOSE 4 Latching valve 4 OPEN/CLOSE 5 Latching valve 5 OPEN/CLOSE 6 Radial valve heater ON 7 Axial valve heater ON 8 Spin valve heaters ON
	1	Reaction Control and Apogee Motor Status Bit 1 Apogee motor 1 OFF 2 Apogee motor 2 OFF 3 Apogee motor 3 OFF 4 Apogee motor 4 OFF 5 Spinup thrusters 1/2 6 Spare 7 Spare 8 Spare

Table 32 (continued)

Main Frame Word	Subcomm Channel	Bit Assignments
8	2	TT&D Status Bit 1 Telemetry encoder 1 PCM mode 2 Telemetry encoder 2 PCM mode 3 Telemetry encoder 1 ON (spinning) 4 Telemetry encoder 2 ON (spinning) 5 Telemetry transmitter A ON 6 Telemetry transmitter B ON 7 Spare 8 Spare
	3	Electrical Power Status Bit 1 Spinning bus paralleled 2 Bypass relay 1 normal 3 Bypass relay 2 normal 4 Despun bus paralleled 5 Spare 6 Spare 7 Spare 8 Spare
	4	Electrical Power Status Bit 1 Thermal charge limit set override 2 Voltage limiter 1 ON 3 Voltage limiter 2 ON 4 Voltage limiter 3 ON 5 Voltage limiter 4 ON 6 Spare 7 Spare 8 Reconditioning discharge ON

Table 32 (continued)

Main Frame Word	Subcomm Channel	Bit Assignments
8	5	Controls Status Bit 1 Despin electronics 1 ON 2 Despin electronics 2 ON 3 Motor drive 1 ON 4 Motor drive 2 ON 5 ANC 1 ON 6 ANC 2 ON 7 Motor driver 1 low/high gain 8 Motor driver 2 low/high gain
	6	Controls Status Bit 1 Command limiter ON 2 Interlock enable 3 Rate command latch 1/2 4 Earth sensor 1 OFF 5 Earth sensor 2 OFF 6 Earth sensor 3 OFF
	7	Control Status Bit 1 Select earth sensor 1 2 Select earth sensor 2 3 Select earth sensor 3 4 SCL enable 5 Spare 6 Spare 7 Spare 8 Spare

Table 32 (continued)

Main Frame Word	Subcomm Channel	Bit Assignments
10	Code	Status Word 10 (8 bits) Attitude Determination Measurement — Bit: 1 2 3 4 5 6 7 8 t_1 Spin period: 0 0 0 1 1 0 0 0 t_2 Sync control reference: 0 0 1 1 1 0 0 0 t_3 Inner sun chord: 0 1 0 0 1 0 0 0 t_4 Outer sun chord: 0 1 0 1 1 0 0 0 t_5 North earth chord: 0 1 1 0 1 0 0 0 t_6 South earth chord: 0 1 1 1 1 0 0 0 t_7 Sun-N earth separation: 1 0 0 0 1 0 0 0 t_8 Sun-S earth separation: 1 0 0 1 1 0 0 0 t_9 N earth to S earth: 1 0 1 0 1 0 0 0 t_{10} Platform pointing
12	—	Status Word 12 (8 bits) Attitude Determination 1/2-16 bit word; bit 1 most significant bit
14	—	Status Word 14 (8 bits) Attitude Determination 1/2-16 bit word; bit 8 least significant bit of 16 bit word included in status word 12 and 14 and coded in status word 10

TABLE 33. TELEMETRY, CHANNEL ASSIGNMENTS FOR ANALOG SUBCOMMUTATOR – SPINNING

Main Frame Word	Subcomm Channel	Channel Assignments
16	0	Battery 1 voltage
	1	Battery 2 voltage
	2	Battery 1 charge/discharge current
	3	Battery 2 charge/discharge current
	4	Battery 1 pack 1 temperature
	5	Battery 1 pack 2 temperature
	6	Battery 2 pack 1 temperature
	7	Battery 2 pack 2 temperature
18	0	Spare
	1	Spare
	2	Spare
	3	Spare
	4	Spare
	5	Spare
	6	Spare
	7	Spare
20	0	Radial jet 1 temperature
	1	Radial jet 2 temperature
	2	Axial jet 1 temperature
	3	Axial jet 2 temperature
	4	Fuel tank 1 temperature
	5	Fuel tank 2 temperature
	6	Hydrazine 1 pressure
	7	Hydrazine 2 pressure
22	0	BAPTA temperature 1
	1	BAPTA temperature 2
	2	Apogee motor temperature 1
	3	Apogee motor temperature 2
	4	Sunshield temperature 1
	5	Sunshield temperature 2
	6	Solar panel temperature 1
	7	Solar panel temperature 2

TABLE 34. TELEMETRY CHANNEL STATUS DIGITAL BIT ASSIGNMENTS – DESPUN

Main Frame Word	Subcomm Channel	Bit Assignments
7		Status Word 7 (8 bits) Despun Encoder Bit 1 Despun decoder 1 execute 2 Despun decoder 2 execute 3 Subframe count 4 Subframe count 5 Subframe count 6 Spare 7 Spare 8 Spare
9		Status Word 9 (8 bits) Despun Encoder Bit 1 Spare 2 Spare 3 Spare 4 Spare 5 Spare 6 Spare 7 Spare 8 Spare
11	0	Communication Status Bit 1 Ku band receiver CMD/LDR forward A ON 2 Ku band receiver CMD/LDR forward B ON 3 Ku band receiver MDR/HDR forward A ON 4 Ku band receiver MDR/HDR forward B ON 5 Antenna tracking modulator driver select A/B (Antenna A) 6 Ku band receiver HDR return 1 A ON 7 Ku band receiver HDR return 1 B ON 8 Antenna tracking modulator driver select A/B (Antenna B)

Table 34 (continued)

Main Frame Word	Subcomm Channel	Bit Assignments
11	1	Communication Status Bit 1 Spare 2 Spare 3 Spare 4 Ku band receiver HDR return 1 bandwidth select 5 Ku band receiver HDR return 1 bandwidth select 6 Ku band receiver HDR return 2 bandwidth select 7 Ku band receiver HDR return 2 bandwidth select 8 Ku band transmitter HDR return 1 A ON
	2	Communication Status Bit 1 Ku band transmitter HDR return 1 B ON 2 Ku band transmitter HDR return 1 TWT select 3 Spare 4 Spare 5 Spare 6 Ku band transmitter MDR/LDR A ON 7 Ku band transmitter MDR/LDR B ON 8 Ku band transmitter MDR/LDR TWT select
	3	Communication Status Bit 1 Ku band transmitter HDR forward 1 A ON 2 Ku band transmitter HDR forward 1 B ON 3 Ku band transmitter HDR forward 1 TWT select 4 Spare 5 Spare 6 Spare 7 UHF transmitter driver A ON 8 UHF transmitter driver B ON

Table 34 (continued)

Main Frame Word	Subcomm Channel	Bit Assignments
11	4	Communication Status Bit 1 UHF power amplifier 1 ON 2 UHF power amplifier 2 ON 3 UHF power amplifier 3 ON 4 UHF power amplifier 4 ON 5 UHF power amplifier 5 ON 6 UHF power amplifier 6 ON 7 Spare 8
	5	Communication Status Bit 1 Spare 2 Spare 3 VHF horizontal receiver 1 A ON 4 VHF horizontal receiver 1 B ON 5 VHF horizontal receiver 2 A ON 6 VHF horizontal receiver 2 B ON 7 VHF horizontal receiver 3 A ON 8 VHF horizontal receiver 3 B ON
	6	Communication Status Bit 1 VHF horizontal receiver 4 A ON 2 VHF horizontal receiver 4 B ON 3 VHF horizontal receiver 5 A ON 4 VHF horizontal receiver 5 B ON 5 VHF vertical receiver 1 A ON 6 VHF vertical receiver 1 B ON 7 VHF vertical receiver 2 A ON 8 VHF vertical receiver 2 B ON

Table 34 (continued)

Main Frame Word	Subcomm Channel	Bit Assignments
11	7	Communication Status Bit 1 VHF vertical receiver 3 A ON 2 VHF vertical receiver 3 B ON 3 VHF vertical receiver 4 A ON 4 VHF vertical receiver 4 B ON 5 VHF vertical receiver 5 A ON 6 VHF vertical receiver 5 B ON 7 VHF receiver select up converter 8 VHF receiver frequency source select
13	0	Communication Status Bit 1 Order wire receiver A ON 2 Order wire receiver B ON 3 S band transponder A ON 4 S band transponder B ON 5 S band transmitter 1 A ON 6 S band transmitter 1 B ON 7 S band transmitter 2 A ON 8 S band transmitter 2 B ON
	1	Communication Status Bit 1 Spare 2 Spare 3 S band transmitter 1 high/low select 4 S band transmitter 2 high/low select 5 Spare 6 S band receiver 1 A ON 7 S band receiver 1 B ON 8 S band receiver 2 A ON

Table 34 (continued)

Main Frame Word	Subcomm Channel	Bit Assignments
13	2	Communication Status Bit 1 S band receiver 2 B ON 2 Spare 3 Spare 4 S band MDR receiver 1 step attenuator IN/OUT 5 S band MDR receiver 2 step attenuator IN/OUT 6 Spare 7 Telemetry encoder 1 ON 8 Telemetry encoder 2 ON
	3	Deployment Status Bit 1 Release support arm Ku band antenna 2 Release center support arm S/Ku band antenna 1 3 Release center support S/Ku band antenna 2 4 Release S/Ku band antenna arm 1 5 Release S/Ku band antenna arm 2 6 Release UHF antenna arm 7 Release Astromast stowage lock 8 Release VHF antenna element 1 to 4 arms
	4	Deployment Status Bit 1 Release VHF antenna element 5 arm 2 Release VHF element 1 from support arm 3 Release VHF element 2 from support arm 4 Release VHF element 3 from support arm 5 Release VHF element 4 from support arm 6 Release VHF element 5 from support arm 7 Release S/Ku band antenna 1 from support arm 8 Release S/Ku band antenna 2 from support arm

Table 34 (continued)

Main Frame Word	Subcomm Channel	Bit Assignments
13	5	Deployment Status Bit 1 Spare 2 Release Ku band antenna from support arm 3 Release UHF antenna from support arm 4 Spare 5 Spare 6 Spare 7 Spare 8 Spare
	6	Power Status Bit 1 Voltage limiter 1 ON 2 Voltage limiter 2 ON 3 Spare 4 Spare 5 Spare 6 Spare 7 Spare 8 Spare
	7	Communication Status Bit 1 Frequency synthesizer A ON 2 Frequency synthesizer B ON 3 Frequency synthesizer status 4 Frequency synthesizer status 5 Frequency synthesizer status 6 Frequency synthesizer status 7 Frequency synthesizer status 8 Frequency synthesizer status
15		Status Word 15 Bit 1 Spare 2 Spare 3 Spare 4 Spare 5 Spare 6 Spare 7 Spare 8 Spare

TABLE 35. TELEMETRY CHANNEL ASSIGNMENTS FOR ANALOG SUBCOMMUTATORS – DESPUN

Main Frame Word	Subcomm Channel	Analog Subcommutators
17	0	Spare
	1	Spare
	2	Spare
	3	Spare
	4	S band power amplifier 1 temperature
	5	S band power amplifier 2 temperature
	6	S band power amplifier 3 temperature
	7	S band power amplifier 4 temperature
19	0	Forward shelf temperature 1
	1	Forward shelf temperature 2
	2	Aft shelf temperature 1
	3	Aft shelf temperature 2
	4	Auxiliary battery voltage
	5	Ku band transmitter A temperature
	6	Ku band transmitter B temperature
	7	Heater bank A current
21	0	Heater bank B current
	1	Heater bank C current
	2	Heater bank D current
	3	Auxiliary battery voltage
	4	Spare
	5	Spare
	6	Spare
	7	Spare
	8	Spare
23	0	BAPTA hub temperature 1
	1	BAPTA hub temperature 2
	2	UHF power amplifier 1 temperature
	3	UHF power amplifier 2 temperature
	4	UHF power amplifier 3 temperature
	5	UHF power amplifier 4 temperature
	6	UHF power amplifier 5 temperature
	7	UHF power amplifier 6 temperature

TABLE 36. COMMAND ASSIGNMENTS

Summary	Despun	Spinning
Communications	122	0
Deployment mechanisms	37	0
Antenna operations	12	0
TT&C	3	11
Power	0	27
Controls	0	26
RCS	0	33
Subtotal	174	97
Spares	81	30
Total	255	127

Communications

Despun

1. Frequency synthesizer A ON, B OFF
2. Frequency synthesizer B ON, A OFF
3. Frequency synthesizer both OFF
4. Master oscillator select A
5. Master oscillator select B
6. Frequency synthesizer A frequency step for S band transmit L O 1
7. Frequency synthesizer B frequency step for S band transmit L O 1
8. Frequency synthesizer A frequency step for S band receive L O 1
9. Frequency synthesizer B frequency step for S band receive L O 1
10. Frequency synthesizer A frequency step for S band transmit L O 2
11. Frequency synthesizer B frequency step for S band transmit L O 2
12. Frequency synthesizer A frequency step for S band receive L O 2
13. Frequency synthesizer B frequency step for S band receive L O 2
14. Ku band receiver CMD/LDR forward A ON, B OFF
15. Ku band receiver CMD/LDR forward B ON, A OFF
16. Ku band receiver CMD/LDR forward both OFF
17. Ku band receiver MDR/HDR forward A ON, B OFF
18. Ku band receiver MDR/HDR forward B ON, A OFF
19. Ku band receiver MDR/HDR forward both OFF
20. Antenna tracking modulator driver select A (antenna A)
21. Antenna tracking modulator driver select B (antenna A)

Table 36 (continued)

22. Ku band receiver HDR return 1 A ON, B OFF
23. Ku band receiver HDR return 1 B ON, A OFF
24. Ku band receiver HDR return 1, both OFF
25. Antenna tracking modulator driver select A (antenna B)
26. Antenna tracking modulator driver select B (antenna B)
27. Antenna tracking modulator driver select A (antenna C)
28. Antenna tracking modulator driver select B (antenna C)
29. Ku band receiver HDR return 1 bandwidth select – 100 MHz
30. Ku band receiver HDR return 1 bandwidth select – 50 MHz
31. Ku band receiver HDR return 1 bandwidth select – 10 MHz
32. Ku band transmitter HDR return 1 A ON, B OFF
33. Ku band transmitter HDR return 1 B ON, A OFF
34. Ku band transmitter HDR return 1, both OFF
35. Ku band transmitter HDR return 1, select TWT A
36. Ku band transmitter HDR return 1, select TWT B
37. Ku band transmitter MDR/LDR A ON, B OFF
38. Ku band transmitter MDR/LDR B ON, A OFF
39. Ku band transmitter MDR/LDR, both OFF
40. Ku band transmitter MDR/LDR, select TWT A
41. Ku band transmitter MDR/LDR, select TWT B
42. Ku band transmitter HDR forward 1 A ON, B OFF
43. Ku band transmitter HDR forward 1 B ON, A OFF
44. Ku band transmitter HDR forward 1, both OFF
45. Ku band transmitter HDR forward 1, select TWT A
46. Ku band transmitter HDR forward 1, select TWT B
47. UHF transmitter driver A ON, B OFF
48. UHF transmitter driver B ON, A OFF
49. UHF transmitter driver, both OFF
50. UHF power amplifier 1 ON
51. UHF power amplifier 1 OFF
52. UHF power amplifier 2 ON
53. UHF power amplifier 2 OFF
54. UHF power amplifier 3 ON
55. UHF power amplifier 3 OFF
56. UHF power amplifier 4 ON
57. UHF power amplifier 4 OFF

Table 36 (continued)

58. UHF power amplifier 5 ON
59. UHF power amplifier 5 OFF
60. UHF power amplifier 6 ON
61. UHF power amplifier 6 OFF
62. VHF horizontal receiver 1 A ON, B OFF
63. VHF horizontal receiver 1 B ON, A OFF
64. VHF horizontal receiver 2 A ON, B OFF
65. VHF horizontal receiver 2 B ON, A OFF
66. VHF horizontal receiver 3 A ON, B OFF
67. VHF horizontal receiver 3 B ON, A OFF
68. VHF horizontal receiver 4 A ON, B OFF
69. VHF horizontal receiver 4 B ON, A OFF
70. VHF horizontal receiver 5 A ON, B OFF
71. VHF horizontal receiver 5 B ON, A OFF
72. VHF horizontal receiver, all OFF
73. VHF vertical receiver 1 A ON, B OFF
74. VHF vertical receiver 1 B ON, A OFF
75. VHF vertical receiver 2 A ON, B OFF
76. VHF vertical receiver 2 B ON, A OFF
77. VHF vertical receiver 3 A ON, B OFF
78. VHF vertical receiver 3 B ON, A OFF
79. VHF vertical receiver 4 A ON, B OFF
80. VHF vertical receiver 4 B ON, A OFF
81. VHF vertical receiver 5 A ON, B OFF
82. VHF vertical receiver 5 B ON, A OFF
83. VHF vertical receivers, all OFF
84. VHF receivers select upconverter A
85. VHF receivers select upconverter B
86. VHF receivers select frequency source A
87. VHF receivers select frequency source B
88. Order wire receiver A ON, B OFF
89. Order wire receiver B ON, A OFF
90. Order wire receiver both OFF
91. S band transponder A ON, B OFF
92. S band transponder B ON, A OFF
93. S band transponder, both OFF

Table 36 (continued)

94. S band transmitter 1 A ON, B OFF
95. S band transmitter 1 B ON, A OFF
96. S band transmitter 1, both OFF
97. S band transmitter 2 A ON, B OFF
98. S band transmitter 2 B ON, A OFF
99. S band transmitter 2, both OFF
100. S band transmitter 1 high level select
101. S band transmitter 1 low level select
102. S band transmitter 2 high level select
103. S band transmitter 2 low level select
104. S band receiver 1 A ON, B OFF
105. S band receiver 1 B ON, A OFF
106. S band receiver 1, both OFF
107. S band receiver 2 A ON, B OFF
108. S band receiver 2 B ON, A OFF
109. S band receiver 2, both OFF
110. S band MDR receiver 1 step attenuator IN
111. S band MDR receiver 1 step attenuator OUT
112. S band MDR receiver 2 step attenuator IN
113. S band MDR receiver 2 step attenuator OUT
114. HDR/MDR/LDR antenna to A
115. HDR/MDR/LDR antenna to B
116. HDR/MDR/LDR antenna to C
117. HDR S/Ku band antenna 1 to A
118. HDR S/Ku band antenna 1 to B
119. HDR S/Ku band antenna 1 to C
120. HDR S/Ku band antenna 2 to A
121. HDR S/Ku band antenna 2 to B
122. HDR S/Ku band antenna 2 to C

Deployment Mechanisms

Despun

1. Release support arm Ku band antenna
2. Release center support S/Ku band antenna 1
3. Release center support S/Ku band antenna 2

Table 36 (continued)

4. Release S/Ku band antenna 1 arm
5. Release S/Ku band antenna 2 arm
6. Release UHF antenna arm
7. Release astromast stowage lock
8. Extend astromast
9. Release AGIPA antenna element 1 to 4 element
10. Release AGIPA antenna element 5 arm
11. Release VHF element 1 from support arm
12. Release VHF element 2 from support arm
13. Release VHF element 3 from support arm
14. Release VHF element 4 from support arm
15. Release VHF element 5 from support arm
16. Sever cable on VHF element 1
17. Sever cable on VHF element 2
18. Sever cable on VHF element 3
19. Sever cable on VHF element 4
20. Sever cable on VHF element 5
21. Unfurl by mechanical drive VHF element 1
22. Unfurl by mechanical drive VHF element 2
23. Unfurl by mechanical drive VHF element 3
24. Unfurl by mechanical drive VHF element 4
25. Unfurl by mechanical drive VHF element 5
26. Release S/Ku band antenna 1 from support arm
27. Release S/Ku band antenna 2 from support arm
28. Release Ku band antenna from support arm
29. Release UHF antenna from support arm
30. Sever cable on S/Ku band antenna 1
31. Sever cable on S/Ku band antenna 2
32. Sever cable on Ku band antenna
33. Sever cable on UHF antenna
34. Unfurl by mechanical drive S/Ku band antenna 1
35. Unfurl by mechanical drive S/Ku band antenna 2
36. Unfurl by mechanical drive Ku band antenna
37. Unfurl by mechanical drive UHF antenna

Table 36 (continued)

Antenna Operations
Despun 1. Step S/Ku band antenna 1 azimuth east 2. Step S/Ku band antenna 2 azimuth east 3. Step Ku band antenna azimuth east 4. Step S/Ku band antenna 1 azimuth west 5. Step S/Ku band antenna 2 azimuth west 6. Step Ku band antenna azimuth west 7. Step S/Ku band antenna 1 elevation south 8. Step S/Ku band antenna 2 elevation south 9. Step Ku band antenna elevation south 10. Step S/Ku band antenna 1 elevation north 11. Step S/Ku band antenna 2 elevation north 12. Step Ku band antenna elevation north
TT&C
Despun 1. Telemetry encoder A ON 2. Telemetry encoder B ON 3. Telemetry encoders both OFF Spinning 1. Telemetry encoder 1 PCM mode 2. Telemetry encoder 2 PCM mode 3. Telemetry encoder 1 ON 4. Telemetry encoder 1 OFF 5. Telemetry encoder 2 ON 6. Telemetry encoder 2 OFF 7. Telemetry encoder 1 FM mode 8. Telemetry encoder 2 FM mode 9. Telemetry transmitter A ON, B OFF 10. Telemetry transmitter B ON, A OFF 11. Telemetry transmitters both OFF

Table 36 (continued)

Power Subsystem
Spinning 1. Voltage limiters OFF 2. Voltage limiter 1 ON 3. Voltage limiter 2 ON 4. Voltage limiter 3 ON 5. Voltage limiter 4 ON 6. Battery 1 discharge ON 7. Battery 2 discharge ON 8. Battery 1 discharge OFF 9. Battery 2 discharge OFF 10. Battery 1 discharge control bypass 11. Battery 2 discharge control bypass 12. Spinning parallel relay OFF 13. Spinning parallel relay ON 14. Battery 1 charge A ON 15. Battery 2 charge A ON 16. Battery 1 charge B ON 17. Battery 2 charge B ON 18. Battery 1 charge OFF 19. Battery 2 charge OFF 20. Battery 1 recondition ON 21. Battery 2 recondition ON 22. Battery 1 recondition OFF 23. Battery 2 recondition OFF 24. Auxiliary battery charge ON 25. Auxiliary battery charge OFF 26. Despun parallel relay ON 27. Despun parallel relay OFF
Controls
Spinning 1. Earth sensors ON 2. Earth sensor 1 OFF 3. Earth sensor 2 OFF

Table 36 (continued)

4. Earth sensor 3 OFF
5. Select earth sensor 1
6. Select earth sensor 2
7. Select earth sensor 3
8. Motor drivers ON
9. Motor driver 1 OFF
10. Motor driver 2 OFF
11. Rate command latch 1
12. Rate command latch 2
13. Despin control electronics 1 and 2 OFF
14. Despin control electronics 1 ON
15. Despin control electronics 2 ON
16. Interlock enable
17. Interlock disable
18. Command limiter ON
19. Command limiter OFF
20. Motor driver 1 low gain
21. Motor driver 1 high gain
22. Motor driver 2 low gain
23. Motor driver 2 high gain
24. Active nutation control 1 ON
25. Active nutation control 2 ON
26. Active nutation control OFF

Reaction Control Subsystem and Apogee Motor

Spinning

1. Axial jet 1
2. Axial jet 2
3. Axial jets 1 and 2
4. Radial jet 1
5. Radial jet 2
6. Latching valve 1 open
7. Latching valve 1 close
8. Latching valve 2 open
9. Latching valve 2 close
10. Latching valve 3 open

Table 36 (continued)

11.	Latching valve 3 close
12.	Latching valve 4 open
13.	Latching valve 4 close
14.	Latching valve 5 open
15.	Latching valve 5 close
16.	Apogee motor squib 1 (decoder 1)
17.	Apogee motor squib 2 (decoder 2)
18.	Apogee motor heaters ON
19.	Apogee motor heater 1 OFF
20.	Apogee motor heater 2 OFF
21.	Apogee motor heater 3 OFF
22.	Apogee motor heater 4 OFF
23.	Spinup valve heaters OFF
24.	Spinup valve heaters ON
25.	Radial valve heater OFF
26.	Radial valve heater ON
27.	Axial valve heater ON
28.	Axial valve heater OFF
29.	Spinup thrusters 1
30.	Spinup thrusters 2
31.	SCL enable
32.	SCL disable
33.	SCL execute

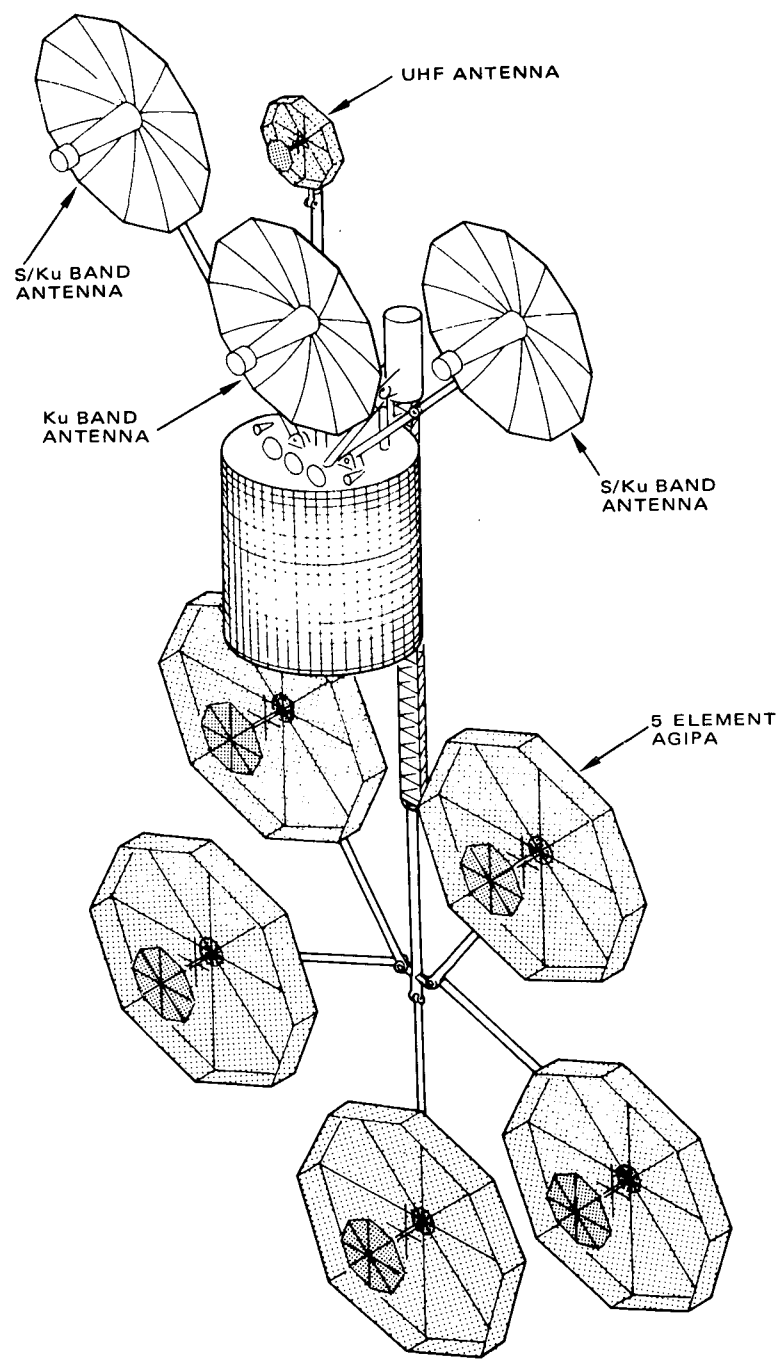

Figure 68. TDRS Antenna Arrangement

4.3.4 Antennas

The arrangement of antennas for the Atlas Centaur launched TDR spacecraft is shown in Figure 68. (This figure is identical to Figure 43 and is repeated here for the reader's convenience.) The antenna arrangement was selected to balance as much as possible the solar torque on the spacecraft.

High gain MDR, HDR, and return link antennas are mounted forward. This position minimizes cable and waveguide runs to electronic equipment mounted in the spacecraft, and also provides for a more rigid and thermally stable mount for these narrowbeam antennas. A forward location of the UHF broadbeam antenna is also selected to minimize power loss in the transmission lines running from the transmitter to the antenna.

The LDR return link is implemented with a five element AGIPA configuration which is deployed aft. The VHF elements are less sensitive to alignment errors and cable runs over the required distance do not result in excessive losses. The antenna is deployed by a system combination of an Astromast and pivoted linkages. The Astromast is a lightweight deployable truss structure which can achieve the long deployment required with a high stiffness and highly compact stowage. The lattice type structure also minimizes shadowing of the solar cell arrays arising from the aft deployment of the LDR return antenna.

Figure 69 shows the stowed configuration of the antenna for the Atlas Centaur launched TDR spacecraft. Stowage of the TDR antenna complement in the Intelsat IV payload fairing requires an extensive amount of folding of these structures. A 4 λ AGIPA size was selected to avoid a more complex deployment or to require an extended length payload fairing. The antenna elements are folded using the umbrella principle being developed by Radiation, Inc. for the high gain S and Ku band antennas.

The TDRS antennas in their operational configuration occupy approximately 25 times the volume available for stowage during launch. Deployment of this antenna configuration is accordingly complicated by the clearances available and because the antennas must be deployed in proper sequence to avoid contact with/or between elements. The aft mounted AGIPA is deployed first (Table 37). Each of the deployment steps up to the point where the Astromast is extended would be by ground command. The remaining deployment would be accomplished by sequentially firing squibs in a specified order. The combination of ground command/time sequenced deployment is to provide a high degree of safety consistent with conservation of command channels (Table 36). The deployment sequence of forward mounted antennas is simpler than that of the aft mounted AGIPA. Each antenna has at most three steps which would be initiated by ground command. The S/Ku band MDR/HDR user link antennas could be deployed either before or after the deployment of the center mounted TDRS to a ground antenna.

TABLE 37. ANTENNA DEPLOYMENT SEQUENCE

Aft	Forward
VHF Antenna Array	S/Ku Band Antennas
Rotate center element support arm 180 degrees	Rotate lower support arms 460 degrees and rotate upper support arms 180 degrees
Rotate astromast assembly 186 degrees	Rotate antennas on gimbal 90 degrees
Extend astromast to deployed length	Deploy parabolic reflectors
Rotate side element support arms	UHF Antenna
Rotate side elements 90 degrees	Rotate support arm 175 degrees
Rotate center element 270 degrees	Rotate antenna 270 degrees
Unfurl and extend all elements	Unfurl and extend antenna
	Ku Band Antenna
	Rotate antenna on gimbal 90 degrees
	Deploy parabolic reflector

4.3.4.1 S/Ku Band Deployable Antennas

The primary objective in the antenna mechanical design is the attainment of minimum mass consistent with adequate structure strength, stiffness, and an antenna stowage within space available for payload. These parameters have been specified to be ±30 g quasi-static acceleration, 50 and 4 Hz minimum frequency for the stowed and deployed antennas, respectively, and the payload envelope available within the standard Intelsat IV fairing.

The S and Ku band dual frequency antenna selected for the TDRS are a deployable rib mesh design of 3.82 meter diameter (Figure 70). The primary surface contour is shaped by 12 aluminum ribs of 3.8 cm diameter and tapered wall thicknesses from 0.015 to 0.03 cm. The reflective mesh contour precision to within 0.025 cm rms is accomplished by the use of a secondary back mesh and adjustable tension ties between front and back mesh. Figure 71 shows the antenna in its stowed configuration.

A central cone supports the S band feed assembly and the Ku band subreflector (Cassegrainian concept-dichroic support structure). The antenna hub measures 45 cm in diameter and houses the mechanical deployment drive and linkage mechanism. Redundant torque spring and motor drives unfurl the reflector in orbit as well as in 1 g environment. This rib

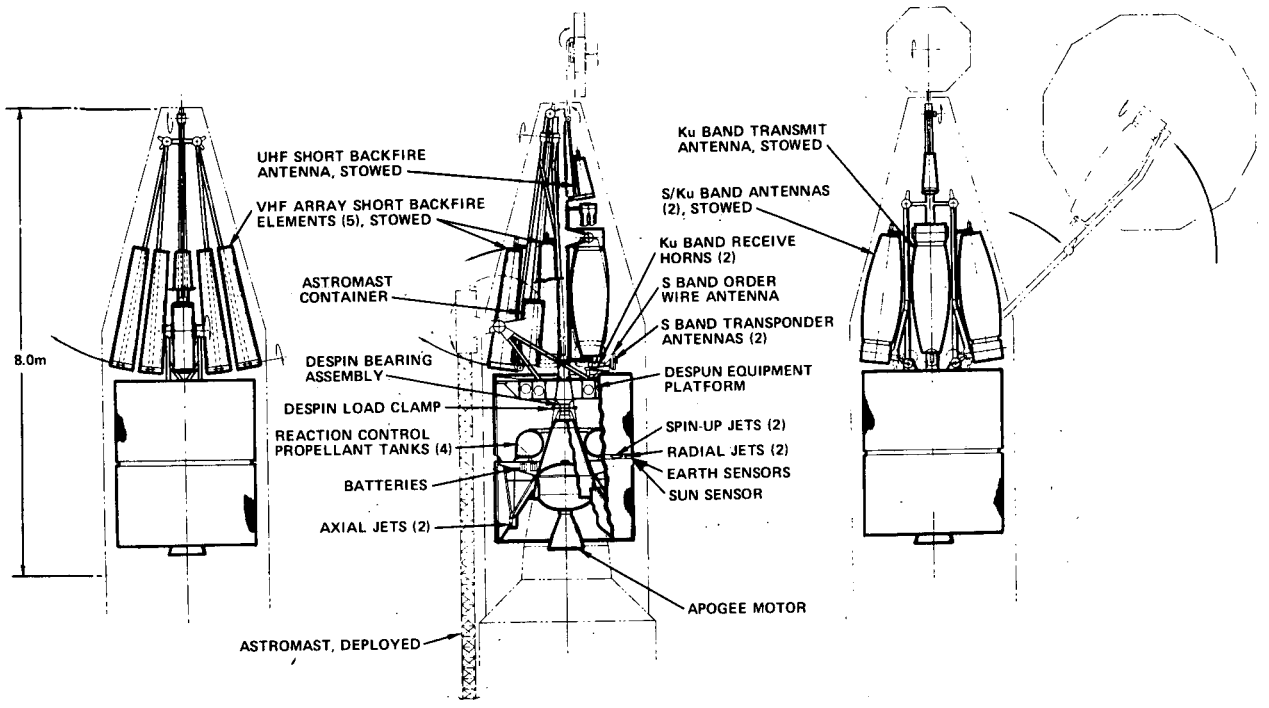

Figure 69. TDRS Stowed Configuration

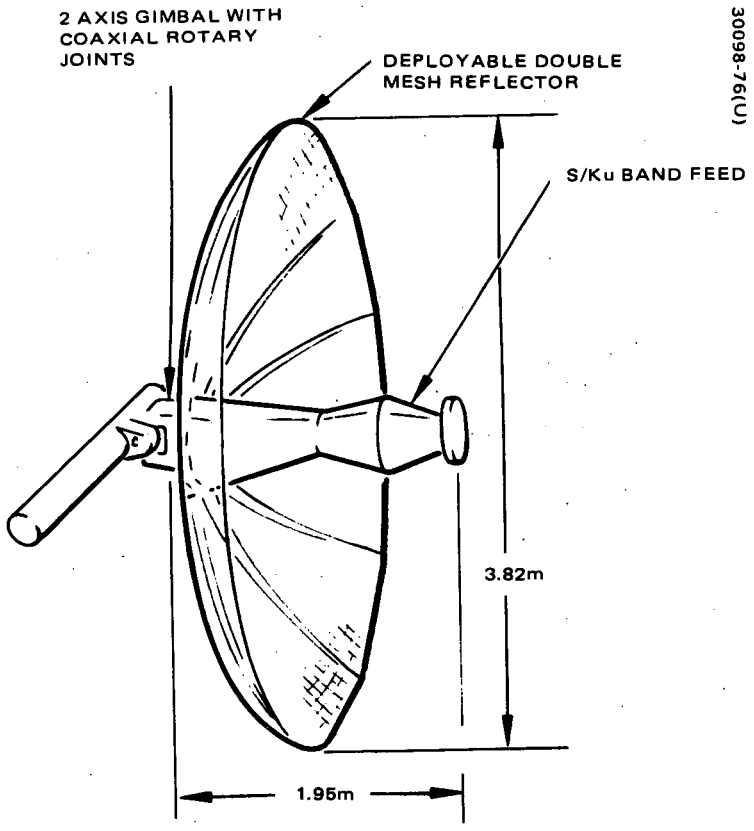

Figure 70. S/Ku Band High Gain Antenna

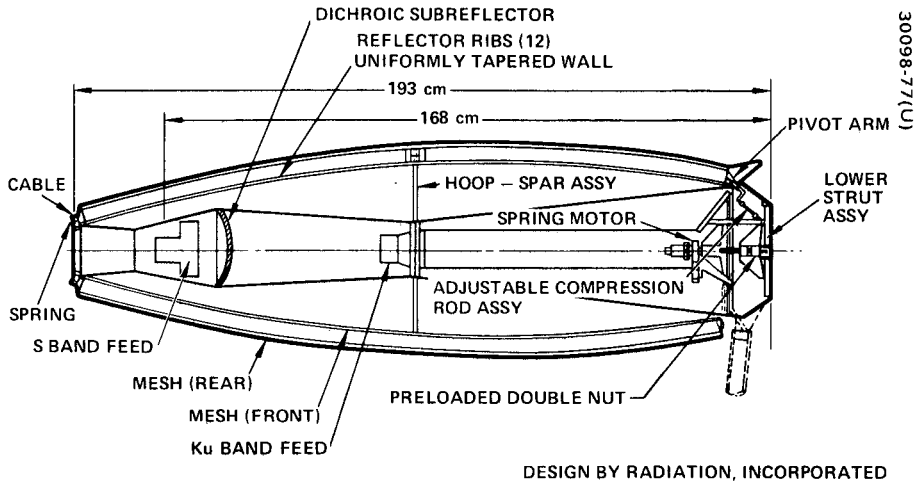

Figure 71. S/Ku Band Deployable Antenna Stowed Configuration

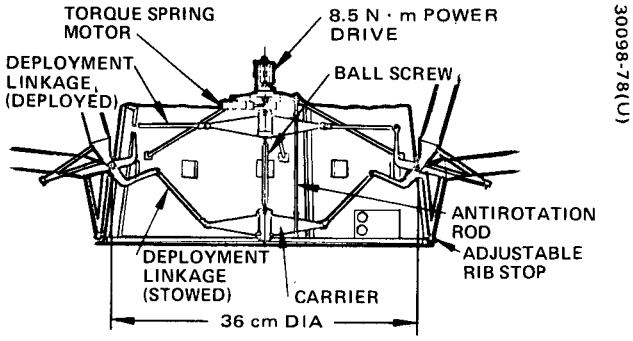

Figure 72. Antenna Mechanical Deployment Drive

dominated mesh antenna system was designed by Radiation, Inc. Its mechanical and RF performance characteristics have been demonstrated in a NASA funded program. The mass estimated by Radiation, Inc., for the 3.82 meter S/Ku band deployable antenna is 8.9 kg.

The reflective mesh is constructed from five-strand bundles of 17.8 micron Chromel-R wire knitted into a wire screen. The mesh is knitted and it is used as a secondary drawing surface for contouring the front mesh while minimizing the antenna mass. The mesh is attached to the ribs in a tensioned state.

Deployment of the reflector from the stowed to the fully open position is precisely controlled to prevent impact loading of the rib structures and mesh, thereby assuring that 1) the preset parabolic surface is not distorted by the deployment action and 2) no mesh loading conditions result that exceed the mesh strength limits. The deployment mechanism shown in Figure 72 utilizes redundant energy drive systems to rotate a ball screw within a recirculating ball nut. The resultant linear motion of the ball nut serves to rotate each rib from the stowed to deployed position through the individual linkages to each rib. The primary drive of this system is a constant torque spring motor. This spring motor provides sufficient energy to deploy the antenna in any orientation under gravity conditions. In a zero gravity condition, the spring motor capability exceeds the deployment energy requirements. A backup drive system of two miniature torque motor functions then as dynamic brakes, controlling the deployment and requiring no electrical power. If required to deliver power, the motors can increase the torque to the ball screw by as much as a factor of four. Latching in the deployed condition is accomplished by driving the ball nut carrier and linkages through an overcenter condition (relative to the pivot arms).

The RF performance parameters for the S and Ku band antennas are summarized in Table 38. In the ground link antenna application operation at Ku band only is required. Without the interference created by use of a second frequency, the antenna exhibits slightly improved RF characteristics (±0.2 dB) and is somewhat lighter (0.7 kg).

4.3.4.2 AGIPA

An Adaptive Ground Implemented Phased Array (AGIPA) has been implemented for the LDR return link from user spacecraft (see Figure 73). The AGIPA consists of five moderate gain backfire antenna elements which are equally spaced on an 8.5 meter circle when deployed. The stowage concept of these VHF elements is essentially that of the S/Ku band rib mesh reflector. The considerably lesser reflector precision requirement at VHF frequency, however, allows use of flex joints at the rib roots for simple deployment mechanization. The primary reflective surface of 4.40 meter diameter employs a 1.25 inch grid mesh and 8 inch aluminum tubular ribs. A central tube supports the crossed dipole feed and a reflective cavity plate (mesh) at $\lambda/4$ and $\lambda/2$ spaced from the primary reflector.

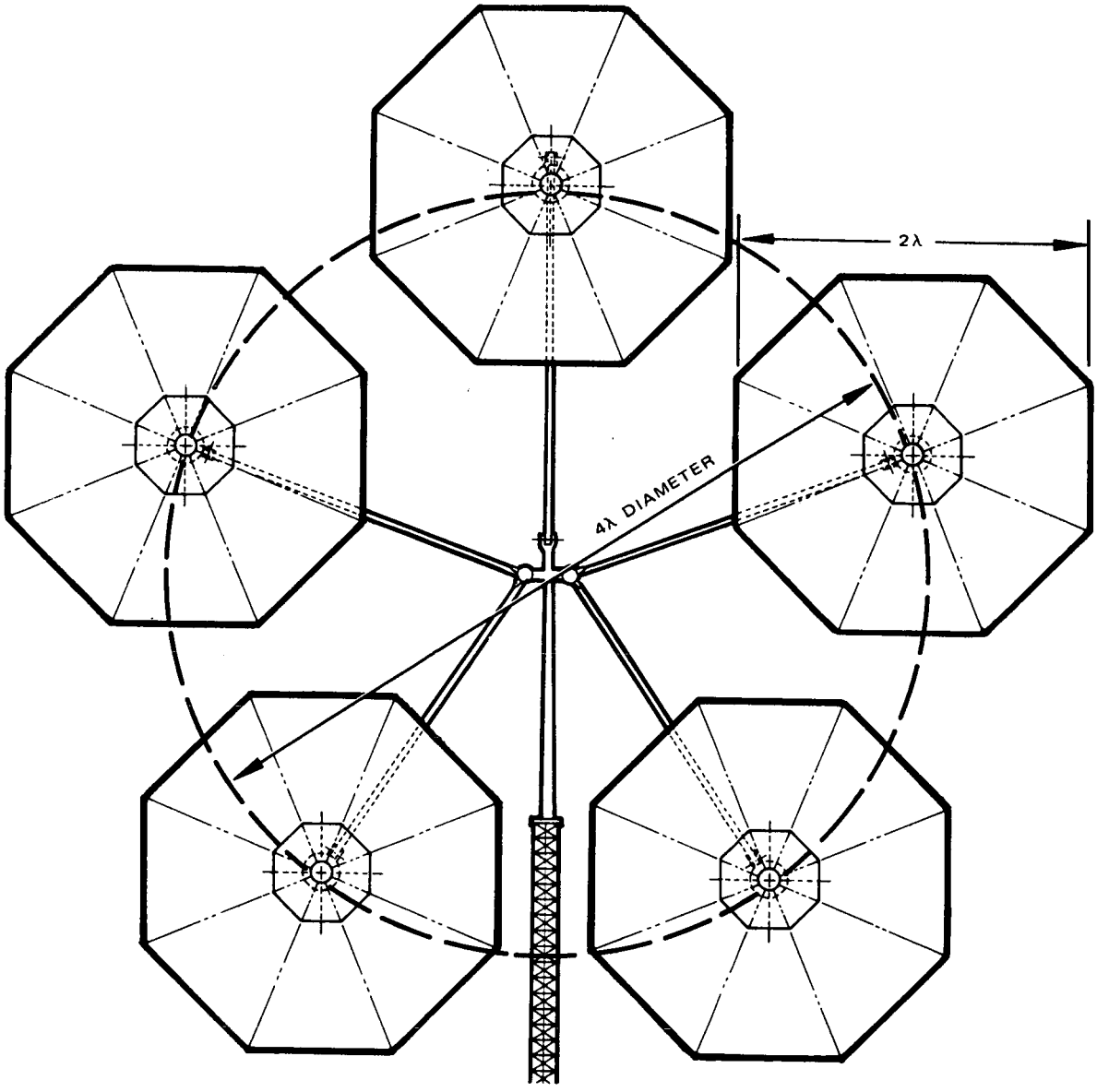

Figure 73. AGIPA Configuration

TABLE 38. S/Ku BAND HIGH GAIN ANTENNA

Frequency Band	S Band		Ku Band	
Frequency, GHz	2.07	2.25	13.7	14.9
Aperture diameter, meters	3.82		3.82	
Aperture area gain, dB	38.4	39.1	54.7	55.6
Spillover and amplitude taper loss, dB	1.35	1.35	0.86	0.86
Phase loss, dB	0.14	0.14	0.04	0.04
Blockage loss, dB	0.19	0.20	0.08	0.08
Crosspolarization loss, dB	0.19	0.20	0.32	0.32
Radome loss, dB	0.19	0.10	0.16	0.16
Dichroic subreflector loss, dB	0.20	0.20	0.20	0.20
Surface tolerance loss, dB	0.02	0.02	0.32	0.36
Mesh I^2R loss	0.05	0.05	0.15	0.15
Hybrid loss, dB	0.20	0.20	N.A.	N.A.
Transmission line loss, dB	0.35	0.35	0.04	0.04
Feed and polarizer I^2R loss, dB	N.A.	N.A.	0.32	0.32
Comparator loss, dB	N.A.	N.A.	0.20	0.20
VSWR loss, dB	0.12	0.12	0.08	0.08
Total losses, dB	2.90	2.93	2.77	2.81
Total efficiency, percent	51.3	51.0	53.0	52.5
Antenna peak gain, dB	35.5	36.2	51.9	52.8
Half power beamwidth, degrees	2.5	2.3	0.37	0.34
Polarization sense	Circular	Circular (orthogonal)	Circular	Circular

The AGIPA system is nested around the antenna support mast in the spacecraft launch configuration. In orbit a deployable lattice truss boom (Astromast-SPAR Aerospace Company) positions the antenna system aft of the spacecraft for balanced solar pressure torque. The openness of the Astromast boom produces less than 1 percent shadowing of the solar cell array at direct sunlight incidence.

Each of the five AGIPA elements employs two coaxial cable feed lines of 1.25 cm Alumnispline which are routed along the structural supports. Dual linear polarization is used. The performance characteristics for the reflector elements are listed in Table 39.

4.3.4.3 Short Backfire Broadbeam Antennas

The short backfire type antenna has been adapted for the broadbeam antenna requirements because of its compact size, minimum mass and complexity. Test data show that this antenna type can develop an aperture

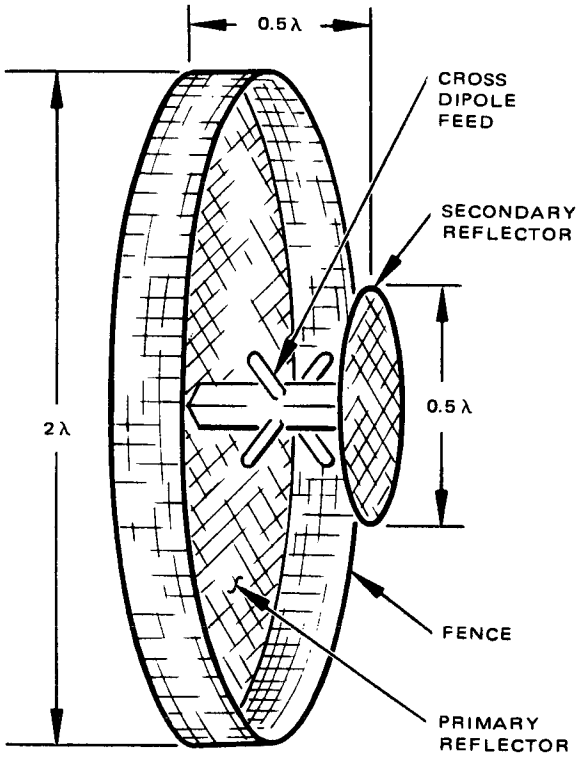

Figure 74. Short Backfire Broadbeam Antenna

TABLE 39. VHF – SHORT BACKFIRE ELEMENT PERFORMANCE

Frequency band, MHz	136 to 138
Aperture diameter meters	4.35
Aperture, gain*, dB	15.0
Reflector surface loss, dB	0.01
Reflector mesh I^2R loss, dB	0.02
Coaxial cable loss, dB	0.03
VSWR loss (I: 3:1), dB	0.08
Total loss, dB	0.14
Antenna peak gain, dB	14.7
Antenna FOV gain, dB (±13°)	12.7
Polarization sense	(Linear: horizontal and vertical)

*L.R. Dog, Backfire Yagi Antenna Measurements.

efficiency of 75 percent for reasonably narrow bandwidths. This antenna configuration is used for the VHF AGIPA, UHF forward link, the S band transponder, and for the order wire service at S band.

The VHF short backfire design, as depicted in Figure 74, has been described previously. The UHF forward link antenna is 148 cm in diameter and about 37.5 cm high. The RF performance data as determined by analysis for an operational frequency of 401 MHz are listed in Table 40.

The S band order wire antenna is electrically identical to the UHF antenna except scaled to S band. The reflector is made from perforated sheet metal for low cost and light weight. Single sense circular polarization is generated by slot fed crossed dipoles. The antenna performance parameters are listed in Table 41. The two S band transponder antennas are essentially identical in design and performance to the order wire antenna.

TABLE 40. UHF ANTENNA PERFORMANCE

Frequency band, MHz	400.5 to 401.5
Aperture diameter, meters	1.3
Aperture gain, dB	15.0
Reflector surface loss, dB	0.02
Reflector mesh I^2R loss, dB	0.08
Hybrid loss, cm rms	(0.635 cm) 0.16 dB
Coaxial cable loss, dB	0.09
VSWR loss (I.3:1), dB	0.08
Total loss, dB	0.43
Antenna peak gain, dB	14.57
Antenna FOV gain, dB (±13°)	12.50
Polarization sense	Circular

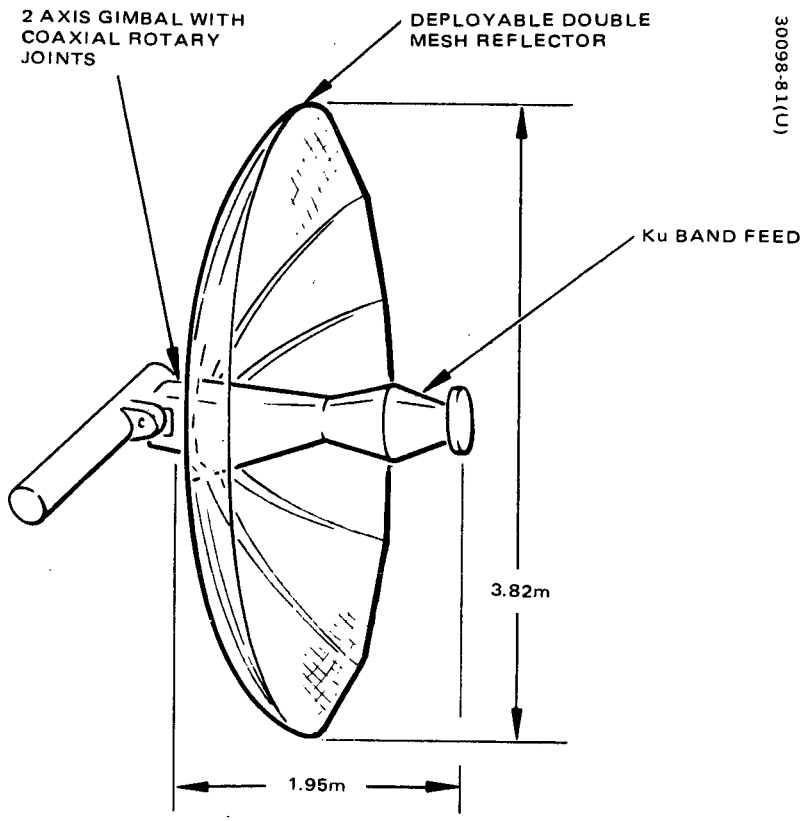

Figure 75. Ku Band High Gain Antenna

TABLE 41. S BAND ORDER WIRE ANTENNA PERFORMANCE

Frequency band, MHz	2200 to 2290
Aperture diameter, cm	26.7
Aperture gain, dB	15.0
Reflector surface loss, dB	0.01
Reflector I^2R loss, dB	0.01
Hybrid loss, dB	0.16
Coaxial cable loss, dB	0.01
VSWR loss (2.0:1), dB	0.50
Total losses, dB	0.69
Antenna peak gain, dB	14.3
Antenna FOV gain, dB (±15 deg)	11.4
Polarization sense	Circular

4.3.4.4 Ku Band Antennas

Two Ku band receive horn antennas provide coverage of the northern hemisphere; both have a circular polarization and a beamwidth of 9 degrees by 18 degrees. An array of two fin-loaded pyramidal horn antennas satisfies the CP beam coverage requirements over the 13.4 to 14.2 GHz transmit frequency. A four-iris square guide polarizer and an orthomode tee are used. For simplicity, the unused orthogonal arm of the orthomode tee has been shorted out. The RF performance characteristics for the Ku band receive horns are summarized in Table 42.

The Ku band transmit antenna is similar to the S/Ku band antenna. Its description and performance characteristics are given in Figure 75 and Table 38, respectively.

TABLE 42. Ku BAND HORN ANTENNA PERFORMANCE

Frequency, GHz	13.7
Aperture area gain ($4\pi A/\lambda^2$), dB	25.1
Amplitude taper and phase losses, dB	1.93
Horn I^2R loss, dB	0.03
Polarizer and transition I^2R loss, dB	0.30
Waveguide loss (30.4 cm), dB	0.25
VSWR loss (1.3:1), dB	0.08
Total losses, dB	2.59
Antenna peak gain, dB	22.5
Antenna Northern Hemisphere gain (±4.0°N-S, ±9.1°E-W), dB	18.5
Polarization sense	Circular

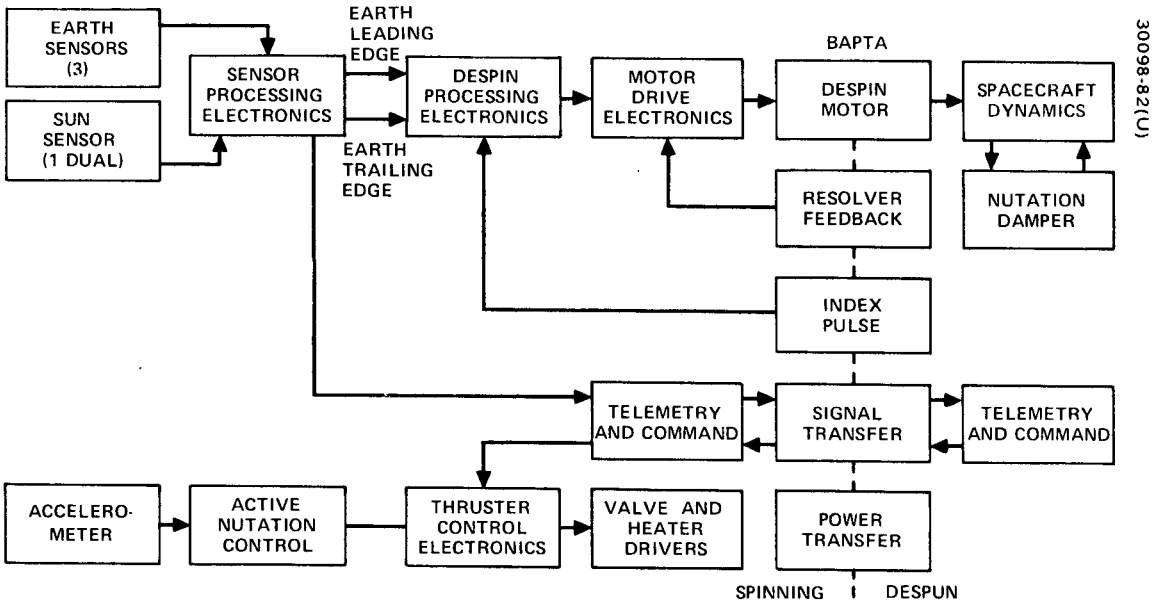

Figure 76. Attitude Control Subsystem

4.3.5 Attitude Control Subsystem

Determination and control of the spacecraft spin axis attitude is similar to that used for TACSAT and Intelsat IV using rotor mounted sun and earth sensors (Figure 76). The sun sensor provides pulse pairs for measurement of the angle between the sun line of sight and the spin axis, while earth sensors provide earth chord width data for attitude measurements. Corrections to the attitude are made using ground commanded pulsing of the jets.

Nutational stability is provided through the passive nutation damper mounted on the despun platform, along with active control through the despin control system and the active nutation control system.

Control of the despun platform is achieved by commanding a torque motor contained in the spinning/despun interface, based on processed information from the spinning earth sensors and master index pulse.

The despin control electronics (DCE) processes the inertial rotor phase information from the ground selected earth sensor, and the relative platform phase information from the master index pulse (sampled once every rotor spin revolution), and generates continuous control torque commands to the BAPTA torque motor. It contains both rate and tracking of the earth. The despin control system contains the loss of sensor detection logic to provide platform rate stability in the event of loss of an earth sensor and accepts ground commands for platform rate control and failure mode ground despin control.

The despin bearing assembly is shown in Figure 77. The despin subsystem performs four primary functions: 1) provides a rotating mechanical interface between the spinning and despun sections of the spacecraft, 2) despins the communications payload and controls compartment position to precisely point the antenna farm toward the earth, 3) provides for transfer of electrical power across the spinning interface, and 4) provides for the transfer of telemetry and command signals across the spinning interface. All these functions, with the exception of despin control, are performed by the BAPTA which is the electrical and mechanical interface between the spinning and despun sections of the spacecraft.

The main structural elements consist of a housing (spinning section), a shaft (despun section), and two angular contact ball bearings. A brushless dc motor is employed which reacts against the spinning housing to despin the shaft. The permanent magnet rotor is an integral part of the despun shaft and the wound stator is an integral part of the spinning housing. The usual requirement for motor brushes is bypassed through the use of a resolver to provide phasing information to the motor drive circuits in the DCE which generate the required rotating magnetic field. The resolver has a wound stator which is an integrated part of the spinning housing and a passive rotor which is an integral part of the despun shaft. An electrical

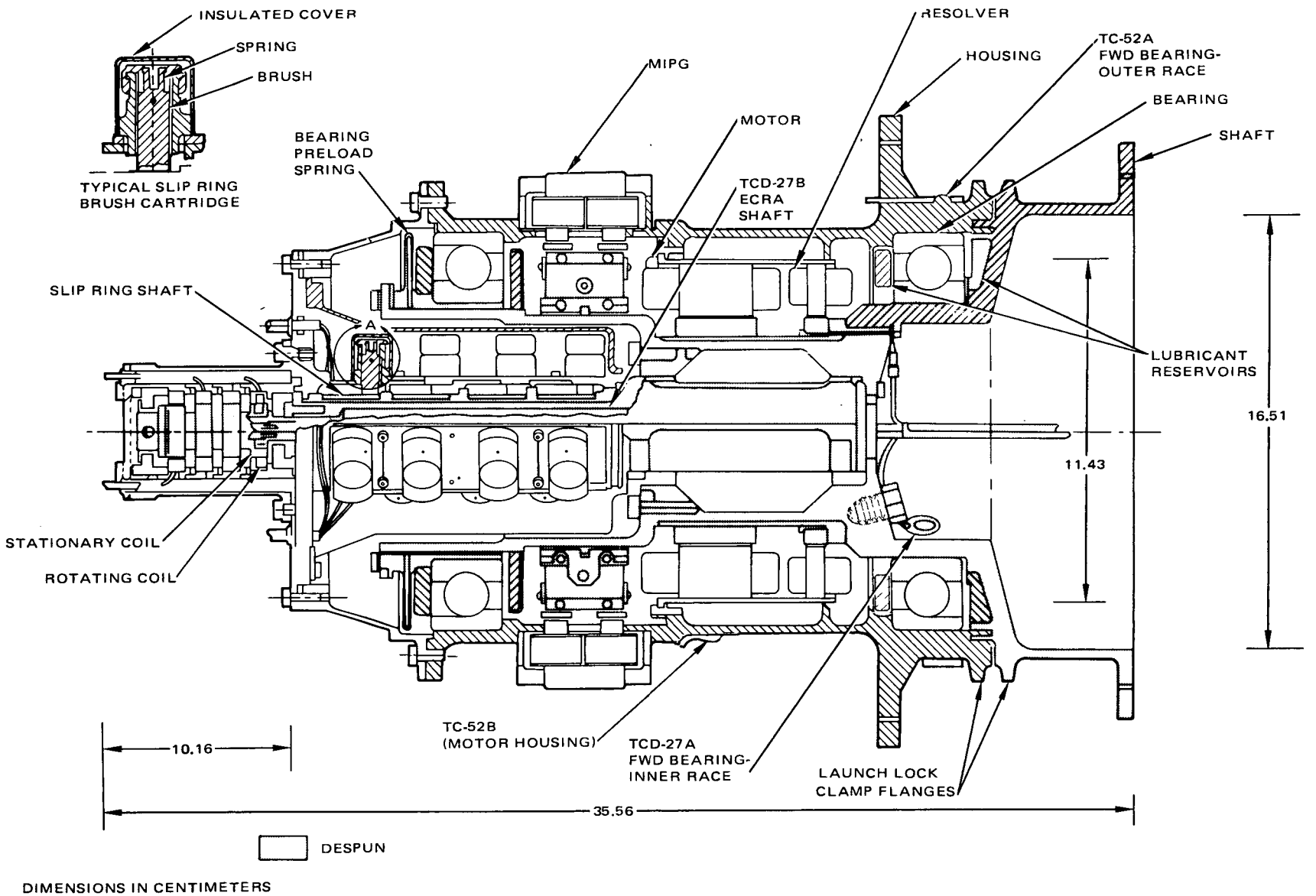

Figure 77. Despin Bearing Assembly

contact ring assembly composed of four brush/slip-ring sets provides for electrical power transfer across the spinning interface. A rotary transformer performs a similar function for telemetry and command signals. A pulse generator composed of two permanent magnets on the despun shaft and redundant coils on the spinning housing is employed to provide relative speed and position data between the spinning and despun sections. The pulse generator data and other data from rotor mounted sensors is used by the despin control electronics to control motor torque and properly despin the BAPTA shaft and the attached communications payload.

Despin motor torque speed characteristics are shown in Figure 78. The motor is essentially a two phase, 16 pole, ac motor which requires in phase sine and cosine driving voltages to generate the required rotating magnetic field. To operate as a dc motor, these sine and cosine voltages must be artifically generated. This is accomplished using a resolver in the BAPTA which is essentially a transformer having both the primary and secondary windings on a stator element and with the transformer core rotor designed to provide sinusoidal variation in the magnetic coupling between the windings as a function of the shaft rotation angle. A precise phase relation is maintained between the motor and resolver rotors by using a common shaft. The resolver is excited by a modulated 1.55 kHz carrier. The sine and cosine resolver outputs are then synchronously demodulated to remove the carrier and then amplified to drive the respective motor windings. The motor has two sine and two cosine windings. One pair (sine and cosine) are driven by the motor drive circuits in a given DCE; however, either DCE can control both motor drive circuits.

The available motor torque with all (four) windings excited is shown. Under stall conditions the maximum torque is 2.5 N-m. As the relative rate increases, a back EMF is developed in the motor stator windings. The torque is limited by the maximum available driving voltage which is 20 volts at the motor winding under worst case and of life conditions.

At 60 rpm and the expected BAPTA temperature of 296 K (heaters on), the maximum friction torque is 0.25 N-m. The friction data is obtained from orbital operation operation on three of the Intelsat IV spacecraft. The Intelsat IV BAPTA has a demonstrated torque margin of 6:1.

An overview of spacecraft control characteristics is presented in Table 43. The performance numbers quoted are estimates based on previous program developments. Areas of design requiring further attention are the effects of structural flexibility, the interaction of the antenna tracking servos and despin control dynamics, and the requirement to blank out spurious signals in the earth sensory arising from the presence of the aft mounted antenna support structure.

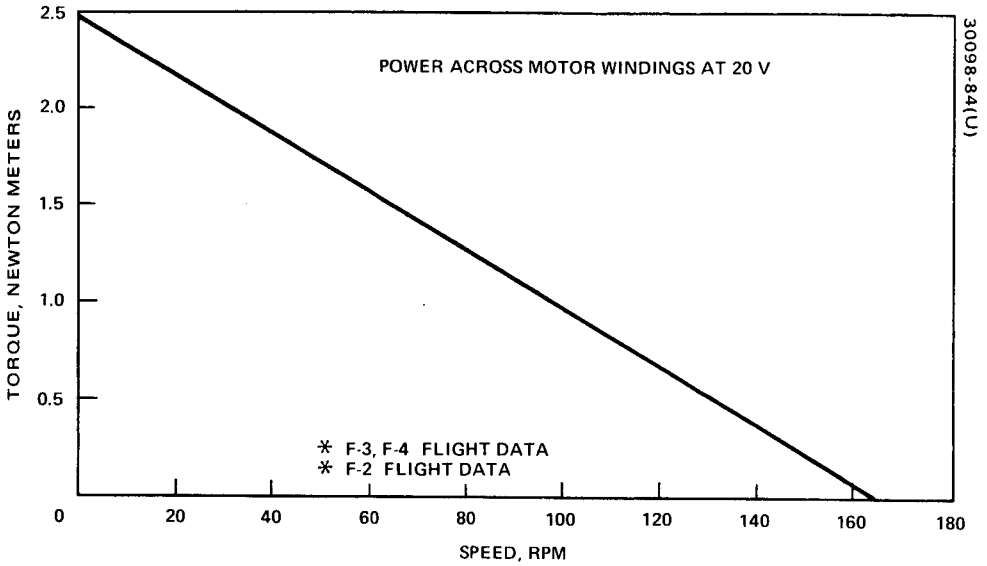

Figure 78. Despin Motor Torque Speed Characteristics

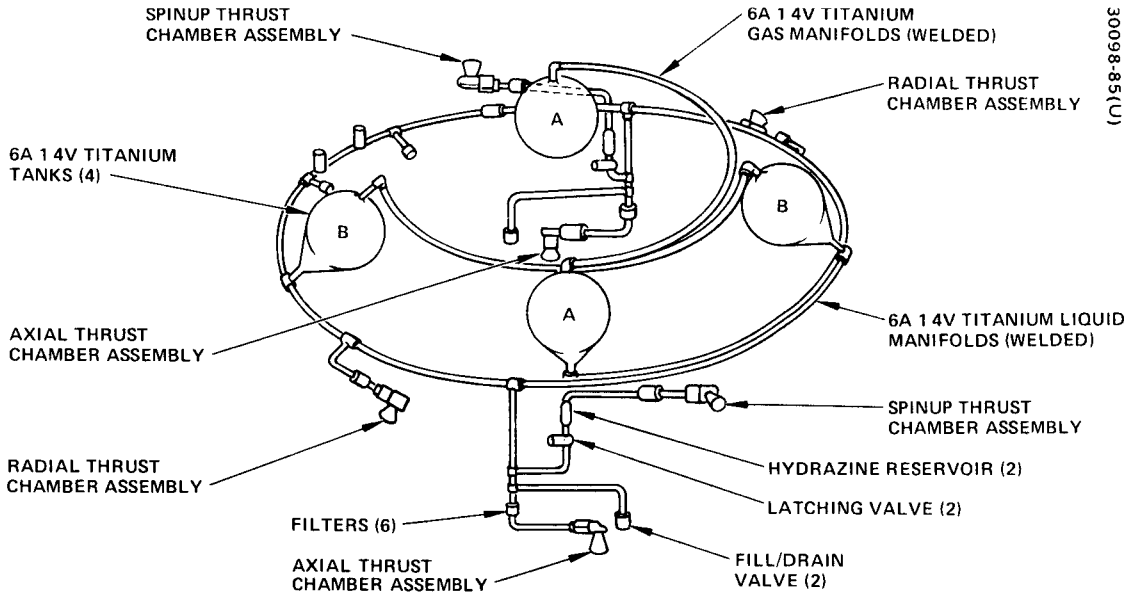

Figure 79. Reaction Control Subsystem

TABLE 43. ATTITUDE CONTROL CHARACTERISTICS SUMMARY

Stabilization	Gyrostat
Spin rate	60 rpm
Nutation frequency	0.08 Hz
Nutation damping time constant	300 seconds maximum
Spin axis orientation	Orbit normal ±0.5 degrees
Spin axis determination axis	0.1 degrees
Platform pointing accuracy	0.2 degrees

4.3.6 Reaction Control Subsystem

The reaction control subsystem is shown schematically in Figure 79. The reaction control subsystem (RCS) uses hydrazine monopropellant to generate thrust, and provides complete hardware redundancy with two independent dual tank subassemblies, each containing half the propellant required for the mission.

Each subassembly utilizes one axial, one radial, and one spinup thrust chamber assembly (TCA). The axial TCA provides a thrust vector parallel to the satellite spin axis; the radial TCA provides a thrust through the spacecraft center of gravity; and the spinup TCA provides a thrust vector 30 degrees from the normal to the spin axis and in a plane normal to the spin axis. Each TCA provides an initial thrust level of 26.7 newtons, decreasing to 12.9 newtons over a tank pressure blowdown ratio of 2.8 to 1 from an initial 1.9 MN/m^2. The TCA propellant inlet valves each contain two series redundant seat/poppet pairs to minimize leakage and two parallel would coils to maximize reliability.

The propellant feed system is of all welded construction to minimize weight and leakage. Liquid and gas manifolds and all component attachments use welded joints. The only mechanical joints in the subsystem are the thrust chamber to propellant valve interface, the propellant valve seats, and the fill and drain valve seats. High strength titanium alloy is used for the tanks, lines, fill and drain valves, pressure transducer housing, filter housing, and propellant reservoirs. Where titanium to stainless steel joints are required, diffusion bonded transition joints are used.

The reaction control subsystem will operate in a pulsed and continuous fire mode. Over the 7 years of in-orbit operation, the tank pressure will vary from 1.72 to 0.69 MN/m^2. Associated with the pressure blowdown is the steady state performance variation shown. The delivered thrust varies from 25.7 to 12.9 newton, while the specific impulse stays nearly constant with an average value of about 225 seconds. When operating in the pulsed

mode, the impulse delivered to the spacecraft varies as a function of the position of the pulse in the train. The TCAs will be controlled by ground command. The proper phasing of the TCAs pulses is achieved by synchronizing firing commands with telemetered sun sensor information. The TCAs will be pulsed nominally 117 ms in duration or, alternately over one full spin cycle. The capability exists to vary the pulse duration from 20 ms to 1000 seconds.

Specific performance requirements for the TDRSS mission are listed below. The associated propellant weights are shown in Table 44.

- Spinup to 60 rpm
- 130 degree precession for alignment of the apogee motor prior to firing
- 120 degree precession for spacecraft operational positioning after firing
- 7 years of solar torque correction

TABLE 44. PROPELLANT AND ΔV BUDGET

Operational Requirement	ΔV, m/s	Propellant Mass, kg	
		TE364-4	SVM-4A + N_2H_4
Spin up (60 rpm)	6.0	1.4	1.3
Attitude control			
Apogee motor pointing (130°)	6.9	3.9	3.5
Initial reorientation (120°)	6.3	3.0	2.9
Solar torque compensation (7 years)	7.7	4.3	4.3
Injection trim	55.5	23.7	22.7
Station change (2 at 4.3 deg/day)	51.2	21.1	20.2
Stationkeeping (7 years)	15.0	6.9	6.7
Contingency (2 percent)	3.0	2.1	2.0
N_2H_4 augmentation	—	—	77.4
Total performance required	146.6	66.4	141.0

- 2 percent margin for jet misalignment compensation
- Injection trim for booster and apogee motor errors
- Two 4.3 deg/day station changes
- 7 years of east-west stationkeeping
- Augment Intelsat IV apogee motor.

The RCS design requirements are summarized in Table 45. The RCS must provide capability for a 146.6 m/sec change in velocity. The cumulative impulse predictability based on spacecraft pointing requirements and verified in thruster qualifications is 20 percent for the first 10 pulses and 10 percent for the remaining pulses in longer trains. The burn time and cold start requirements are derived from the mission sequence.

TABLE 45. RCS DESIGN REQUIREMENTS

Performance		
ΔV		
Cumulative impulse predictability for a given engine		146.6 m/sec
10 pulses		20 percent
10 pulses		10 percent
Burn time steady state*	spin up	135 seconds
	Apogee augmentation	7700 seconds
Number of pulses*	Axial	22,500
	Radial	33,000
Mass		
Subsystem dry		18.0 kg
Propellant and pressurant		
with augmentation		141.0 kg
without augmentation		64.4 kg
Environment		
Temperature range		283 to 338 K
Vibration and acceleration		Same as Intelsat IV

*Total for subsystem

A temperature range of 283 to 338 K has been set to be compatible with the hydrazine. The vibration and acceleration levels are assumed to be the same as the Intelsat IV satellite (HS 312) requirements.

Figure 79 shows the arrangement of the RCS. It is a redundant design (except for propellant), selected to provide high reliability with a minimum of components. Malfunction of any single valve or thruster will not result in loss of any subsystem function. The RCS is assembled as a unitized, all-welded module of high strength 6 Al-4V titanium alloy. Stainless steel components are welded into the system by diffusion bonded, coextruded titanium-to-steel transition joints. The only mechanical joints in the RCS are the thrust chamber-to-propellant valve interfaces, the propellant valve redundant seats (upstream of the previously mentioned interface), and the redundantly sealed fill and drain valve.

Table 46 summarizes the component mass, previous use, and number required per spacecraft. Power is supplied from the attitude control subsystem, except for heaters, whose required 10 watts of power are supplied by the power subsystem.

Identical thruster propellant control valves, selected because of demonstrated superior reliability, are used on all thrusters. The valve is a torque motor actuated unit which employs series redundant tungsten carbide seats and poppets. It is of welded construction and hydrazine does not contact electrical components. It is held closed by a combination of spring forces and permanent magnet forces. When power is applied, electromagnetic forces overcome these closing forces, and the valve opens. When power is removed, the valve closes. Leakage of each individual valve seat may be measured at any time prior to launch if the RCS is free of liquid.

Redundant axial, radial, and spinup thrusters are provided. All utilize Shell 405 catalyst (Grade ABSG) to decompose the hydrazine into hot gases which are expelled through a converging-diverging nozzle to produce thrust. The thrusters are fabricated of L-605 alloy, which is resistant to nitriding and has excellent high temperature physical properties. Each has a flow trim orifice in the inlet line, which is readily removable to adjust the Δp of the thruster.

All thrust chambers will operate satisfactorily in either the pulse or steady state modes. The propellant valve may be readily removed for cleaning or replacement without disturbing the thrust chamber. The nominal thrust level of each of the six thrusters used is 22.24 newtons.

The four propellant tanks operate in the blowdown mode and employ no propellant management devices. The liquid-gas interface is controlled by the centrifugal forces resulting from spacecraft spin. The tanks, made of 6 Al-4V titanium, are conispherical. Each has two ports: a liquid outlet

TABLE 46. RCS COMPONENTS

Component	Number per RCS	Unit Mass, kg	Hughes Part No.	Manufacturer	Previous Program Qualifications
Thruster, 22.24 newtons	6	0.54	3193400	Hughes	HS 312
Propellant valve all thrusters	6	Included in thruster weight	253393	Hydraulic Research and Manufacturing Co.	HS 312, HS 318, HS 333
Tanks	4	2.36	251976-1	Precision Sheet Metal	HS 312, HS 318
Reservoirs	2	0.11	252694	Hughes	HS 318
Filters	6	0.14	318406-100	Vacco Industries	HS 312, HS 318, HS 333
Latching valves	4	0.27	3181404-100	Carleton Controls Corp.	HS 312, HS 318
Fill/drain valves	1	0.18	3181407-100	Hughes	HS 312, HS 318, HS 333
Transducer	1	0.14	318415-100	Edcliff	HS 312, HS 318, HS 333, ATS, HS 308
Lines and fittings	1	1.36		Hughes	HS 312, HS 318, HS 333
Transition tubes	17	Included in mass of lines and fittings	25238	Nuclear Metals Div., Whittaker Corp.	HS 312, HS 318, HS 333
Welded tees	10		252437	Hughes	HS 312, HS 318, HS 333

at the apex of the conical section, and a gas port, 180 degrees opposed. The included angle of the conical section is 85 degrees. This permits total removal of liquid by spinning (in-orbit) or by gravity (during ground operations). At launch, each tank will contain approximately 16.6 kg of fuel, which is substantially less than the 34 kg that the tank contains for Intelsat IV. Tanks can, therefore, be topped off to match launch vehicle payload capability at time of launch, thereby providing some excess maneuvering capability or propellant redundancy. Anticipated launch pressure is 1.83 MN/m^2.

Each of the five latching valves is housed in a welded stainless steel body. A belville spring provides the force to latch the valve in either the open or closed position, after removal of power from the actuation solenoid. The valve seat is a stainless steel-to-teflon interface. Moving parts are isolated from propellant contact by a welded metal bellows, which also balances poppet loads.

The latch valves are used to isolate the two half systems. In the event of a thruster failure or valve failed closed, the interconnect valves can be opened to permit the propellant to flow to the redundant thruster. The other two latch valves are used to trap propellant in the spinup system. Upon separation from the booster, the spacecraft is in zero g; the position of the propellant, relative to tank outlets is uncertain. That portion of the RCS between the latching valves and the two spinup thrusters is full of propellant and the valves are closed prior to launch, trapping enough fuel in the reservoirs to initiate spinup, even if the tank outlet is unported. Upon separation, all latching valves are opened and system pressure is applied to the reservoirs. Both spinup thrusters are fired steady state, initiating spacecraft rotation, and centrifugal force causes the fuel to settle and fill the lines, providing an uninterrupted flow to the spinup thrusters.

A high capacity filter, with 10 microns absolute rating, is provided upstream of each propellant valve. It consists of electrochemically etched discs mounted concentrically on a perforated tube. The entering fluid exits through the tortuous paths etched into the discs which are encased in a welded titanium housing.

As all propellant tank gas phases are interconnected, a single potentiometer type transducer in which pressure is sensed by an aneroid capsule of stainless steel is used. The deflection of this capsule is transmitted through a pushrod to the wiper of a linear wound resistance element.

A single manually operated and direct acting fill and drain valve is used. The primary seal is formed between a tungsten carbide ball and the titanium body. Since these materials permit the application of high closing torques, zero leakage is repeatedly achieved. A redundant mechanical cap seal is installed for launch.

Manifolds are fabricated from seamless tubing, (0.635 outside diameter and 0.051 cm thick walls) of 6 Al-4V titanium alloy. Branch lines are accommodated by tee fittings. Stainless steel components are welded into the system by means of transition joints. These coextrusions of 6 Al-4V titanium and 304L stainless steel provide a transition of properties from one to the other. All connections are butt-welded by an automatic tube welder which produces preprogrammed, continuous tungsten inert gas (TIG) welds without the use of sleeves, rings, or filler material.

The RCS subsystem is identical to the Intelsat IV RCS and is performing successfully on all four spacecraft launched to date. The Hughes 22.24 newton thruster and the propellant tank will be used on all follow on Intelsat IVs. Every component is identical to an existing component qualified for flight on other Hughes spacecraft programs.

The propellant valves, fill and drain valve, and latching valves are the only moving mechanical assemblies used. These valves are all fully qualified and have been successfully used on the Intelsat IV and HS 318 spacecrafts.

All components proposed are in use on other Hughes programs, as are the equipment, techniques, and procedures for manufacture, assembly, and test. No RCS development effort will be required. Minor additional qualification of components may be required, depending on the environmental requirements.

4.3.7 Electrical Power Subsystem

The electrical power subsystem provides power for operating command and data links for LDR, MDR, and HDR users. In addition, a voice link will be provided to orbiting manned spacecraft. With the user spacecraft in an approximately 100 minute orbit, an S band forward voice link can be operated up to a maximum of 50 percent of the time. No UHF voice link is provided. Voice operation on the return links is unrestricted except for time sharing the S/Ku band antenna with various users. These power requirements include a 7 to 10 percent contingency reserved for future growth. The power requirement for the different operating modes for both the sunlit and eclipse portion of the orbit are shown in Table 47. Power subsystem performance is described in Table 48.

The power levels required for the TDRS mission can be achieved using an Intelsat IV size solar cell array with currently available higher efficiency solar cells. This minimum change is planned for all programs which will use the Intelsat IV spacecraft in the future. The voltage limiters are identical with those used on Telesat, whereas the power electronics are those of Intelsat IV.

TABLE 47. ELECTRICAL POWER REQUIREMENTS

Equipment	Watts at 24.5 Volts			
	Eclipse Season		Solstice Season	
	Command Mode	Intermittent S Band Voice	Command Mode	Intermittent S Band Voice
HDR return Tx (Ku)	30	30	30	30
LDR/MDR return Tx (Ku)	9	9	9	9
HDR forward Tx (Ku)	27	27	27	27
MDR forward Tx no. 1 (S)				
Command	25	25	25	25
Voice and data				
MDR forward Tx no. 2 (S)				
Command	25	–	25	–
Voice and data	–	100	–	100
LDR forward Tx (UHF)				
Command and data	146	146	146	146
S band transponder	24/2	24/2	24/2	24/2
Receivers, processors, etc.	43	43	43	43
Telemetry, tracking and command	16	16	16	16
Antenna position control	12	12	12	12
Despin control	20	20	20	20
Thermal control	6	6	6	6
Power electronics	1	1	1	1
Battery charging	109	36	36	36
Distribution losses	14	14	14	14
Power required	512/490	514/492	439/417	514/492
Contingency	60/82	58/80	101/123	26/48
Solar power available	572	572	540	540

TABLE 48. ELECTRICAL POWER SUBSYSTEM PARAMETERS

Parameter	Performance Requirement
Solar cell arrays	
Number of buses	2
Polarity	Positive
Voltage end of life at maximum power	24.5 volts
Maximum voltage limited to	33.0 volts
Maximum power end of life	572 watts eclipse season
Maximum power end of life	540 watts summer solstice
Battery Discharge	
Set point for automatic discharge	24.1 $\pm$ 0.15 volts
Voltage transient on battery turn-on	+9.0 volts maximum step charge
Discharge turn-off	By ground command
Minimum bus voltage during battery discharge	24.1 volts
Battery Charge	
Battery charge current	1.2A per battery at end of 7 years (1.45 A max)
Battery charge command	
2/3 charge array	One on command per battery
1/3 charge array	One on command per battery
All charge arrays	One off command per battery
Battery reconditioning	
Discharge current	0.030 ampere nominal
Command	On/off command for each battery
Shunts	
Rating	25 amperes (200 mv output)
Number provided	6

The basic configuration of the power subsystem is shown in Figure 80. The solar array provides sufficient power to support all communication loads and also charge batteries simultaneously in eclipse season. There are two batteries with twenty-five cells each. The cells are 18 ampere-hours in size.

The power subsystem is a positive polarity, two bus system, each bus powering approximately one-half the spacecraft load. The buses are designed to operate independently over the total spacecraft operating life. However, for unexpected operating modes, bus paralleling relays are provided.

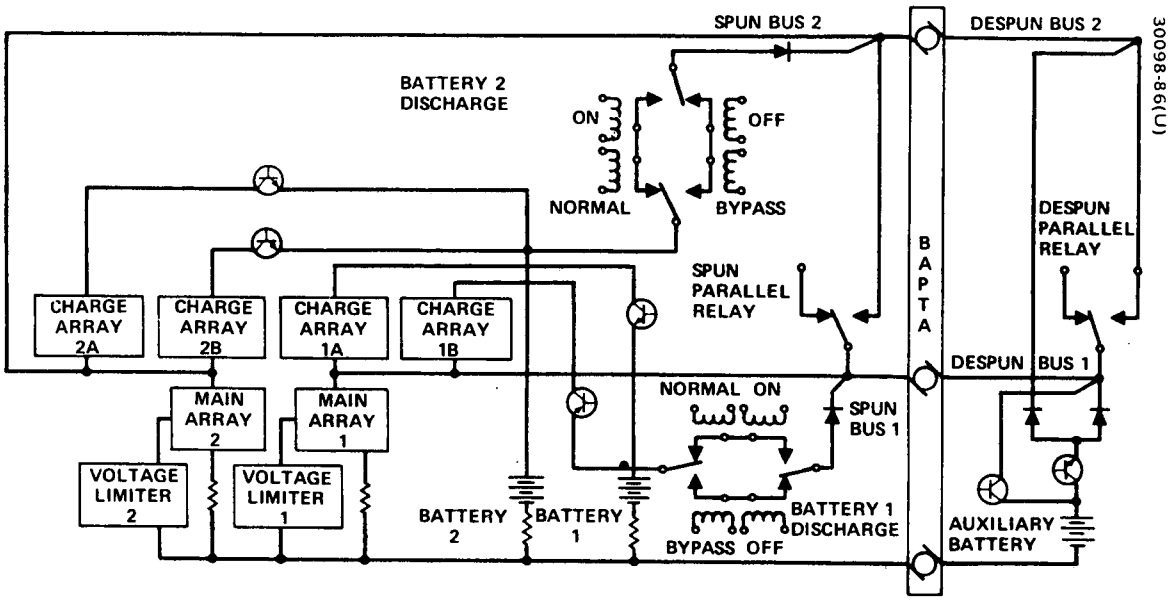

Figure 80. Electrical Power Subsystem

The solar array consists of two spinning solar panels termed main array 1 and main array 2. Each main array forms a spacecraft bus, the negative panel terminal being connected to the bus through a shunt. Performance data on each panel can be monitored separately. Power is supplied from each panel directly to loads on the spinning section and through slip rings to the loads on the despun section. The solar array design data are listed in Table 49.

Charge arrays, designated 1a, 1b, 2a, and 2b, are connected as shown through commandable switches to the batteries. The charge arrays for each battery have current ratings in a 1 to 2 ratio, so that 1/3, 2/3, or 3/3 of available charge current may be selected.

Battery operation is designed to be semiautomatic. Low bus voltage causes the battery to be automatically connected to the bus and a command is required to disconnect the battery from the bus. Each battery has two charge arrays with each array individually commandable.

Operation of the battery systems can be controlled manually as on Intelsat IV. During the eclipse season, the battery is commanded on as eclipse is entered and is subsequently commanded off when eclipse is completed. Battery charging is controlled entirely by ground command.

During noneclipse seasons, the battery can be trickle charged continuously if desired or stored and recharged periodically. Capability for battery reconditioning is provided.

TABLE 49. SOLAR ARRAY DESIGN DATA

Solar Array End of 7 Years Power Output	
Summer solstice	540W
Eclipse season	572W
Solar Panels	
Number of panels	2
Geometric shape	Cylindrical
Diameter	2.38 meters
Length/panel	1.37 meter
Mass, per panel	
Substrate	17.0 kg
Cells, wire, diodes, connector, etc.	19.9 kg
Total	39.9 kg
Solar Cells	
Type of cell, cm	2 x 6, n/p silicon
Coverglass thickness	0.3 mm
Cell thickness	0.3 mm (nominal)
Minimum average power per lot	181 mW
Test voltage	0.445 ±0.002 volt
Cell temperature	298 K ±2 K
Illumination level	139.6 mW/cm^2
Illumination spectrum	Air mass zero equivalent

The battery configuration data are shown in Table 50. Consideration during spacecraft design was given to battery thermal design and configuration. The 7 year life requirement for the battery emphasized maintaining temperatures as low as possible, preferably not greater than 298 K. Examination of specific available mounting areas and pack configurations resulted in selection of a multipack (four 3-cell packs, one 6-cell pack, one 7-cell pack) arrangement for each 25 cell battery. Physical location of these packs is on the spacecraft ribs (1.25 mm thick). Rib and pack flatness are controlled to ±0.25 mm and RTV 11 is used as a filler for thermal control. Additional thermal control is achieved by commanding charge from full to minimum when 110 percent of the discharged energy has been returned.

TABLE 50. BATTERY CONFIGURATION DATA

Batteries		
Number of batteries		2
Type of battery		Nickel-cadmium
Number of cells in series		25
Nameplate capacity per battery		18 ampere-hours
Maximum depth of discharge		60 percent
Charge rate		C/15 minimum
Charge mode		Constant current
Cell Packs	**No. per Battery**	**Mass, each (kg)**
Cells per pack	3, 6, and 7	
3-cell packs	4	2.9
6-cell packs	1	5.6
7-cell packs	1	6.4
Cells		
Minimum cell discharge voltage		1.15 volt
Cell type		Hermetically sealed rectangular

End of life charge rate is 1.2 amperes, which is C/15 when related to nameplate cell rating. The temperature profile of the battery resulting from the passive thermal design is ideal for efficient charging of nickel-cadmium cells at a relatively low rate. A typical temperature profile permits the charge to occur between temperatures of 277 K and 298 K. For conservatism, full charge is not turned on until the cell temperature is above 277 K.

Two commandable relay assemblies which are used to parallel the buses are provided, one on each side of the slip ring assembly. This arrangement permits cross connection of loads and buses in the event of failure.

Spacecraft power distribution is achieved through redundant wiring via two separate buses. The spinning and despun grounds are structurally isolated at the BAPTA (bearing and power transfer assembly) to prevent current flow through the BAPTA bearings.

Mechanical relays were used to connect batteries to the bus for discharge, thus minimizing the voltage drop, saving at least one battery cell, and minimizing both series and shunt dissipation in the controller. Disadvantages of the relay circuit are the need for manual control and the transient imposed on the bus by relay actuation.

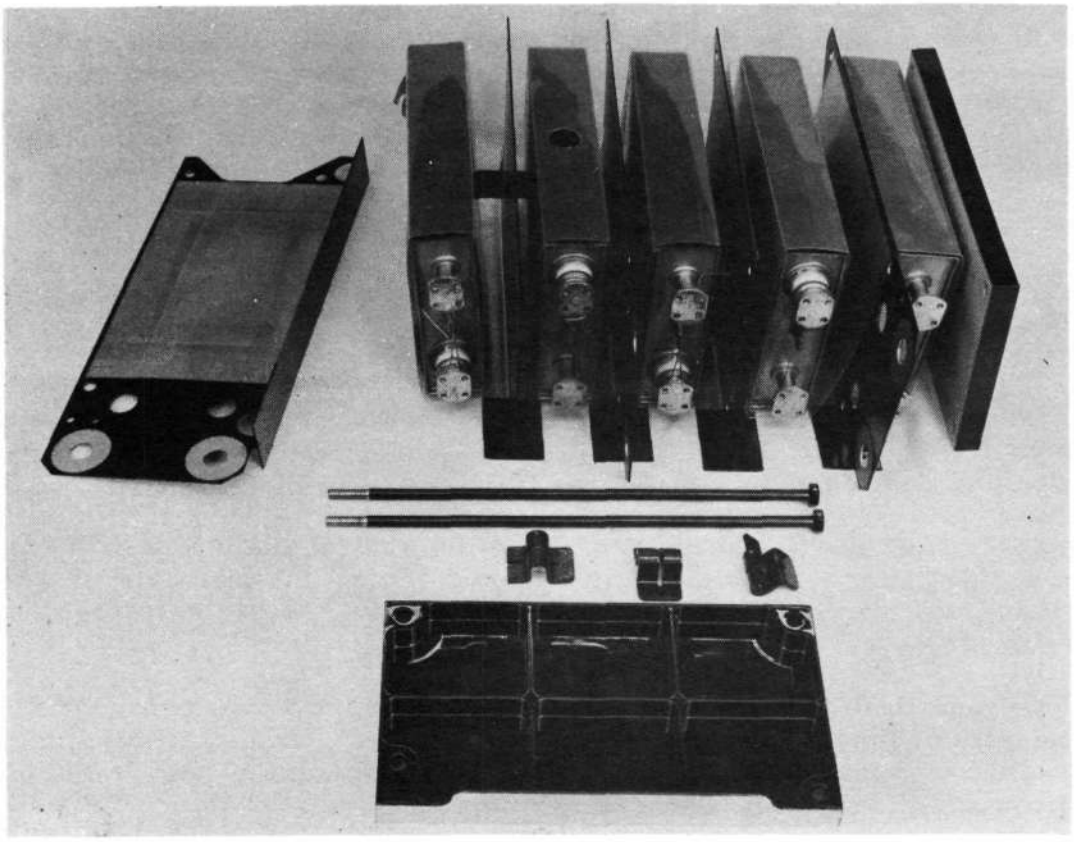

Figure 81. Typical Battery Pack Construction (Photo A24833)

Typical battery pack construction is shown in Figure 81. Controls for both batteries are located in a single electronics assembly. This assembly includes commandable switches for selecting the desired charge current, and power relays for connecting the battery to the bus. These power relays can be opened or closed on command and also close automatically when bus voltage drops below the set point. Commandable reconditioning switches are also located inside the battery controllers.

Ground controlled operation of the relay type battery control is a practical rather than inherent limitation. Automatic operation of discharge control is implemented by sensing the output voltage and causing relay turn on at the desired lower bus limit. The Intelsat IV design incorporates this capability by using a delay circuit that permits relay actuation only after the low voltage signal is present for at least 250 milliseconds. Without this delay feature, the panel ripple voltage at the 1 rpm spin speed would cause actuation.

To prevent loss of a battery due to relay failure, two relays are used as shown in Figure 82. Normal failure of this type of relay, according to Hughes experience, is circuit closure in either of the two positions, rather than hang up of the arm in neither contact position.

The second relay, termed the backup relay, is commanded to the normal position prior to launch and is not intended to be used again. All automatic and command functions are then applied to the automatic relay.

Spacecraft power users (e. g. , communications and telemetry and command subsystems) provide their own regulators and converters. All spacecraft units provide current limiting resistors, fusing resistors, or filament fuses.

Voltage limiters maintain solar panel output voltage below 33 volts independently of load after emerging from eclipse. These limiters provide a minimum heat dissipation on the despun platform during launch and orbit acquisition and also during powered down operation.

Solar panel tap limiters are used to hold the bus voltage below 33 volts, dumping surplus solar panel power at beginning of life by shunting or eliminating the current supplied by the tapped strings to the main bus. Tap limiters also clamp the bus after exiting eclipse. Four tap limiters, each shunting a separate section of the array (1/8 of total array in each section), are provided. The limiters have set points separated by 0. 1 volt, so that operation is incremental.

The bus voltage varies between the upper voltage limit (33 volts) determined by the cold solar panel emerging from eclipse and the lower limit (23. 8 volts) of the battery discharge control set point. When the discharge control set point is reached, the battery is switched directly to the bus, which results in a step voltage increase of up to 10 volts on the bus. All spacecraft using systems have been designed to accept this voltage transient. However, for conservative operation, it is recommended that battery turn on be manually controlled during the eclipse season. This is done by commanding the battery on as eclipse is entered before the panel voltage decreases to the automatic set point, thus minimizing the transient effect.

C-3

4.3.8 Apogee Motor

The SVM-4A motor built by Aerojet for the Hughes Intelsat IV can serve as the synchronous apogee motor for an improved Atlas-Centaur launch. This motor has been successful on all four Intelsat IV launches to date. It is undersized for the improved Atlas-Centaur launch vehicle separated mass capability of 1720 kg. A payload match can be obtained by using the maximum amount of additional hydrazine that can be stored in the existing Intelsat IV reaction control subsystem, 77.4 kg, and performing a 6 degree perigee plane change during transfer orbit injection. The SVM-4A is shown in Figure 83. Its major performance characteristics are presented in Table 51.

The SVM-4A motor is 93.2 cm in diameter and 153.2 cm in overall length. It has a nominal total mass of 706.8 kg with 642.3 kg of propellant.

It produces a nominal vacuum total impulse of 1.82 MNS at 294.3K, an average vacuum thrust of 55,511 newtons, and a duration of 33.1 seconds. It has an operating temperature range of 277.6 K to 305.4 K, is capable of temperature cycling over a range between 266.5 and 316.5 K, and has an age life of at least 5 years when stored at approximately 302.6 K. The maximum expected operating pressure is 7.04 MN/m^2 at 311.K; at maximum expected operating pressure, the predicted thrust is 76,100 newtons (maximum thrust).

The grain is a cast-in-case, internal-burning configuration cast with carboxy-terminated polybutadiene propellant. The grain is fully bonded to the internal chamber insulation, except at the aft head where a released

TABLE 51. NOMINAL SVM-4A ROCKET MOTOR CHARACTERISTICS
(At 294.3 K and VAC)

Duration, seconds	33.1
Average thrust, Newtons	57,379
Total impulse, MNs	1.82
Average operating pressure, MN/m^2	5.1
Propellant mass, kg	642.3
Loaded mass, kg	706.8
Operating temperature range, K	277.6 to 305.4
Specific impulse, seconds	289.2
Expansion ratio	40:1

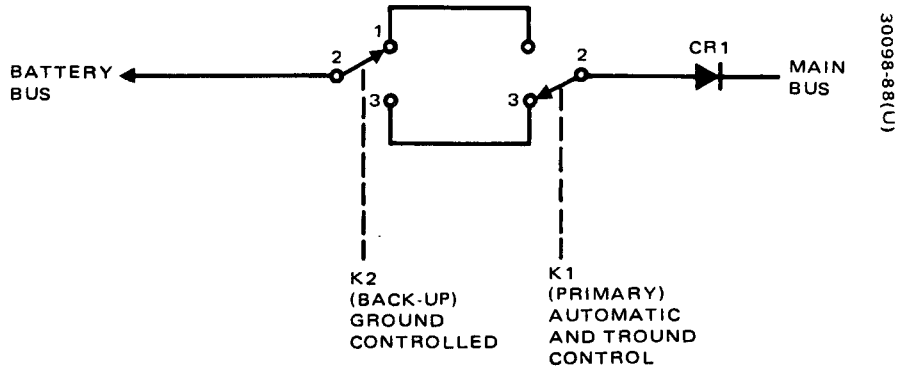

Figure 82. Simplified Diagram of Discharge Relay-Contact Configuration

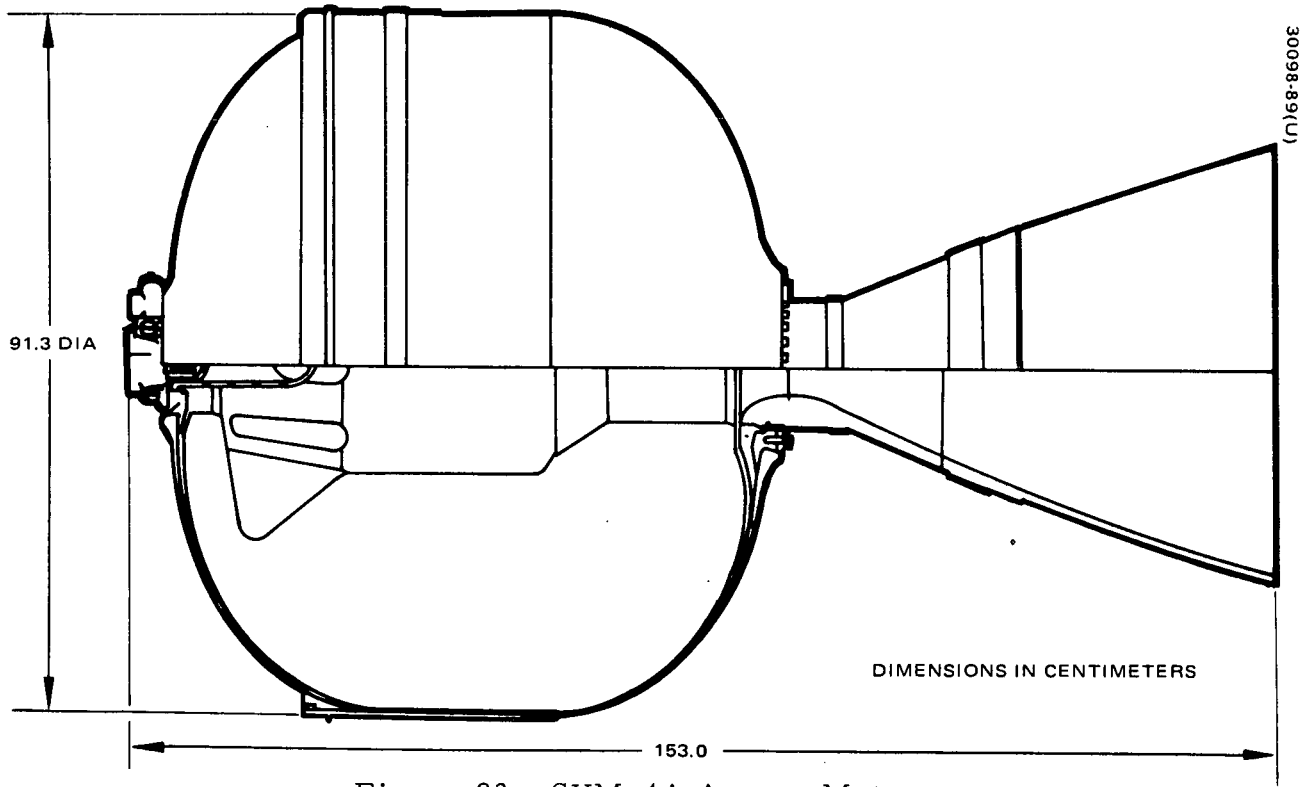

Figure 83. SVM-4A Apogee Motor

boot is used for stress relief. A finocyl grain design with eight fins in the forward head is used to achieve high volumetric loading and low grain stresses. The propellant is AGC ANB-3066, which is the same as that used in the Intelsat II, Intelsat III, and Minuteman motors. When the 40:1 expansion ratio nozzle is employed, the specific impulse is 289.6 seconds.

The motor is statically and dynamically balanced. The propellant is trimmed during manufacture to control the total impulse within ±1.0 percent at 294.3 K.

The chamber is fabricated of filament-wound glass and epoxy resin and insulated internally with silica-filled Buna-N rubber. The preimpregnated glass rivings have a minimum ultimate tensile strength of 3.036 N/m^2. Aluminum alloy polar bosses are incorporated into the chamber structure to provide attachment provisions for the igniter, nozzle, and safe and arming device.

The nozzle has a silver-infiltrated tungsten throat and composite plastic exit section. The ignition system consists of a remotely operable electric safe-and-arm device and a boron potassium nitrate (BPN) charge contained in a perforated glass/phenolic premolded chamber.

Control of motor temperatures within the required band of 278 to 305 K is accomplished by means of a heater and insulation blanket. The heater is a 30 watt unit, installed around the nozzle attach flange area and extending down past the nozzle throat. The motor case and nozzle throat are covered by a multilayered low emissivity aluminized Kapton blanket.

A second candidate apogee motor is a modified version of the TE-M-364-4 to be built by Thiokol for the FLTSATCOM program. The FLTSATCOM will be launched from the improved Atlas-Centaur. Thus, the motor will match the full payload capability of the improved Atlas-Centaur launch vehicle at an optimum design point. The currently estimated payload for the improved Atlas-Centaur into synchronous transfer orbit is 1720 kg exclusive of the Intelsat IV payload adapter. The FLTSATCOM motor is being designed by Thiokol for a payload of 1814 kg. Therefore, the FLTSATCOM motor may need to be off-loaded approximately 4.4 percent in propellant mass to give the correct performance for a payload of 1720 kg.

The FLTSATCOM motor is in an early stage of design; therefore, the design and performance features given herein are preliminary. The motor is an extended spherical solid propellant rocket motor designed to operate in a space environment as an apogee motor. The motor has a major diameter of 0.96 meter and an overall length of 1.58 meters. The motor mass fraction is 0.91.

The motor total mass sized for a payload mass of 1720 kg is 886.6 kg. Of this, 809.6 kg is propellant and 77 kg is inert mass. The nominal burnout mass is 70.2 kg.

The total impulse is 2.29 MNS at 283.1 K. The propellant specific impulse is 288.1 seconds, and the effective specific impulse is 285.9 seconds. The action time is 42.7 seconds. The average thrust is 53,311 newtons, with a maximum thrust of 59,136 newtons.

The flange for spacecraft attachment is integral with the case. The principal components of the assembly are: a high expansion, contoured, composite plastic nozzle assembly; an elongated spherical titanium case; an asbestos-filled polyisoprene insulation system; an electromechanical safe and arm pyrogen ignition system; and a composite ammonium perchlorate polyhydrocarbon (CTPB) propellant.

The motor is shown in Figure 84. Its major performance characteristics are summarized in Table 52.

4.3.9 Spacecraft Mechanical Design

The Intelsat IV spacecraft was chosen for use in the TDRS Phase II vehicle design. This spacecraft configuration is shown in Figure 85. It consists of a spinning section and a continuously earth-oriented despun section. The despin bearing assembly (BAPTA) at the apex of the conical thrust tube is the interface between the despun and spun sections. The despun section contains the communications repeater, the antennas, antenna positioners, the antenna positioner control electronics, nutation dampers, a small portion of the electrical power subsystem, and the majority of the telemetry and command subsystem. The spun section contains the attitude and orientation subsystem, the major portion of the electrical power subsystem, the despin control electronics, the attitude sensors, accelerometers, the apogee motor, and a portion of the telemetry and command subsystem. A cross section of the spacecraft is shown in Figure 85.

The despun portion of the spacecraft comprises the antenna support assembly and the communication service module. The despun compartment is 2.20 meters in diameter and built around a central hub from which six

TABLE 52. NOMINAL TE-M-364-X ROCKET MOTOR CHARACTERISTICS
(At 283.1 K and VAC)

Duration, seconds	42.7
Average thrust, Newtons	53,311
Total impulse, MNs	2.29
Propellant mass, kg	809.6
Loaded mass, kg	886.6
Specific impulse, seconds	288.1

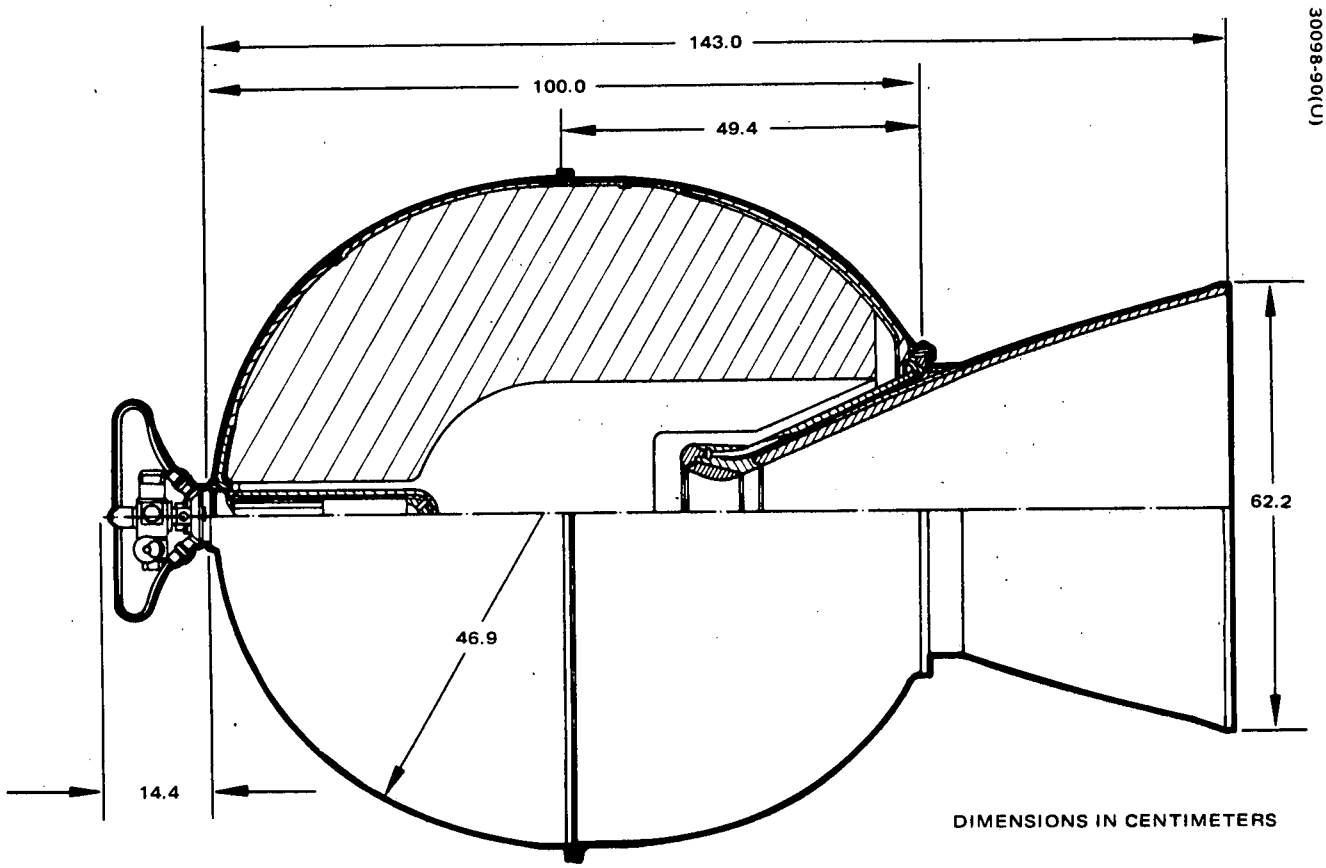

Figure 84. TE-M-364-X Apogee Motor

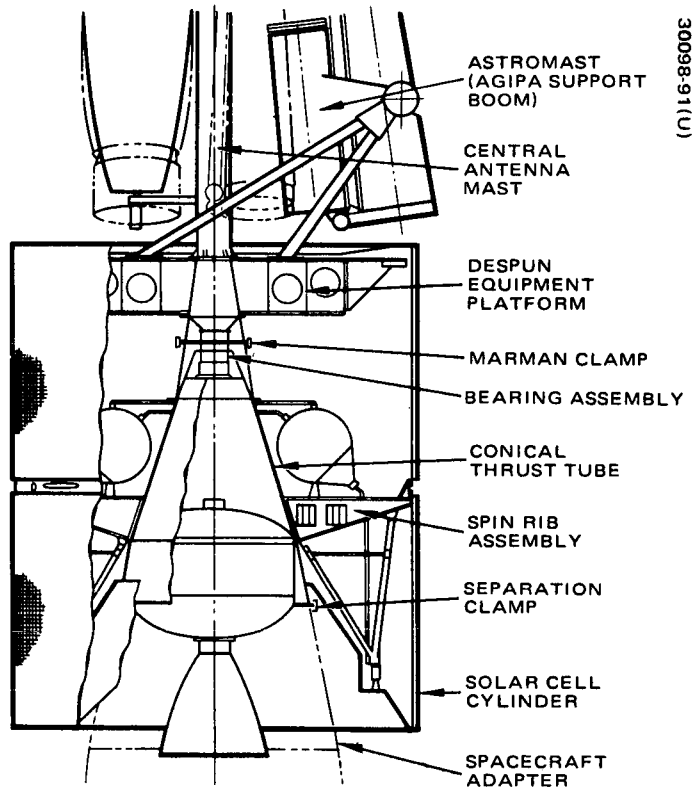

Figure 85. Primary Structural Elements

ribs extend radially. The central hub is an assembly made of machined aluminum rings and skins riveted together. It is conical in shape and attaches to the despun flange of the BAPTA. It also supports the antenna mast. The despun ribs are riveted to the central hub. The compartment decks are of honeycomb sandwich construction and use aluminum facesheets.

The antenna support mast is constructed from lightweight beryllium tube sections of about 20 cm diameter. The wall thickness of this mast is selected so that a minimum cantilever frequency of 10 Hz is achieved to avoid excessive dynamic coupling with the boost vehicle. The antenna support arms which pivot off the central mast do not function as primary load carrying members during launch. Their dimensions are defined by the minimum stiffness of the deployed antenna assembly in orbit.

The interface between despun and spun portions of the spacecraft is the BAPTA which contains a pair of bearings, a dc brushless motor, and slipring assemblies for electrical power transfer and for signal transfer.

The BAPTA is bypassed during launch by a structural cone and a Marman type clamp. Following release, the clamp moves outboard and is restrained radially on the despun portion of the spacecraft.

The spun portion of the spacecraft incorporates a conical core to support the encoders, decoders, squib and solenoid driver, despin control electronics, and the apogee motor.

The battery packs are bolted to the eight ribs extending radially from the central cone. The four positioning and orientation tanks are mounted on ribs and also supported laterally at the top. The two axial thrusters are located 92 cm radially outboard of the spacecraft centerline, diametrically opposite each other, and 115 cm aft of the spun bulkhead. These thruster/valve assemblies and associated components are supported by tubular tripod structures.

A thin bulkhead covers the tops of the ribs. This assembly provides a mounting surface for the heater switches, parallel relay, and the eight solar panel attach brackets which are also utilized as ground handling lift points. The two solar panels are cantilevered from these common brackets. The sun sensor and earth sensors are provided view fields through the 7.5 cm space between the solar panels. The radial and spinup thrusters exhaust through this central band. The sensors, accelerometers, radial thrusters, and spinup thrusters are attached to intercostals between the rib ends.

The forward conical sunshield and the aft thermal barrier are bolted to the edges of the forward and aft solar panels, respectively. The inner circumference of the conical sunshield supports an aluminized teflon laminate closure. The aft thermal barrier, a conically shaped assembly, is attached at the aft end of the solar panel and is anchored at its forward edge just below the apogee motor mounting ring.

The apogee motor is restrained within the basic conical structure of the spacecraft by 36 radial bolts.

The spacecraft is secured to the adapter during launch by a two-piece band assembly (see Figure 86) which is tensioned by two pyrotechnic bolts located 180 degrees apart. When one or both bolts are blown, the band separates and the sectors are retracted axially onto clamp catchers on the adapter. Separation of the spacecraft from the adapter is effected by the extension of eight springs positioned at equal intervals around the interior periphery of the separation ring of the adapter. At four of the eight spring locations there are plunger switches; two switches provide separation indication to the spacecraft and two provide indication to the booster telemetry system.

4.3.9.1 Structural Design

The primary structure of the spacecraft is made up of four basic assemblies: the antenna support structure, the despun compartment, the spun section, and the booster adapter. The important structural link on orbit is the BAPTA. The BAPTA shaft and housing are made of titanium alloy and are supported in a machined aluminum alloy conical section. The central conical structure of the spun assembly, the spun bulkhead, and the adapter are made up of three magnesium rings and skins. The BAPTA cone, the forward ring of the central conical structure, and the spun rib assemblies are made from aluminum alloy materials.

The despun compartment central hub is a machined member which supports 1) the antenna assembly through a bolt circle on its forward end; 2) the BAPTA shaft through a bolt circle on its aft end; and 3) the despun ribs, whose vertical inboard flanges are bonded and bolted to the cylindrical portion of the hub. The despun shelves are bolted to radial flanges on the hub as well as to the cap sections of the ribs. The six ribs are machined from aluminum alloy plates. The angle sections which join the lower extremities of the ribs are formed from aluminum alloy sheet. The shelves provide closures at the top and bottom; they, as well as the outrigger shelf, are made of aluminum alloy honeycomb core bonded to aluminum alloy face sheets. All face sheets except that on the forward inboard shelf are 0.025 cm thick. The forward inboard face sheet is chemically milled to provide a thickness variation, as required for heat transfer, from 0.025 cm at the inner radial portion adjacent to the hub to 0.12 cm at the outer portion. The honeycomb shelves incorporate more than 700 inserts for both attachments supported between the face sheets by syntactic foam to provide structural restraint. With few exceptions, all bolt attachments for units are made unidirectionally, i.e., units on the lower surface of the aft shelf are bolted into inserts and do not protrude into the forward surface and those on the forward surface are attached with bolts which do not extend through the aft surface.

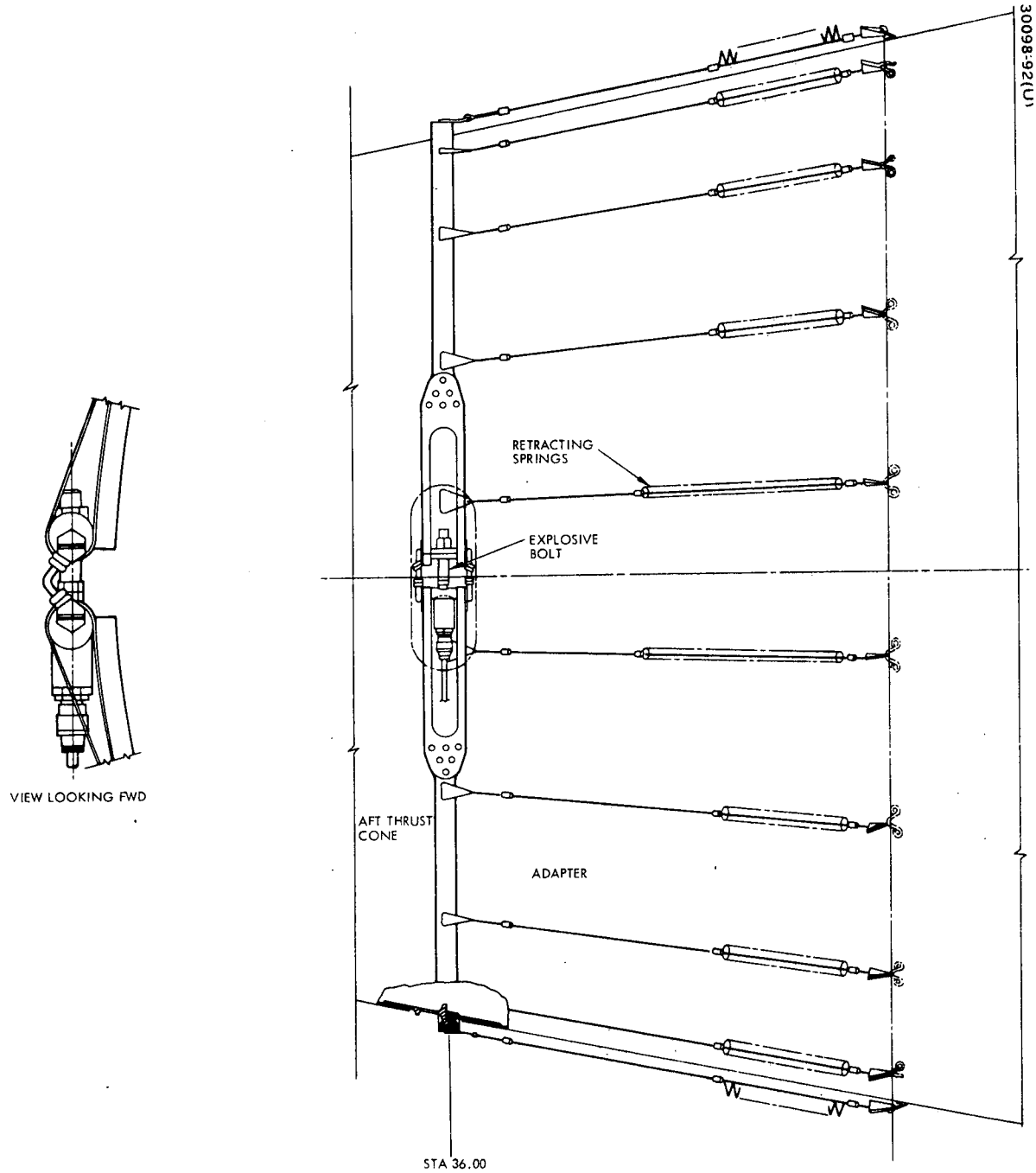

Figure 86. Separation Clamp Installation

The forward outboard shelf extends in a cantilever fashion from a bolted attachment to the horizontal bottom surface of the TWT support tees at the periphery of the basic hub structure. It is additionally supported near its mid-span by tubular members attached at twelve equally spaced perimeter locations. The lower ends of the tubular members are supported in pairs by fittings at the lower outboard extremity of each of the six ribs. The outrigger shelves incorporate tee sections stiffeners on the upper suface to provide support stiffness to the TWT power supplies.

The central cone of the spun section is an assembly of three machined and formed conical skin assemblies and four machined rings. Each magnesium skin section is flat machined to within 0.002 cm of minimum required thickness and is then formed into its conical shape with one or two joggled longitudinal lap seams dependent upon diameter.

The forward ring of aluminum alloy provides an axial bolt circle for attachment of the BAPTA and the radial support ties from the tops of the positioning and orientation tanks. The forward skin section provides a mounting surface for four machined aluminum brackets located at four orthogonal locations. These four brackets are the mounting locations for the spun encoders and decoders, the despin control electronics units, the squib and solenoid drivers, and the battery control electronics. The cross sectional areas of the machined brackets are set by requirements for thermal conduction between the units and the conical shelf which provides a radiation/conduction path.

The second ring at the base of the forward skin is machined from aluminum ring forging. It provides the upper support for the inboard end of the eight spinning ribs as well as the attachment for the inner perimeter of the thin magnesium sheet mounted on the rib tops.

The next, intermediate, skin section is formed into the conical shape from a single magnesium sheet with one longitudinal joggled seam. It provides an attachment for eight longitudinal angle members which are shear attachments for the inboard ends of the rib webs.

The closing machined aluminum ring on the intermediate section is the most complex of the rings. It provides an attachment for the lower inboard ends of the eight ribs and, most important, provides for the support/alignment of the apogee motor. The apogee motor mounting bolts pass through a series of 36 equally spaced radial holes.

The aft section, below the apogee motor mount ring, incorporates two magnesium sheets formed to the conical shape. The aft ring is machined to provide a mating surface for the separation clamp. It also includes provisions for supporting separation switches/pads and separation spring pads. Late additions to this ring are the four torsion keys attached to the aft surface of the inboard flange of the ring.

The rib assembly includes eight back-to-back stiffened pairs of C channels of formed sheet aluminum alloy for ribs, an 0.05 cm thick magnesium coversheet, and eight box section intercostal closures joggled at their ends to mate with the C shape edge of each rib. Fittings are attached at alternate ribs to provide a base mount for the positioning and orientation tanks.

Brackets are mounted on the rib intercostals to provide support for two radial jets, two spinup jets, two earth sensors, two accelerometers, an earth sensor, a series of connectors for ground operation, and two electrical umbilicals for prelaunch and launch interconnect with the boost vehicle. One intercostal also has a bracket to support one end of the apogee motor S&A view tube which extends inboard through a second support near the central cone to a point adjacent to the indicator window on the S&A assembly on the forward end of the apogee motor.

Four of the rib extremities also provide fittings to attach the outboard members of the positioning and orientation axial jet support structure. The inboard attachment of the third primary member of the axial jet support is at the apogee motor mount ring. From these three points the tripod assembly extends aft to an apex fitting machined to accept the tubular members. This fitting is the mounting location for the axial jet support bracket and also provides attachment for the fill and drain valve. The remaining components along the axial propellant lines are supported by a series of channel sections attached to the basic tripod support. Additional structural support is provided radially by a tubular member extending from a channel section across the two outboard members of the tripod to the central cone.

The two cylindrical solar panels are cantilevered from machined fittings mounted at the ends of each spinning rib. The solar panel substrate to which the solar cell arrays are bonded form a continuous 2 cm thick cylinder that is 2.38 meters in diameter and 1.38 meters long. They are of sandwich construction. The face sheets and edge closures are made of fiberglass. The edge closures consist of eight U shaped spliced sectors at each end. Into these closures are bonded metal inserts used for structural attachments.

The forward solar shield is attached to the forward solar panel. The substrate which supports the silvered quartz mirrors is an all aluminum honeycomb sandwich. The substrate is made with the minimum cone angle to provide structural support to the mirrors and inboard teflon laminate shield without excessive deflection.

The inboard sunshield is attached to the conical substrate by clips and has stiffening wires run between support clips to prevent any appreciable response to spacecraft nutation. The laminate itself is a special bonded sandwich consisting of 0.005 cm aluminum foil and 0.005 cm aluminized teflon.

The aft thermal barrier, supported at the aft end of the solar panel, is a conically shaped assembly which is a basic 0.002 cm thick stainless steel support for a two layer nickel sheet, ceramic mat sandwich. It is anchored at its forward edge by 12 tension springs attached just below the apogee motor mounting ring. "Dormer windows" are included in two places in the aft thermal barrier through which the axial jets protrude.

The adapter provides the structural interface with the Centaur boost vehicle. The forward end is a machined aluminum ring forging which provides one half of the separation interface held by the Vee band clamp. The skin is made from two flat machined magnesium skin formed into a conical shape and joined at two joggled longitudinal seams. The aft end is a machined aluminum ring which is bolted to the Centaur payload support structure.

4.3.9.2 Spacecraft Structure Analysis

Preliminary loads and dynamic spacecraft analysis were conducted for the TDRS design in support of system analysis (see Table 53). Three quasi-static load conditions that were critical in the Intelsat IV design have applied for structure sizing. The first load condition represents the Atlas Centaur burn condition and consists of a uniform ±2.5 g's lateral load along the total spacecraft length, combined with -7.5 g's and ±3.0 g axial. This condition follows the past philosophy of combining simultaneously the worst lateral and axial load factors, even though in reality they may occur at different periods during ascent flight.

A second quasi-static loading condition is used to design for non-uniform loading of the type that occurs during the Atlas Centaur maximum

TABLE 53. DESIGN LOAD CONDITIONS

Type	Condition/Level	Event
Quasi static accelerations	A) ±2.5 g lateral -7.5 g, +3 g axial	Atlas/Centaur burn
	B) Nonuniform lateral g, -3.75 g axial	Launch release and maximum dynamic air load (aq)
	C) 4R lateral (R in meters), -11 g axial	Apogee motor burn
Transient flight loads	Loads predicted by coupled spacecraft/boost vehicle dynamic analysis	Engine ignition and cutoffs

air load and launch release flight events. This type of loading is characterized by relatively high lateral loads on the appendages at the top of the spacecraft.

The third condition consists of the apogee motor ultimate load factor of -11.0 g combined with centrifugal loading g's of 4R where R is the radius in meter from the centerline of the spacecraft. The -11.0 g represents an allowance of -10.0 g for unsteady load effects, superimposed on the -10.0 g peak acceleration produced by the apogee motor.

Final structure validation for flight is achieved by coupled booster/spacecraft analysis that computes steady state and maximum dynamic responses to the various flight event transients.

4.3.9.3 Dynamic Analysis

During the TDRSS study Phase II, two math models of the proposed spacecraft structure were generated to determine dynamic characteristics of the liftoff and orbital spacecraft configurations. In addition, maximum quasi static loading conditions were applied to the liftoff math model in order to develop maximum structural element loading for stress analysis purposes.

Details of the liftoff math model are shown in Figures 87 and 88. The model consists of 38 mass points. The spun section model is identical to that of the Intelsat IV design. A cone was added between the spun and despun spacecraft sections to provide the primary load path around the BAPTA. The BAPTA itself is not locked as it was in the Intelsat IV application. The cone carries 97 percent of the load and the BAPTA 3 percent at liftoff. After release of a Marman band prior to AKM burn, the BAPTA assumes 100 percent of the load.

The orbital model consists of 37 mass points with the spacecraft antennas supported off the despun platform and positioned both forward and aft of the spacecraft body. The orbital model is shown in Figure 89. The mode shapes and frequencies are calculated for a nonspinning free-free spacecraft. The mode shapes and frequencies for both the liftoff and orbit conditions are tabulated on Tables 54 and 55, respectively. The results of the orbital math model analysis are used as input to the DASFA computer program for predicting the spinning spacecraft dynamic response and interactions with the attitude control system.

Two separate loading conditions were analyzed for the liftoff cases: X and Y lateral axes combined with a -3.75 g's axial load. The load curve used is an extrapolation of that used for the Intelsat IV design. It consists of an exponentially tapering lateral acceleration profile having a maximum value of 30 g's at the tip of the antenna mast and a base acceleration of 2.5 g's. This loading curve is shown in Figure 90.

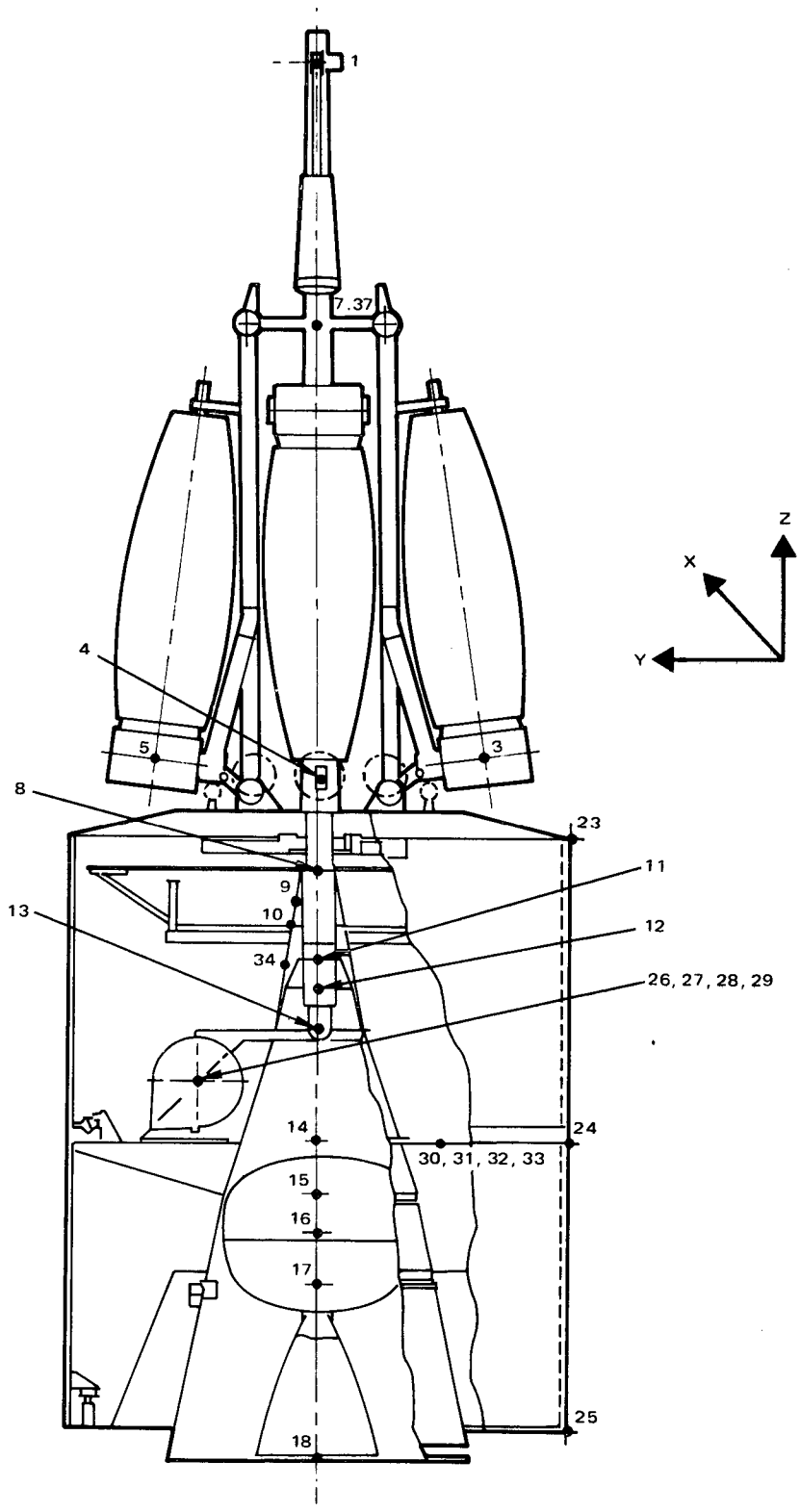

Figure 87. TDRSS Liftoff Mathematical Model 1

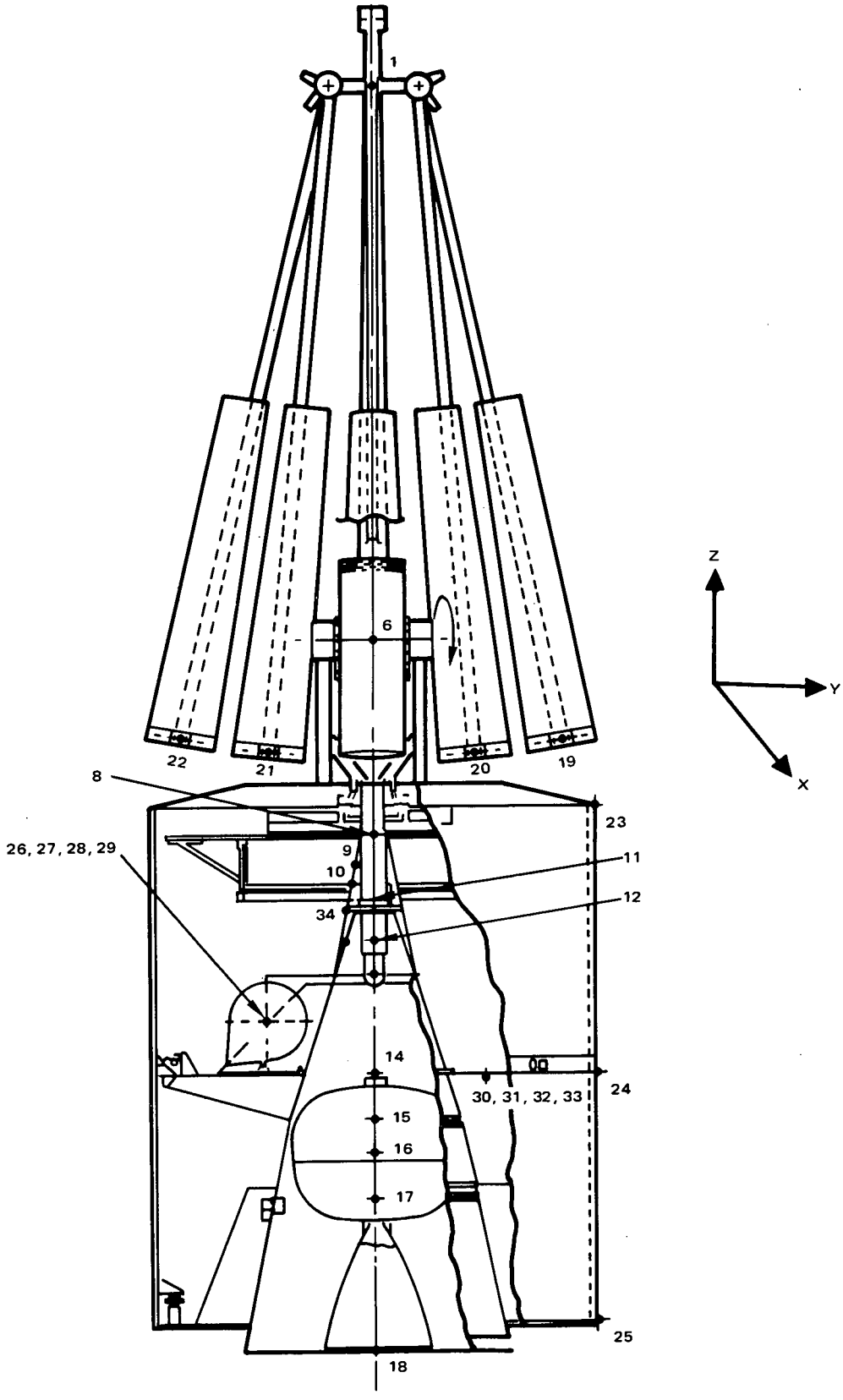

Figure 88. TDRSS Liftoff Mathematical Model 2

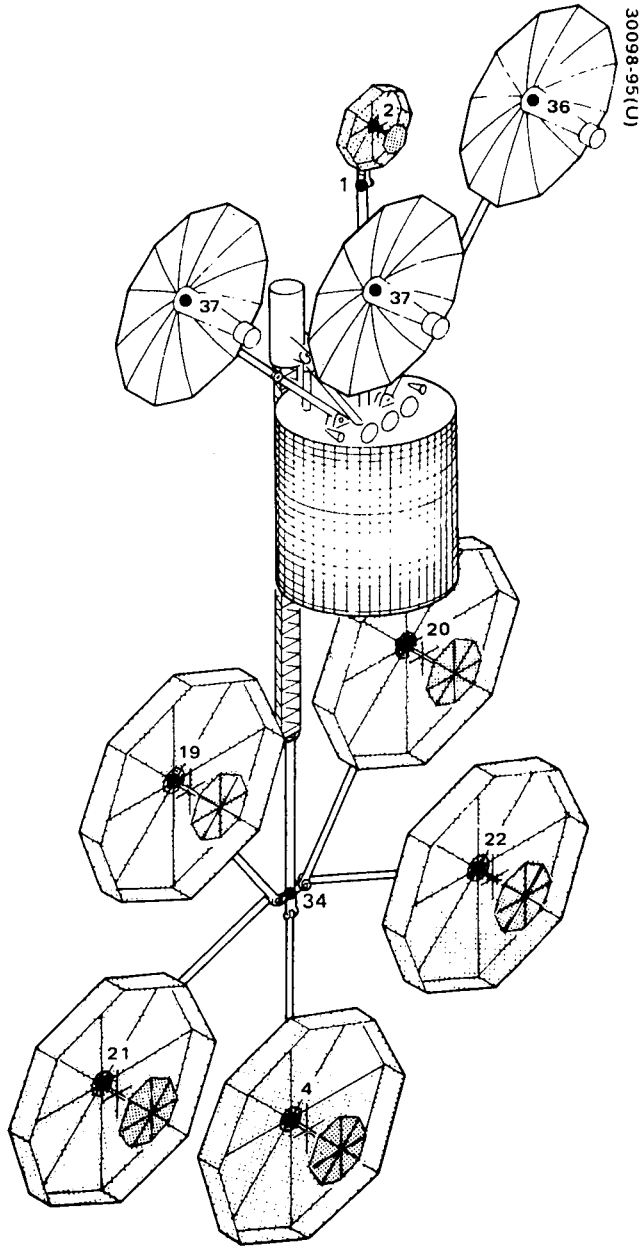

Figure 89. TDRSS Orbital Configuration Math Model

TABLE 54. LIFTOFF CONFIGURATION MODE SHAPES AND FREQUENCIES

Mode No.	Frequency, Hz	Component	Direction
1	6.04	Antenna mast	X
2	6.07	Antenna mast	Y
3	12.83	Astro mast	Y
4	15.91	Astro mast	Y
5	16.76	Spacecraft	X
6	18.4	Spacecraft	Y
7	21.17	Astro mast	X
8	23.67	Lower antenna support	X
9	23.92	Lower antenna support	Y
10	24.0	Solar panel	Y
11	24.45	RCS tanks	X
12	24.72	Antenna support	X
13	25.0	Antenna support	X
14	26.31	RCS tanks	X, Y
15	26.6	Antenna mast	Y
16	27.21	Antenna mast	X
17	29.0	Solar panel	θZ
18	29.7	Spacecraft	Y
19	30.1	Spacecraft	X
20	30.74	Despun shelf	θZ

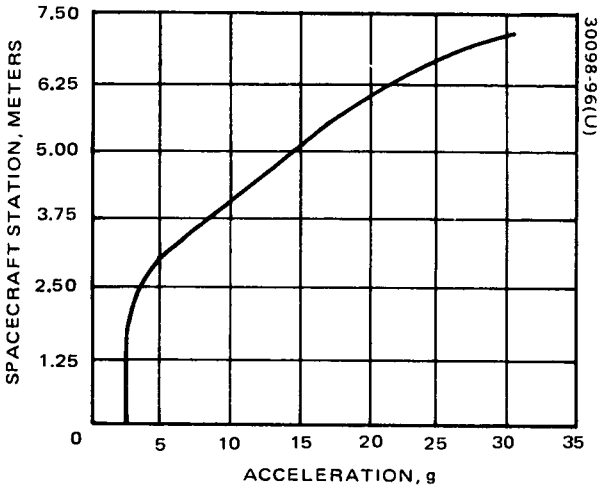

Figure 90. Quasi-Static Nonuniform Lateral Loading Curve to be Combined With -3. 75 g Axially

The loads reacted in the structure from the application of the X and Y lateral loading conditions combined with an axial compressive loading were used in establishing element sizes and for determining maximum structure/deflections.

The maximum shear and bending moment on the BAPTA occurs during the application of the X-axis loads. A shear of 14900N combined with a bending moment of 1360N-m is reacted by the BAPTA between mass stations 11 and 38. The cone bridging the BAPTA carries the remainder of the load; 44, 500N shear and 52, 600 N-m bending moment at the Marman clamp station 34. The loads applied to the BAPTA are below the maximum load carrying capacity of the Intelsat IV BAPTA.

4. 3. 9. 4 Interactions Between Flexible Antenna Structures and Attitude Dynamics

Dynamic analyses of the TDRS spacecraft have been performed to determine the effects of despun antenna flexibility on the antenna beam

TABLE 55. ORBIT CONFIGURATION MODE SHAPES AND FREQUENCIES

Mode No.	Frequency, Hz	Component	Direction
1-6	Rigid Body	Spacecraft	6 DOF
7	0.638	Aft antenna	Y
8	0.728	Forward antennas	X
9	1.0	Aft antennas	X
10	1.43	Aft antennas	Y
11	1.55	Aft antennas	Y
12	1.627	Aft antennas	X
13	1.77	Forward antennas	X
14	1.97	Forward antennas	Z
15	2.188	Aft antenna	Y
16	2.19	Forward antenna	Y
17	2.3	Aft antennas	X
18	2.57	Aft antennas	Z
19	2.65	Aft antennas	X
20	2.69	Aft antennas	Y, Z

pointing errors and on the nutational stability of the vehicle. Time histories were generated showing the motion of the spacecraft with rotor dynamic unbalance, and the response of the spacecraft to attitude control jet pulsing.

An eigenvalue analysis of the linearized equations of motion was also performed. The vehicle was found to be nutationally stable (as expected) and the pointing errors of the main antenna beams were determined to be quite small.

The despun antenna assembly is massive and its motion dominates the overall spacecraft attitude dynamics. The despin control system and the selected nutation damper were found to require extremely long periods for reducing dynamic motion of the despun section.

The present TDRS conceptual design is a gyrostat spacecraft with a very large and massive despun antenna farm, as shown in Figure 89. This large, low-vibration-frequency structure will interact strongly with the attitude dynamics of the spacecraft, thereby influencing the pointing accuracy of the various antennas.

The dynamic interactions of the large, flexible, despun structure with the overall vehicle dynamics were investigated by first determining the in-orbit vibrational frequencies of the system. As part of this effort,

coupling terms were developed which indicated which structural vibration mode should most strongly couple with the vehicle dynamics. Another by-product of this study was a verification of the attitude stability of the spacecraft in the presence of flexible antennas.

With this information, time histories of vehicle motion were generated under several conditions to gain more insight into the attitude dynamics.

The first step in this dynamic analysis was to model the flexible despun portion of the spacecraft as an assemblage of lumped masses and interconnecting flexible structural members, then to determine the natural vibration frequencies and corresponding mode shapes (i.e., the structure's deformation pattern). The structure was analyzed assuming that it was cantilevered from a rigid base at the BAPTA. The BAPTA was considered to be flexible; experimental data obtained from tests on the INTELSAT IV BAPTA were used. (The value used was 0.144×10^6 N-m/rad.) This idealization was used in the MARS program in order to find the normal modes of vibration of interest. The first six fundamental vibration frequencies determined in this manner are listed in Table 56.

The truncated modal representation of the flexible structure obtained from the MARS analysis was assembled along with the overall spacecraft inertias, rotor spin rate and inertia, and despin control system characteristics to form a dynamic model of the orbital spacecraft configuration. The spacecraft parameters used are listed in Figure 91. The despin control system was assumed to consist of a proportional loop and a rate loop; i.e., the control torque was represented by

$$T = C\dot{\theta} + K\theta$$

TABLE 56. STRUCTURAL FREQUENCIES

Cantilever Frequency (cps)	In-Orbit Frequency (cps)
0.366	0.422
0.387	0.436
0.883	3.4
1.12	
1.243	
1.247	
	1.01
	1.52
	1.74

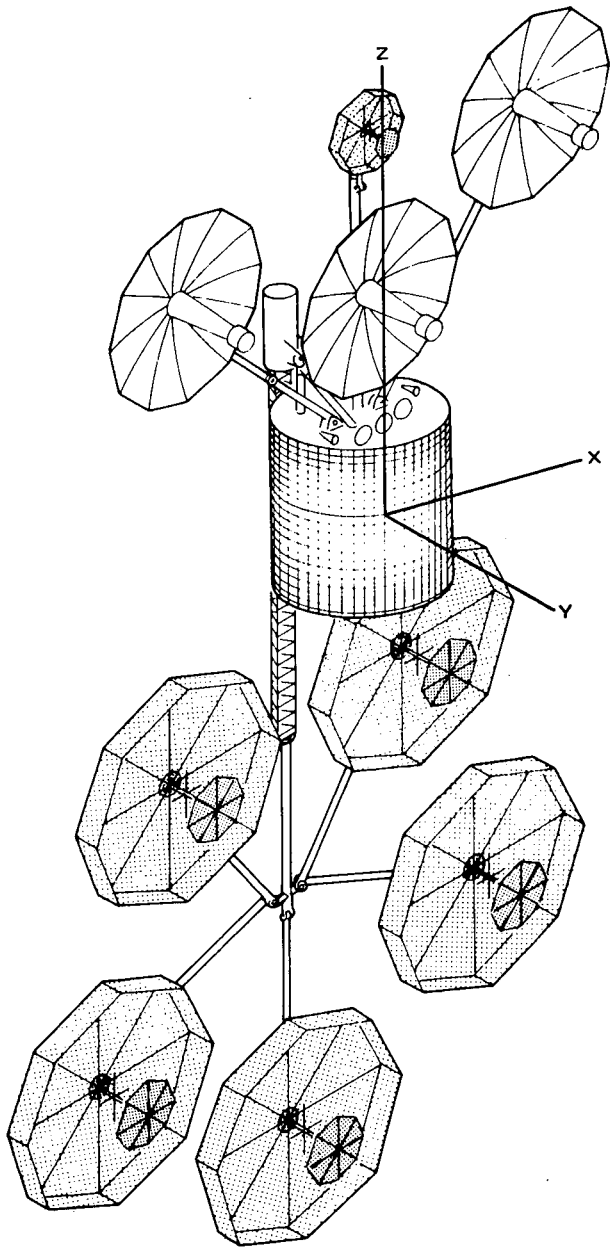

SPACECRAFT INERTIA MATRIX:

$$\begin{bmatrix} 9000 & 0 & 328 \\ 0 & 8300 & 0 \\ 328 & 0 & 1260 \end{bmatrix} \text{ kg - m}^2$$

ROTOR SPIN INERTIA:

191 kg - m^2

ROTOR SPIN RATE:

1 Hz

Figure 91. TDRS Configuration, Inertia Property Matrix and Coordinate System

where T is the torque and θ the platform azimuth angle error. The values used in this representation were (Ref. 1)

$$C = 186.5 \text{ Nm/rad/sec}$$

$$K = 2.34 \text{ m/N/rad}$$

The nutation damper characteristics selected for this model were

damping:	$C_c = 0.155$ N sec/m
spring constant:	$K_d = 0.0081$ N/m
moment arm:	$L_d = 3.05$ m
mass	$m_d = 0.454$ kg

The dynamic model was assembled using a computer program, INTERFACE, which was generated specifically for handling dynamic systems with flexible appendages (Ref. 2). The assembled model was subjected to an eigenvalue analysis using the library routine, DYNEIG. This analysis verified the overall attitude stability of the system, as all eigenvalues had positive real parts.

The eigenvalue analysis also revealed the in-orbit vibration frequencies of the system. Typically, transverse vibrations increase somewhat in frequency compared to the cantilever values due to the presence of less constraint at the base. Torsional frequencies about the spin axis increase greatly compared to the fixed base case, since now the base is free except for a typically very "soft" despin control system. The first six in-orbit frequencies determined from the eigenvalue analysis are listed in Table 56 alongside the cantilever frequencies obtained from the MARS program. The first two in-orbit modes, which are transverse bending modes, can be related to the corresponding first two cantilever modes and illustrate the moderate upward shift in frequency which occurs for such modes. The next mode is the torsion mode about the spin axis and displays the large shift in frequency. The next three in-orbit modes cannot be put into one-to-one correspondence with the next three cantilever modes; they are actually a mixture of these modes. However, note that one of these in-orbit modes has a frequency of 1.01 cps. This mode would be excited by any rotor dynamic imbalance because of the 1 cps spin rate of the rotor. Hence, the structural design ought to be modified in order to shift this frequency and avoid resonance.

Another feature of the INTERFACE program is the generation of "effective dynamic inertia" matrices which indicate the degree of coupling

of each mode of vibration with the overall spacecraft dynamics. To explain briefly, the equations of motion of the spacecraft with attached flexible appendages will be of the form (see Ref. 3)

$$I\,\underline{\ddot{\theta}} + B\,\underline{\dot{\theta}} + \Delta^T\underline{\ddot{\eta}} = \underline{t} \tag{1}$$

where

I = total spacecraft inertia matrix

B_T = gyroscopic matrix

Δ = modal participation matrix

$\underline{\theta}$ = spacecraft angular motion coordinates

$\underline{\eta}$ = flexible appendage modal coordinates

$\underline{t}$ = external torques

The equations of motion of the appendages will be of the form

$$\underline{\ddot{\eta}} + \left[2\zeta_i\omega_i\right]\underline{\dot{\eta}} + \left[\omega_i^2\right]\underline{\eta} + \Delta\underline{\ddot{\theta}} = 0 \tag{2}$$

where

$\left[2\zeta_i\omega_i\right]$ = diagonal modal damping matrix

$\left[\omega_i^2\right]$ = diagonal generalized stiffness matrix

When Equation (2) is substituted into Equation (1), the result is

$$(I - \Delta^T\Delta)\,\underline{\ddot{\theta}} + B\,\underline{\dot{\theta}} - \Delta^T\left\{\left[2\zeta_i\omega_i\right]\underline{\dot{\eta}} + \left[\omega_i^2\right]\underline{\eta}\right\} = \underline{t}$$

The matrix $\Delta^T\Delta$ is a 3 x 3 matrix which represents the inertia of the appendage relative to the spacecraft center-of-mass; it is composed of the sum of individual 3 x 3 matrices for each vibration mode. These "effective dynamic inertia" matrices are a most direct indication of the importance of each vibration mode and the axes about which its coupling is strongest. The six matrices corresponding to the six retained vibration modes are given on

$$\begin{bmatrix} 6280 & 0 & 490 \\ 0 & 5550 & 0 \\ 490 & 0 & 1047 \end{bmatrix}$$

TOTAL APPENDAGE INERTIA MATRIX (RELATIVE TO SPACECRAFT CENTER-OF-MASS), kg - m^2

3008-8-81(U)

MODE 1

$$\begin{bmatrix} 1950 & 0 & 316 \\ 0 & 0 & 0 \\ 316 & 0 & 51 \end{bmatrix}$$

MODE 2

$$\begin{bmatrix} 0 & 0 & 0 \\ 0 & 1640 & 0 \\ 0 & 0 & 0 \end{bmatrix}$$

MODE 3

$$\begin{bmatrix} 244 & 0 & -107 \\ 0 & 0 & 0 \\ -107 & 0 & 462 \end{bmatrix}$$

MODE 4

$$\begin{bmatrix} 3080 & 0 & 149 \\ 0 & 0 & 0 \\ 149 & 0 & 6.8 \end{bmatrix}$$

MODE 5

$$\begin{bmatrix} 14.9 & 0 & -84 \\ 0 & 0 & 0 \\ -84 & 0 & 450 \end{bmatrix}$$

MODE 6

$$\begin{bmatrix} 0 & 0 & 0 \\ 0 & 3000 & 0 \\ 0 & 0 & 0 \end{bmatrix}$$

EFFECTIVE DYNAMIC INERTIA MATRICES, kg - m^2

Figure 92. Effective Dynamic Inertia Matrices

Figure 92. These matrices display, for example, that the second and sixth modes are essentially rocking of the appendage about the Y-axis, and that the sixth mode is much more strongly coupled than the second. Similarly, the first and fourth modes are also rocking modes about the X-axis, and the fourth mode is more dominant than the first. The third and fifth modes involve torsion about the Z-axis and are about equal in importance.

The analyses of the dynamic interactions of flexible members on the despun platform, despin control system, and rigid rotor were performed using the DASFA computer program. This digital computer program uses the dynamic model assembled in the INTERFACE program to obtain time histories of spacecraft and appendage motions for various conditions. The conditions which were examined in this study were the presence of a dynamic imbalance on the rotor and the effect of pulsing an attitude control jet.

The response of the spacecraft to a rotor dynamic imbalance of 1.35 kg-m^2 is shown in Figures 93 to 95. The spacecraft was started with zero initial conditions, so that the imposition of the rotor imbalance in the simulation acted as a perturbation to the motion. Hence, the portion of the attitude motion which is nutation is actually a transient which would eventually die out if the simulation were carried out far enough.

Figure 93 is a polar plot of the motion of the spin axis in inertial space over a period of 100 seconds. (The nutation period for this vehicle is

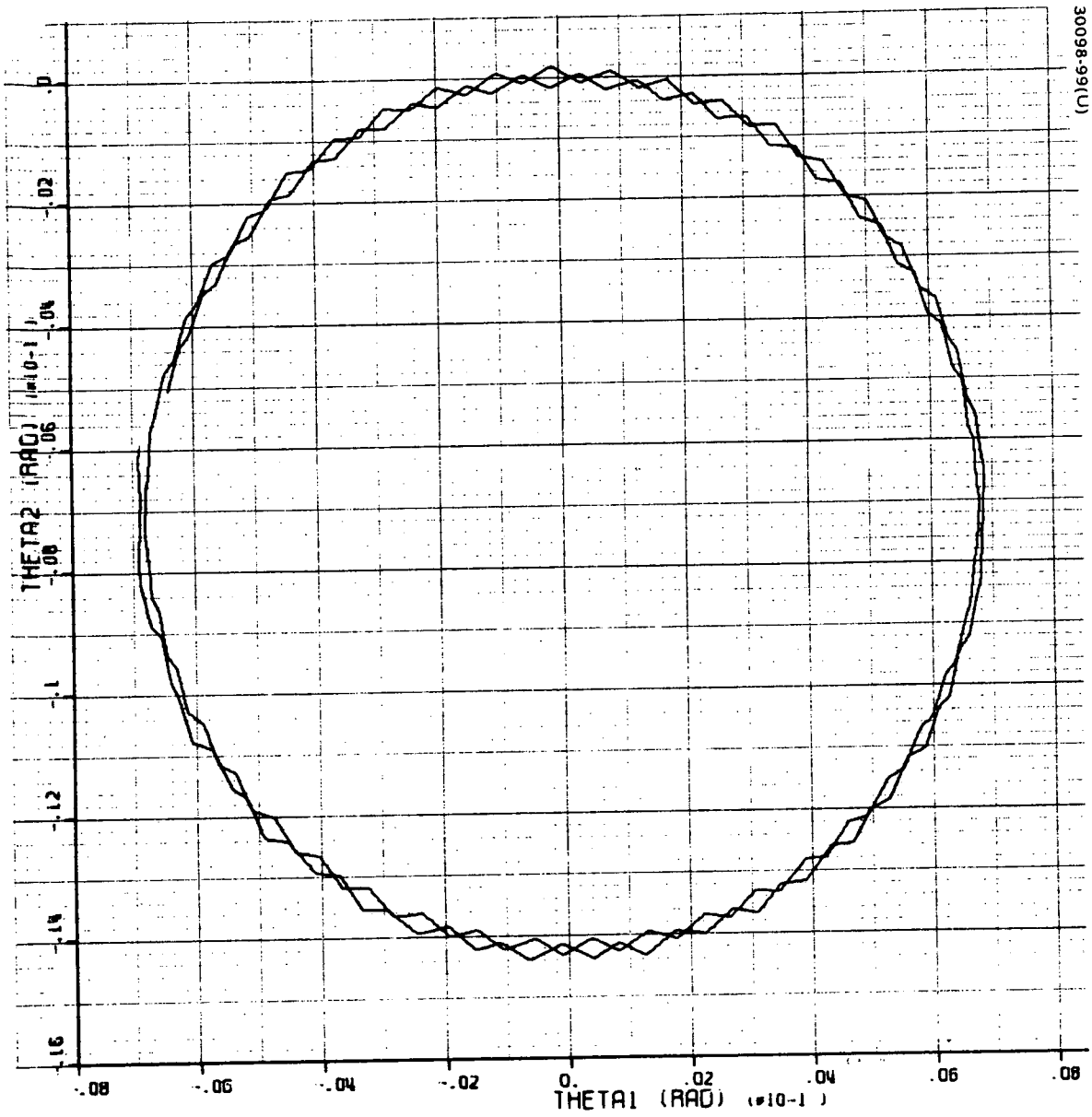

Figure 93. Spin Axis Motion - Rotor Imbalance

45 seconds.) The radius of the circular pattern represents the nutation angle induced by the rotor imbalance, whereas the small scale ripple superimposed on the nutation is the spin-axis wobble. This 1 cps wobble motion will remain after the transient nutation has died out. The fact that the spin axis trace decays very little over the two nutation cycles shown verifies that the relatively small nutation damper would require a very long time to reduce the nutation. The predicted time constant, using Reference 5, is about 14 hours. This could be improved somewhat using a larger damper further from the spin axis, but the time constant would still be of the order of hours. This is due mainly to the very large transverse inertia of the vehicle and the resulting low nutation frequency. The most effective way of controlling nutation would be to provide shaping in the despin control system which would use the large despun platform product-of-inertia to actively reduce nutation.

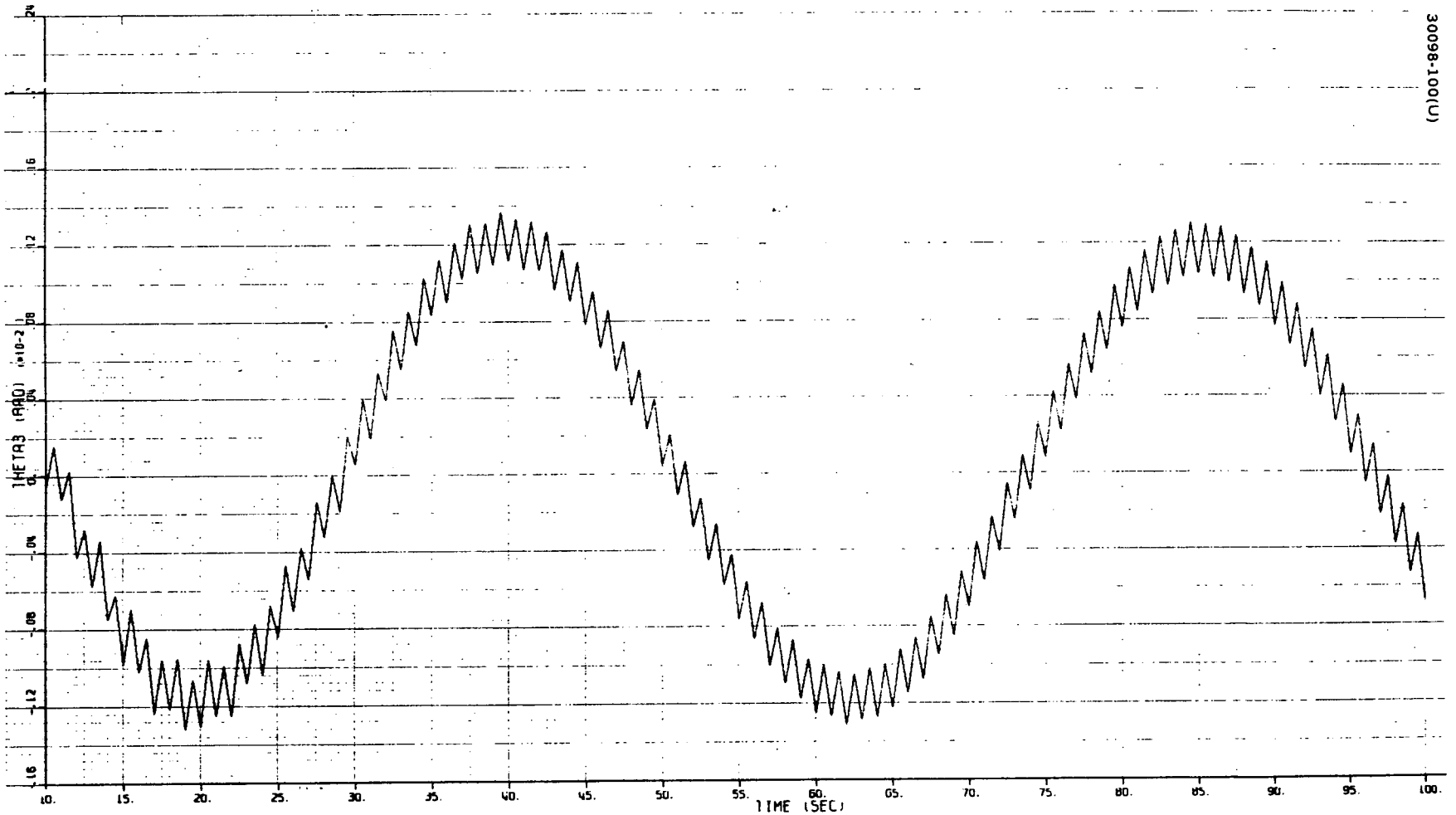

Figure 94. Despun Member Azimuth Motion - Rotor Imbalance

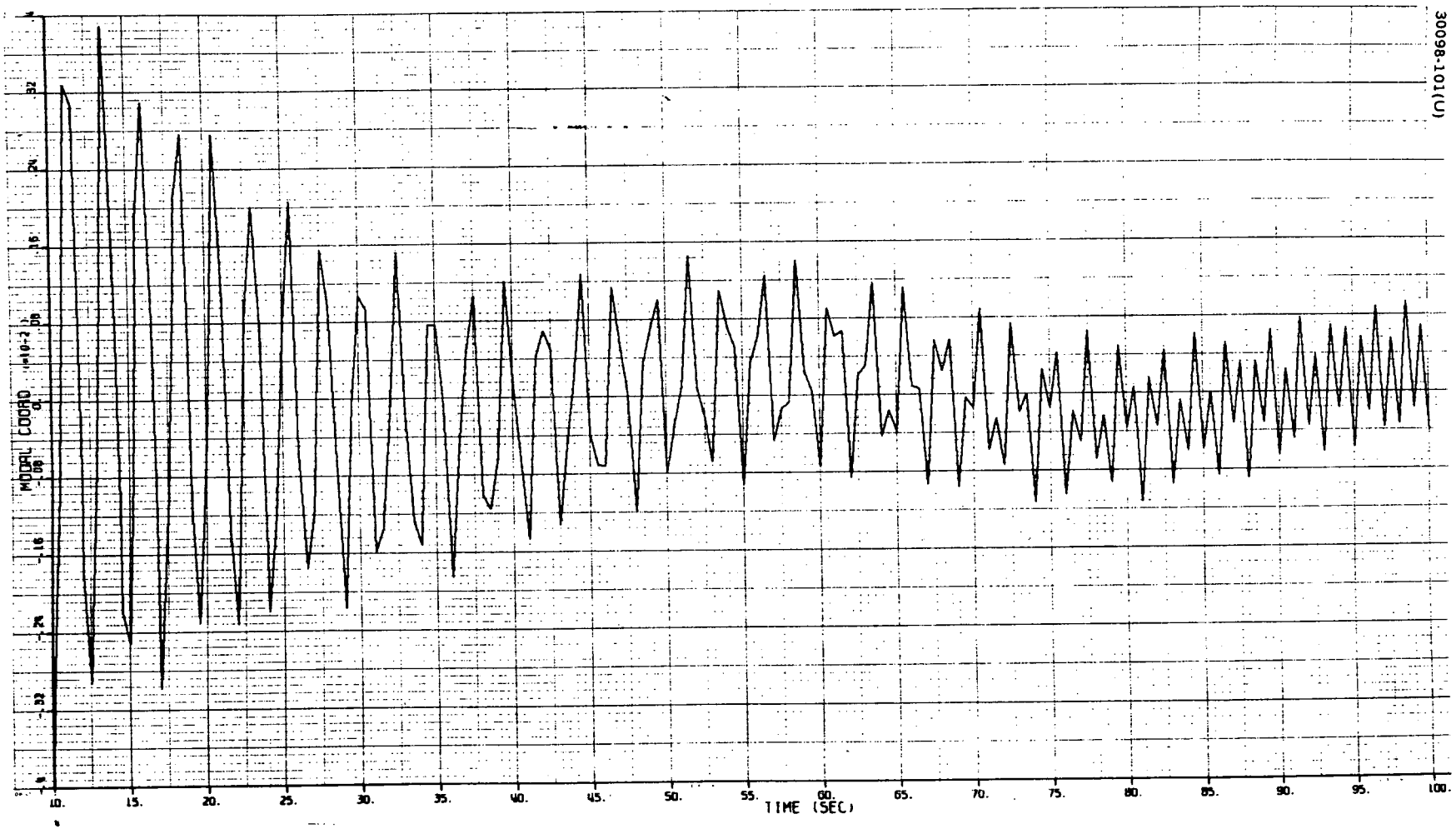

Figure 95. First Vibration Mode Amplitude - Rotor Imbalance

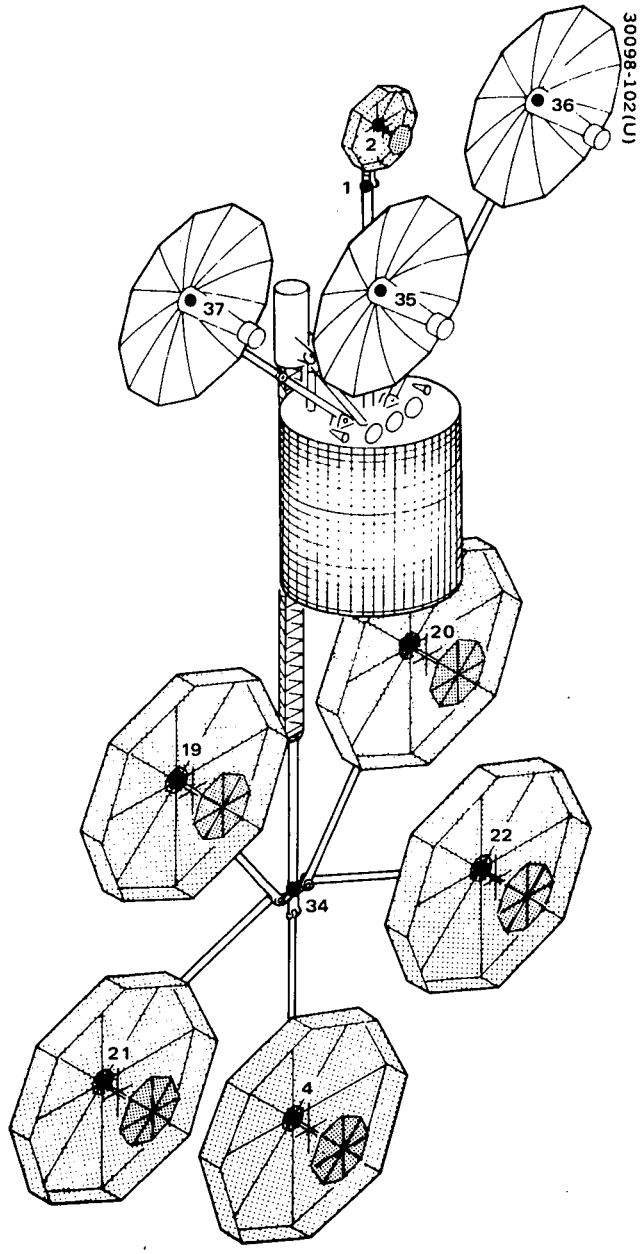

Figure 96. TDRS Orbital Configuration Math Model

Figure 94 is a time history of the platform azimuth motion. The product-of-inertia coupling of this azimuthal motion with the nutation causes the excursions shown. It can be seen that this motion decays very little over two cycles; this indicates that the postulated despin control system is "soft" so that it has little effect on these azimuth motions caused by product-of-inertia coupling. Once nutation has been damped out of the system, the 1 cps rotor wobble disturbance will remain. This motion has an amplitude of

$$2.2 \times 10^{-4} \text{ rad/kg m}^2 \text{ rotor dynamic imbalance}$$

Figure 95 shows the response of the first vibration mode to the imbalance. Here, the induced transient effectively damps out after about 70 seconds, and the motion becomes a steady-state one driven by the rotor wobble.

As part of the DASFA simulation, the total deflections of two representative antennas were monitored. Figure 96 shows some of the mass points used in the original MARS finite element model of the structure. The lowest antenna reflector (pt. 4) and one of the upper reflectors (pt. 37) were chosen for monitoring. In particular, the rotational deflections of these members about their Z-axes were recorded. The maximum amplitudes of these steady state motions (after the initial transient has damped out) are

$$\text{pt. 4:} \quad 5.53 \times 10^{-4} \text{ rad/kg m}^2 \text{ rotor dynamic imbalance}$$

$$\text{pt. 37:} \quad 1.25 \times 10^{-4} \text{ rad/kg m}^2 \text{ rotor dynamic imbalance}$$

These values should be added to the platform azimuth motion given previously to obtain the total motion. Since the antenna beam is swung through twice this angle, the maximum beam pointing error for any antenna reflector is, for mass point 4,

$$2 \times (7.5 \times 10^{-4} + 3 \times 10^{-4}) = 2.1 \times 10^{-3} \text{ rads}$$

per 1.355 kg m^2 of rotor imbalance. This value can then be used with a specified allowable beam pointing error to determine the maximum permissible rotor dynamic imbalance.

The other condition examined in the DASFA simulation involved the response of the vehicle to an attitude control jet pulse. A torque impulse of 0.13 Nm/sec, about the Y-axis was imposed on the vehicle after 10 seconds of quiescence. The responses are displayed on Figures 97 to 99. Figure 97 illustrates the induced nutation, Figure 98 the platform azimuth motion (again brought about by product-of-inertia coupling with the nutation), and Figure 99 the response of the first vibration mode. The same deflections were monitored as were followed for the case of rotor imbalance.

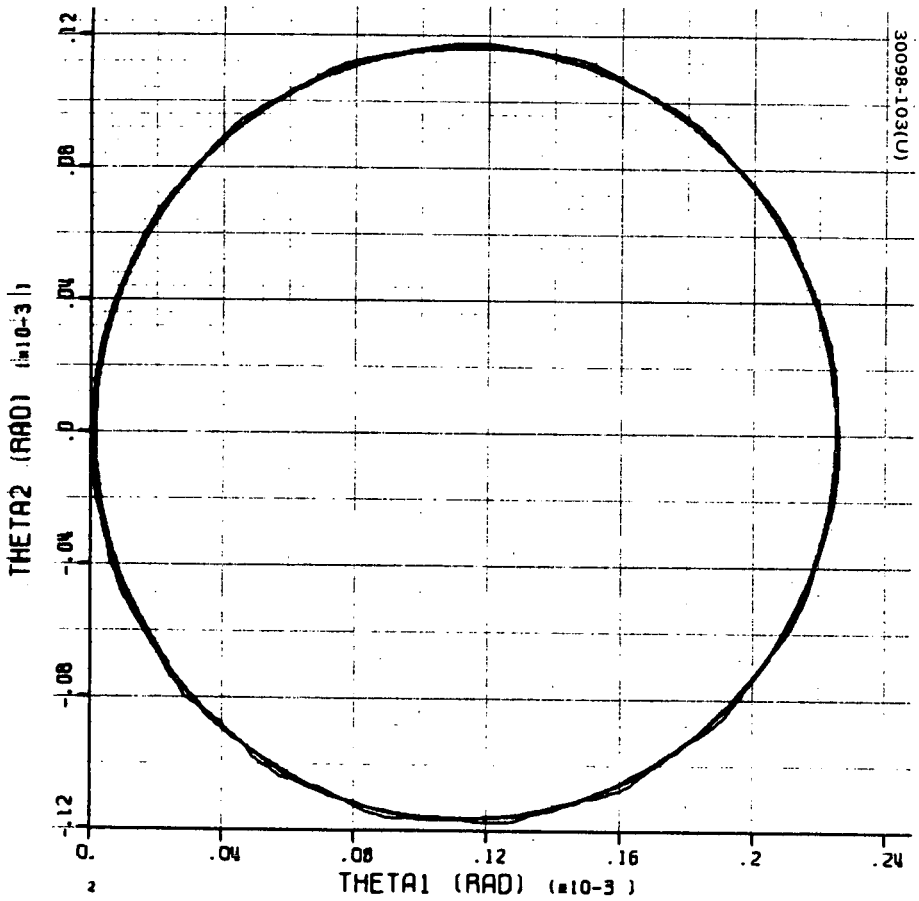

Figure 97. Spin Axis Motion - Jet Pulse

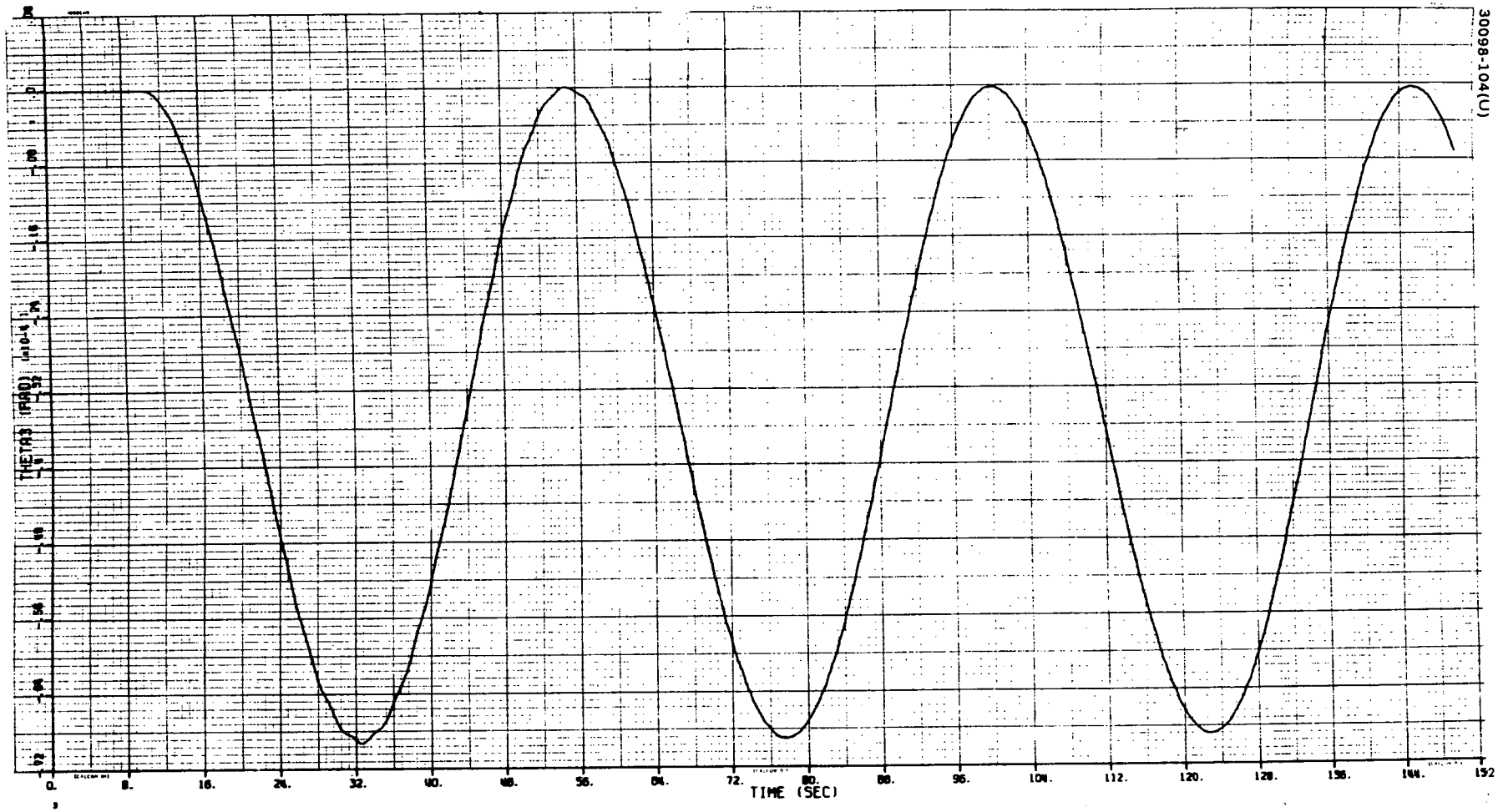

Figure 98. Despun Member Azimuth Motion - Jet Pulse

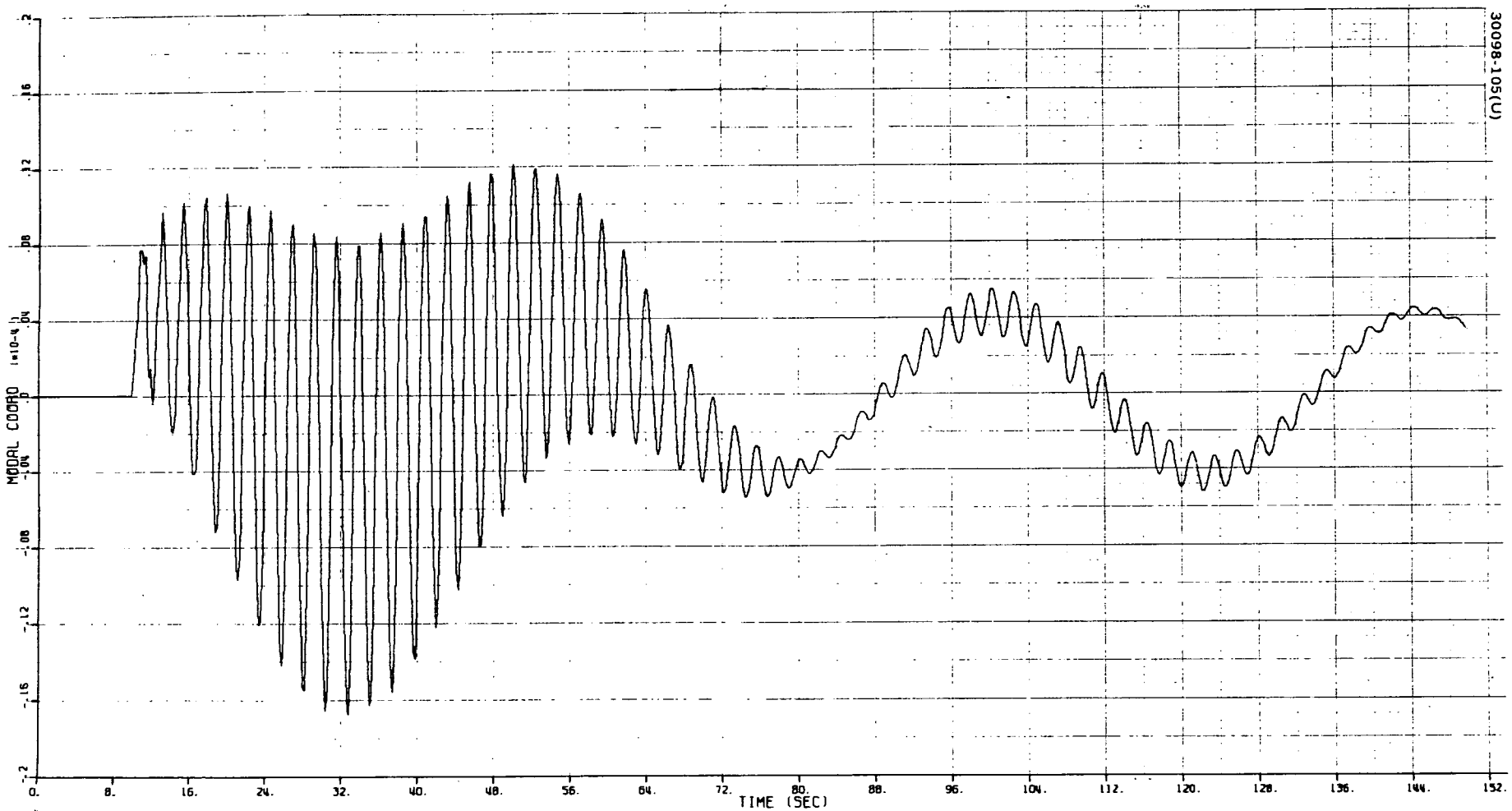

Figure 99. First Vibration Mode Amplitude - Jet Pulse

The maximum excursions for this case, normalized to the torque impulse, were

nutation:	2.25×10^{-3} rad
platform azimuth motion:	7×10^{-4} rad
mass pt. 4, θ_Z deflection:	1.26×10^{-6} rad
mass pt. 37, θ_Z deflection:	5.53×10^{-5} rad

Here, the worst case for beam-pointing error is the induced nutation; it would cause a maximum error per unit impulse of

$$4.5 \times 10^{-3} \text{ rad}$$

This value could be used to establish a specification for attitude control jet torque impulses.

In conclusion, the interactions can be summarized as follows:

- The nutation frequency of the vehicle is low (0.22 cps) and it does not couple with any of the structural frequencies of the flexible despun antenna farm, whose lowest in-orbit frequency is 0.42 cps.
- The despun segment of the TDRS spacecraft is massive and any motion of it will dominate the overall spacecraft dynamics.
- The nutation damper parameters and simplified despin control system model used in the simulation represent systems which are "soft" and therefore many minutes or even hours are needed for performing attitude control. However, the massiveness of the despun antenna farm means that perturbations caused by disturbances such as rotor dynamic imbalance and control jet pulsing are quite small.
- The flexible structure interactions with the vehicles attitude dynamics do not seriously degrade its performance.

4.3.9.5 References

1) Adams, G. J., personal communication

2) "Interface: Description and User's Manual," Hughes TIC in preparation

3) Likins, P. W., and Gale, A. H., "Analysis of Interactions Between Attitude Control Systems and Flexible Appendages," Proceedings of the 19th International Astronautical Congress, (New York, 1968), Vol. 2, pp. 67-90, Pergamon Press, 1970

4) Cloutier, G. J., "DASFA User's Manual," Hughes TIC 4112.21/88, 30 May 1972.

5) Cloutier, G. J., "Nutation Damper Design Principles for Dual-Spin Spacecraft," Journal of the Astronautical Sciences, Vol. XVI, No. 2, pp. 79-87, March-April 1969.

6) Cooley, H. H., "Dynamic Analysis of Atlas Centaur Launched TDRS Configuration," Hughes IDC 4112.22/369 (HS337/0130), 22 January 1973.

4.3.10 Thermal Control

The spacecraft thermal control system must provide an adequate temperature environment for all satellite subsystems during a mission life of 5 years in synchronous orbit. The orbital design must be compatible with survival and/or operation of all subsystems during transfer to synchronous orbit, apogee motor burn, and on-orbit operations. Table 57 presents the subsystem temperature requirements that have been established for the TDRS.

The overall thermal design concept employed for TDRS is one of passive thermal control, similar to Intelsat IV, which takes advantage of both the temperature averaging that results from uniform spin rate of the vehicle solar panel and the containment of the sun within ±30 degrees of the orbit plane. The key features of the thermal design are identified in Figure 100. Radiation is the dominant mode of heat transfer between major spacecraft elements. The temperatures of the spinning structure and low power dissipation regions are controlled by maximizing the radiation coupling to the solar panel. The batteries are hard mounted to the structural ribs in order to provide thermal fin capability. The lines and valves of both the axial and radial thrusters are provided with molded blanket heaters (a heater system of 0.03 watt/meter propellant line and 0.75 watt per thruster is used) that prevent any portion of the system from reaching the freezing point of hydrazine at any time during the operational life of the spacecraft. These heater elements are wrapped with low emittance aluminum tape to minimize the heater power requirements. During eclipse the hydrazine tanks are maintained above the freezing point with multilayer insulation.

Most of the power dissipating units are grouped on a despun platform across the forward end of the solar panel. Platform dissipation is radiated to a despun intermediate radiating surface provided between the platform and space. The high dissipating units are uniformly distributed to minimize thermal gradients on the shelf. A second surface finish of aluminized teflon for the intermediate surface serves to attenuate the temperature variation of the despun platform with respect to solar incidence angle. Temperature sensitivity of the platform is further attenuated by radiation coupling to the stable solar panel boundary.

TABLE 57. SUBSYSTEM TEMPERATURE REQUIREMENTS

Equipment	Design Range K	Eclipse Minimum K
Despun		
Transmitters, receivers, and other repeater electronics	267 to 311	261
Telemetry and command electronics	267 to 311	261
S band antenna positioner	222 to 367	222
Antenna mast and cabling	200 to 367 Mast deflections due to diametral temperature different 0.28	200
VHF and S band antenna	117 to 395	117
Spinning		
Apogee motor	278 to 306	278
Despin bearing	273 to 311	284
Despin electronics	267 to 323	261
Batteries*	273 to 300	273
Solar panel	222 to 297	172
RCS tanks	278 to 333	278
lines	278 to 367	278
valves	278 to 339	278

*No overcharge.

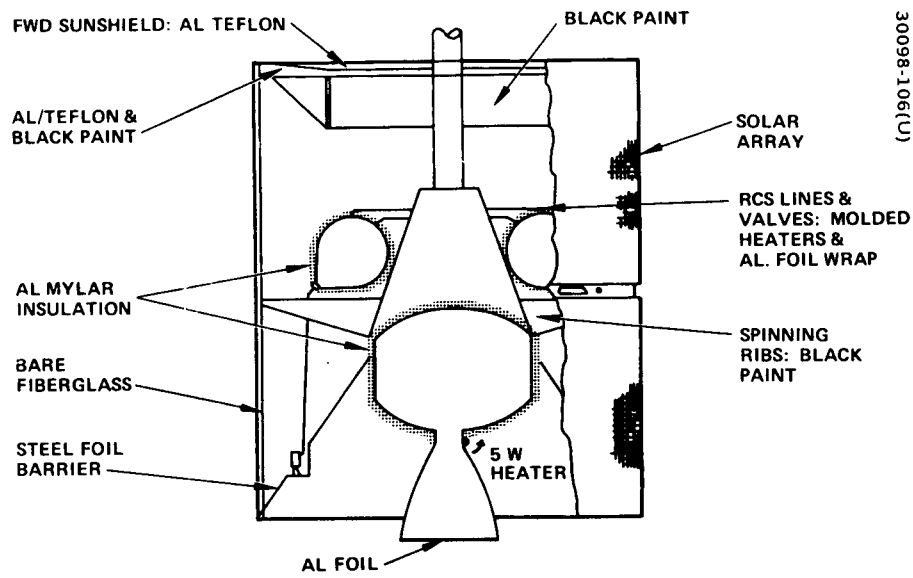

Figure 100. Spacecraft Thermal Control

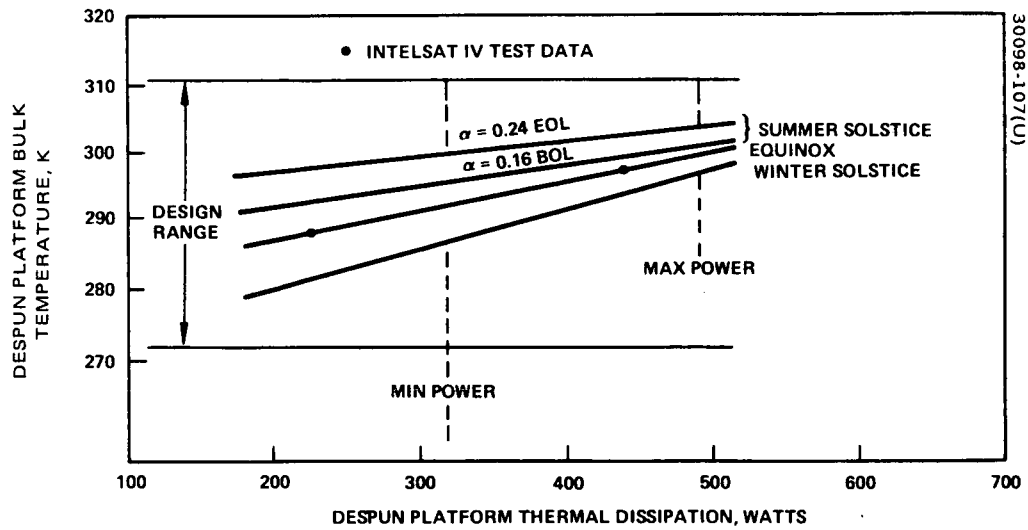

Figure 101. Despun Platform Power - Temperature Performance

The antenna masts will be treated as needed with a combination of aluminum foil and second surface aluminized teflon strips in order to limit both the thermal bending of the mast and the peak temperature of the cabling that will be attached to the mast. The antenna elements will have high emittance finishes only to the extent necessary to limit peak temperature below 422 K in any critical areas.

The apogee motor has an aluminized Kapton multilayer insulation blanket to protect the spacecraft from postfiring thermal soakback. Additional thermal isolation is provided around the aft end and around and over the nozzle to limit undesirable local temperatures near the nozzle throat during the transfer orbit. In addition to this isolation, an active heater on the nozzle throat is provided to the baseline to assure adequate temperature control of this critical element. The aft end of the spacecraft is closed and protected from apogee motor plume heating by a thermal barrier. A maximum surface temperature of 920 K is expected on the aft barrier during motor firing.

The power-temperature performance characteristics of the platform design are shown in Figure 101. The temperature performance is well within the equipment design range for the extremes in season and operating mode. Further, the end of life performance of the degraded teflon sun shield appears adequate for this mission. The figure contains two Intelsat IV test data points for reference.

5. ATLAS CENTAUR LAUNCHED TDRS OPTION 1

The Atlas Centaur launched TDRS Option 1 (AC01) configuration, Figure 102, is similar to the baseline configuration. The principal configuration change is the addition of a fourth 3.82 meter paraboloid reflector antenna for HDR service. The additional power requirements necessitate an extension of the solar cell array approximately 30 cm in length. A longer payload fairing is needed in order to accommodate the larger configuration; an extension of approximately 75 cm is required.

The key subsystem changes for AC01 are listed in Table 58. The additional mass of electronics, antennas, power supply, and supporting structure impacts the baseline configuration by requiring more efficient apogee injection propulsion to obtain more injected mass in synchronous orbit. The spacecraft bus for this optional design is similar to some of the extended capability Intelsat IV configurations currently under study. This configuration for TDRS more fully utilizes the capabilities of the improved Atlas Centaur launch vehicle.

The communications subsystem for AC01 is described in Figure 103. The increased capability provided by the addition of a second HDR channel to the baseline configuration requires approximately 24 kg of electronics and the power consumption is increased by 76 watts. Interchangeability of the Ku band channels and antennas is provided by means of interconnection switches and transmission lines. Equipment mass and power requirements are listed in Table 59.

The antennas used for Option AC01 are identical to those employed in the baseline design but with the addition of a second Ku transmit antenna and its positioner and position controller. The added Ku band antenna is of the same design as the one shown on the baseline, a deployable rib mesh design 3.82 meters in diameter. The primary surface is shaped by ribs of tapered wall thickness. The reflective mesh is contoured to a precesion of 0.025 cm by the use of a secondary back mesh and adjustable tension ties between the two meshes.

Power demand for the HDR service is doubled. The larger power demand requires larger batteries and more battery power during solar eclipses. This in turn requires more battery charge power and the total power demand increases 95 watts relative to the baseline configuration.

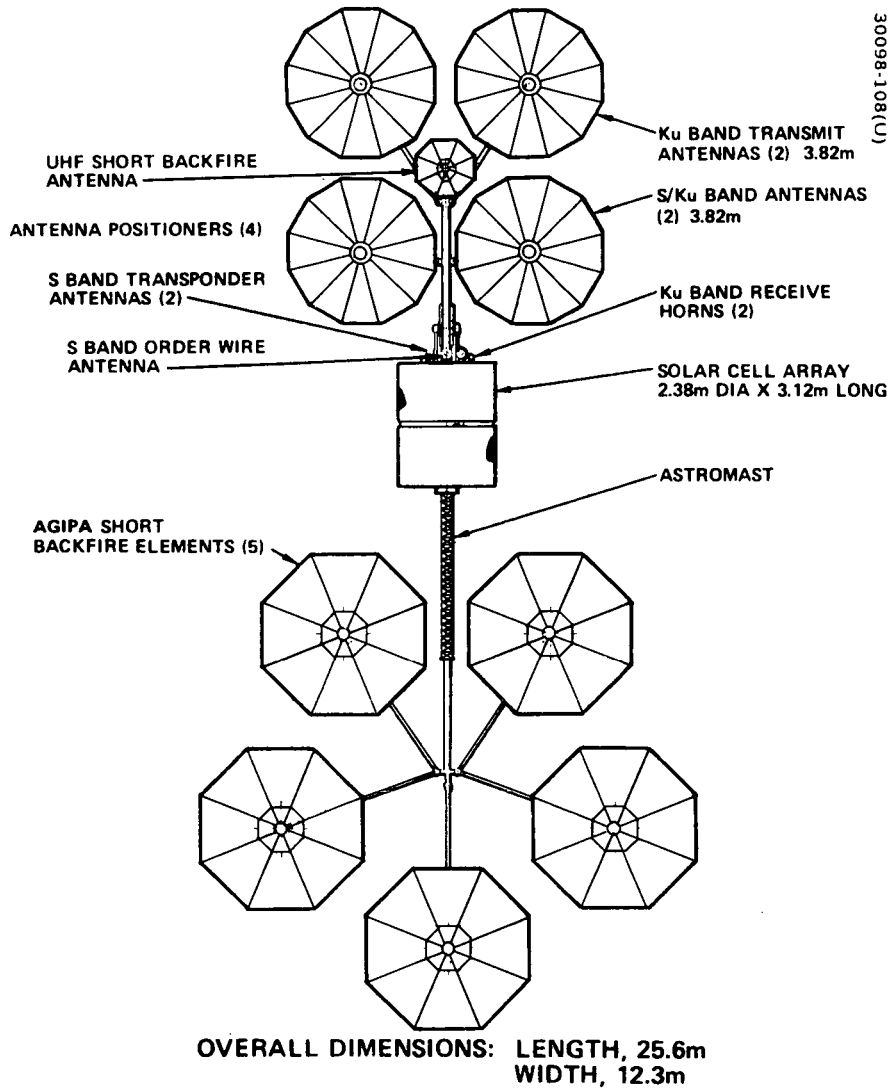

Figure 102. Atlas-Centaur Launched TDRS Option 1

TABLE 58. KEY SUBSYSTEM CHANGES FOR ACO1

Repeater

- Add redundant complement of HDR forward and return equipment
- Upgrade frequency synthesizer

Antennas

- Add one Ku band antenna with positioner, positioner controller, and waveguide

Electrical Power

- Increase size of solar cell array and batteries by approximately 10 percent

Propulsion

- Select optimized rocket motor to maximize injected payload

Structure

- Redesign forward deployment to accommodate fourth 3.82 meter antenna
- Increase length of solar cell array substrate
- Extensive use of lightweight beryllium structures

Thermal Control

- Add insulation for fourth antenna support strut
- Incorporate thermal and solar radiation barriers

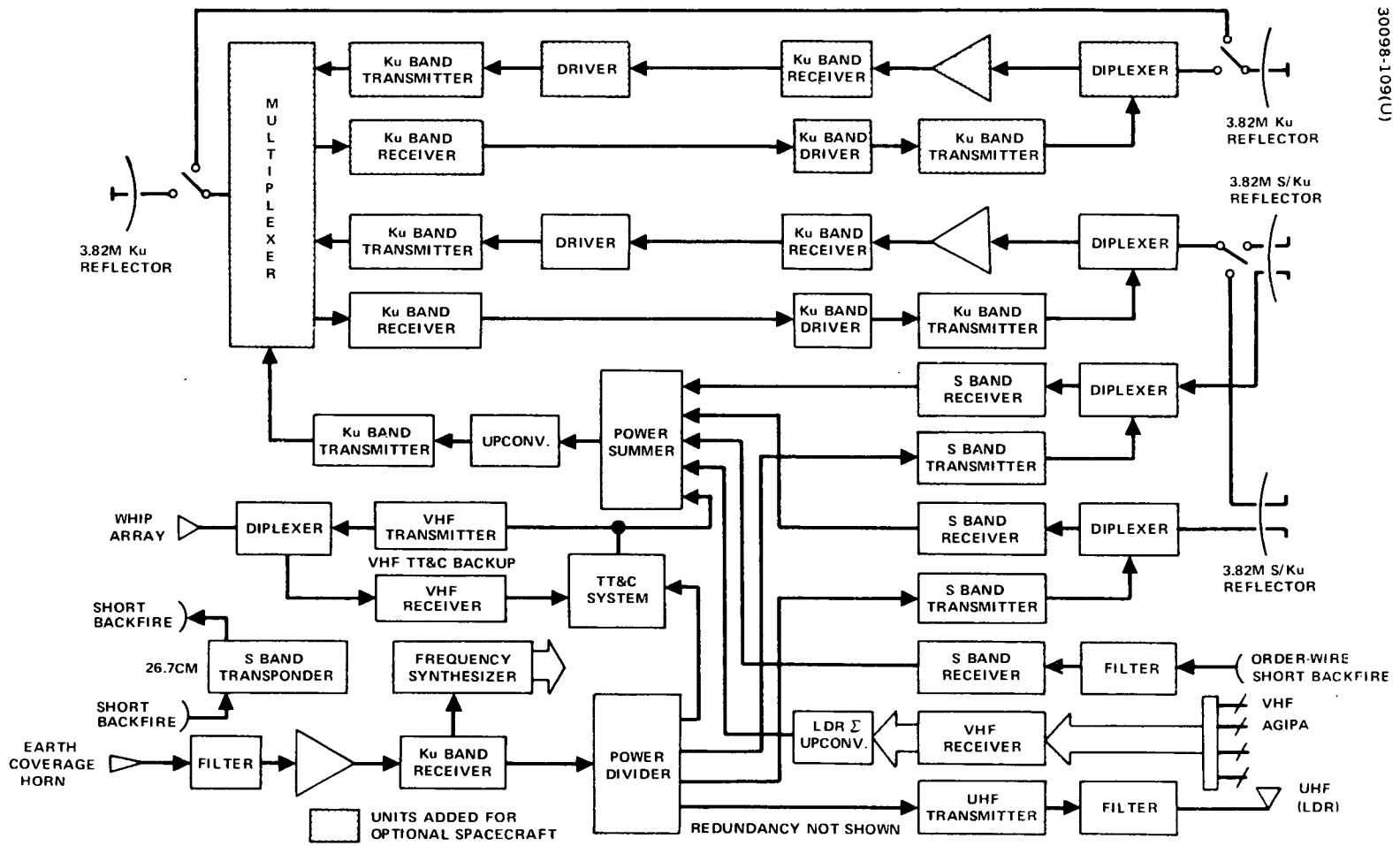

300898-109(U)

Figure 103. Telecommunications Subsystem for AC01

The solar cell array is sized to a convenient increment of solar cells for a total increase of 98 watts. The power budget for AC01 is given in Table 60. The power subsystem performance figures appear in Table 61.

A summary of the solar panel design parameters is presented in Table 62. The solar panel length is increased 0.15 meter. Oversized solar cells, 2.36 by 6.23 cm, are incorporated to utilize the increased panel length without either increasing the end of life bus voltage or resorting to a complicated layout configuration.

The increased equipment mass and larger power supply and structure have necessitated a new spacecraft design in order to obtain a reasonable margin for spacecraft mass. The spacecraft mass summary for AC01 is given in Table 63. A more efficient apogee injection motor utilizing double base propellant is incorporated into the design. Extensive use of graphite composite and beryllium structures is also required. Some savings of mass could possibly be made by more extensive interconnection of repeater equipment together with some reduction in redundancy. This design, however, uses a fully redundant electronic equipment complement.

Component mass estimates are tabulated in Table 64. Most of the equipment is similar to that presented for the baseline configuration.

TABLE 59. MASS AND POWER REQUIREMENTS FOR REPEATER COMPONENTS

	Spacecraft Quantity	Mass, kg	DC Power
Transmitter, HDR/MDR/LDR Return		16.8	70.0
Antenna switches	2	0.4	–
Multiplexer (3 transmit and 1 receive)	1	0.5	–
TWT and EPC	6	8.2/2.3	67.6
Driver upconverter	6	3.3	2.4
Summer	1	0.3	–
Transmitter, HDR Forward		12.0	54.0
Antenna switches	6	1.2	–
Diplexer (transmit receive)	2	0.4	–
TWT and EPC	4	8.2	52.4
Driver upconverter	4	2.2	1.6
Receiver, CMD/LDR Forward		3.4	2.1
TDA and BPF	2	0.7	0.4
Mixer/amplifier and phase lock loop	2	2.5	1.7
Hybrid and divider	1	0.1	–
EPC	1	0.1	–
Receiver; HDR Return		12.7	20.0
Tracking modulator	3	3.3	3.4
Preamplifier	4	5.0	10.8
Mixer/amplifier/filter (redundant)	4	2.4	1.2
Tracking demodulator	4	1.8	3.6
EPC	1	0.2	11.0
Receiver, MDR/HDR Forward		5.1	5.8
Tracking modulator	1	1.1	1.7
BPF	1	0.1	–
Mixer/amplifier/filters	2	2.9	2.0
Antenna tracking demodulator	1	0.9	1.8
EPC	1	0.1	0.3
Transmitter, MDR Forward		17.4	100/25
Driver (redundant)	6	8.1	410
Power amplifier (4 of 6)	3	3.9	96/21
Diplexer and cable	3	5.1	
EPC	3	0.3	–

Table 59 (continued)

	Spacecraft Quantity	Mass, kg	DC Power
Receiver, MDR Return		4.5	17.5
Preamplifier	6	2.4	15.0
Mixer/filter/amplifier/attenuator (redundant)	6	1.8	1.5
EPC	3	0.3	1.0
Receiver, Order Wire		1.9	1.7
BPF	1	1.1	–
Preamplifier	2	0.2	0.5
Mixer/filter amplifier/mixer amplifier (redundant)	2	0.5	1.0
EPC	1	0.1	0.2
Transponder, S band		4.0	24.0/2.0
Receiver	2	0.6	1.0
Transmitter	2	0.9	22.0
Frequency reference	2	0.3	1.0
Filter	1	2.2	–
Transmitter, LDR Forward		4.6	146.0
Driver	2	0.6	6.0
Power amplifier (4 of 6)	6	1.5	140.0
Summer and switch	1	0.5	–
LPF	1	1.0	–
Cable	1	0.9	–
EPC	1	0.1	–
Receiver, LDR Return		6.4	9.6
Preamplifier/BPF/amplifier	20	1.7	1.0
LO frequency source and selector	2	0.2	0.3
Preamplifier/mixer/amplifier (8 channels)	20	1.1	7.0
BPF/limiter/summer	1	0.7	–
Mixer/amplifier/filter	2	0.1	0.8
EPC	1	0.1	0.5
Cable and integrated package		2.5	–
Frequency Synthesizer		8.5	7.8
Master oscillators and multiplier		8.4	7.3
EPC		0.1	0.5

TABLE 60. POWER BUDGET FOR AC01

Equipment	Watts at 24.5 volts			
	Eclipse Season		Solstice Season	
	Command Mode	Intermittent S Band Voice	Command Mode	Intermittent S Band Voice
HDR return transmitter (Ku band)	61	61	61	61
LDR/MDR return transmitter (Ku band)	9	9	9	9
HDR forward transmitter (Ku band)	54	54	54	54
MDR forward transmitter no. 1 (S band)				
Command	25	25	25	25
Voice and data				
MDR forward transmitter no. 2 (S band)				
Command	25	–	25	–
Voice and data		100		100
LDR forward transmitter (UHF)				
Command and data	146	146	146	146
Voice				
S band transponder	24/2	24/2	24/2	24/2
Receivers, processors, etc.	65	65	65	65
Telemetry, tracking, and command	16	16	16	16
Antenna position control	12	12	12	12
Despin control	20	20	20	20
Thermal control	6	6	6	6
Power electronics	1	1	1	1
Battery charging	134	45	45	0
Distribution losses	15	15	15	15
Power required	613/591	596/574	524/502	554/532
Contingency	57/79	74/96	108/120	78/100
Solar power available	670	670	632	632

TABLE 61. POWER SUBSYSTEM PERFORMANCE

Parameter	Performance Requirement
Solar Cell Arrays	
Number of buses	2
Polarity	Positive
Voltage end of life at maximum power	24.5 volts
Maximum voltage limited to	33.0 volts
Maximum power end of life	670 watts eclipse season 632 watts summer solstice
Battery Discharge	
Set point for automatic discharge	24.1 ±0.15 volts
Voltage transient on battery turn-on	+9.0 volts maximum step charge
Discharge turn-off	By ground command
Minimum bus voltage during battery discharge	24.1 volts
Battery Charge	
Battery charge current	1.45A per battery at end of 7 years (1.75 A max)
Battery charge command	
2/3 charge array	One on command per battery
1/3 charge array	One on command per battery
All charge arrays	One off command per battery
Battery Reconditioning	
Discharge Current	0.035 A nominal
Command	On/off command for each battery
Shunts	
Rating	30 A (200 mv output)
Number provided	6

TABLE 62. SOLAR CELL ARRAY DESIGN CHARACTERISTICS

Solar Array End of 7 Years Power Output	
Summer solstice	632 W
Eclipse season	670 W
Solar Cell Arrays	
Number of panels	2
Geometric shape	Cylindrical
Diameter	2.38 meters
Length/Panel	1.52 meters
Mass, per array	
Substrate	18.5 kg
Cells, wire, diodes, connector, etc.	21.6 kg
Total	40.1 kg
Solar Cells	
Type of cell, cm	2.36 x 6.23 cm n/p silicon
Coverglass thickness	0.3 mm
Cell thickness	0.33 mm (nominal)
Minimum average output per lot	522 mA
Test voltage	0.445 ±0.002 volt
Cell temperature	298K ±2K
Illumination level	139.6 mW/cm^2
Illumination spectrum	Air mass zero equivalent
Solar Cell Array Design Factors	
Voltage	
Fabrication loss	1.000
Radiation damage	0.9275
Instrumentation error	1.000
Temperature coefficient for V_{oc}	-2.25 mV/K
Temperature coefficient for V_{mp}	-2.1 mV/K
Diode loss	0.94 volt
Current	
Fabrication loss	0.980
Radiation damage	0.8792
Transmission loss factor	0.98
Instrumentation error	1.000
Effective illuminated area factors	0.3183
Curvature edge effect	0.9616
Effective intensity ratio	
Summer solstice	0.8884
Equinox	1.0000
Temperature coefficient for I_{sc}	107 A/K
Temperature coefficient for I_{mp}	84.0 A/K
Ripple	0.98

TABLE 63. SPACECRAFT MASS SUMMARY FOR AC01

Subsystem	Mass, kg
Repeaters	97.3
Telemetry, tracking, and command	19.5
Antennas	113.5
Attitude control	32.8
Reaction control	18.0
Electrical power	107.7
Wire harness	30.0
Apogee motor burn out	52.0
Structure	230.0
Thermal control	30.0
Contingency	129.2
Spacecraft, final orbit	860.0
Hydrazine synchronous orbit	63.0
Spacecraft, initial orbit	923.0
Apogee motor expendables	782.0
Spacecraft, transfer orbit	1705.0
Hydrazine, transfer orbit	5.0
Spacecraft, separation	1710.0
Spacecraft adapter	61.0
Payload at launch	1771.0*

*Extended payload fairing.

TABLE 64. SUBSYSTEM AND COMPONENT MASS FOR AC01

Subsystem/Item	Quantity		Mass, kg
	Available	Required	
Repeater Subsystem			97.3
Transmitter, LDR/MDR/HDR return	2	1	16.8
Transmitter, HDR forward	4	2	12.0
Receiver, CMD/LDR forward	2	1	3.4
Receiver, HDR return	4	2	12.7
Receiver, MDR/HDR forward	2	1	5.1
Transmitter, MDR forward	6	3	17.4
Receiver, MDR return	6	3	4.5
Receiver, Order wire	2	1	1.9
Transponder, S band	2	1	4.0
Transmitter, LDR forward	2	1	4.6
Receiver, LDR return	20	10	6.4
Frequency synthesizer	2	1	8.5
Telemetry and Command Subsystem			19.5
Despun decoder	2	1	2.7
Despun encoder and multiplexer	2	1	4.2
Spun decoder	2	1	2.7
Spun encoder and multiplexer	2	1	5.0
Despun squib driver	1	1	3.5
Spun squib and solenoid driver	1	1	0.9
Latching valve/heater driver	1	1	0.5
Antenna subsystem			113.5
Paraboloid reflector, Ku band	1	1	7.9
Horns, Ku band	2	2	0.5
Paraboloid reflector, S and Ku bands	3	3	26.7
Backfire, S band	2	2	1.0
Backfire, UHF	1	1	2.5
Backfire, VHF	5	5	30.5
Bicone, S band	1	1	1.0
Antenna positioner	4	4	16.8
Positioner controller	4	4	3.6
Coax waveguide			22.0
Attitude control subsystem			32.8
BAPTA	1	1	13.7
Earth sensors	3	2	2.8
Sun sensors	1	1	0.1

Table 64 (continued)

Subsystem/Item	Quantity		Mass, kg
	Available	Required	
Despun control electronics	2	1	4.4
Active nutation control	2	1	1.8
Nutation damper	2	1	10.0
Reaction control subsystem			18.0
Tanks	4	4	9.5
Thrusters	6	3	3.0
Filters	4	4	0.6
Valves fill vent	1	1	0.3
Valves batching	5	5	0.5
Pressure transducer	2	2	0.5
Plenum chambers	2	2	0.2
Manifold fittings			2.3
P-O pressurant			1.1
Electrical power subsystem			107.7
Solar cell arrays	2	2	43.2
Batteries	2	2	57.6
Battery controller	2	2	2.6
Heater controllers	1	1	1.1
Miscellaneous hardware			0.5
Voltage limiter	6	4	2.7
Wire harness			30.0
Apogee motor burn out	1		52.0
Structure			230.0
Solar array substrate	2	2	38.0
Spin structure	1	1	45.0
Despun equipment platform	1	1	50.0
Equipment support	1	1	20.0
Antenna support	—	—	65.0
Despun clamp	1	1	7.0
Balance mass			5.0
Thermal control			30.0
Spin thermal equipment	1	1	20.0
Despun thermal equipment	1	1	10.0